Year : 2017

AMINO ACID RESTRICTION AND HYDROGEN SULFIDE IN VASCULAR HOMEOSTASIS

Longchamp Alban

Longchamp Alban , 2017, AMINO ACID RESTRICTION AND HYDROGEN SULFIDE IN VASCULAR HOMEOSTASIS

Originally published at : Thesis, University of Lausanne

Posted at the University of Lausanne Open Archive http://serval.unil.ch
Document URN : urn:nbn:ch:serval-BIB_C9484BB47AB80

UNIL | Université de Lausanne
Faculté de biologie et de médecine

AMINO ACID RESTRICTION AND HYDROGEN SULFIDE IN VASCULAR HOMEOSTASIS

Thèse de doctorat

MD - PhD

présentée à la

Faculté de biologie et de médecine
de l'Université de Lausanne

par

Alban LONGCHAMP

Médecin diplômé de la Confédération Helvétique

Jury

Prof. Peter Vollenweider, président et répondant MD-PhD
Prof. Jacques-Antoine Haefliger, directeur de thèse
Prof. Charles Keith Ozaki, co-directeur de thèse
Prof. James R. Mitchell, expert
Prof. Xavier Berard, expert
Prof. Thierry Pedrazzini, expert

Lausanne 2017

UNIL | Université de Lausanne

Ecole doctorale

Ecole Doctorale

Doctorat MD-PhD

Imprimatur

Vu le rapport présenté par le jury d'examen, composé de

Président·e	Monsieur Prof. Peter **Vollenweider**
Directeur·trice de thèse	Monsieur Prof. Jacques-Antoine **Haefliger**
Co-Directeur·trice de thèse	Monsieur Prof. Charles Keitz **Ozaki**
Répondant·e	Monsieur Prof. Peter **Vollenweider**
Expert·es	Monsieur Prof. Xavier **Berard**
	Monsieur Prof. James R. **Mitchell**
	Monsieur Prof. Thierry **Pedrazzini**

le Conseil de Faculté autorise l'impression de la thèse de

Monsieur Alban LONGCHAMP

Médecin diplômé de la Confédération Suisse

intitulée

AMINO ACID RESTRICTION AND HYDROGEN SULFIDE IN VASCULAR HOMEOSTASIS

Lausanne, le 15 septembre 2017

pour Le Doyen
de la Faculté de Biologie et de Médecine

Prof. Peter Vollenweider

ACKNOWLEDGEMENTS

I would like to thank the jury, for evaluating this work and providing valuable comment throughout the thesis: Prof. P. Vollenweider, Prof. J.-A. Haefliger, Prof C.- Keith Ozaki, Prof. James R. Mitchell, Prof. Xavier Bérard, Prof. T. Pedrazzini.

I would like to thank my parents, Nicole and Jean-Paul Longchamp, as well as my brother and sisters Grégoire, Justine and Ella. They have always been supportive. My family offered happiness, culture and education. Beyond education, they made of us decent human being. I'll never thank them enough for it.

I would also like to thank Prof. J-M Corpataux, who initially served as my master thesis advisor. I first discovered surgery, especially vascular surgery through him. As a medical student, he was the reason I chose to become a vascular surgeon. He guided me in my professional career and was always available. His leadership, passion, hunger for excellence and willingness to teach me on the ward and in the OR made of him a key person in my life. With Dr. S. Déglise and Prof. H.-B Ris, they not only believed in me when I decided to leave to the United States but made it possible, providing moral and financial support.

After graduating in 2012, I spent one year in Prof. J.-A. Haefliger's lab. It was during these initial stages of my education I confirmed my desire to pursue an academic career path, and become a "clinician-scientist." Jacques-Antoine guided me toward this path and has been a great mentor. He wasn't only a great scientist to me, but also a great friend, and shared our common interest in gastronomy and sport. In 2013, with his help, I was accepted in the MD-PhD Program at the University of Lausanne / EPFL. His lab, encompass amazing scientist Florent, Florian, Loic, and Martine that every day they invested time for me and taught me the basis of laboratory work. Especially Florent, thank you for spending so many hours training me, and for sharing with me your passion for science.

In December 2013 I joined the Ozaki and Mitchell lab in Boston. They are not only the best scientists I have ever met but they are amazing human beings. They showed the best side of their culture with me. Prof. C. Keith Ozaki is a model of kindness, scientific and personal achievement. He shared with me his passion of surgery, academia and science, as well as his love for country music and steak in Nashville, or fishing in Florida. Thank you. Jay welcomed in his lab with opened arms, he always had faith in me was available at any time for some

precious advices. I was so lucky to meet someone as open minded as Jay. His scientific rigor and excellence taught me to always think outside the box. Thank you for being such a great mentor. Jays created the most amazing atmosphere in the lab. I was lucky enough to meet and work with Chris, at the time they discovered the role of H_2S. Thank you Chris for sharing your expertise, you have inspired me in your work. I'll always be grateful for your guidance.

I want to thank people in Jays, Dr. Ozaki's lab and at Harvard, including some that became great friends: Kaspar, Neslon, Lear, Humberto, Pedro, Mike, Issam, Kent, Eylul, Ming, Gaurav, Andrew, Abhi, Tea, Dr D. A Sinclair and Dr. C. Chen.

I also want to thank my friends in Switzerland. They always supported me in my decision and made me feel home, thank you Yann, Raphael, Swenn, Adrien, Rémi, Jonas, Florian and Céline.

Finally, I want to thank my girlfriend Justina. You have always been understanding and provided time and moral support when I needed it the most.

ABSTRACT

Dietary Restriction (DR), defined as reduced food intake without malnutrition, was first described nearly a century ago to extend lifespan in rats. Since then, DR has been extensively studied, in a multitude of organisms, and evidence supports that DR increases lifespan and confers protection against age-associated diseases such as hypertension, ischemia of the limbs, heart or brain.

Angiogenesis, the formation of new blood vessels by endothelial cells (EC), is crucial for the protection and recovery from blood vessel occlusion. Hypoxia is the best understood pro-angiogenic trigger, but therapies targeting this pathway have largely failed to demonstrate long-term benefits.

Here, we hypothesized that a nutrient-based pathway regulates angiogenesis independent of hypoxia. We found that dietary sulfur amino acid restriction (methionine and cysteine) promoted VEGF expression and capillary growth in skeletal muscle of mice independent of hypoxia or the transcription factor HIF1α, instead requiring the amino acid-sensing translation initiation factor eIF2α kinase GCN2 and the transcription factor ATF4. GCN2/ATF4 activation increased cystathionine-γ-lyase expression and pro-angiogenic hydrogen sulfide (H_2S) production. In human EC, H_2S boosted glycolytic ATP production by inhibiting mitochondrial electron transport, and was required for angiogenesis triggered by amino acid deprivation, exercise or local VEGF overexpression.

H_2S is an endogenously produced gas with broad protective effects on the vascular system, and can be measured in blood serum. Using a cohort of patients undergoing vascular surgery (for advanced occlusive disease) and matched healthy patients, we found that healthy patients had the highest serum H_2S production. Importantly, among patients that underwent surgery for vascular disease, the percentage of survival in the low H_2S (defined as < median) was lower compared to high H_2S (defined as > median) suggesting that it may serve as an easily quantified measure with biological significance with regards to vascular health.

RESUME

La restriction alimentaire (RA), définie comme une réduction des apports alimentaires sans malnutrition, fut décrite il y a près d'un siècle. Depuis, la RA a été étudiée dans une multitude d'organismes, démontrant que la RA permet d'augmenter l'espérance de vie et de protéger contre les maladies associées à l'âge telles que l'hypertension, l'ischémie cardiaque, cérébrale et des membres inférieurs.

L'angiogenèse, soit la formation de nouveaux vaisseaux sanguins par les cellules endothéliales (EC), protège et facilite la récupération lors d'une occlusion vasculaire (ischémie). L'hypoxie est le stimulus pro-angiogénique le plus étudié; cependant, les thérapies ciblant cette voie ont à l'heure actuelle largement échouées. Nous avons donc émis l'hypothèse qu'une voie indépendante, nutrio-sensible, pouvait réguler la formation de nouveaux vaisseaux. Nos résultats suggèrent que la restriction d'acides aminés soufrés (méthionine et cystéine) favorise l'expression du factor de croissance vasculaire VEGF et la croissance capillaire *in-vivo*, indépendamment de l'hypoxie ou de l'HIF1α mais nécessitant la kinase GCN2 et le facteur de transcription ATF4.

L'activation de GCN2/ATF4 augmente l'expression de cystathionine-y-lyase et la production de sulfure d'hydrogène (H_2S), connu pour ses propriétés pro-angiogéniques. Dans les EC humaines, le H_2S favorise l'angiogenèse en inhibant le transport d'électrons mitochondrials, stimulant la production d'ATP glycolytique.

H_2S est un gaz produit de manière endogène avec des effets protecteurs sur le système vasculaire, et peut être mesuré dans le sérum. Dans une cohorte de patients hospitalisés pour une maladie vasculaire occlusive avancée et de patients sains nous avons constaté que les taux sériques d'H_2S étaient plus élevés chez les patients sains. De plus, parmi les patients qui ont subi une intervention chirurgicale pour les maladies vasculaires, la survie à 6 et 24 mois était plus élevée chez les patients avec un taux préopératoire élevé d'H_2S. En conclusion, nos résultats démontre qu'une RA, via H_2S participent à la fonction du système vasculaire et pourrait jouer un rôle majeur dans la survie/ récupération des patients ayant subi un intervention vasculaire.

AASR Amino acid starvation response

ABBREVIATIONS

AMPK	AMP-activated kinase
ATF4	Activating transcription factor 4
CBS	Cystathionine β- synthase
CGL (CSE, CTH)	Cystathionine-gamma-lyase
CPT1	Carnitine palmitoyltransferase 1
Cyst	Cysteine
DR	Dietary restriction
EC	Endothelial cell
eIF2α	Eukaryotic translation initiation factor α
ERAS	Enhanced recovery after surgery
FAO	Fatty acid oxidation
FGF21	Fibrobalst growth factor 21
GCN2	General control nonderepressible 2
H_2S	Hydrogen Sulfide
HUVECs	Human Umbilical Vein Endothelial Cells
IGF-1	Insulin growth factor-1
IRI	Ischemia Reperfusion Injury
Met	Methionine
MR	Methionine Restriction
mTORC	Mechanistic target of rapamycin
NO	Nitric Oxide
PAD	Peripheral artery disease
RA	Restriction alimentaire
VEGF	Vascular endothelial growth factor
VEGR2	Vascular endothelial growth factor receptor 2

TABLE OF CONTENTS

INTRODUCTION

Dietary restriction

When the food intake of an organism is reduced to below what they would eat if given unlimited access to food, but not so much that they are malnourished, they age at a slower rate and live longer (1). This phenomenon of dietary restriction (DR), defined as reduced nutrient/energy intake without malnutrition, is the most potent intervention to increase lifespan and decrease the incidence and severity of age-related diseases from single-celled yeast to fruit flies to non-human primates (2).

While long term DR prolong life, more recent data indicate that short-term DR (in the range of days to weeks) can increases resistance to multiple forms of stress, that range from chemotherapy to surgical ischemia reperfusion injury (IRI) (8–11). For example, 2-4 days of water-only fasting is sufficient for protection in models of IRI to the liver or the kidney, a model that is relevant to organ transplantation (3). Similarly, 6-7 days of reduced total food or isolated protein intake protects against warm ischemia reperfusion injury to brain, liver or kidney (4-6). Importantly, short-term protein restriction or fasting also protect from chronic re-occlusive vascular wall adaptations, such as intimal hyperplasia, which can result in recurrent end-organ ischemia, loss of limb, reduced brain function, or even death (7).

Despite strong evidence of the evolutionary conservation of DR benefits in humans (8), voluntary food restriction is impractical for most people. Thus, uncovering common nutritional and molecular mechanisms that require either minimal dietary alterations, or can be targeted by pharmacological interventions, is of great significance (9, 10).

Nutritional requisite

Although protein is equal in caloric content to carbohydrate, restriction of protein (but not sugar or fat) contribute to dietary preconditioning beyond its caloric value (**Figure 1**) (4, 11).

Importantly, preconditioning against surgical stress in rodents can be achieved without enforced food restriction (caloric restriction) by using diets reduced in or lacking protein (amino acid restriction, protein free regimen, **Figure 1**). This is an important difference when considering clinical translational potential due to the difficulties inherent in enforced restriction of food intake

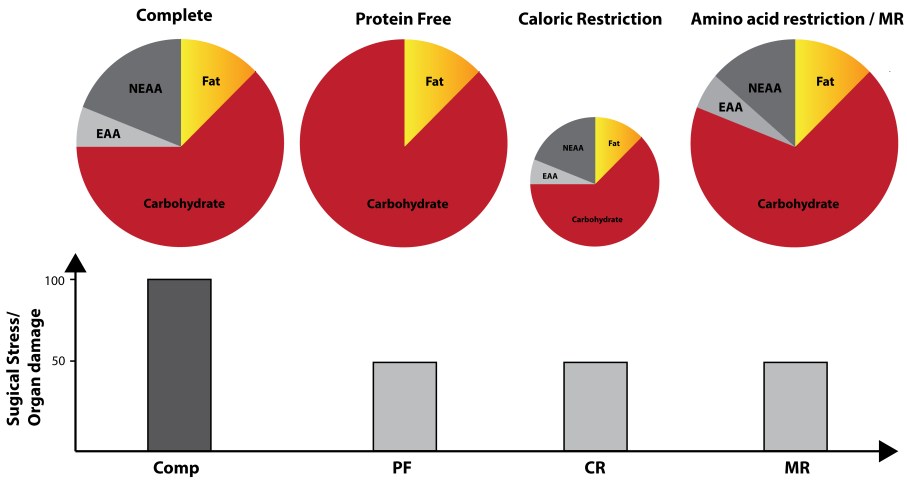

Figure 1: Schematic of diets in which 18% of calories are contributed by protein (complete), sucrose (PF), NEAAs (NEAA only), or EEAs (EAA only, *top*). Mice preconditioned with these diets were protected against various form of surgical stress (*bottom),* including ischemia reperfusion injury to the heart, brain, liver, kidney or limbs.

even for short periods of time.

It is also important to note that different organs can have different requirements for protection even against the same injury. For example, while in the renal IRI model both protein and calorie restriction contribute additively to organ protection (12), protein restriction alone contributes disproportionately to organ protection against hepatic IRI (11). Much future work is required in order to determine the optimal balance of calories from protein vs. sugar and fat, as well as the total calorie intake, for optimal stress resistance, which itself will likely depend on the specific surgery as well as patient-specific risk factors.

Methionine restriction

Restriction of sulfur amino acids methionine (Met) and cysteine (Cys) is common to numerous DR regimens across evolutionary boundaries and is thus a potential shared nutritional trigger of DR benefits. Orentreich's initial studies demonstrated that the inception of methionine restriction (MR) early in life increased median and maximum lifespan by 30 and

40%, respectively (13). In mammals, MR benefits actually require combined methionine and cysteine restrictions (14), and thus could be more accurately referred to as sulfur amino acid (SAA) restriction. MR also extends lifespan and stress resistance in yeast (15) flies (16), worms (17) and rodents (13, 18). In humans, MR has been used to complement cancer treatment (19) and to improve metabolic fitness (20, 21). Evidence in favor of a mechanistic overlap stems from fly studies, in which DR-mediated lifespan extension can be abrogated by giving essential amino acids (EAA) including Met, but not EAA lacking Met (22). We also recently showed SAA abrogated benefits of stress resistance in mice (23, 24).

Amino acid sensing and molecular basis for DR benefits

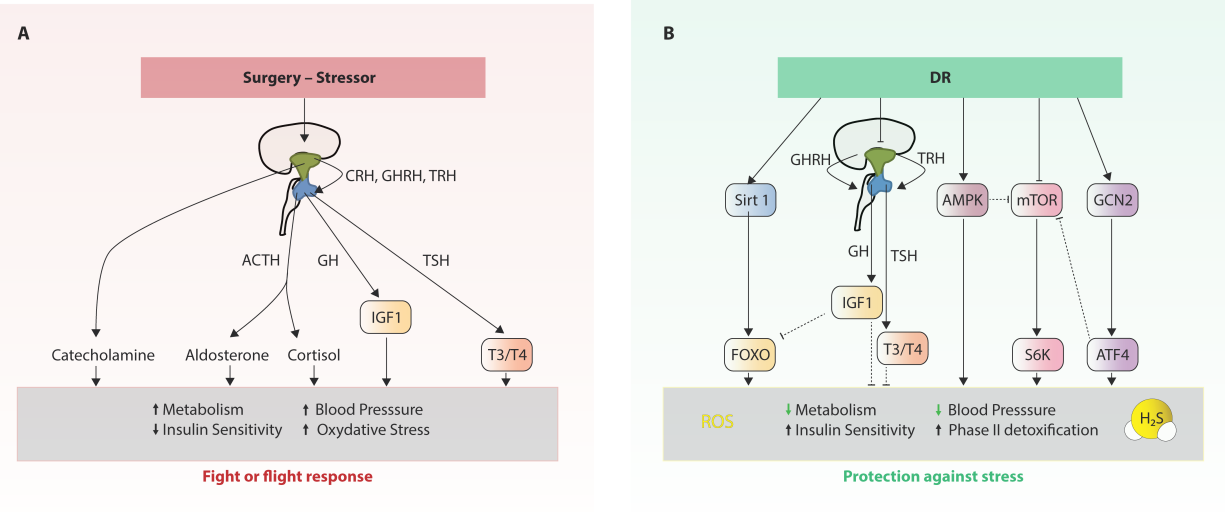

Figure 2: **Effects of dietary restriction on surgical stress. A**, model of the metabolic response to surgical stress. Surgery perturbs metabolic and immune homeostasis through effects on afferent (autonomic and sympathetic) nerve input from the area of trauma leading to local and systemic catecholamine release, increased levels of proinflammatory acute phase reactants, metabolic adaptations including glycogen mobilization, and vascular changes including vasoconstriction and increased heart rate. Parallel activation of the hypothalamic-anterior pituitary-adrenomedullary axis promotes release of cortisol from the adrenal cortex, resulting in a partially counterbalancing response characterized by protein and fat mobilization, immunosuppression, and dampening of the action of anabolic hormones such as IGF1/insulin and testosterone. **B**, Conserved molecular signaling that regulate longevity and and stress resistance in vertebrates. Dietary restriction controls the activity of various signal transduction pathways either directly or indirectly through the reduced levels of circulating growth factors such as IGF-1 and the thyroid hormone thyroxine (T4) and triiodothyronine (T3). In this model propose that the mechanism of surgical stress resistance caused by modulation of these nutrient signaling pathways include a transient increase in free radical superoxide (ROS) and hydrogen sulfide (H_2S) production. Sirt 1 indicates Sirtuin 1; AMPK, AMP-activated protein kinase; FOXO, forkhead box O transcription factors; IGF-1, insulin-like growth factor 1; mTOR, mammalian target of rapamycin; S6K, S6 kinase; GCN2, general control nonderepressible 2; ATF4, Activating Transcription Factor 4 ROS, reactive oxygen species; H_2S, hydrogen sulfide.

The ability to sense and respond to fluctuations in environmental nutrient levels is requisite for life (25). During food excess, nutrient-sensing pathways engage anabolism and storage, whereas scarcity triggers nutrient mobilization via internal storage degradation. In the context of DR, it is therefore coherent that the same pathways sensing nutrients are involved in DR benefits.

General control nonderepressible 2:

Proteins are synthetized in the ribosome, which incorporates amino acids into a nascent polypeptide by the sequential binding of a specific transfer RNA (tRNA) covalently linked to its cognate amino acid. Amino-acid-specific aminoacyl tRNA synthetases (aaRSs) execute the loading of amino acids to their cognate tRNAs, and uncharged tRNAs accumulate when levels of free amino acids are minimal. The general control nonderepressible 2 (Gcn2) protein is a serine/threonine protein kinase that contains two central regulatory regions, a histidyl-tRNA synthetase-like domain (HisRS) and a C-terminal domain (CTD), which function together to sense nutrient depletion(26-30). Typically upon DR, low levels of one or more amino acids promote accumulation of uncharged cognate tRNAs. Uncharged tRNAs directly activate the kinase domain of GCN2, facilitating phosphorylation of the eukaryotic translation initiation factor α (eIF2α). Phosphorylated eIF2α reduces general translation initiation efficiency, it promotes translational up-regulation mRNAs with specific regulatory sequences upstream of the initiating Met codon, including the activating transcription factor 4 (ATF4) (31). ATF4 in turns stimulates expression of target genes involved in non-essential amino acid biosynthesis, amino acid transport, collectively known as the amino acid starvation response (30) (**Figure 2**). Interestingly, deprivation of a single amino acid can result in deacylation of non-cognate tRNAs as well. For example, leucine starvation of auxotrophic yeast results in accumulation of uncharged serine and threonine tRNAs in addition to leucine tRNAs (30, 32).

Because GCN2 regulates adaptive changes to perceived amino acid deficiency, mice lacking this protein appear normal in the absence of such a challenge. This is not the case for one of its downstream effectors, ATF4. ATF4-knockout mice display multiple developmental abnormalities and are smaller than control littermates (33). Cells lacking ATF4 require excess non-EAAs including cysteine (or antioxidants such as glutathione or *N*-acetylcysteine) (34). In addition, cells lacking ATF4 have reduced levels of CSE, the enzyme responsible for the

conversion of cystathionine to cysteine (35). Moreover, elevated ATF4 levels have been described in liver and isolated fibroblasts of long-lived, stress-resistant rodent models including hypopituitary Snell dwarf mice (36), and are associated with extended longevity upon nutrient deprivation, altered ribosomal function, or rapamycin treatment in yeast (37).

In the context of dietary preconditioning against IRI, GCN2 is required for protection from renal and hepatic ischemia reperfusion injury induced by dietary tryptophan deficiency (4). However, GCN2 does not appear to be required for preconditioning by total protein deprivation (11, 12), likely due to redundancy in protein-sensing mechanisms including mTORC1 as described below. GCN2 can also be activated pharmacologically by the proline tRNA synthase inhibitor halofuginione (38). In mice, pretreatment with halofuginone protects against renal IRI in a GCN2-dependent manner (4).

Mechanistic target of rapamycin complex 1:

In all eukaryotes, the mechanistic target of rapamycin (mTOR) is a conserved Ser/Thr kinase comprised of three essential and evolutionarily conserved core subunits (mTOR, Raptor and mLST8) forming mTOR complex 1 (mTORC1). This kinase integrates information on energy, amino acid and growth factor availability to cell fate decisions regarding anabolism or catabolism, including cell growth and autophagy (39-42). Under nutrient/energy restriction, mTORC1 is activated to stimulate anabolic processes that convert nutrients and energy into macromolecules, including protein, lipid and nucleic acids (**Figure 2**). Interestingly, while GCN2 can detect the absence of any amino acid, the presence of specific amino acids such as leucine (43, 44) or argininie (45) is sensed specifically by the protein complex mTORC1.

At the lysosome level, entry of amino acids, promotes Ragulator activity. In this manner, amino acids stimulate the formation of $RagA/B^{GTP}$–$RagC/D^{GDP}$ heterodimers, which bind directly to mTORC1 and recruit the inactive kinase complex to the lysosomal surface for its activation.

Activated mTORC1 promotes protein synthesis via mRNA translation through two sets of direct downstream targets: the eukaryotic initiation factor 4E (eIF4E)-binding proteins (4E–BP1 and 2) and the ribosomal S6 kinases (S6K1 and 2)(25, 39, 40, 46-48).

In the context of DR inhibition of mTORC1 (49, 50) or its direct target, S6K (51) promotes lifespan and healthspan. Importantly, we recently showed that in mice, one week on protein free diet reduced hepatic mTORC1, coinciding with protection against hepatic IRI (11). Whether this is a direct result of reduced amino acid (leucine) levels, or more likely a reduction of growth factor levels also required for mTORC1 activation, remains to be determined. However consistent with the importance of reduced mTORC1 in dietary preconditioning, liver-specific deletion of the upstream mTORC1 repressor gene TSC1 (The LTsc1KO mice), results in constitutive hepatic mTORC1 activation independent of diet, and prevents protein restriction from preconditioning against hepatic IRI (11, 24). Rapamycin (Sirolimus) is a partial mTORC1 inhibitor used in humans to prevent T and B cell-mediated organ transplant rejection, and also as a vascular stent coating to prevent intimal hyperplasia (52). In mice, long-term rapamycin treatment extends longevity (49, 50), but does not protect mice from hepatic IRI despite reducing hepatic mTORC1 signaling (11).

AMP-activated kinase:

AMP-activated kinase (AMPK) is a conserved energy-sensing protein kinase present in all eukaryotes as heterotrimers comprising catalytic α subunit and regulatory β and γ subunits. AMPK is allosterically activated when cellular energy is low via AMP and/or ADP as well as by several upstream kinases, e.g. serine/threonine kinase 11 (LKB1), Ca^{2+}/calmodulin-dependent protein kinase kinase β (CaMKKβ) and transforming growth factor-β-activated kinase 1 (TAK1)(53). It also reduces anabolic mTORC1 signaling by phosphorylating the mTORC1 inhibitor, TSC2.

Activation of AMPK promotes energy production by increasing glucose uptake in the short term and facilitating a switch to oxidative metabolism in the long term.

AMPK is activated upon fasting or DR regimens involving enforced food restriction (**Figure 2**); somewhat surprisingly it is also activated upon protein restriction independent of calorie intake (12). Due to essential nature of AMPK function and redundancy in catalytic AMPK subunit genes, genetic experiments to test the requirement in dietary preconditioning have not yet been performed. However, AMPK activation by the allosteric activator 5-aminoimidazole-4-carboxamide ribonucleotide (AICAR) protects against ischemic injury in rats when given at high doses before injury (54). AMPK activation by the endogenous lipokine adiponectin, which is increased upon DR, is also essential for the cardioprotective effects of DR against myocardial infarction (55)

Hydrogen Sulfide

Hydrogen sulfide (H_2S) is a gas easily identified by its distinctive odor of rotten eggs. While toxic at high levels, H_2S produced endogenously by CGL or CBS (**Figure 4**) acts on the vasculature and the brain as a signaling molecule to reduce blood pressure (56) and prevent neurodegeneration (57). Low levels of exogenous H_2S also extends lifespan of worms (18, 24) and induce suspended animation in mammals (58). H_2S has numerous other cardiovascular benefits, including pro-angiogenesis in vitro and in vivo (59, 60), reduced vascular restenosis

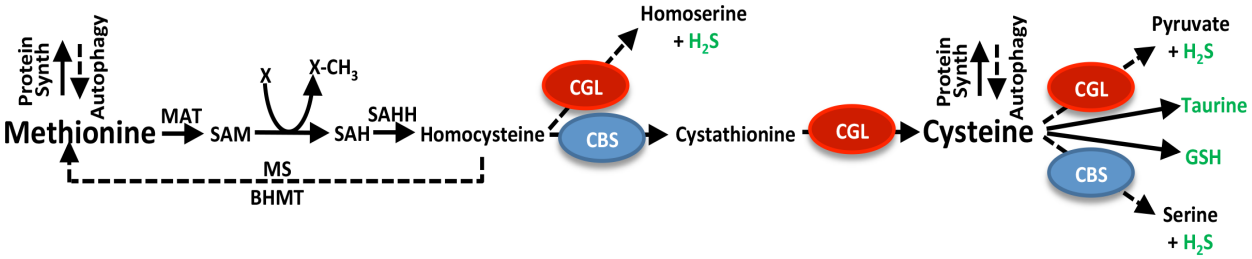

Figure 3: Model of the transmethylation and transsulfuration pathway (TSP). Arrows trace sulfur from Met to Cys through various metabolites and downstream cellular processes via the enzymes Cystathionine Beta- Synthase (CBS) and Cystathionine Gamma-Lyase (CGL). Metabolites in green (taurine, GSH and H_2S) have demonstrated potential to protect against IRI. MAT: methionine adenosyl transferase, SAM: S- Adenosylmethionine, SAH: S-Adenosylhomocysteine, SAHH: S-adenosylhomocysteine hydrolase, MS: Methionine synthase, BHMT: Betaine homocysteine methyltransferase. Picture and Legend from Hine et al, Cell 2015.

(intimal hyperplasia)(61, 62), anti-atherosclerotic activity (63), and reduced binding of neutrophils to the wall of blood vessel (64). On the other hand, in humans, serum H_2S concentration declines with age (65) and the levels of the H_2S producing enzymes are reduced in patients suffering vascular diseases (66, 67). We have recently demonstrated that mice lacking the H_2S-producing enzyme CGL fail to gain the protective effects of DR, while adenoviral overexpression of CGL in the liver, or delivery of H_2S itself, recapitulate DR-like benefits without the need for any dietary intervention (24). Thus, a model has emerged in which the well-known benefits of multiple DR regimens are linked to a common effector molecule: endogenous H_2S gas produced as part of an adaptive response to nutrient/energy deficiency.

Whether free H_2S is a circulating gasotransmitter that acts as a paracrine, or autocrine molecule is still being debated and difficult to address (68, 69). However, the enzyme CGL secreted by endothelial cells (EC)s and hepatocytes circulates in the plasma/serum, and actively produces H_2S in human blood (70), which may be critical for the systemic vascular benefits of H_2S (71). H_2S has many potential mechanisms of action, including sulfhydration, or formation of –SSH moieties on surface-exposed Cys residues, of an ever-growing list of protein targets (57, 68, 72-75). In ECs, for example, such targets include the Kir6.2 regulatory subunit of the K_{ATP} channel and the VEGF receptor leading to vessel relaxation and angiogenesis, respectively (73, 75). H_2S also has direct antioxidant properties, and can participate in mitochondrial energy production by donating electrons to the mitochondrial electron transport chain protein SQR, with a potential role in protection from organ ischemia (76, 77).

Angiogenesis

Structure of the vasculature

The vascular system of the human body is comprised of an extensive network of arteries, capillaries, and veins that deliver oxygen and nutrients to every part of the body, remove waste and provide gateways for patrolling immune cells (78) (**Figure 4**). Small blood vessels (capillaries), consist only of endothelial cells (ECs), whereas larger vessels are organized in three distinct histological layers (**Figure 4,** *right*): the intima, the media and the

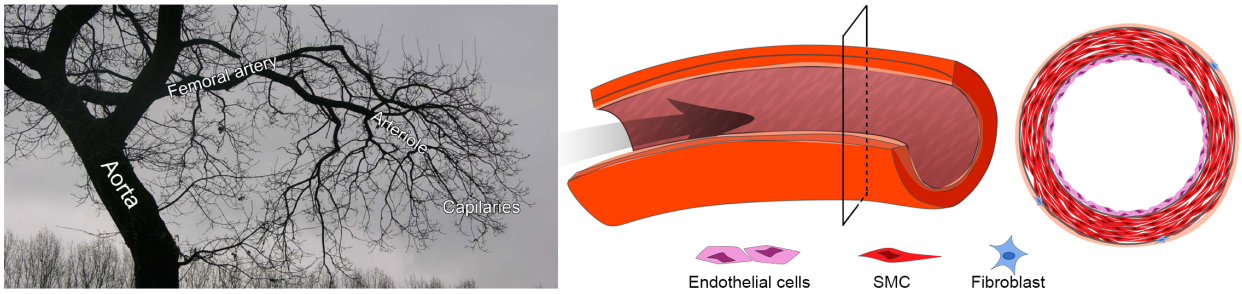

Figure 4: *Left:* The vascular tree. Graphical representation of the major arteries, from the aorta to small sized arteries to the capillaries, formed of one single layer of endothelial cells. Picture adapted from: https://www.flickr.com/photos/43635707@N00/131520207/in/photostream/.
Right: Schematic of an artery: The inner layer (intima) is formed by the endothelium, separated to the media by the internal elastic laminae. The media containing smooth muscle cells (SMCs) is lining on the external elastic laminae. The outer layer, the adventitia consists of connective tissue including fibroblasts.

adventitia. The intima, consists of a single layer of ECs surrounded by circularly arranged elastic bands or internal elastic laminae. The media mainly consists of SMCs and, which controls the caliber of the vessel. The external layer is entirely made of connective tissue. It also contains nerves and capillaries supplying vessel, especially in the larger vessels.

Endothelial cells

The endothelium, line the inner surface of all vessel. It is not only a barrier, between the circulating blood and organs but has a central role in maintain vascular homeostasis. It secretes numerous para-, endo- and auto-crine molecules such as nitric oxide (NO) (79) and H_2S (68). ECs are plastic cells, that can switch between growth states (80), and undergo multiple

developmental and functional transitions during fetal, neonatal and adult life. This plasticity is crucial to maintain a healthy microvascular network, providing adequate blood supply to organs throughout life and during metabolic stresses (81). Inadequate vessel maintenance or growth causes ischemia in diseases such as myocardial infarction, stroke, and neurodegenerative or obesity-associated disorders, whereas excessive vascular growth or abnormal remodeling promotes many ailments including cancer, inflammatory disorders, and eye disease (82).

Mechanism

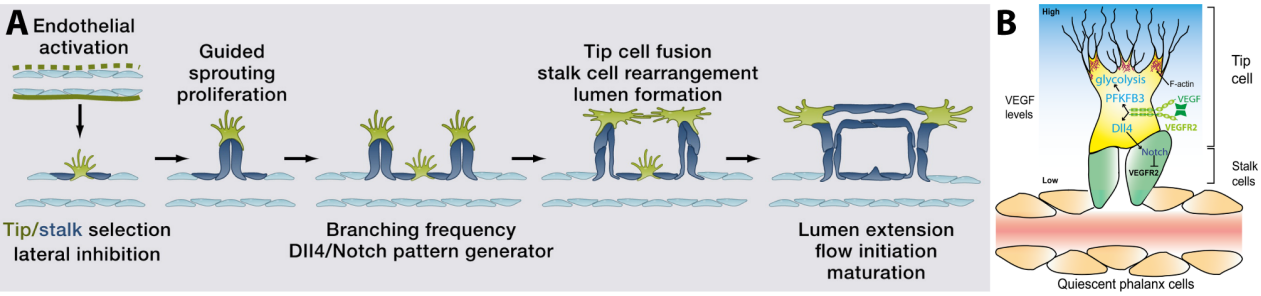

Figure 5: A: Steps of vessel sprouting: (1) tip/stalk cell selection; (2) tip cell navigation and stalk cell proliferation; (3) branching coordination; (4) stalk elongation, tip cell fusion, and lumen formation; and (5) perfusion and vessel maturation. Picture and legend from Potente M et al., Cell 2011. **B**: Schematic overview of a growing vessel sprout. In tip cells at the leading front of a newly formed vessel sprout, binding of VEGF to VEGFR2 induces upregulation of Dll4. In the adjacent EC, Dll4-dependent activation of Notch decreases the expression of VEGFR2, thereby preventing this EC to adopt a tip cell phenotype and inducing stalk cell differentiation. Stalk cells proliferate and elongate the sprout. Quiescent "phalanx" cells line established vessels (bottom). VEGFR2 signaling in the tip cells also increases the expression of the glycolytic enzyme PFKFB3 and enhances glycolytic energy production. Glycolytic enzymes are concentrated in the lamellipodia and filopodia, colocalizing with actin filaments (F-actin). This compartmentalization of glycolysis with F-actin provides local, rapid ATP production needed for actin-cytoskeletal remodeling required for migration. Tip cell is indicated in yellow, stalk cells in green, and phalanx cells in orange. Picture and legend from Vandekeere S et al., Microcirulation 2016

Angiogenesis is the formation or sprouting of new blood vessels from existing ones. Perhaps most well characterized mechanism is oxygen deprivation (hypoxia) that stabilizes the transcription factor hypoxia inducible factor 1 (HIF1α, (83), stimulating proangiogenic signals such as vascular endothelial growth factor (VEGF). Upon stimulation, ECs become motile, invasive and protrude filopodia (**Figure 5**). These tip cells at the forefront of the vascular branch extend long filopodia and navigate but rarely proliferate, probing the environment for guidance

cues (82, 84). Following tip cells, stalk cells proliferate, elongate some filopodia and establish a lumen. Finally, blood flow, the establishment of a basement membrane, and the recruitment of mural cells (pericyte) stabilize new connections (**Figure 5**) (82). The sprouting process iterates until the hypoxia is relieved by subsequent improved tissue perfusion, abrogating proangiogenic signals and re-establishing quiescence.

VEGF

Given the complexity of a process such as angiogenesis, it is remarkable that a single growth factor, VEGF, regulates angiogenesis so predominantly. VEGF (also known as VEGF-A) is the main component of the VEGF family. The major proangiogenic signal is generated from the ligand-activated VEGF receptor-2 (VEGFR-2, also known as FLK1) (85). Neuropilins such as NRP1 and NRP2 are VEGF co-receptors, which enhance the activity of VEGFR-2. Similar to VEGFR-2 deficiency, the loss of VEGF aborts vascular development (84). VEGF is also reduced in diabetic patients, which correlates with poor angiogenesis following soft tissue injury and impaired wound healing (86, 87). Activating VEGFR-2 mutations cause vascular tumours (88). VEGFRs are tyrosine kinase receptors carrying an extracellular domain for ligand binding, a transmembrane domain, and a cytoplasmic domain, including a tyrosine kinase domain. The cytoplasmic domain harbors binding site for the SH2 domain of the p85 subunit in the PI3-kinase complex and to activate the PI3K pathway, crucial for ECs growth (89). In addition, the SH2 domain of PLCγ binds to the 1175-PY site of VEGFR-2. The PLCγ-PKC-MAPK pathway is highly activated upon VEGF bounding and is a crucial signal for ECs proliferation (90, 91). Interestingly, VEGF stimulates H_2S production from EC. In turn, H_2S sulfhydrates the VEGFR2, that increases its dimerization, *trans*-autophosphorylation and activation (73).

Metabolic requirements

Blood vessels transport nutrients to energy-utilizing tissues, and hence, vessels as well as proangiogenic signals can affect metabolism (92). The opposite is also true, where metabolic

node affects vessel growth. For example, in condition of nutrient deprivation, the PGC-1a/ERR-a pathway mediates exercise-induced angiogenesis (93). Similarly, energy deprivation, increases cellular levels of AMP, activating AMPK, which induces VEGF-driven angiogenesis (82). Moreover, FOXO1 transcription factor, unregulated during fasting, promotes endothelial quiescence by antagonizing MYC, which leads to a coordinated reduction in the proliferative and metabolic activity of ECs (94). Interestingly, FOXO is controlled by SIRT1, a member of the sirtuin family of NAD^+-dependent deacylases that mediate the health benefits of dietary restriction and, in the case of SIRT1 can extend lifespan when overexpressed (95, 96).

Recent data indicate that ECs generate up to 85% of their ATP via glycolysis and are thus "addicted" to glucose (**Figure 6**) (80). Importantly, VEGF stimulates glycolysis. On the other hand, the loss of the glycolytic activator PFKFB3 in ECs impaired filopodia/lamellipodia, migration and ultimately vessel formation (**Figure 5B**). Despite the significantly lower energy yield per molecule of glucose via glycolysis (2 ATP) vs. oxidative metabolism (34 ATP), glycolysis offers other advantages to ECs. For instance, anaerobic glucose metabolism enables ECs to vascularize avascular anoxic tissues, an activity that would not be possible if they would rely primarily on oxidative glucose metabolism.

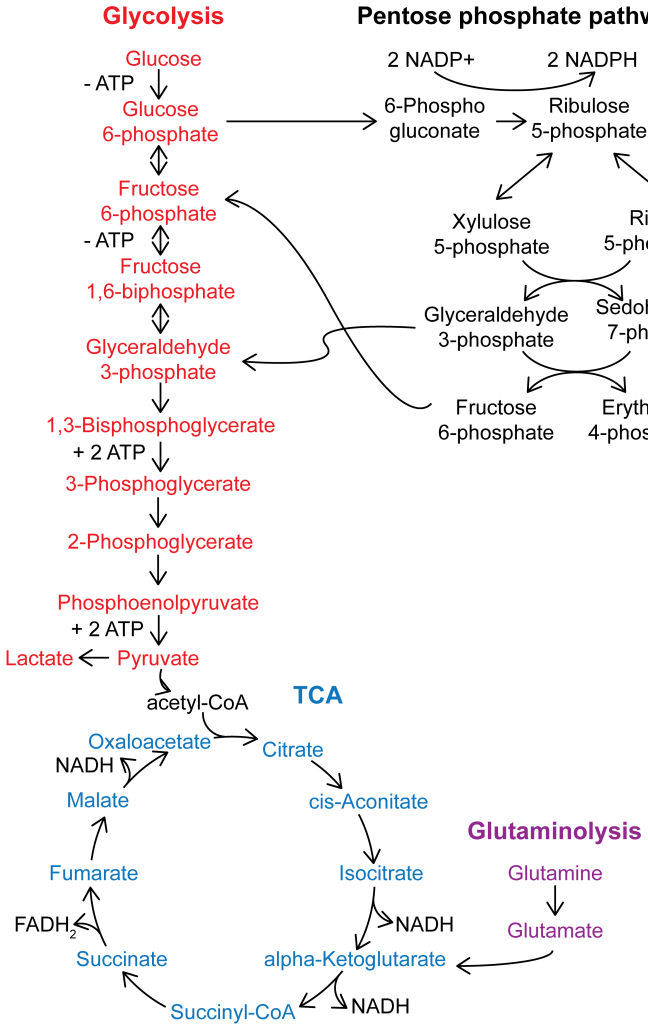

Figure 6: Overview of general metabolism.

Furthermore, glycolysis can generate more molecules of ATP in a shorter time span as compared to oxidative metabolism, thus rapidly providing ECs with the necessary energy to sprout and form new vessels, and thereby quickly restore oxygen supply to the surrounding tissue.

In normal conditions, fatty acid β-oxidation (FAO) contributes to less than 5% of the total amount of ATP in ECs (97). Surprisingly, new data demonstrated that FAO is also essential for de novo nucleotide synthesis and angiogenesis (98). Carnitine palmitoyltransferase 1 (CPT1) controls the transfer of long-chain fatty acids into the mitochondria, where they are oxidized, and is the rate-controlling step of FAO. In ECs, CPT1A silencing reduced FAO and impaired de novo synthesis of deoxyribonucleotides for DNA replication. Subsequently, vessel sprouting was reduced due to decreased EC proliferation. By contrast, CPT1A knock down did not affect EC migration or motility. Finally, in mice, pharmacological CPT1 blockade inhibited pathological ocular angiogenesis (97, 98).

References

1. Fontana L, Partridge L, Longo VD. Extending healthy life span--from yeast to humans. Science. 2010;328(5976):321-6.
2. Speakman JR, Mitchell SE. Caloric restriction. Mol Aspects Med. 2011;32(3):159-221.
3. Sumimoto R, Southard JH, Belzer FO. Livers from fasted rats acquire resistance to warm and cold ischemia injury. Transplantation. 1993;55(4):728-32.
4. Peng W, Robertson L, Gallinetti J, Mejia P, Vose S, Charlip A, et al. Surgical stress resistance induced by single amino acid deprivation requires Gcn2 in mice. Sci Transl Med. 2012;4(118):118ra11.
5. Mitchell JR, Verweij M, Brand K, van de Ven M, Goemaere N, van den Engel S, et al. Short-term dietary restriction and fasting precondition against ischemia reperfusion injury in mice. Aging Cell. 2010;9(1):40-53.
6. Varendi K, Airavaara M, Anttila J, Vose S, Planken A, Saarma M, et al. Short-term preoperative dietary restriction is neuroprotective in a rat focal stroke model. PLoS One. 2014;9(4):e93911.
7. Mauro CR, Tao M, Yu P, Treviño-Villerreal JH, Longchamp A, Kristal BS, et al. Preoperative dietary restriction reduces intimal hyperplasia and protects from ischemia-reperfusion injury. J Vasc Surg. 2014.
8. Levine ME, Suarez JA, Brandhorst S, Balasubramanian P, Cheng CW, Madia F, et al. Low protein intake is associated with a major reduction in IGF-1, cancer, and overall mortality in the 65 and younger but not older population. Cell Metab. 2014;19(3):407-17.
9. Hine C, Kim HJ, Zhu Y, Harputlugil E, Longchamp A, Matos MS, et al. Hypothalamic-Pituitary Axis Regulates Hydrogen Sulfide Production. Cell Metab. 2017;25(6):1320-33.e5.
10. Longchamp A, Harputlugil E, Corpataux JM, Ozaki CK, Mitchell JR. Is Overnight Fasting before Surgery Too Much or Not Enough? How Basic Aging Research Can Guide Preoperative Nutritional Recommendations to Improve Surgical Outcomes: A Mini-Review. Gerontology. 2017;63(3):228-37.
11. Harputlugil E, Hine C, Vargas D, Robertson L, Manning BD, Mitchell JR. The TSC complex is required for the benefits of dietary protein restriction on stress resistance in vivo. Cell Rep. 2014;8(4):1160-70.
12. Robertson LT, Treviño-Villarreal JH, Mejia P, Grondin Y, Harputlugil E, Hine C, et al. Protein and Calorie Restriction Contribute Additively to Protection from Renal Ischemia Reperfusion Injury Partly via Leptin Reduction in Male Mice. J Nutr. 2015.
13. Orentreich N, Matias JR, DeFelice A, Zimmerman JA. Low methionine ingestion by rats extends life span. J Nutr. 1993;123(2):269-74.
14. Elshorbagy AK, Valdivia-Garcia M, Mattocks DA, Plummer JD, Smith AD, Drevon CA, et al. Cysteine supplementation reverses methionine restriction effects on rat adiposity: significance of stearoyl-coenzyme A desaturase. J Lipid Res. 2011;52(1):104-12.
15. Ruckenstuhl C, Netzberger C, Entfellner I, Carmona-Gutierrez D, Kickenweiz T, Stekovic S, et al. Lifespan extension by methionine restriction requires autophagy-dependent vacuolar acidification. PLoS Genet. 2014;10(5):e1004347.
16. Troen AM, French EE, Roberts JF, Selhub J, Ordovas JM, Parnell LD, et al. Lifespan modification by glucose and methionine in Drosophila melanogaster fed a chemically defined diet. Age (Dordr). 2007;29(1):29-39.

17. Cabreiro F, Au C, Leung KY, Vergara-Irigaray N, Cochemé HM, Noori T, et al. Metformin retards aging in C. elegans by altering microbial folate and methionine metabolism. Cell. 2013;153(1):228-39.
18. Miller DL, Roth MB. Hydrogen sulfide increases thermotolerance and lifespan in Caenorhabditis elegans. Proc Natl Acad Sci U S A. 2007;104(51):20618-22.
19. Thivat E, Durando X, Demidem A, Farges MC, Rapp M, Cellarier E, et al. A methionine-free diet associated with nitrosourea treatment down-regulates methylguanine-DNA methyl transferase activity in patients with metastatic cancer. Anticancer Res. 2007;27(4C):2779-83.
20. Lees EK, Król E, Grant L, Shearer K, Wyse C, Moncur E, et al. Methionine restriction restores a younger metabolic phenotype in adult mice with alterations in fibroblast growth factor 21. Aging Cell. 2014;13(5):817-27.
21. Lees EK, Krol E, Shearer K, Mody N, Gettys TW, Delibegovic M. Effects of hepatic protein tyrosine phosphatase 1B and methionine restriction on hepatic and whole-body glucose and lipid metabolism in mice. Metabolism. 2015;64(2):305-14.
22. Grandison RC, Piper MD, Partridge L. Amino-acid imbalance explains extension of lifespan by dietary restriction in Drosophila. Nature. 2009;462(7276):1061-4.
23. Hine C, Mitchell JR. Calorie restriction and methionine restriction in control of endogenous hydrogen sulfide production by the transsulfuration pathway. Exp Gerontol. 2015;68:26-32.
24. Hine C, Harputlugil E, Zhang Y, Ruckenstuhl C, Lee BC, Brace L, et al. Endogenous hydrogen sulfide production is essential for dietary restriction benefits. Cell. 2015;160(1-2):132-44.
25. Efeyan A, Comb WC, Sabatini DM. Nutrient-sensing mechanisms and pathways. Nature. 2015;517(7534):302-10.
26. Wek SA, Zhu S, Wek RC. The histidyl-tRNA synthetase-related sequence in the eIF-2 alpha protein kinase GCN2 interacts with tRNA and is required for activation in response to starvation for different amino acids. Mol Cell Biol. 1995;15(8):4497-506.
27. Ramirez M, Wek RC, Hinnebusch AG. Ribosome association of GCN2 protein kinase, a translational activator of the GCN4 gene of Saccharomyces cerevisiae. Mol Cell Biol. 1991;11(6):3027-36.
28. Wek RC, Jackson BM, Hinnebusch AG. Juxtaposition of domains homologous to protein kinases and histidyl-tRNA synthetases in GCN2 protein suggests a mechanism for coupling GCN4 expression to amino acid availability. Proc Natl Acad Sci U S A. 1989;86(12):4579-83.
29. Zhu S, Wek RC. Ribosome-binding domain of eukaryotic initiation factor-2 kinase GCN2 facilitates translation control. J Biol Chem. 1998;273(3):1808-14.
30. Gallinetti J, Harputlugil E, Mitchell JR. Amino acid sensing in dietary-restriction-mediated longevity: roles of signal-transducing kinases GCN2 and TOR. Biochem J. 2013;449(1):1-10.
31. Grallert B, Boye E. GCN2, an old dog with new tricks. Biochem Soc Trans. 2013;41(6):1687-91.
32. Zaborske JM, Narasimhan J, Jiang L, Wek SA, Dittmar KA, Freimoser F, et al. Genome-wide analysis of tRNA charging and activation of the eIF2 kinase Gcn2p. J Biol Chem. 2009;284(37):25254-67.

33. Yang X, Matsuda K, Bialek P, Jacquot S, Masuoka HC, Schinke T, et al. ATF4 is a substrate of RSK2 and an essential regulator of osteoblast biology; implication for Coffin-Lowry Syndrome. Cell. 2004;117(3):387-98.
34. Harding HP, Zhang Y, Zeng H, Novoa I, Lu PD, Calfon M, et al. An integrated stress response regulates amino acid metabolism and resistance to oxidative stress. Mol Cell. 2003;11(3):619-33.
35. Dickhout JG, Carlisle RE, Jerome DE, Mohammed-Ali Z, Jiang H, Yang G, et al. Integrated stress response modulates cellular redox state via induction of cystathionine γ-lyase: cross-talk between integrated stress response and thiol metabolism. J Biol Chem. 2012;287(10):7603-14.
36. Li W, Miller RA. Elevated ATF4 function in fibroblasts and liver of slow-aging mutant mice. J Gerontol A Biol Sci Med Sci. 2015;70(3):263-72.
37. Kubota H, Obata T, Ota K, Sasaki T, Ito T. Rapamycin-induced translational derepression of GCN4 mRNA involves a novel mechanism for activation of the eIF2 alpha kinase GCN2. J Biol Chem. 2003;278(23):20457-60.
38. Sundrud MS, Koralov SB, Feuerer M, Calado DP, Kozhaya AE, Rhule-Smith A, et al. Halofuginone inhibits TH17 cell differentiation by activating the amino acid starvation response. Science. 2009;324(5932):1334-8.
39. Zoncu R, Efeyan A, Sabatini DM. mTOR: from growth signal integration to cancer, diabetes and ageing. Nat Rev Mol Cell Biol. 2011;12(1):21-35.
40. Jewell JL, Russell RC, Guan KL. Amino acid signalling upstream of mTOR. Nat Rev Mol Cell Biol. 2013;14(3):133-9.
41. Dibble CC, Elis W, Menon S, Qin W, Klekota J, Asara JM, et al. TBC1D7 is a third subunit of the TSC1-TSC2 complex upstream of mTORC1. Mol Cell. 2012;47(4):535-46.
42. Dibble CC, Manning BD. Signal integration by mTORC1 coordinates nutrient input with biosynthetic output. Nat Cell Biol. 2013;15(6):555-64.
43. Saxton RA, Knockenhauer KE, Wolfson RL, Chantranupong L, Pacold ME, Wang T, et al. Structural basis for leucine sensing by the Sestrin2-mTORC1 pathway. Science. 2016;351(6268):53-8.
44. Wolfson RL, Chantranupong L, Saxton RA, Shen K, Scaria SM, Cantor JR, et al. Sestrin2 is a leucine sensor for the mTORC1 pathway. Science. 2016;351(6268):43-8.
45. Chantranupong L, Scaria SM, Saxton RA, Gygi MP, Shen K, Wyant GA, et al. The CASTOR Proteins Are Arginine Sensors for the mTORC1 Pathway. Cell. 2016;165(1):153-64.
46. Chantranupong L, Wolfson RL, Sabatini DM. Nutrient-sensing mechanisms across evolution. Cell. 2015;161(1):67-83.
47. Sancak Y, Peterson TR, Shaul YD, Lindquist RA, Thoreen CC, Bar-Peled L, et al. The Rag GTPases bind raptor and mediate amino acid signaling to mTORC1. Science. 2008;320(5882):1496-501.
48. Sancak Y, Bar-Peled L, Zoncu R, Markhard AL, Nada S, Sabatini DM. Ragulator-Rag complex targets mTORC1 to the lysosomal surface and is necessary for its activation by amino acids. Cell. 2010;141(2):290-303.
49. Harrison DE, Strong R, Sharp ZD, Nelson JF, Astle CM, Flurkey K, et al. Rapamycin fed late in life extends lifespan in genetically heterogeneous mice. Nature. 2009;460(7253):392-5.

50. Lamming DW, Ye L, Katajisto P, Goncalves MD, Saitoh M, Stevens DM, et al. Rapamycin-induced insulin resistance is mediated by mTORC2 loss and uncoupled from longevity. Science. 2012;335(6076):1638-43.
51. Selman C, Tullet JM, Wieser D, Irvine E, Lingard SJ, Choudhury AI, et al. Ribosomal protein S6 kinase 1 signaling regulates mammalian life span. Science. 2009;326(5949):140-4.
52. Waldner M, Fantus D, Solari M, Thomson AW. New perspectives on mTOR inhibitors (rapamycin, rapalogs and TORKinibs) in transplantation. Br J Clin Pharmacol. 2016.
53. Hardie DG, Ross FA, Hawley SA. AMPK: a nutrient and energy sensor that maintains energy homeostasis. Nat Rev Mol Cell Biol. 2012;13(4):251-62.
54. Lempiäinen J, Finckenberg P, Levijoki J, Mervaala E. AMPK activator AICAR ameliorates ischaemia reperfusion injury in the rat kidney. Br J Pharmacol. 2012;166(6):1905-15.
55. Shinmura K, Tamaki K, Saito K, Nakano Y, Tobe T, Bolli R. Cardioprotective effects of short-term caloric restriction are mediated by adiponectin via activation of AMP-activated protein kinase. Circulation. 2007;116(24):2809-17.
56. Yang G, Wu L, Jiang B, Yang W, Qi J, Cao K, et al. H2S as a physiologic vasorelaxant: hypertension in mice with deletion of cystathionine gamma-lyase. Science. 2008;322(5901):587-90.
57. Paul BD, Snyder SH. H_2S signalling through protein sulfhydration and beyond. Nat Rev Mol Cell Biol. 2012;13(8):499-507.
58. Blackstone E, Morrison M, Roth MB. H2S induces a suspended animation-like state in mice. Science. 2005;308(5721):518.
59. Cai WJ, Wang MJ, Moore PK, Jin HM, Yao T, Zhu YC. The novel proangiogenic effect of hydrogen sulfide is dependent on Akt phosphorylation. Cardiovasc Res. 2007;76(1):29-40.
60. Polhemus DJ, Kondo K, Bhushan S, Bir SC, Kevil CG, Murohara T, et al. Hydrogen sulfide attenuates cardiac dysfunction after heart failure via induction of angiogenesis. Circ Heart Fail. 2013;6(5):1077-86.
61. Shi YX, Chen Y, Zhu YZ, Huang GY, Moore PK, Huang SH, et al. Chronic sodium hydrosulfide treatment decreases medial thickening of intramyocardial coronary arterioles, interstitial fibrosis, and ROS production in spontaneously hypertensive rats. Am J Physiol Heart Circ Physiol. 2007;293(4):H2093-100.
62. Zhao X, Zhang LK, Zhang CY, Zeng XJ, Yan H, Jin HF, et al. Regulatory effect of hydrogen sulfide on vascular collagen content in spontaneously hypertensive rats. Hypertens Res. 2008;31(8):1619-30.
63. Wang Y, Zhao X, Jin H, Wei H, Li W, Bu D, et al. Role of hydrogen sulfide in the development of atherosclerotic lesions in apolipoprotein E knockout mice. Arterioscler Thromb Vasc Biol. 2009;29(2):173-9.
64. Zanardo RC, Brancaleone V, Distrutti E, Fiorucci S, Cirino G, Wallace JL. Hydrogen sulfide is an endogenous modulator of leukocyte-mediated inflammation. FASEB J. 2006;20(12):2118-20.
65. Chen YH, Yao WZ, Geng B, Ding YL, Lu M, Zhao MW, et al. Endogenous hydrogen sulfide in patients with COPD. Chest. 2005;128(5):3205-11.
66. Islam KN, Polhemus DJ, Donnarumma E, Brewster LP, Lefer DJ. Hydrogen Sulfide Levels and Nuclear Factor-Erythroid 2-Related Factor 2 (NRF2) Activity Are Attenuated in the Setting of Critical Limb Ischemia (CLI). J Am Heart Assoc. 2015;4(5).

67. Beard RS, Bearden SE. Vascular complications of cystathionine β-synthase deficiency: future directions for homocysteine-to-hydrogen sulfide research. Am J Physiol Heart Circ Physiol. 2011;300(1):H13-26.
68. Wang R. Physiological implications of hydrogen sulfide: a whiff exploration that blossomed. Physiol Rev. 2012;92(2):791-896.
69. Olson KR. Is hydrogen sulfide a circulating "gasotransmitter" in vertebrate blood? Biochim Biophys Acta. 2009;1787(7):856-63.
70. Bearden SE, Beard RS, Pfau JC. Extracellular transsulfuration generates hydrogen sulfide from homocysteine and protects endothelium from redox stress. Am J Physiol Heart Circ Physiol. 2010;299(5):H1568-76.
71. Bian JS, Yong QC, Pan TT, Feng ZN, Ali MY, Zhou S, et al. Role of hydrogen sulfide in the cardioprotection caused by ischemic preconditioning in the rat heart and cardiac myocytes. J Pharmacol Exp Ther. 2006;316(2):670-8.
72. Altaany Z, Ju Y, Yang G, Wang R. The coordination of S-sulfhydration, S-nitrosylation, and phosphorylation of endothelial nitric oxide synthase by hydrogen sulfide. Sci Signal. 2014;7(342):ra87.
73. Tao BB, Liu SY, Zhang CC, Fu W, Cai WJ, Wang Y, et al. VEGFR2 functions as an H2S-targeting receptor protein kinase with its novel Cys1045-Cys1024 disulfide bond serving as a specific molecular switch for hydrogen sulfide actions in vascular endothelial cells. Antioxid Redox Signal. 2013;19(5):448-64.
74. Gao XH, Krokowski D, Guan BJ, Bederman I, Majumder M, Parisien M, et al. Quantitative H2S-mediated protein sulfhydration reveals metabolic reprogramming during the integrated stress response. Elife. 2015;4:e10067.
75. Mustafa AK, Gadalla MM, Sen N, Kim S, Mu W, Gazi SK, et al. H2S signals through protein S-sulfhydration. Sci Signal. 2009;2(96):ra72.
76. Módis K, Coletta C, Erdélyi K, Papapetropoulos A, Szabo C. Intramitochondrial hydrogen sulfide production by 3-mercaptopyruvate sulfurtransferase maintains mitochondrial electron flow and supports cellular bioenergetics. FASEB J. 2013;27(2):601-11.
77. Olson KR, Deleon ER, Gao Y, Hurley K, Sadauskas V, Batz C, et al. Thiosulfate: a readily accessible source of hydrogen sulfide in oxygen sensing. Am J Physiol Regul Integr Comp Physiol. 2013;305(6):R592-603.
78. Carmeliet P, Jain RK. Principles and mechanisms of vessel normalization for cancer and other angiogenic diseases. Nat Rev Drug Discov. 2011;10(6):417-27.
79. Palmer RM, Ferrige AG, Moncada S. Nitric oxide release accounts for the biological activity of endothelium-derived relaxing factor. Nature. 1987;327(6122):524-6.
80. De Bock K, Georgiadou M, Schoors S, Kuchnio A, Wong BW, Cantelmo AR, et al. Role of PFKFB3-driven glycolysis in vessel sprouting. Cell. 2013;154(3):651-63.
81. Rivard A, Fabre JE, Silver M, Chen D, Murohara T, Kearney M, et al. Age-dependent impairment of angiogenesis. Circulation. 1999;99(1):111-20.
82. Potente M, Gerhardt H, Carmeliet P. Basic and therapeutic aspects of angiogenesis. Cell. 2011;146(6):873-87.
83. Liu Y, Cox SR, Morita T, Kourembanas S. Hypoxia regulates vascular endothelial growth factor gene expression in endothelial cells. Identification of a 5' enhancer. Circ Res. 1995;77(3):638-43.

84. Carmeliet P, Jain RK. Molecular mechanisms and clinical applications of angiogenesis. Nature. 2011;473(7347):298-307.
85. Nagy JA, Dvorak AM, Dvorak HF. VEGF-A and the induction of pathological angiogenesis. Annu Rev Pathol. 2007;2:251-75.
86. Mace KA, Yu DH, Paydar KZ, Boudreau N, Young DM. Sustained expression of Hif-1alpha in the diabetic environment promotes angiogenesis and cutaneous wound repair. Wound Repair Regen. 2007;15(5):636-45.
87. Greenhalgh DG. Wound healing and diabetes mellitus. Clin Plast Surg. 2003;30(1):37-45.
88. Buysschaert I, Schmidt T, Roncal C, Carmeliet P, Lambrechts D. Genetics, epigenetics and pharmaco-(epi)genomics in angiogenesis. J Cell Mol Med. 2008;12(6B):2533-51.
89. Shibuya M. Vascular Endothelial Growth Factor (VEGF) and Its Receptor (VEGFR) Signaling in Angiogenesis: A Crucial Target for Anti- and Pro-Angiogenic Therapies. Genes Cancer. 2011;2(12):1097-105.
90. Takahashi T, Ueno H, Shibuya M. VEGF activates protein kinase C-dependent, but Ras-independent Raf-MEK-MAP kinase pathway for DNA synthesis in primary endothelial cells. Oncogene. 1999;18(13):2221-30.
91. Takahashi T, Yamaguchi S, Chida K, Shibuya M. A single autophosphorylation site on KDR/Flk-1 is essential for VEGF-A-dependent activation of PLC-gamma and DNA synthesis in vascular endothelial cells. EMBO J. 2001;20(11):2768-78.
92. Fraisl P, Mazzone M, Schmidt T, Carmeliet P. Regulation of angiogenesis by oxygen and metabolism. Dev Cell. 2009;16(2):167-79.
93. Arany Z, Foo SY, Ma Y, Ruas JL, Bommi-Reddy A, Girnun G, et al. HIF-independent regulation of VEGF and angiogenesis by the transcriptional coactivator PGC-1alpha. Nature. 2008;451(7181):1008-12.
94. Wilhelm K, Happel K, Eelen G, Schoors S, Oellerich MF, Lim R, et al. FOXO1 couples metabolic activity and growth state in the vascular endothelium. Nature. 2016;529(7585):216-20.
95. Haigis MC, Sinclair DA. Mammalian sirtuins: biological insights and disease relevance. Annu Rev Pathol. 2010;5:253-95.
96. Satoh A, Brace CS, Rensing N, Cliften P, Wozniak DF, Herzog ED, et al. Sirt1 extends life span and delays aging in mice through the regulation of Nk2 homeobox 1 in the DMH and LH. Cell Metab. 2013;18(3):416-30.
97. Cantelmo AR, Brajic A, Carmeliet P. Endothelial Metabolism Driving Angiogenesis: Emerging Concepts and Principles. Cancer J. 2015;21(4):244-9.
98. Schoors S, Bruning U, Missiaen R, Queiroz KC, Borgers G, Elia I, et al. Fatty acid carbon is essential for dNTP synthesis in endothelial cells. Nature. 2015;520(7546):192-7.

AIM OF THE STUDY

Dietary restriction (DR), defined as reduced food intake without malnutrition is best known for extending lifespan in experimental model organisms, but also increases resistance to a variety of clinically relevant stressors, including those associated with surgery. Recently we discovered that hydrogen sulfide (H_2S) is increased upon DR in the liver and plays an essential role in mediating DR benefits the context of surgical stress (Chapter 1).

Angiogenesis, the formation of new blood vessels by endothelial cells (ECs), is an adaptive response to nutrient/oxygen deprivation orchestrated by vascular endothelial growth factor (VEGF) during ischemia (e.g. vessel occlusion or tumorigenesis) or exercise. Hypoxia is the best-understood trigger of VEGF expression via the transcription factor HIF1a. Nutrient deprivation is inseparable from hypoxia upon ischemia, yet its role in angiogenesis is poorly characterized. Interestingly, H_2S was shown by others to promote angiogenesis. In the second part of this work, we found that restricting the intake of dietary sulfur-containing amino acids methionine and cysteine promote angiogenesis. We then tested the functional consequences of increased capillary density in rodent preclinical models. We have made progress towards understanding the underlying molecular mechanisms, including the role of upstream amino acid-sensing pathways and downstream effector molecules such as hydrogen sulfide. We also worked to elucidate practical methods for increasing angiogenesis through dietary methionine restriction in the shortest time period and with the minimal restriction of nutrients, with the long-term goal of translating such benefits to clinically relevant applications (Chapter 2).

Finally, H_2S that is endogenously produced gas, with broader protective effects on the vascular system. H_2S can also be measured in blood serum, but the biological significance or predictive value with regard to vascular health is unknown. Using lead acetate methods and mass spectrometry we quantified H_2S in patients undergoing vascular surgery including carotid endarterectomy (n=49), open lower extremity arterial revascularization (n=44) or major leg

amputation (n=22) as well as in 20 control patients. We found that control patients that did not require cardiovascular surgery had the highest serum H_2S production capacity and free Sulfur. Moreover, we pre-operative serum H_2S levels predicted post-operative survival (Chapter 3). These date built up on the importance of H_2S in vascular homeostasis. The will serve as basis to develop guidelines for brief DR or pharmacological DR mimetics such as increasing endogenous H_2S production to precondition against the stress and potential complications of surgery.

RESULTS

Chapter 1: Is Overnight Fasting before Surgery Too Much or Not Enough? How Basic Aging Research Can Guide Preoperative Nutritional Recommendations to Improve Surgical Outcomes: A Mini-Review

This work has been published in 2016 in Gerontology

Summary

Dietary restriction (DR) is best known for extending lifespan in experimental model organisms, but also increases resistance to a variety of clinically relevant stressors, including those associated with surgery. Extended periods of DR, lasting months to years, are required for optimal longevity benefits in rodents, but short-term dietary preconditioning (less than 1 week) remarkably protects from acute injury. Here, we discuss recent advances in our understanding of the mechanistic basis of short-term DR and fasting in the context of surgical stress resistance, including upstream amino acid sensing by the GCN2 and mTORC1 pathways, and down- stream effector mechanisms including increased insulin-dependent prosurvival signaling and elevated endogenous hydrogen sulfide production. We also review the current trend in preoperative nutrition away from preoperative fasting and towards carbohydrate loading. Finally, we discuss the rationale for the nonmutually exclusive use of brief DR or pharmacological DR mimetics to precondition against the stress and potential complications of surgery.

Experimental Section / Mini-Review

Gerontology

Gerontology
DOI: 10.1159/000453109

Received: May 2, 2016
Accepted: November 7, 2016
Published online: January 5, 2017

Is Overnight Fasting before Surgery Too Much or Not Enough? How Basic Aging Research Can Guide Preoperative Nutritional Recommendations to Improve Surgical Outcomes: A Mini-Review

Alban Longchamp[a, b] Eylul Harputlugil[a] Jean-Marc Corpataux[c]
C. Keith Ozaki[b] James R. Mitchell[a]

[a]Department of Genetics and Complex Diseases, Harvard T.H. Chan School of Public Health, and [b]Department of Surgery and the Heart and Vascular Center, Brigham and Women's Hospital and Harvard Medical School, Boston, MA, USA; [c]Department of Vascular Surgery, Centre Hospitalier Universitaire Vaudois, and Lausanne University, Lausanne, Switzerland

Key Words
Dietary restriction · Surgery · Surgical stress · Nutrition · Hydrogen sulfide · Amino acid sensing · Ischemia · Longevity · Enhanced recovery after surgery

Abstract
Dietary restriction (DR) is best known for extending lifespan in experimental model organisms, but also increases resistance to a variety of clinically relevant stressors, including those associated with surgery. Extended periods of DR, lasting months to years, are required for optimal longevity benefits in rodents, but short-term dietary preconditioning (less than 1 week) remarkably protects from acute injury. Here, we discuss recent advances in our understanding of the mechanistic basis of short-term DR and fasting in the context of surgical stress resistance, including upstream amino acid sensing by the GCN2 and mTORC1 pathways, and downstream effector mechanisms including increased insulin-dependent prosurvival signaling and elevated endogenous hydrogen sulfide production. We also review the current trend in preoperative nutrition away from preoperative fasting and towards carbohydrate loading. Finally, we discuss the rationale for the nonmutually exclusive use of brief DR or pharmacological DR mimetics to precondition against the stress and potential complications of surgery.

Introduction

In 1935, Clive McCay reported that dietary restriction (DR), or reduced food intake without malnutrition, extends lifespan of laboratory rats [1, 2]. Since that time, longevity extension by DR has been demonstrated in numerous experimental organisms from yeast to non-human primates [1]. DR is thought to extend longevity by reducing the rate of aging, making it a key tool in aging research. However, since maximal lifespan extension requires long-term adhesion, antigeronic clinical applications have never been considered feasible due to the obvious difficulties associated with long-term voluntary food restriction. Indeed, while prospective clinical trials show that DR can reduce risk factors for diabetes, cardiovascular disease, and cancer, they also highlight problems with long-term compliance [3, 4].

KARGER

E-Mail karger@karger.com
www.karger.com/ger

0304–324X/17/0000–0000$39.50/0

James R. Mitchell
Department of Genetics and Complex Diseases
Harvard T.H. Chan School of Public Health
655 Huntington Ave., Building 2-121, Boston, MA 02115 (USA)
E-Mail jmitchel@hsph.harvard.edu

Fortunately, DR confers other important benefits that do not require long periods of food restriction, including increased resistance to multiple forms of acute stress. One of the biggest planned stressors many people will face in their life is that of major elective surgery, which carries inherent risks of complications, such as perioperative stroke and myocardial infarction (MI).

A novel concept in surgical risk mitigation emerging from basic research on DR and aging is dietary preconditioning, or short-term DR lasting one week or less prior to surgery [5]. In rodent models of surgical stress ranging from ischemia reperfusion injury (IRI) to vascular restenosis (intimal hyperplasia), short-term DR or fasting before surgery, followed by a return to normal food intake after surgery, leads to improved outcomes [6–10].

Here, we will provide an update on recent advances in our understanding of the nutritional basis, nutrient sensing mechanisms, and downstream effectors of protection by short-term DR and fasting in preclinical models of surgical stress. Finally, we will discuss the translational potential of DR and DR mimetics before surgery in relation to current practices.

The Surgical Stress Response and Associated Complications

Surgery is an invasive medical intervention involving an incision, with major surgery typically describing procedures in which a body cavity is entered. Like many types of acute injury, surgery perturbs metabolic and immune homeostasis through effects on afferent (autonomic and sympathetic) nerve input from the area of trauma leading to local and systemic catecholamine release, increased levels of proinflammatory acute phase reactants, metabolic adaptations including glycogen mobilization, and vascular changes including vasoconstriction and increased heart rate. Parallel activation of the hypothalamic-anterior pituitary-adrenomedullary axis promotes release of cortisol from the adrenal cortex, resulting in a partially counterbalancing response characterized by protein and fat mobilization, immunosuppression, and dampening of the action of anabolic hormones such as insulin and testosterone [11]. Together, these effects result in a transient increase in metabolic rate that scales in amplitude and duration with the severity of the insult (Fig. 1a).

From an evolutionary standpoint, the selective advantage conferred by these coordinated stress responses likely involves staunching hemorrhage and redirecting stored energy to immune function and tissue repair to promote survival following acute injury. However, in any given surgical patient, such vasoconstrictive, prothrombotic and proinflammatory responses can also precipitate ischemia (inadequate blood supply), which underlies a range of surgical complications such as renal dysfunction, myocardial ischemia or stroke.

Risk assessments prior to surgery focus on the potential for a perioperative major adverse cardiovascular event (MACE), a composite of potential negative outcomes including MI and death (either MI-related or all-cause mortality), but also sometimes stroke or the need for urgent revascularization [12]. Estimations of risk, including the revised cardiac risk index (RCRI) or the American College of Surgeons National Surgical Quality Improvement Program risk (ACS-NSQIP), are based on patient characteristics such as age, renal function, metabolic status, cardiac and neurological history, and results of physical examination prior to surgery, but also on the type of surgery performed. For example, the majority of cardiac surgeries are performed on an ischemic, nonbeating heart achieved by cross-clamping the aorta (thus interrupting coronary artery perfusion), with systemic blood circulation achieved via extracorporeal circulation (ECC). In addition to IRI to the heart, ECC itself causes a systemic inflammatory response leading to activation of circulating leukocytes and a prothrombic state potentially contributing to cardiac dysfunction [13, 14].

Surgery also carries a risk of non-MACE complications specific to a particular procedure. For example, complications of open abdominal aortic aneurysm repair include limb, pelvic, mesenteric and spinal ischemia, while repair of aortic lesions involving the renal arteries carries increased risk of renal failure (due to inflow artery cross-clamping) which directly relates to the ischemic time [15]. Interestingly, while risk assessment is standard practice in deciding if the benefits of a given surgery outweigh its risks, interventional prophylactic approaches to reduce patient-based risk factors prior to surgery are not.

Short-Term DR Preconditions against Surgical Stress in Rodent Models

The term DR is used here to describe a variety of dietary regimens with overlapping functional benefits including extended longevity, improved metabolic fitness and increased stress resistance. While the nutritional basis of DR is described in more detail below, such regimens can generally be divided into two categories. The first involves calorie restriction, for example by daily restriction

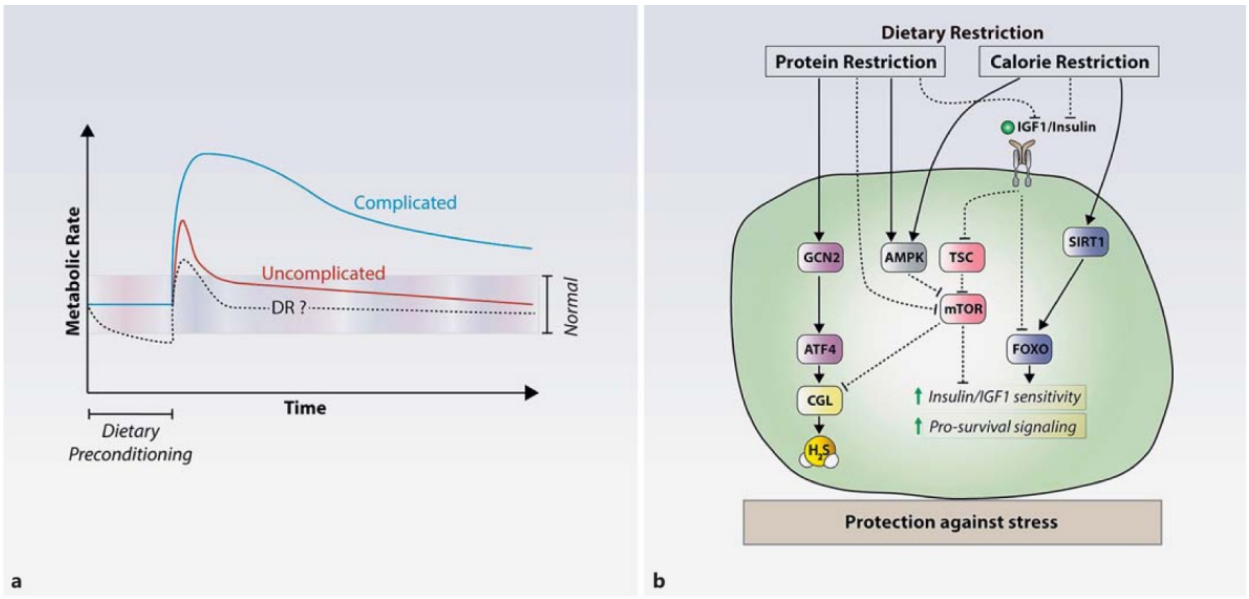

Fig. 1. Potential effects of DR on surgical stress resistance. **a** Model of the metabolic response to uncomplicated elective surgery vs. surgery in which complications such as MI, renal failure, or stroke occur. Also modeled is how DR affects metabolic rate prior to surgery as well as the metabolic response to surgical stress. **b** Cellular mechanisms of protection by dietary preconditioning. Dietary protein or essential amino acid restriction activates general control nonderepressible 2 (GCN2), AMP-activated protein kinase (AMPK), and sirtuin 1 (SIRT1) and represses mammalian target of rapamycin complex 1 (mTORC1) nutrient/energy sensing signal transduction pathways, resulting in increased hydrogen sulfide (H_2S) production by the transsulfuration pathway enzyme cystathionine γ-lyase (CGL) and improved insulin/insulin-like growth factor 1 (IGF-1) receptor sensitivity. H_2S can protect against acute stress via numerous mechanisms including direct antioxidant action, while improved insulin/IGF-1 sensitivity allow for increased prosurvival signaling, contributing to overall stress resistance. ATF4, activating transcription factor 4; FOXO, forkhead box O1; ROS, reactive oxygen species.

of food intake or periods of intermittent fasting. The second involves special diets reduced in specific nutrients such as protein, but fed on an ad libitum (unlimited) basis without enforced food/calorie restriction. Because DR and starvation are by definition mutually exclusive states, the duration of treatment is of critical importance, particularly in cases involving severe food restriction or diets lacking essential nutrients such as protein or individual essential amino acids.

As with any regimen necessitating dietary alterations, duration is also of critical importance when considering practical translation to the clinic. For the purposes of this review, we define short-term as a week or less, and long-term as greater than 1 week. Historically, DR benefits including life span extension, improved metabolic fitness and even decreased injury in preclinical models of surgical stress including IRI to heart or brain [16, 17] were originally described in association with long-term DR regimens lasting months to years and thus with little practical translational potential. However, more recent experiments designed to test the timing of onset of DR benefits make it clear that rapid onset is an evolutionarily conserved property of DR-mediated stress resistance [18]. For example, 2–4 days of water-only fasting is sufficient for protection in models of organ injury including cold IRI, a model of organ storage prior to reattachment that is relevant to organ transplantation [19]. Similarly, 6–7 days of reduced total food or isolated protein intake protects against warm IRI to brain, liver or kidney [8, 10, 20] relevant both to surgical procedures involving intentional interruption of blood flow, as well as unintended surgical complications including heart attack or stroke. Importantly, short-term protein restriction or fasting also protect from chronic re-occlusive vascular wall adaptations, such as intimal hyperplasia, which can result in recurrent end-organ ischemia, loss of limb, reduced brain function, or even death [7]. Because the etiology of hemodynamically-driven intimal hyperplasia is distinct from IRI, this finding demonstrates the ability of

short-term DR to protect against multiple different kinds of surgery-associated acute and chronic complications.

While the protective effects of short periods of DR prior to surgery are becoming evident in preclinical models of surgical stress as described above, still very little is known about the ability of DR after injury (postconditioning) to confer any protection, with some studies showing no effect [8] and others some efficacy [21]. Additionally, the relevance of refeeding after surgery in mice that are restricted prior to surgery is unknown. Finally, whether the integrated neuroendocrine/metabolic response to surgery is dampened by dietary preconditioning, and to what extent this affects surgical outcome, remains to be examined (Fig. 1a).

Nutritional Requirements for Dietary Preconditioning against Surgical Stress

Classic DR regimens, often referred to as caloric restriction, involve restriction of total food intake resulting in proportional reduction of calories in the form of carbohydrates, fats, and protein. In experimental rodents, the amount of restriction leading to longevity benefits is typically in the range of 30–40%, although benefits have been observed up to near the point of starvation around 60% restriction [22]. Logistically, there are a variety of ways to accomplish DR, ranging from daily allotment of a fixed amount of food to alternating periods of fasting and ad libitum food intake, with enforced periods of food restriction as the common denominator.

While protein is equal in caloric content to carbohydrate, restriction of protein (but not sugar or fat) can contribute to dietary preconditioning beyond its caloric value [20, 23]. Although the extension of this finding to longevity has been questioned [24], preconditioning against surgical stress in preclinical models can be leveraged without enforced food restriction by using diets reduced in or lacking protein. This is an important difference when considering clinical translational potential due to the difficulties inherent in enforced restriction of food intake even for short periods of time.

Dietary protein is composed of approximately 20 amino acids present in different ratios depending on the source of protein. Of these, mammals can synthesize adequate amounts of approximately 10 "nonessential" amino acids, while the remaining "essential amino acids" must be obtained from the diet. In many animals including mammals, recent data indicate that the benefits of protein restriction are controlled by the restriction specifically of one or more essential amino acids [20, 25, 26].

Two different experimental approaches have been used to distinguish the contribution of individual or combinations of amino acids to DR benefits. In the first, amino acids are removed and replaced with sucrose or the nonessential amino acid glycine for comparison between two otherwise isocaloric diets. Using this approach, a number of different individual essential amino acids have been shown to confer DR benefits, including tryptophan, leucine, and methionine [20]. One drawback to this approach in rodents is the voluntary reduction in food intake commonly associated with such incomplete or unbalanced diets, which makes it difficult to separate the effects of specific amino acid depletion from those of overall calorie restriction. Future studies are thus required to fully disentangle the effects of amino acid restriction from overall calorie restriction, as well as to rigorously test the relative contributions of each of the 10 essential amino acids, alone or in combination, to the benefits of DR.

A second, complementary approach to assess the role of amino acids in DR benefits independent of their caloric value is to start on a restricted background (e.g., 50% DR) and add back individual or combinations of amino acids. Using this approach, increased longevity and reduced fecundity were shown to be responsive to essential amino acid re-addition in fruit flies, with a particular role for the sulfur-containing essential amino acid, methionine, and downstream effects on insulin signaling [27]. Interestingly, in the context of DR-mediated preconditioning against hepatic IRI in mice, readdition of Met and/or Cys also abrogates benefits in part through reduction of endogenous hydrogen sulfide (H_2S) generation [26]. Whether or not individual amino acids contribute through a common mechanism or independently through amino acid-specific mechanisms remains to be worked out, although examples of both will be provided in the molecular effector mechanisms section below.

It is also important to note that different organs can have different requirements for protection even against the same injury. For example, while in the renal IRI model both protein and calorie restriction contribute additively to organ protection [6], protein restriction alone contributes disproportionately to organ protection against hepatic IRI [23]. Much future work is thus required in order to determine the optimal balance of calories from protein versus sugar and fat, as well as the total calorie intake, for optimal stress resistance, which itself will likely depend on the specific surgery and its associated patient-specific risk factors.

Nutrient-/Energy-Sensing Mechanisms Implicated in Dietary Preconditioning

The ability to sense and adjust to fluctuations in environmental nutrient/energy levels is requisite for life. In mammals, nutrient/energy sensing and neuroendocrine signaling are intricately linked in order to rapidly engage anabolism and storage in times of food excess, or mobilization and catabolism in times of scarcity. In the context of DR, it is thus not surprising that nutrient/energy sensing and hormonal pathways have been implicated in pleiotropic DR benefits [28]. While modulation of key hormonal pathways including growth hormone, insulin/insulin-like growth factors (IGFs), and the fasting hormone FGF21 have all been associated with longevity extension by DR in rodents [29], we will focus on the amino acid and energy-sensing molecules general control nonderepressible 2 (GCN2), mechanistic target of rapamycin complex 1 (mTORC1), AMP-activated kinase (AMPK), and sirtuin-1 (SIRT1) because of their proven involvement specifically in experimental models of surgical stress resistance (Fig. 1b).

GCN2

Dietary deficiency in protein-coding amino acids is intricately linked to modulation of protein translation and stress responses through the GCN2 serine/threonine protein kinase. Typically upon dietary protein starvation or consumption of an imbalanced protein source (e.g., a monodiet consisting of rice is relatively deficient in the essential amino acid lysine), low levels of one or more amino acids promote accumulation of uncharged cognate tRNAs. Uncharged tRNAs directly activate the kinase domain of GCN2, facilitating phosphorylation of the eukaryotic translation initiation factor-α (eIF2α). While this reduces general translation initiation efficiency, it promotes translation of specific transcripts including activating transcription factor 4 (ATF4), and increased expression of target genes involved in nonessential amino acid biosynthesis, amino acid transport, and other stress responses [25]. This cascade of events is described alternately as the amino acid starvation response (specifically when GCN2 phosphorylates eIF2α) or more generally as the integrated stress response when any of the four eIF2α kinases are activated upon different stresses (e.g., PERK/ER stress, HRI/iron stress, PKR/viral infection). Interestingly, elevated ATF4 levels have also been described in liver and isolated fibroblasts of long-lived, stress-resistant rodent models including hypopituitary Snell dwarf mice [30], and are associated with extended longevity upon nutrient deprivation, altered ribosomal function, or rapamycin treatment in yeast [31].

In the context of dietary preconditioning against IRI, GCN2 is required for protection from renal and hepatic IRI induced by dietary tryptophan deficiency [20]. However, GCN2 does not appear to be required for preconditioning by total protein deprivation [6, 23], likely due to redundancy in protein-sensing mechanisms including mTORC1 as described below. GCN2 can also be activated pharmacologically by the proline tRNA synthase inhibitor halofuginone [32], originally described as an antimalarial agent and currently used in humans against scleroderma and in a clinical trial in patients with progressive advanced solid tumors (NCT00027677) [33]. In mice, pretreatment with halofuginone protects against renal IRI in a GCN2-dependent manner [20]. Nonetheless, despite providing proof-of-principle of GCN2 activation as a target for preconditioning against renal injury, the narrow window of efficacy for halofuginone due to on-target toxicity make it a less plausible strategy than DR itself.

mTORC1

While GCN2 can detect the absence of any amino acid, the presence of specific amino acids such as leucine is sensed by the protein complex mTORC1, a serine/threonine kinase that integrates information on amino acid, energy, and growth factor availability in order to effect cell fate decisions regarding anabolism versus catabolism [34, 35]. Amino acids are sensed by mTORC1 via an upstream mechanism involving the Rag family GTPases and a regulatory complex referred to as the Ragulator [36] that anchors mTORC1 at the lysosomal surface.

Hepatic mTORC1 activity is reduced in mice preconditioned on a protein-free diet for 1 week, coinciding with protection against hepatic IRI [23]. Whether this is a direct result of reduced amino acid (leucine) levels, or more likely a reduction of growth factor levels also required for mTORC1 activation, remains to be determined. However consistent with the importance of reduced mTORC1 in dietary preconditioning, liver-specific deletion of the upstream mTORC1 repressor gene TSC1, results in constitutive hepatic mTORC1 activation independent of diet, and prevents protein restriction from preconditioning against hepatic IRI [23]. Interestingly, preconditioning by tryptophan restriction alone does not require the TSC complex, suggesting that different mechanisms might be mediating the effects of individual amino acid and total protein-deficient diets, potentially via parallel action of GCN2 and mTORC1 pathways [23].

Rapamycin (Sirolimus) is a partial mTORC1 inhibitor used in humans to prevent T and B cell-mediated organ transplant rejection, and also as a vascular stent coating to prevent intimal hyperplasia [37]. In mice, long-term rapamycin treatment extends longevity [38, 39], but does not protect mice from hepatic IRI despite reducing hepatic mTORC1 signaling [23]. Thus, in the context of dietary preconditioning, reduced mTORC1 signaling may be necessary but insufficient for protection. Alternately, side effects of rapamycin including reduced insulin sensitivity may have a larger negative impact in the context of hepatic IRI than in longevity extension [38]. Thus, despite having identified 2 amino acid-sensing pathways targetable with pharmacological agents, much work remains to be done in order to understand how to use such agents to successfully mimic the beneficial effects of dietary preconditioning.

AMPK

AMPK is a conserved energy-sensing protein kinase present in all eukaryotes as heterotrimers comprising catalytic α-subunit and regulatory β- and γ-subunits. AMPK is allosterically activated when cellular energy is low via AMP and/or ADP as well as by several upstream kinases. Activation of AMPK promotes energy production by increasing glucose uptake in the short term and facilitating a switch to oxidative metabolism in the long term. It also reduces anabolic mTORC1 signaling by phosphorylating the mTORC1 inhibitor, TSC2. AMPK is activated upon fasting or DR regimens involving enforced food restriction. Somewhat surprisingly, it is also activated upon protein restriction independent of calorie intake [6]. Like mTORC1 signaling with which AMPK is intricately intertwined, this could reflect a change in the growth factor environment induced by protein restriction, resulting in a metabolic state resembling energy deficiency. The essential nature of AMPK function and redundancy in catalytic AMPK subunit genes complicates testing the genetic requirement for AMPK in dietary preconditioning. However, AMPK activation by the allosteric activator 5-aminoimidazole-4-carboxamide ribonucleotide (AICAR) protects against ischemic injury in rats when given at high doses before injury [40]. AMPK activation by the endogenous adipokine adiponectin, which is increased upon DR, is also essential for the cardioprotective effects of DR against MI [41].

SIRT1

Under conditions of nutritional and environmental stress (fasting, DR, and exercise), the NAD+-dependent deacetylase SIRT1 stimulates mitochondrial biogenesis, energy homeostasis and cell survival by regulating the acetylation and activity of transcription factors, including the peroxisome roliferator-activated receptor-γ coactivator-1α (PGC-1α) and forkhead box O (FOXO) [42, 43]. In the context of surgical stress, SIRT1 activation protects in mouse models of hepatic IRI and stroke (middle cerebral artery occlusion), while genetic ablation increases sensitivity to these injuries [44, 45]. In addition, 3 months of 40% DR preconditioning protects in an ex vivo model of myocardial IRI via an eNOS-dependent increase in SIRT1 [46]. Sirtuins have attracted considerable attention as drug targets and are discussed in detail elsewhere [47, 48]. Of interest, hepatocytes treated with either the sirtuin activators resveratrol or SRT1720 were protected in an in vitro model of IRI [49]. In vivo, treatment of mice with sirtuin activator 3 reduced infarct volume following middle cerebral artery occlusion [44].

Molecular Effector Mechanisms Underlying Dietary Preconditioning

Because of the plethora of physiological and molecular changes that occur even upon short-term restriction of a single essential amino acid from the diet, identification of critical downstream mechanisms of DR-mediated protection against surgical stress is challenging. Elucidation of upstream nutrient-sensing pathways such as GCN2 and mTORC1, for which genetic full-body or tissue-specific knockout models are available, has proven a critical step forward. Using experimental designs in which dietary interventions are combined with genetic models lacking upstream nutrient sensors that fail to gain protection upon DR, two major downstream mechanisms involving increased prosurvival insulin signaling and endogenous H_2S production have recently been elucidated.

Increased Prosurvival Insulin Signaling

Improved insulin sensitivity is one of the metabolic hallmarks common to extended longevity models including interventions such as DR, and genetic models of reduced signaling through the growth hormone/insulin/IGF/mTORC1 axis [28]. DR improves insulin sensitivity in part through lowering circulating insulin levels. This in turn reduces mTORC1 activity and its associated feedback inhibition of insulin receptor signaling, facilitating improved insulin sensitivity [50].

Mice lacking TSC1 specifically in hepatocytes (LiTsc1KO) display constitutive hepatic mTORC1 activity and profound hepatic insulin resistance due to feed-

back inhibition of insulin receptor signaling, even upon DR despite low circulating insulin levels [23]. In the hepatic IRI model, LTsc1KO mice fail to gain the benefit of dietary preconditioning in part due to insulin resistance. Consistent with this, specific inhibition of insulin signaling via genetic deletion of the insulin receptor in hepatocytes, or via pharmacological inhibition with the PI3K inhibitor wortmannin in wild-type mice, significantly impinges on the ability of short-term DR to protect against hepatic IRI [23].

How does the DR-mediated improvement in hepatic insulin sensitivity contribute to protection from hepatic IRI? In addition to regulating energy metabolism, insulin can act as a prosurvival factor via negative regulation of apoptosis. Consistent with this mechanism of action, circulating insulin levels and antiapoptotic signaling are both increased in the hours after liver reperfusion in wild-type mice preconditioned on DR, while this effect is absent in mice with constitutive insulin resistance [23]. Taken together, these data suggest that a major mechanism of DR action is via increased insulin sensitivity prior to an injury, which then facilitates increased prosurvival signaling and reduced hepatocyte apoptosis after injury. Interestingly, GCN2 activation upon amino acid restriction also improves insulin sensitivity [51], and this correlates with increased resistance to IRI [20].

It is important to note that as with insulin, reduced circulating IGF-1 is characteristic of numerous genetic and dietary models of extended longevity [52]. In rodents, short-term fasting reduces IGF-1 and protects against chemotherapeutic toxicity [53]. Protein/amino acid restriction also decreases IGF-1 in rodents, as it does in humans [54] in a GCN2-dependent manner [20]; however, whether or not this plays a role in dietary preconditioning against surgical stress remains untested.

Benefits of reduced IGF-1 are thought to work through activation of stress resistance pathways normally suppressed by insulin/IGF-1 signaling, for example expression of antioxidant-encoding genes [53]. However, increased IGF-1 is also associated in many contexts with increased stress resistance and improved outcome after IRI [55]. How can both increased and decreased IGF-1 signaling be beneficial? In the context of acute stress resistance, as long as both of these mechanisms are separated in time relative to the acute stress, they are not necessarily mutually exclusive: reduced IGF-1 signaling during the dietary preconditioning period may increase FOXO-dependent antioxidant gene expression, while increased antiapoptotic IGF-1 signaling after injury may prevent cell death as described above for insulin.

Increased Endogenous H_2S

H_2S is a gas easily identified by its distinctive odor of rotten eggs. Although toxic at high levels, endogenously produced H_2S by one of three evolutionarily conserved enzymes is now recognized to have pleiotropic cytoprotective, anti-inflammatory and vasodilatory effects resulting in cardioprotection and resistance to ischemic injury [26, 56]. In the context of dietary preconditioning against hepatic IRI, mice lacking the H_2S-producing enzyme cystathionine γ-lyase (CGL) fail to gain the protective effects of DR. Furthermore, adenoviral overexpression of CGL in the liver, or delivery of H_2S itself, recapitulate DR-like benefits without the need for any dietary intervention [26]. These findings establish the importance of endogenously produced H_2S in DR-mediated protection from hepatic IRI.

H_2S has numerous potential mechanisms of action, including sulfhydration, or formation of –SSH moieties on surface-exposed Cys residues, of an ever-growing list of protein targets. In endothelial cells, for example, such targets include the Kir6.2 regulatory subunit of the K_{ATP} channel and the VEGF receptor leading to vessel relaxation and angiogenesis, respectively [57, 58]. H_2S also has direct antioxidant properties, and can participate in mitochondrial energy production by donating electrons to the mitochondrial electron transport chain protein SQR, with a potential role in protection from ischemia. Since pharmacological delivery of H_2S also protects in models of surgical stress, as well as more broadly in preclinical models of cardiovascular disease [26], it remains to be seen if supplementation with exogenous sources of H_2S, or increased endogenous H_2S production through dietary or other means, will ultimately turn out to be more beneficial in the context of surgical stress resistance.

Implications for Clinical Translation in Surgery

The findings that short-term fasting or restriction of food intake – on the order of days to a week – leads to robust functional benefits in rodents has profound implications for the mechanism of DR action in mammals. Rather than previous notions of DR as an intervention whose benefits accumulate over long periods of time due to reduced calorie intake, DR is now viewed as a rapid adaptation to the mild stress of calorie and/or nutrient deprivation with the potential to protect against many other forms of stress. This new understanding has important practical implications for attempts to leverage DR against clinically relevant endpoints, including planned surgery.

If future clinical trials identify brief DR regimens or pharmacological DR mimetics that are safe and effective against the stress and potential complications of surgery, how would this change current preoperative nutritional standards? With few exceptions such as bariatric surgery discussed below, there is currently no consensus on what should or should not be eaten up to 1 day prior to surgery, so long as the patient is not suffering from malnutrition. Starting from the day before surgery, optimization of nutrition is a cornerstone (along with preoperative counseling, standardized analgesic and anesthetic regimens, and early mobilization after surgery) of enhanced recovery after surgery (ERAS) protocols for perioperative care designed to achieve early recovery after surgical procedures [59, 60]. ERAS nutritional optimization calls for preoperative oral carbohydrate loading, including 100 g of carbohydrate administered the day before and 50 g the day of the surgery, and is designed to alleviate surgery-induced insulin resistance and reduce patient discomfort in the form of hunger and thirst [59, 60].

A concept that is embedded in ERAS nutritional guidelines – namely that a catabolic state prior to surgery is undesirable, or even detrimental – has also influenced the long-standing "NPO after midnight" recommendation designed to prevent bronchoaspiration during anesthesia. Current guidelines have shortened the fasting period to 8 h after a meal containing fat or meat, and to 2 h after ingestion of clear fluids including beverages designed for carbohydrate loading [61]. Based on these current practices, extending the fasting regimen, or simply reducing protein/calorie intake, for a period of days prior to surgery specifically to leverage benefits associated with DR would thus represent a paradigm shift in perioperative nutrition.

Although long-term DR has been popularized for its ability to extend longevity, it is still largely unknown in the clinical literature and often confused with starvation. Furthermore, long-term DR has been associated with impaired wound healing and immunosuppression in animal models, and thus suspected of potentially increasing risk of bacterial infection [16, 62]. Nonetheless, a form of preoperative DR is already the standard of care in one surgical intervention, albeit for a different reason. In the context of bariatric surgery, current preoperative guidelines call for low- or very-low-calorie diets (although typically with protein supplementation) to reduce liver mass and facilitate the surgical procedure [63]. Importantly, studies specifically designed to test the potential efficacy of short-term DR in clinical applications, including living organ donor surgery [64, 65] and chemotherapy treatment [66, 67], have demonstrated safety and feasibility in these patient populations. Thus, while short-term DR/fasting appears feasible and safe in select populations, efficacy in mitigating risk more broadly in elective surgery, and in particular in high-risk individuals and procedures, remains to be rigorously tested.

Conclusions

Long-term DR is a well-established interventional method of life span and health span extension across species under defined experimental conditions, with some metabolic health benefits in humans confirmed in prospective clinical trials [3, 4, 68]. Short-term DR or fasting prior to surgery preconditions against a variety of complications in preclinical models [6, 8, 10, 20, 23, 26]. Currently, the duration of preoperative fasting used as an "anesthetic precaution" in humans is likely too short to tap into DR benefits, while the progressive clinical application of ERAS nutritional guidelines promotes an alternate although not mutually exclusive concept of increased nutrition immediately prior to surgery. Future clinical trials are required to test the safety, feasibility, and potential efficacy of short-term DR, including extended periods of fasting, to reduce risk of surgical complications and improve outcomes. If successful, this approach has the potential to change the paradigm for preoperative nutritional care based on concepts derived from research into the basic biology of aging.

References

1 Speakman JR, Mitchell SE: Caloric restriction. Mol Aspects Med 2011;32:159–221.
2 McCay CM, Crowell MF, Maynard LA: The effect of retarded growth upon the length of life span and upon the ultimate body size. 1935. Nutrition 1989;5:155–171; discussion 172.
3 Ravussin E, Redman LM, Rochon J, Das SK, Fontana L, Kraus WE, Romashkan S, Williamson DA, Meydani SN, Villareal DT, Smith SR, Stein RI, Scott TM, Stewart TM, Saltzman E, Klein S, Bhapkar M, Martin CK, Gilhooly CH, Holloszy JO, Hadley EC, Roberts SB; CALERIE Study Group: A 2-year randomized controlled trial of human caloric restriction: feasibility and effects on predictors of health span and longevity. J Gerontol A Biol Sci Med Sci 2015;70:1097–1104.

Chapter 2: Amino acid restriction triggers angiogenesis via GCN2/ATF4 regulation of VEGF and H_2S production.

This work is pending revision in Cell

Summary

Angiogenesis, the formation of new blood vessels by endothelial cells (ECs), is an adaptive response to nutrient/oxygen deprivation orchestrated by vascular endothelial growth factor (VEGF) during ischemia (e.g. vessel occlusion or tumorigenesis) or exercise. Hypoxia is the best-understood trigger of VEGF expression via the transcription factor HIF1α. Nutrient deprivation is inseparable from hypoxia upon ischemia, yet its role in angiogenesis is poorly characterized. Here, dietary sulfur amino acid restriction in mice promoted VEGF expression and capillary growth in skeletal muscle independent of hypoxia or HIF1α, instead requiring the amino acid-sensing eIF2α kinase GCN2 and the transcription factor ATF4. GCN2/ATF4 activation also increased cystathionine-γ-lyase expression and pro-angiogenic hydrogen sulfide (H_2S) production. H_2S boosted glycolytic ATP production by inhibiting mitochondrial electron transport in ECs, and was required for angiogenesis triggered by amino acid deprivation, exercise or local VEGF overexpression. Amino acid deprivation is thus a powerful pro-angiogenic trigger independent of hypoxia.

Amino acid restriction triggers angiogenesis via GCN2/ATF4 regulation of VEGF and H_2S production

Alban Longchamp[1,2], Teodelinda Mirabella[3,4], Abhirup Das[5,6], Christopher Hine[1], Lear E. Brace[1], Issam Ben-Sahra[1], Nelson Knudsen[1], J. Humberto Treviño-Villarreal[1], Pedro Mejia[1], Ming Tao[2], Gaurav Sharma[2], Rui Wang[7], Jean-Marc Corpataux[8], Jacques-Antoine Haefliger[8], Kyo Han Ahn[9], Chih-Hao Lee[1], Brendan D. Manning[1], David A. Sinclair[5,6], Christopher Chen[3,4], C. Keith Ozaki[2], and James R. Mitchell[1]*

[1]Department of Genetics and Complex Diseases, Harvard T. H. Chan School of Public Health, Boston, MA 02115, USA

[2]Department of Surgery and the Heart and Vascular Center, Brigham & Women's Hospital and Harvard Medical School, Boston, MA 02115 USA

[3]Tissue Microfabrication Lab, Department of Biomedical Engineering Boston University, Boston, MA 02215, USA

[4]Wyss Institute for Biologically Inspired Engineering Centre for Life Science Boston Building, 3 Blackfan Circle, Boston, MA 02115, USA

[5]Laboratory for Aging Research, Department of Pharmacology, School of Medical Sciences, The University of New South Wales, Sydney NSW 2052, Australia

[3]Glenn Center for the Biological Mechanisms of Aging, Department of Genetics, Harvard Medical School, Boston, MA 02115, USA

[7]Cardiovascular and Metabolic Research Unit, Laurentian University, Sudbury, ON, Canada

[8]Department of Vascular Surgery, Laboratory of Experimental Medicine, Centre Hospitalier Universitaire Vaudois, Lausanne, Switzerland.

[9]Department of Chemistry, Centre for Electro-Photo Behaviors in Advanced Molecular Systems, Postech, 77 Cheongam-Ro, Nam-Gu, Pohang, Republic of Korea

*Correspondence to: jmitchel@hsph.harvard.edu

655 Huntington Ave. Building 2-121, Boston, MA 02115

Telephone: (617) 432-7286

Fax: (617) 432-5368

Highlights

*Sulfur amino acid restriction triggers angiogenesis independent of hypoxia or HIF1α

*GCN2/ATF4 pathway regulates VEGF and CGL expression upon amino acid restriction

*CGL-dependent H_2S production in ECs is required for skeletal muscle angiogenesis

*H_2S triggers EC glycolysis and migration via mitochondrial respiration inhibition

Summary

Angiogenesis, the formation of new blood vessels by endothelial cells (ECs), is an adaptive response to nutrient/oxygen deprivation orchestrated by vascular endothelial growth factor (VEGF) during ischemia (e.g. vessel occlusion or tumorigenesis) or exercise. Hypoxia is the best-understood trigger of VEGF expression via the transcription factor HIF1α. Nutrient deprivation is inseparable from hypoxia upon ischemia, yet its role in angiogenesis is poorly characterized. Here, dietary sulfur amino acid restriction in mice promoted VEGF expression and capillary growth in skeletal muscle independent of hypoxia or HIF1α, instead requiring the amino acid-sensing eIF2α kinase GCN2 and the transcription factor ATF4. GCN2/ATF4 activation also increased cystathionine-γ-lyase expression and pro-angiogenic hydrogen sulfide (H_2S) production. H_2S boosted glycolytic ATP production by inhibiting mitochondrial electron transport in ECs, and was required for angiogenesis triggered by amino acid deprivation, exercise or local VEGF overexpression. Amino acid deprivation is thus a powerful pro-angiogenic trigger independent of hypoxia.

Introduction

Angiogenesis is the formation of new blood vessels from existing ones through sprouting, proliferation and migration of endothelial cells (ECs). In adult mammals, angiogenesis is a critical adaptive response to a wide variety of normal and pathophysiological conditions characterized by inadequate supply of oxygen and nutrients, ranging from tissue ischemia upon vessel occlusion or tumorigenesis to endurance exercise.

Hypoxia is the best-understood trigger of angiogenesis, stabilizing the oxygen-sensitive transcription factor hypoxia inducible factor (HIF)-1α in multiple cell types and promoting expression of the master regulator of angiogenesis, vascular endothelial growth factor (VEGF). VEGF expression can also be induced by the transcriptional co-activator PGC1α upon oxygen/nutrient deprivation through an ERR-α-dependent, HIF-1α independent pathway (Arany et al., 2008).

VEGF acts via binding to EC-specific cell-surface tyrosine kinase receptors (VEGFR2), triggering an orchestrated cascade of signal transduction via the PI3K and MAPK pathways involving critical second messengers nitric oxide (NO) and cyclic GMP (cGMP) and changes in gene expression facilitating EC migration, proliferation and vessel formation (Olsson et al., 2006). VEGF-mediated angiogenesis is potentiated by the NAD+-dependent deacetylase SIRT1, which deacetylates and inactivates FOXO transcription factors (Potente et al., 2007) involved in negative regulation of EC migration and tube formation (Potente et al., 2005). VEGF signalling also triggers changes in cellular energy metabolism, namely increased glucose uptake and glycolysis, necessary to provide rapid energy for EC migration (De Bock et al., 2013).

Hydrogen sulfide (H_2S) is a pro-angiogenic gas produced in ECs upon VEGF stimulation (Papapetropoulos et al., 2009) primarily by the transsulfuration enzyme cystathionine-gamma-lyase (CGL) (Wang, 2012). Like NO, which in addition to activating cGMP synthesis functions through post-translational modification (S-nitrosylation) of target proteins (Fukumura et al.,

2006), H_2S promotes angiogenesis through post-translational modification (sulfhydration) and activation of at least two proximal signal transduction components, VEGFR2 (Tao et al., 2013) and eNOS (Altaany et al., 2014; Coletta et al., 2012). VEGF-induced angiogenesis is compromised upon genetic CGL deficiency in aorta explant assays *ex vivo* (Papapetropoulos et al., 2009), as is neovascularization following arterial occlusion *in vivo* (Kolluru et al., 2015). However, the mechanism by which VEGF stimulates endogenous H_2S production, as well as the relative contribution of H_2S vs. NO to angiogenesis, remains unclear (Katsouda et al., 2016).

In addition to hypoxia, nutrient depletion is a hallmark of tissue ischemia that ECs must contend with in order to perform angiogenesis and restore tissue homeostasis. While PGC1α responds to nutrient deprivation independent of hypoxia, and can drive VEGF production by muscle cells, it is not activated in ECs themselves (Arany et al., 2008). Furthermore, pharmacological approaches to promote angiogenesis under conditions of chronic ischemia by targeting PGC1α or HIF1α have to date been unsuccessful (Chu and Wang, 2012). Thus a deeper understanding of the mechanisms underlying angiogenesis is needed in order to restore vascular health in the context of tissue ischemia without promoting tumor growth, both of which increase upon aging.

Dietary restriction (DR), defined as reduced nutrient/energy intake without malnutrition, is best known for its ability to extend lifespan, improve metabolic fitness and increase stress resistance (Colman et al., 2009; Fontana et al., 2010; Hine et al., 2015). Dietary restriction specifically of sulfur amino acids (methionine and cysteine), also known simply as methionine restriction (MR), leads to many of these same benefits but without enforced restriction of total calorie intake (Miller et al., 2005; Orentreich et al., 1993; Perrone et al., 2013).

We recently reported that both DR and MR increase CGL expression and endogenous H_2S production in liver *in vivo* and in hepatocytes *in vitro*, and that increased H_2S is necessary and sufficient for short-term DR-mediated stress resistance upon ischemic injury (Hine et al., 2015). However, the mechanisms underlying nutrient regulation of CGL expression and H_2S

production, and the potential of DR to modulate angiogenesis via H_2S, remain unknown. DR promotes revascularization and recovery in a model of femoral artery ligation in rodents (Kondo et al., 2009), and maintains vascular health in rodents and non-human primates in part by preserving capillary density in skeletal muscle (Omodei and Fontana, 2011). Although the mechanism remains unknown, this could occur in part via SIRT1, which is activated in some tissues upon DR (Cantó and Auwerx, 2009; Wang, 2014) and required for VEGF-dependent angiogenesis (Potente et al., 2007). On the other hand, protection afforded by DR against cancer in rodent models is thought to occur in part through inhibition of angiogenesis, thus preventing tumor neovascularization (Hursting et al., 2013).

Here, we identified dietary restriction of sulfur amino acids as a novel pro-angiogenic trigger promoting rapid growth of new capillaries in skeletal muscle. This occurred through coordinate regulation of VEGF and CGL expression and H_2S production in multiple cell types, including ECs, via an amino acid sensing mechanism independent of hypoxia, HIF1α or PGC1α, but dependent on SIRT1. We also identified the requirement for CGL-derived H_2S in VEGF-dependent angiogenesis, and a novel mechanism of pro-angiogenic H_2S action in ECs involving a switch from oxidative to glycolytic metabolism.

Results

Dietary sulfur amino acid restriction induces functional angiogenesis via increased VEGF *in vivo*

We tested the potential of isolated nutrient restriction independent of ischemia or hypoxia to impact angiogenesis *in vitro* using a model of sulfur amino acid restriction (Hine et al., 2015). Human umbilical vein endothelial cell (HUVEC) cultured in media lacking methionine (Met, M) and cysteine (Cys, C) for 16 hrs displayed increased VEGF mRNA expression and protein secretion into the media (Fig. 1A). This correlated with increased pro-angiogenic potential, including migration (Fig. 1B) and formation of capillary-like structures (tube formation,

Fig. 1C). M&C deprivation also increased sprout length in HUVEC spheroid cultures, an effect that was abrogated by the VEGF receptor inhibitor SU5416 (Fig. 1D).

We next tested the requirement for SIRT1 in angiogenesis induced by M&C deprivation. SIRT1 is activated upon DR in some tissues (Cantó and Auwerx, 2009; Wang, 2014) and required for VEGF-mediated angiogenesis in ECs under conditions of oxidative stress *in vitro* and maintenance of vascular density upon aging *in vivo* (Das et al., see accompanying manuscript). Blocking SIRT1 activity with the inhibitor EX527 significantly reduced HUVEC tube formation upon M&C deprivation, with the main effects occurring at the branch points (Fig. 1E, FigS1A). Thus, the pro-angiogenic pathway triggered by amino acid (M&C) deprivation of ECs is dependent on both VEGF and SIRT1 activity.

To test the potential of dietary sulfur amino acid restriction to increase angiogenesis *in vivo*, mice were given *ad libitum* access to a Met restricted (MR) diet that is reduced in Met and lacking Cys (Miller et al., 2005; Orentreich et al., 1993; Perrone et al., 2013). Young adult wildtype (WT) mice on MR for 2 mo maintained a lower body weight despite normal food intake

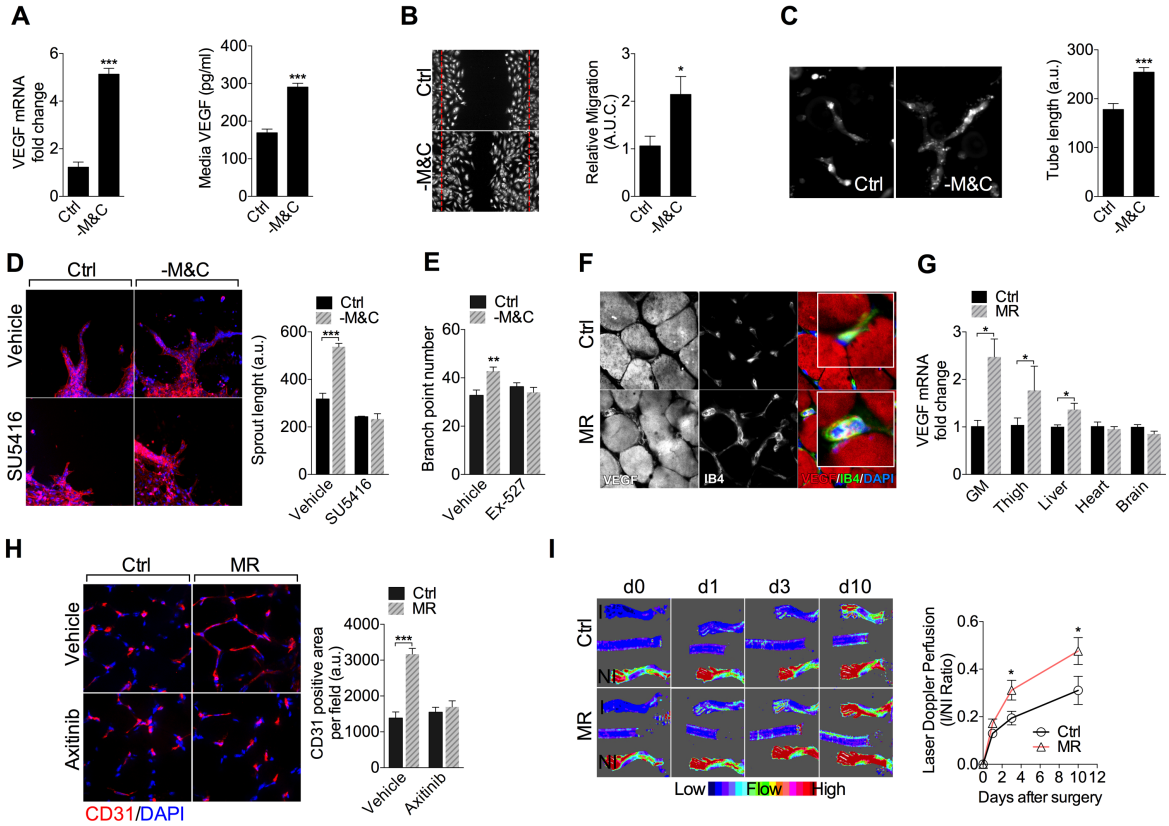

Figure 1: Dietary sulfur amino acid restriction induces functional angiogenesis via increased VEGF *in vivo*

(**A**) VEGF mRNA levels (left) and secreted protein concentration in the media (right) of HUVEC cultured in control (Ctrl) or sulfur amino acid deficient (-M&C) media for 16 hrs. **(B)** Representative wound closure (left, 10X magnification at time = 20 hr; dotted lines indicate boundary of the scratch wound at time = 0 hr) and area under the curve (A.U.C., right) from HUVEC in the indicated media. (**C**) Representative capillary-like structures (left, tube formation at 40X magnification) and mean tube length quantification (right) in HUVEC cultured in the indicated media for 24 hrs. (**D**) Representative images (left, 40X magnification) and quantification (right) of sprouting EC spheroids in the indicated media +/- VEGFR2 inhibitor SU5416 for 24 hrs. (**E**) Quantification of tube branch points per field of view in HUVECs seeded onto growth factor-replete Matrigel and incubated with in the indicated media +/- SIRT1 inhibitor Ex-527 for 18 hrs. All cell-based assays were repeated at least 3 times. (**F**) Representative transverse sections of gastrocnemius muscle stained for VEGF (left, 40X magnification), IsolectinB4 (IB4, middle, 40X magnification) and merged (VEGF red, IB4 green, DAPI blue; right, insert 160X magnification) in mice preconditioned for 2 mo on control (Ctrl) or methionine restricted (MR) diets. (**G**) Expression of VEGF mRNA in the indicated organ (GM, gastrocnemius muscle) of mice on Ctrl or MR diets as indicated for 2 mo; n = 3-7/group. (**H**) Representative transverse sections (left, 40X magnification) and quantification (right) of gastrocnemius muscle stained for endothelial marker CD31 in mice fed for 2 wks on Ctrl or MR diets with or without VEGFR2 inhibition (Axitinib); n=4-5/group. (**I**) Longitudinal Doppler imaging of blood flow in WT mice preconditioned on Ctrl or MR diets as indicated for 1 mo prior to femoral artery occlusion (I, ischemic; NI, non-ischemic). Left: representative infrared images on the indicated day after occlusion. Right: quantification of blood-flow recovery; n=7-8 per group. Error bars indicate SEM; $*P < 0.05$, $**P < 0.005$, $***P < 0.001$ compared to Ctrl by Student's t test.

relative to mice fed a control diet containing normal Met and Cys levels (Fig. S1B). Co-immunostaining for VEGF and the EC marker isolectin B4 (IB4) revealed increased VEGF protein in both muscle fibers and ECs upon MR (Fig. 1F). Expression of VEGF mRNA was also significantly increased upon MR in different muscle beds (gastrocnemius, thigh) and to a lesser extent in the liver, but not in the brain or heart (Fig. 1G). Interestingly, increased VEGF transcription was observed upon different DR regimens that shared a reduction in sulfur amino acids, including protein calorie restriction (PCR, consisting of a Protein-free diet fed at 40% Calorie Restriction) or 3 d of water-only fasting (Fast) (Fig. S1C).

Strikingly, MR resulted in increased vascular density in skeletal muscle as determined by immunostaining (Fig. 1H) and flow cytometric analysis (Fig. S1D, E) for the EC marker CD31. Consistent with VEGF dependence, this effect was blocked by the VEGF receptor inhibitor axitinib at a dose previously shown to inhibit neovascularization *in vivo* (Ma and Waxman, 2008) (Fig. 1H, Fig. S1E).

The functional significance of MR-induced neovascularization was tested in a model of ischemic injury induced by femoral artery occlusion. Mice were preconditioned on MR or control diets for 1 mo prior to surgical artery occlusion and returned to a complete diet after surgery (Fig. S1E). The return of blood flow indicative of neovascularization was then followed over 10 d using laser Doppler imaging (Fig. S1F). Although blood flow was similarly interrupted in both groups immediately after occlusion (d0), return of blood flow was markedly accelerated in MR preconditioned mice relative to the control group, with significant improvement as early as 3 d after ischemia (Fig. 1I). These data are consistent with neovascularization induced by dietary amino acid restriction as a critical factor in the improved physiological response to acute blood flow cessation.

GCN2-dependent, hypoxia independent regulation of VEGF and angiogenesis upon amino acid restriction

We next sought to determine the mechanism of increased VEGF expression upon M&C deprivation. Stabilization of the transcription factor HIF1α upon hypoxia is the best characterized trigger of VEGF expression in multiple cell types including ECs and myocytes (Liu et al., 1995). However, consistent with normoxic conditions, VEGF expression upon M&C deprivation in cultured HUVECs was unaffected by HIF1α RNAi knock-down (KD) (Fig. S2A, B) and coincided with a reduction of HIF1α protein levels (Fig. 2A). The transcriptional co-activator PGC1α can also induce VEGF independently of HIF1α upon total nutrient/growth factor deprivation in specific cell types including myocytes although not in ECs (Arany et al., 2008). Consistent with this, endogenous PGC1α mRNA expression in HUVECs was very low and unaffected by M&C deprivation (Fig. S2C*)*, while exogenous PGC1α overexpression in HUVECs failed to modulate VEGF expression (Fig. S2D*)*. Therefore, VEGF induction upon M&C deprivation in ECs occurred independently of hypoxia or the canonical HIF1α and PGC1α pathways.

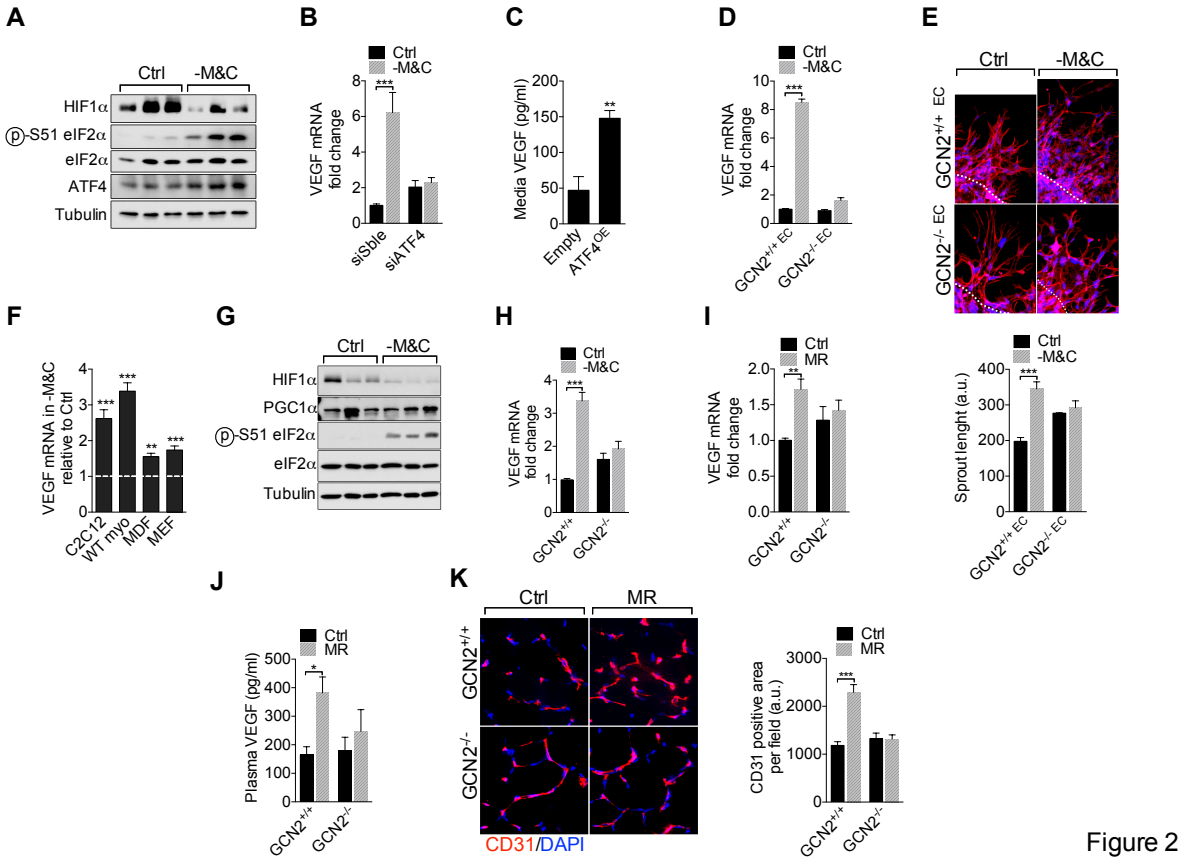

Figure 2

Figure 2: GCN2-dependent, hypoxia independent regulation of VEGF and angiogenesis upon amino acid restriction

(**A**) Western blot of HIF1α, eIF2α (p-Ser51, total) and ATF4 in HUVEC cultured in control (Ctrl) or sulfur amino acid deficient (-M&C) media for 16 hrs. (**B**) Relative VEGF mRNA expression in HUVEC 2 d after transfection with ATF4 or control scrambled siRNA and cultured in the indicated media for 16 hrs. (**C**) Secreted VEGF protein concentration in the media of HUVEC 2 d after transfection with an ATF4 overexpressing ($ATF4^{OE}$) or control construct (Empty). (**D**) VEGF mRNA expression in $GCN2^{+/+}$ and $GCN2^{-/-}$ primary mouse EC cultured in the indicated media for 16 hrs. (**E**) Representative images (top, 40X magnification) and quantification (bottom) of $GCN2^{+/+}$ and $GCN2^{-/-}$ sprouting EC spheroids cultured in the indicated media for 24 hrs. All cell-based assays were repeated at least 3 times. (**F**) VEGF mRNA in C2C12, WT myotubes, MDF and MEF cultured in M&C deficient media relative to control (Ctrl) media for 16 hrs. (**G**) Western blot of HIF1α, PGC1α, eIF2α (p-Ser51, total) in C2C12 cultured in control (Ctrl) or sulfur amino acid deficient (-M&C) media for 16 hrs. (**H**) VEGF mRNA expression in $GCN2^{+/+}$ and $GCN2^{-/-}$ primary mouse EC cultured in control (Ctrl) or sulfur amino acid deficient (-M&C) media for 16 hrs. (**I-K**) VEGF mRNA expression in skeletal muscle (**I**), plasma VEGF (**J**) and representative transverse sections (left, 40X magnification) and quantification (right) of gastrocnemius muscle stained for CD31 (**K**) in $GCN2^{+/+}$ or $GCN2^{-/-}$ mice fed for 2-4 wks on Ctrl or MR diets; n=5-6/group. Error bars indicate SEM; **P* < 0.05, ***P* < 0.005, ****P* < 0.001 compared to Ctrl by Student's t test.

The amino acid starvation response (AASR) is triggered by direct binding of uncharged cognate tRNAs to the general control nonderepressible 2 (GCN2) kinase, resulting in

phosphorylation of its direct target, eukaryotic translation initiation factor 2 α (eIF2α) and translational derepression of select mRNAs, including that encoding the transcription factor ATF4 (Wek et al., 1995). The AASR has been implicated in DR-mediated resistance to ischemia reperfusion injury (Peng et al., 2012), but has not been assessed in ECs. Consistent with GCN2 activation upon M&C deprivation in ECs, Western blot analysis revealed increased eIF2α phosphorylation and ATF4 expression (Fig. 2A) and increased expression of the ATF4 target ASNS (Fig. S2E). ATF4 was required for VEGF transcriptional upregulation upon M&C deprivation (Fig. 2B; Fig. S2E), while ATF4 overexpression alone increased VEGF secretion independent of nutrient deprivation (Fig. 2C; Fig. S2F). The requirement for GCN2 upstream of eIF2α/ATF4 was tested in primary ECs isolated from WT and GCN2$^{-/-}$ mice (Fig S2G). Similar to HUVECs, M&C deprivation significantly increased VEGF and ASNS expression (Fig. 2D; Fig. S2H), and sprout length (Fig. 2E) in WT ECs, each of which was abrogated in the absence of GCN2.

Because VEGF can be secreted by many cell/tissue types, including muscle fibers, we next asked if GCN2/ATF4 regulated VEGF expression upon M&C deprivation in other cell types. In all cell lines tested, including mouse primary skeletal myotubes, C2C12 myotubes, primary dermal fibroblasts (MDF) and spontaneously immortalized mouse embryonic fibroblasts (MEF), M&C deprivation significantly increased VEGF expression (Fig. 2F). In C2C12 myotubes, this induction of VEGF coincided with increased eIF2α phosphorylation (Fig. 2G) and ATF4 activity (Fig. S2I) and reduced HIF1α protein levels (Fig. 2G). Notably, it was unaffected by HIF1α RNAi knock-down (KD) under normoxic (20%) or hypoxic (<1%) oxygen tensions (Fig. S2J-L), consistent with independent regulation of VEGF upon oxygen and nutrient deprivation in myotubes as observed in ECs.

Finally, the genetic requirement for GCN2 was tested *in vitro* and *in vivo*. VEGF induction in primary skeletal myotubes upon M&C restriction *in vitro* required GCN2 (Fig. 2H).

Similarly, increased VEGF mRNA expression in muscle (Fig. 2I), circulating VEGF protein in plasma (Fig. 2J) and increased vascular density (Fig. 2K) upon 2-4 wks of MR were lost in GCN2KO mice. Taken together, these data reveal amino acid restriction and the GCN2/ATF4-dependent AASR as a novel trigger of increased VEGF expression and angiogenesis independent of hypoxia, HIF1α or PGC1α.

VEGF signalling and AASR converge on endothelial H_2S production by CGL

VEGF promotes angiogenesis in part by stimulating CGL-dependent production of the pro-angiogenic gas H_2S in ECs (Lin et al., 2013; Papapetropoulos et al., 2009), however mechanisms of CGL regulation in ECs and the importance H_2S in angiogenesis remain poorly understood. Recently we found that dietary sulfur amino acid restriction increases CGL expression and H_2S production in multiple cell and tissue types (Hine et al., 2015), prompting us to test the potential contribution of CGL-dependent H_2S to angiogenesis in the context of amino acid restriction.

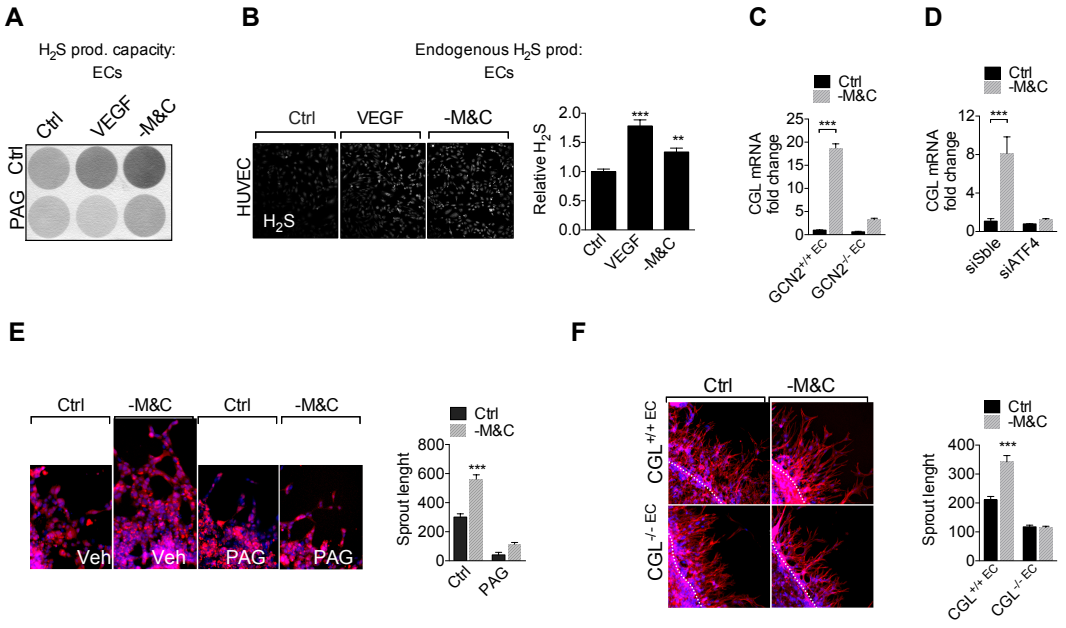

Figure 3

Figure 3: VEGF signalling and AASR converge on endothelial H_2S production by CGL
(**A**) Representative H_2S production capacity as indicated by black lead sulfide formation from EC deprived of M&C for 16 hr or treated with VEGF (50 ng/ml) in the presence or absence of the CGL inhibitor propargylglycine (PAG, 100 μM) as indicated. (**B**) Representative (left) endogenous H_2S production and quantification of the intensity (right) using an H_2S-specific fluorescent probe in HUVEC upon treatment with VEGF (50 ng/ml) or cultured in media lacking sulfur amino acids (-M&C). (**C**) CGL mRNA expression in $GCN2^{+/+}$ and $GCN2^{-/-}$ primary mouse EC cultured in control (Ctrl) or sulfur amino acid deficient (-M&C) media for 16 hrs. (**D**) CGL mRNA expression in HUVEC 2 d after transfection with ATF4 or control scrambled siRNA and cultured in the indicated media for 16 hrs. (**E**) Representative images (left, 40X magnification) and quantification (right) of HUVEC spheroids cultured in control media (Ctrl) or media lacking M&C (-M&C) for 24 hrs in the presence of vehicle (Veh) or CGL inhibitor PAG (100 μM). (**F**) Representative images (left, 40X magnification) and quantification (right) of $CGL^{-/-}$ primary EC sprouts in control media (Ctrl) or media lacking M&C (-M&C) for 24 hrs. All cell-based assays were repeated at least 3 times. Error bars indicate SEM; ***$P < 0.001$ compared to Ctrl within genotype by Student's t test.

Two complementary assays were used to test the ability of M&C deprivation to stimulate H_2S production specifically in ECs. In the first, the ability of cells to produce H_2S in the presence of excess added substrate (cysteine) is visualized by the highly selective interaction between H_2S and lead acetate to form the black precipitate, lead sulfide. In the second, endogenous H_2S production is visualized with a sensitive and selective fluorescent probe added to live cells or fresh-frozen tissue sections without the need for exogenous substrate (Singha et al., 2015). Both assays revealed a significant increase in H_2S production upon M&C deprivation similar in magnitude to exogenous VEGF addition and sensitive to the CGL inhibitor PAG (Fig. 3A, B). Nutrient deprivation also boosted endogenous H_2S production in primary hepatocytes, while VEGF did not because hepatocytes lack VEGFR2 (Fig. S3A).

We next tested the potential contribution of the GCN2-dependent AASR to CGL mRNA regulation. Like VEGF mRNA, CGL mRNA was strongly induced in ECs upon M&C deprivation, and this was lost in ECs lacking GCN2 (Fig. 3C) or upon ATF4 knockdown (Fig. 3D; Fig. S2E). Importantly, VEGF mRNA was not affected by the absence of CGL (Fig. S3B), consistent with CGL and VEGF as independent downstream targets of the AASR. Interestingly, exogenous VEGF increased CGL (but not CBS or 3-MST) mRNA and protein expression in ECs independent of nutrient deprivation (Fig. S3C, D), suggestive of a positive feedback loop between VEGF and CGL expression.

The functional relevance of endothelial CGL-derived H_2S in angiogenic potential *in vitro* was assessed in the EC spheroid assay. Increased sprout length of EC spheroids upon M&C deprivation was prevented by CGL inhibition with PAG in HUVECs (Fig. 3E) and by genetic CGL ablation ($CGL^{-/-}$) in mouse ECs (Fig. 3F). Thus, CGL is required for angiogenesis induced by M&C deprivation *in vitro*.

CGL is necessary and sufficient for angiogenesis *in vivo*

We next tested the requirement for CGL-derived H_2S in angiogenesis triggered by nutrient deprivation *in vivo*. CGL is thought to be the major H_2S producer in ECs *in vivo (Wang, 2012)*, which we confirmed using the H_2S-specific P3 probe in fresh-frozen sections of gastrocnemius muscle from CGL WT and KO mice (Fig. 4A). P3 fluorescence indicative of endogenous H_2S production co-localized with $CD31^+$ cells in WT but not CGLKO mice, further suggesting ECs as the major producer of endogenous H_2S in this tissue (Fig. 4A). Quantification of P3 intensity in WT and CGLKO mice fed Ctrl vs. MR diets for 2wks confirmed a CGL-dependent increase in EC H_2S production upon MR *in vivo* (Fig. 4B). Coincident with failure to increase H_2S, CGLKO mice demonstrated no increase in capillary density upon MR *in vivo* as in the WT group (Fig. 4C). Taken together, CGL-derived H_2S is required for angiogenesis triggered by nutrient deprivation.

We next asked if CGL-derived H_2S is sufficient to promote angiogenesis independent of amino acid restriction. Overexpression of CGL in gastrocnemius muscle of WT mice via intra-muscular injection of CGL-overexpressing adenovirus increased muscle H_2S production capacity (Fig. S4A) and vascular density (Fig. 4D) independent of any other pro-angiogenic stimulus, suggesting that CGL-derived H_2S is sufficient to trigger angiogenesis.

To test this apparent general requirement for CGL-derived H_2S in angiogenesis independent of the upstream stimulus, we induced angiogenesis by either treadmill exercise training, a potent stimulus for angiogenesis in adult skeletal muscle (Rowe et al., 2014), or by

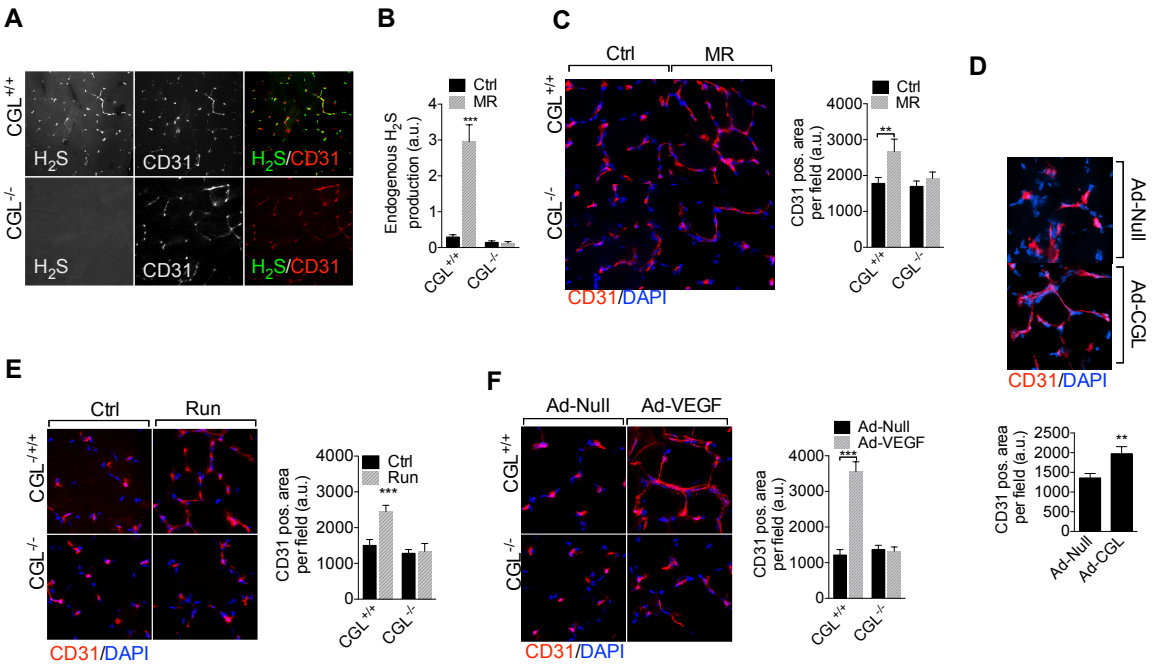

Figure 4

Figure 4: CGL is necessary and sufficient for angiogenesis *in vivo*

(**A**) Representative transverse sections (20X magnification) of gastrocnemius muscle from $CGL^{+/+}$ and $CGL^{-/-}$ mice stained for CD31 and endogenous H_2S. (**B**) Quantification of endogenous H_2S production in $CD31^+$ EC in the gastrocnemius muscle of $CGL^{+/+}$ and $CGL^{-/-}$ mice fed for 2 wks on Ctrl or MR diets as indicated; n=4-5/group. (**C**) Representative transverse section (left, 40X magnification) and quantification (right) of gastrocnemius muscle stained for CD31 from $CGL^{+/+}$ and $CGL^{-/-}$ mice fed for 2 wks on Ctrl or MR diets as indicated; n=4-5/group. (**D**) Representative transverse sections of gastrocnemius muscle stained for CD31 (left, 40X magnification) and quantification (right) 2 wks after Ad-Null or Ad-CGL injections; n=4/group. (**E**) Representative transverse section (left, 40X magnification) and quantification (right) of gastrocnemius muscle stained for CD31 from $CGL^{+/+}$ and $CGL^{-/-}$ mice subjected to low intensity running (exercised) vs. control (sedentary) for 1mo; n=5-6/group. (**F**) Representative transverse sections of gastrocnemius muscle stained for CD31 (left, 40X magnification) and quantification (right) from $CGL^{+/+}$ and $CGL^{-/-}$ mice 6 d after intramuscular injection of control (Ad-Null) or $VEGF_{165}$ -expressing (Ad-VEGF) adenovirus; n=4/group. Error bars indicate SEM; $^{**}P < 0.005$, $^{***}P < 0.001$ compared to Ctrl by Student's t test.

VEGF overexpression via intra-muscular injection of VEGF-overexpressing (ad-$VEGF_{165}$) adenovirus. Exercise training increased endogenous VEGF mRNA expression in WT mice (Fig. S4B), while both exercise training (Fig. 4E) and local VEGF overexpression via adenoviral gene delivery (Fig. 4F) increased capillary density in WT but not CGLKO mice. Taken together, these data indicate that CGL-mediated H_2S production is necessary for VEGF-mediated neovascularization *in vivo* independent of the upstream pro-angiogenic stimulus.

H_2S promotes glucose uptake and ATP generation by glycolysis for EC migration

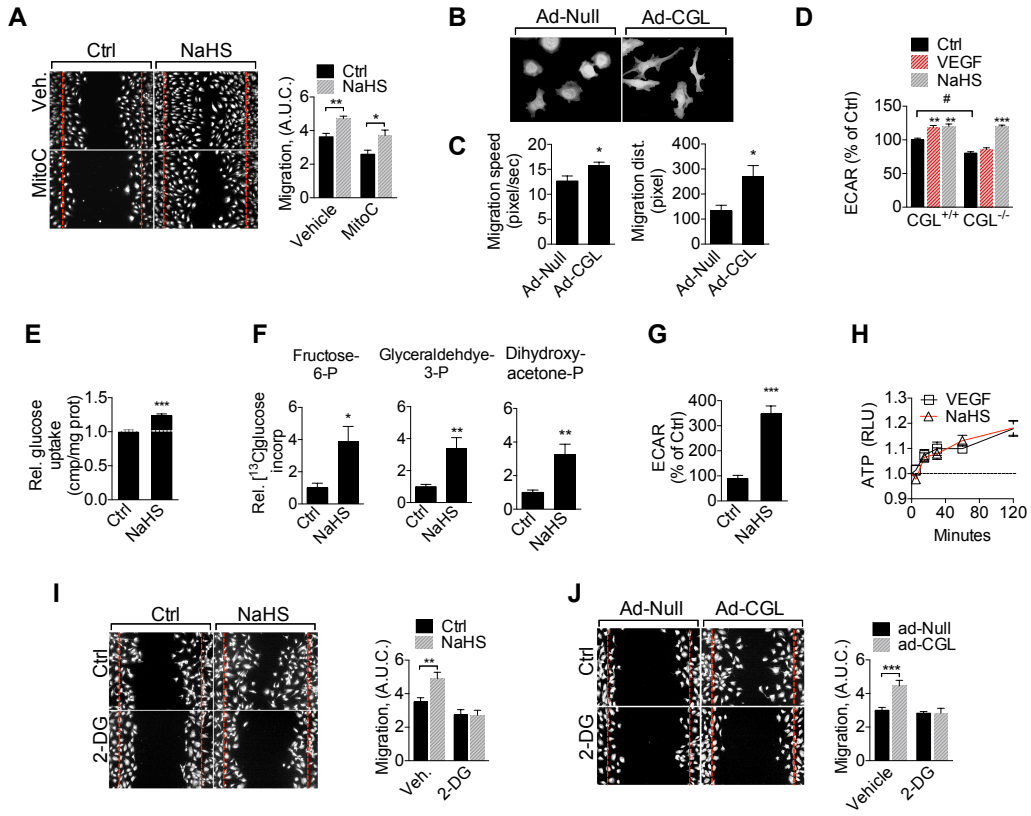

Figure 5

Figure 5: H_2S promotes glucose uptake and ATP generation by glycolysis for EC migration

(**A**) Time-dependent wound closure (left) and quantification (right, A.U.C., area under the curve) in HUVEC +/- 100μM NaHS in the presence of vehicle or mitomycin C (MitoC) to inhibit proliferation. (**B, C**) Representative images (**B**) and quantification (**C**) of migration speed (left) and distance (right) from time-lapse video imaging of GFP+ HUVEC infected with control (Ad-Null) or CGL adenovirus (Ad-CGL) as indicated. (**D**) Extracellular acidification rate (ECAR) indicative of glycolysis in $CGL^{+/+}$ and $CGL^{-/-}$ primary mouse EC pretreated for 1 hr with VEGF (50 ng/ml) or NaHS (100 μM). (**E**) Relative glucose uptake in HUVEC pretreated with NaHS for 1 hr. (**F**) C13-labeled metabolite levels measured by mass spectrometry-scaled intensity in C13 glucose pulsed HUVEC pretreated for 1 hr +/- NaHS (100 μM). (**G**) Extracellular acidification rate (ECAR) indicative of glycolysis in HUVEC pretreated for 1 hr with NaHS (100μM). (**H**) Time dependent ATP production in HUVEC treated with 100 μM NaHS at time=0. (**I, J**) Representative wound closure (left) and quantification (right, A.U.C) from HUVEC treated with 100 μM NaHS in the presence of vehicle or 1 mM 2-DG (**I**) or infected with a control (Ad-Null) or CGL adenovirus (Ad-CGL) at multiplicity of infection 50 (**J**) in the presence of vehicle or the glycolysis inhibitor 2-deoxyglucose (2-DG, 1mM). All cell-based assays were repeated at least three times. Error bars indicate SEM; $*P < 0.05$, $**P < 0.005$, $***P < 0.001$ compared within genotype to Ctrl by Student's t test.

CGL is a promiscuous enzyme that can convert cystathionine to cysteine as part of the

transsulfuration pathway, but that can also use cysteine to produce H_2S and serine. We thus sought to directly test H_2S as the CGL metabolite relevant to angiogenesis. H_2S delivery in the form of NaHS promoted EC proliferation/migration indicative of increased angiogenic potential in the wound closure assay (Fig. 5A). Blocking proliferation with mitomycinC (MitoC) only partially reduced H_2S-induced wound closure (Fig. 5A), consistent with migration as a critical factor in H_2S-induced angiogenic potential. To confirm the effects of CGL on migration, time-lapse video imaging of GFP^+ HUVECs revealed that cells overexpressing CGL (Ad-CGL) formed lamellipodial projections over larger areas (Fig. 5B) coincident with increased migration speed and greater cell body displacement (Fig. 5C).

To determine where in the VEGF signal transduction pathway H_2S acts to promote EC migration, we first considered signalling events proximal to VEGF in which H_2S has been previously implicated, including sulfhydration and activation of VEGFR2 (Tao et al., 2013) and eNOS (Altaany et al., 2014; Coletta et al., 2012). However, eNOS inactivation using RNAi KD (sieNOS) or L-NG-nitroarginine methyl ester (L-NAME) had no effect on the pro-angiogenic activity of CGL/H_2S on migration in the wound closure assay *in vitro* (Fig. S5A-E). Similarly, L-NAME failed to block angiogenesis *in vivo* (Fig. S5F), consistent with a critical role for H_2S in angiogenesis downstream of (or redundant with) eNOS activation, and prompting us to consider pro-angiogenic mechanisms of H_2S action further downstream of proximal VEGF signaling.

Cell migration requires rapid ATP generation to facilitate actin cytoskeleton rearrangement, which in ECs is met by increasing glycolytic metabolism (De Bock et al., 2013; Schoors et al., 2014). We thus examined glucose uptake and oxidative vs. glycolytic energy metabolism as a function of genetic and pharmacological H_2S modulation in ECs. Consistent with the pro-angiogenic effect of increased glycolysis, treatment of WT mouse ECs with either VEGF or NaHS stimulated glycolytic metabolism as evidenced by an increase in extracellular acidification rate (ECAR, Fig. 5D). In CGLKO ECs, glycolysis under basal conditions was significantly reduced relative to WT controls, and this was rescued to WT levels by exogenous

H_2S (NaHS) administration, while VEGF failed to boost glycolysis (Fig. 5D). In HUVECs, NaHS similarly boosted glucose uptake (Fig. 5E) and glycolysis as shown by increased accumulation of glycolytic metabolites in ^{13}C-glucose-labeled cells (Fig. 5F) and increased ECAR (Fig. 5G; Fig. S5G). This induction of glycolysis upon NaHS administration was unaffected by axitinib or L-NAME (Fig. S5H), and thus most likely mediated downstream of proximal VEGFR2 signalling. Importantly, exogenous VEGF and H_2S boosted intracellular ATP levels over a similar rapid time course (Fig. 5H). Consistent with the importance of glycolysis and ATP generation in EC migration, the pro-migratory effects of exogenous H_2S addition or CGL overexpression were blocked by the glycolysis inhibitor 2-deoxy-D-glucose (2-DG; Fig. 5I, J).

H_2S shifts oxidative/glycolytic balance by transient inhibition of mitochondrial electron transport

By what mechanism does H_2S promote glucose uptake and glycolysis in ECs? H_2S has been reported to sulfhydrate and activate GAPDH (Mustafa et al., 2009), a rate-limiting step in glycolysis (Shestov et al., 2014). However, preventing sulfhydration by addition of the reducing agent dithiothreitol (Mustafa et al., 2009) had no effect on induction of glucose uptake by NaHS (Fig. S6A).

Inhibition of oxidative phosphorylation can also precipitate a rapid shift to glycolysis subsequent to transient ATP depletion and initiation of adaptive responses including AMPK activation, which boosts glucose uptake and glycolytic metabolism (Wheaton et al., 2014). Consistent with such a role for H_2S in regulation of oxidative/glycolytic balance, CGLKO ECs displayed increased oxygen consumption under basal conditions relative to WT cells (Fig. 6A) and decreased acetyl-CoA entry into the TCA cycle (Fig. S6B). AMPK was activated within 5 min of NaHS treatment (Fig. 6B) and returned to baseline after 30min, while treatment with an AMPK inhibitor (Compound C) prevented the increase in glycolysis, glucose uptake and migration (Fig. 6C; Supplemental Fig. 6C, D). Because of the rapid and transient nature of

AMPK activation, we hypothesized that brief treatment with H_2S would be sufficient to trigger EC migration. Indeed, 10min NaHS treatment was sufficient to promote EC migration during the subsequent 12hr period, and that this was blocked by pharmacological AMPK inhibition (Fig.

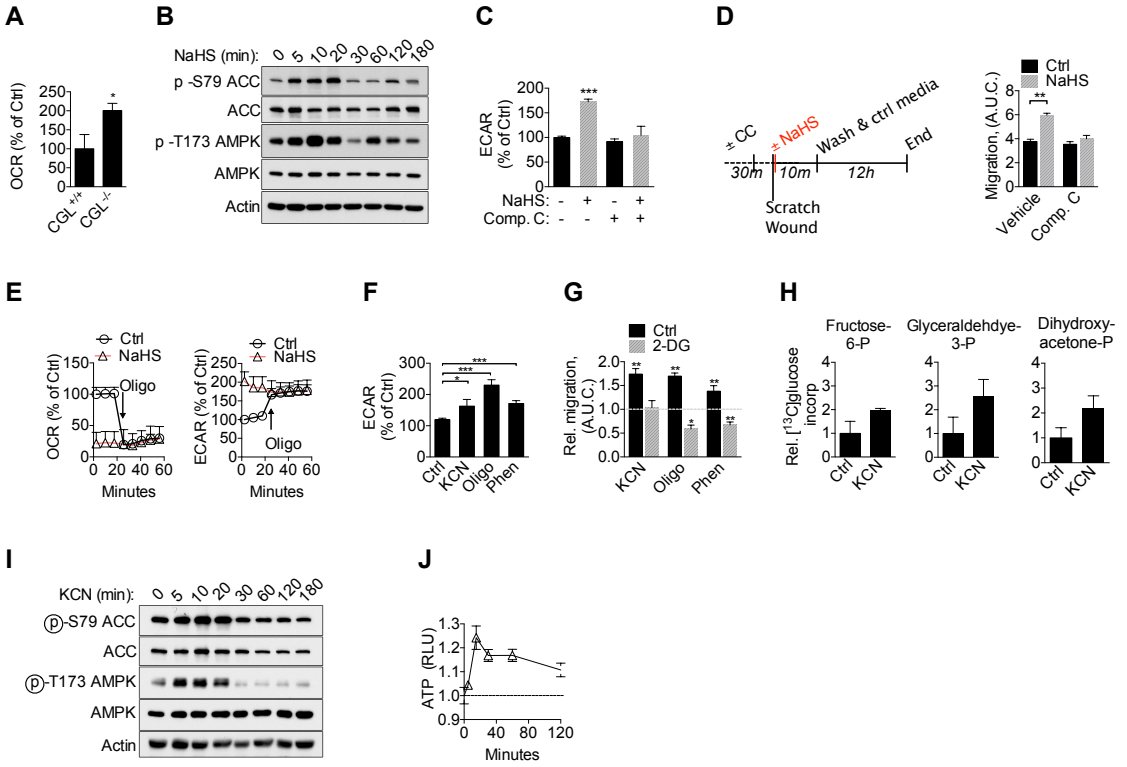

Figure 6

Figure 6: H_2S shifts oxidative/glycolytic balance by transient inhibition of mitochondrial electron transport

(**A**) Basal oxygen consumption rate (OCR) indicative of mitochondrial respiration in $CGL^{+/+}$ and $CGL^{-/-}$ primary mouse EC. (**B**) Western blot of ACC (pSer79, total) and AMPK (Thr172, total) in HUVEC treated with NaHS at the indicated time. (**C**) Extracellular acidification rate (ECAR) indicative of glycolysis in HUVEC pretreated for 1 hr with NaHS (100μM) +/- the AMPK inhibitor Compound C (Comp. C) as indicated. (**D**) Schematic of the experiment (left) and time-dependent wound closure quantification (migration A.U.C., right) in HUVEC treated with NaHS for 10 min in the presence of vehicle or Comp. C (10μM). (**E**) OCR (left) and ECAR (right) over time in HUVEC pretreated for 2 hrs with 100μM NaHS followed by oligomycin (oligo, 2.5μM) injection at the indicated time. (**F**) ECAR in HUVEC pretreated for 2 hrs with cyanide (KCN, 10μM), oligomycin (2μM) or phenformin (Phen, 500μM) expressed as a percent of control over time after addition of 10mM glucose. (**G**) Relative wound closure (migration A.U.C.) expressed as fold change relative to control in HUVEC treated with oligomycin (2μM), phenformin (500μM) or cyanide (10μM) +/- 2DG (1mM) as indicated. (**H**) C13-labeled metabolite levels measured by mass spectrometry-scaled intensity in C13 glucose pulsed HUVEC in the presence or absence of KCN. (**I**) Western blot of ACC (pSer79, total) and AMPK (Thr172, total) in HUVEC treated with KCN (10μM) at the indicated time. (**J**) ATP production in HUVEC treated with KCN at the indicated time. All cell-based assays were repeated at least three times. Error bars indicate SEM; **P* < 0.05, ***P* < 0.005, ****P* < 0.001 compared within genotype to Ctrl by Student's *t* test.

6D). Finally, treatment of ECs with NaHS resulted in a concomitant shift from oxidative phosphorylation to glycolysis that was not further affected upon addition of the Complex V inhibitor oligomycin (Fig. 6E).

A previously established mechanism of H_2S action responsible for its toxicity at high concentrations is non-competitive inhibition of Complex IV of the mitochondrial electron transport chain (ETC) (Wang, 2012). In order to assess the specific contribution of ETC inhibition to the pro-angiogenic activity of H_2S, we compared H_2S to another Complex IV inhibitor, cyanide, as well as oligomycin and the Complex I inhibitor, phenformin. Each ETC inhibitor increased EC glycolysis (Fig. 6F; Fig. S6E) and stimulated 2-DG-sensitive EC migration (Fig. 6G; Fig. S6F) without increasing H_2S (Fig. S6G). Metabolic tracing studies using ^{13}C-glucose (D-Glucose-1,2-$^{13}C_2$) confirmed similar effects of cyanide (KCN) on glycolysis (Fig. 6H), glucose uptake (Fig. S6H), AMPK activation (Fig. 6I) and intracellular ATP (Fig. 6J) as previously observed for H_2S. Importantly, ETC inhibition did not induce EC apoptosis under the same conditions (Fig. S6I). Together, these data are consistent with a mechanism of H_2S action in angiogenesis involving transient inhibition of mitochondrial respiration by direct inhibition of ETC, resulting in a shift from oxidative phosphorylation to glycolysis.

Discussion

A model for a previously unrecognized pro-angiogenic pathway activated by dietary amino acid restriction and controlled by the GCN2/ATF4-dependent AASR is presented in Fig. 7. While VEGF production was the major output of this pathway in muscle fibers, CGL and H_2S production appeared to dominate in ECs. The genetic requirement for CGL in angiogenesis triggered by nutrient deprivation, exercise or VEGF injection strongly suggests an essential role for H_2S in VEGF-mediated angiogenesis independent of the upstream trigger. Finally, we uncovered a mechanistic role for H_2S in boosting rapid anaerobic ATP production via inhibition

of mitochondrial oxidative phosphorylation in ECs, the first time that this otherwise toxic mode of H_2S action has associated with a beneficial outcome.

Translational implications for pro-angiogenic effects of dietary amino acid restriction and SIRT1 activation

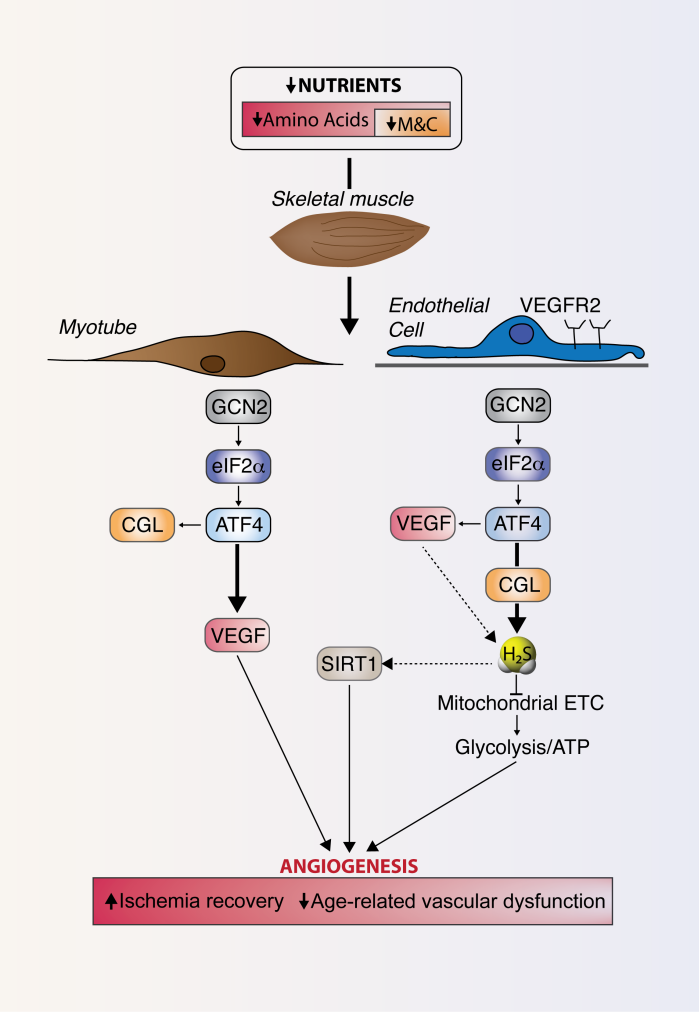

Figure 7

Figure 7: Model for the role of amino acid deprivation in the regulation of angiogenesis through the GCN2/ATF4 amino acid starvation pathway independent of hypoxia, and the role of CGL-mediated H_2S production in the regulation of glycolysis and EC migration downstream of VEGF signaling.

While hypoxia is the best-characterized trigger of VEGF expression and angiogenesis upon vessel occlusion, solid tumor growth or exercise training, oxygen and nutrient restriction are inextricably linked under these circumstances. Yet, little is known about how ECs respond to nutrient restriction independently of hypoxia.

Here, we found that the GCN2/ATF4-dependent AASR was not only activated in ECs upon amino acid restriction independent of hypoxia, but was itself a powerful pro-angiogenic trigger. Activation of this pathway increased VEGF expression in multiple cell types *in vitro* and tissues *in vivo*, and additionally controlled CGL expression and H_2S production in ECs.

These findings reveal the AASR as a new target for modulation of angiogenesis by pharmacological or even dietary manipulations. This has therapeutic value for example in the context of limb ischemia, a major complication of cardiovascular disease and diabetes that is not amenable to treatment by exercise. In the context of cancer chemotherapy, where inhibition of angiogenesis is desired, it is also important to recognize the AASR as an independent pathway with the ability to contribute to tumor vascularization.

Additionally, in an accompanying manuscript, Das et al. report an important interaction between H_2S and SIRT1 in the regulation of angiogenesis in the context of oxidative stress and aging. In ECs subject to oxidative stress *in vitro*, exogenous H_2S potentiated the pro-angiogenic effects of NAD+ supplementation (via NMN addition). As with M&C-induced angiogenesis under normal conditions (Fig. 1E), this effect was dependent on SIRT1 (Das et al.). Strikingly, H_2S/NMN supplementation in old mice reversed age-associated loss of muscle vascular density and improved exercise performance (Das et al.). Although the mechanism by which H_2S augments SIRT1 function remains to be worked out, these data suggest that H_2S and SIRT1 function in a critical axis regulating angiogenesis with the potential to mitigate or reverse oxidative stress-induced and aging-related changes in vascular health.

Loss of vascular function is associated with many of the age-related diseases that restrict human healthspan, including hypertension, atherosclerosis, heart failure, stroke, neurodegeneration and complications of type II diabetes (Askew et al., 2005; Duscha et al., 1999; Rivard et al., 1999; Stern et al., 2003). While many of these phenotypes are ameliorated or reversed by DR in experimental models (Ahmet et al., 2011; Winnik et al., 2015), future experiments are required to determine to what degree increased angiogenic potential contributes to these benefits, and the role of SIRT1 activation (Haigis and Sinclair, 2010; Naiman et al., 2012; Satoh et al., 2013) and increased H_2S production (Hine et al., 2015) in this process. Nonetheless, the potential to modulate these pathways with pharmacological agents

holds promise for leveraging the benefits of DR on vascular health without the need for reduced food intake.

Transcriptional, post-translational and substrate-level regulation of CGL and H_2S production by diet

Previously we found that CGL mRNA and protein levels, as well as hepatic H_2S production capacity, are increased upon DR and repressed by dietary sulfur amino acids, but the molecular requirements for dietary control of H_2S production were not elucidated (Hine et al., 2015). Here, we revealed a requirement for the AASR in the coordinate regulation of CGL as well as VEGF upon nutrient restriction. In all cells tested, sulfur amino acid deprivation increased CGL and VEGF gene expression via the integrated stress response through GCN2 activation and ATF4 stabilization (Lee et al., 2008). Interestingly, additional regulation of H_2S production appeared to occur in ECs on a post-translational level, as evidenced by rapidly increased H_2S production upon VEGF addition, possibly via calcium-calmodulin stimulation of CGL (Yang et al., 2008). Future studies will be required in order to determine the relative contributions of GCN2/ATF4-dependent transcriptional regulation of CGL and VEGF-dependent post-translational activation of H_2S production. Moreover, despite the crucial importance of CGL in ECs (here) and hepatocytes (Hine et al., 2015), the potential role of other H_2S-generating enzymes, CBS or 3-MST, present in other tissues *in vivo* must also be considered.

The use of a fluorescent probe to visualize H_2S production in frozen sections *in vivo* also allowed us to confirm that endogenous H_2S was increased upon amino acid restriction. This was not possible in our previous study (Hine et al., 2015) in which the lead sulfide method was employed because of the requirement for addition of exogenous cysteine as substrate in this assay. Nonetheless, the increase in endogenous H_2S production by CGL in ECs upon removal of its substrate, Cys, from the diet presents an apparent paradox. It should be pointed out, however, that the source of free Cys for H_2S generation by CGL is not currently known, but

could come from pools distinct from diet-derived or de novo-produced Cys. For example, cytoplasmic glutathione levels which are in the millimolar concentration range could be utilized to produce Cys, as could lysosomal Cys produced upon autophagy, which is also increased in the context of nutrient deficiency. In support of this latter notion, the benefits of MR on longevity in yeast require autophagy (Ruckenstuhl et al., 2014).

Mechanisms of H_2S action in ECs

While the major mechanism by which H_2S is thought exert its biological activities is through post-translational modification of target proteins via sulfhydration of surface-exposed cysteine residues, thus altering protein activity (Mishanina et al., 2015), H_2S can also alter the function of metal-containing proteins via direct interaction with metallocenters. A classic example of this is sulfide coordination of the copper-heme iron complex in Complex IV of the mitochondrial ETC that reversibly inhibits terminal electron transfer to oxygen (Nicholls and Kim, 1982).

Our data regarding inhibition of mitochondrial respiration in the pro-angiogenic effects of H_2S in ECs is consistent with the importance of this latter mechanism of H_2S action in biology, not only for its toxicity at high H_2S concentrations, but also for its ability to alter cellular oxidative/glycolytic energy balance at physiological levels. EC generate 85% of their ATP via glycolysis, and are thus “addicted” to glucose (De Bock et al., 2013). Despite the significantly lower energy yield per molecule of glucose via glycolysis (2 ATP) vs. oxidative metabolism (34 ATP), glycolysis offers other advantages to ECs. For instance, anaerobic glucose metabolism enables ECs to vascularize avascular anoxic tissues, an activity that would not be possible if they would rely primarily on oxidative glucose metabolism. Furthermore, glycolysis can generate more molecules of ATP in a shorter time span as compared to oxidative metabolism, thus rapidly providing ECs with the necessary energy to sprout and form new vessels, and thereby quickly restore oxygen supply to the surrounding tissue.

The effects of H_2S on cellular energy metabolism may also have important implications for cancer, both in terms of therapeutic inhibition of angiogenesis (Schoors et al., 2014) as well as in energy metabolism of the tumor itself. Interestingly, a number of tumors and cancer cells lines upregulate GCN2 (Lehman et al., 2015; Wang et al., 2013) or H_2S production (Bhattacharyya et al., 2013; Sen et al., 2015; Sonke et al., 2015; Szabo et al., 2013), and thus possibly contributing to the Warburg effect through inhibition of mitochondrial respiration.

In the context of ageing, genetic alteration of the worm electron transport chain that reduced mitochondrial function results in a longer lifespan (Dillin et al., 2002; Lee et al., 2003). This is potentially counterintuitive, as normal ageing in humans as well as premature aging in mouse models is also associated with reduced mitochondrial function (Short et al., 2005; Trifunovic et al., 2004). Although further experiments are required, the notion that H_2S is a reversible inhibitor of Complex IV could explain the difference between it and cyanide, a lethal compound that irreversibly inhibits the same ETC component. In support of this idea, mice with transient or partial deletion of various mitochondrial electron transport components prolong life, (Liu et al., 2005) while severe mitochondrial impairment shortens lifespan of worms (Rea et al., 2007).

Experimental Procedures

Mice

All experiments were performed with the approval of the Harvard Medical Area or Boston University Institutional Animal Care and Use Committee (IACUC). 8-14 wk old male or female C57BL/6 mice (The Jackson Laboratory, Bar Harbor, ME) were used for all experiments unless otherwise indicated. Male and female $CGL^{+/+}$ and $CGL^{-/-}$ mice on a mixed 129/C57BL/6 background (Yang et al., 2008) and GCN2 KO and control mice on a C57BL/6 background (Peng et al., 2012) were bred at our facility.

Dietary regimens: Mice were given *ad libitum* (AL) access to food and water unless otherwise indicated. Experimental diets were based on Research Diets D12450B with approximately 18% of calories from protein (hydrolysed casein or individual crystalline amino acids (Ajinomoto) in the proportions present in casein), 10% from fat and 72% from carbohydrate. MR diets containing 1.5g Met/kg food and lacking Cys (Miller et al., 2005) in the context of a 14% protein/ 76% carbohydrate calorie diet were provided AL. In experiments with $CGL^{+/+}$ and $CGL^{-/-}$ mice, the control diet was supplemented with 4.3g Cys/kg food to compensate for the inability of $CGL^{-/-}$ mice to make Cys. AL food intake per gram of body weight was monitored daily for several days and used to calculate calorie restriction (CR) based on initial animal weights. Protein free diets were kept isocaloric by replacing casein/amino acids with an equal weight of sucrose and provided either AL or 40-50% CR as indicated. Animals were fed daily with fresh food between 6pm and 7pm. Water-only fasting was accomplished by transferring mice to a fresh cage with free access to water but without food for 3 d.

Pharmacological interventions: Axitinib and L-NAME were supplemented at a daily dose of ~30mg/kg/d and 80mg/kg/d respectively in the food as previously described (Alonso et al., 2010; Ma and Waxman, 2008).

Adenoviral-mediated gene delivery: Local overexpression of CGL or VEGF in gastrocnemius was accomplished by intramuscular injection of 40 µl of 10^9 PFUs of an

adenovirus-type 5 (dE1/E3) containing the CMV promoter driving expression of the mouse CGL gene (Ad-mCTH/CGL, Genbank RefSeq BC019483, ADV-256305 Vector Biolabs) or the human VEGF gene (Ad-hVEGFA165 Genbank RefSeq NM_001171626, Vector Biolabs) or the negative control virus Ad-CMV-Null (1300 Vector Biolabs) once weekly for 2 wks.

Hindlimb ischemia model

12 wk old C57BL/6 (wild-type) WT mice were anaesthetized with isoflurane and body temperature maintained on a circulating heated water pad. Following a 1 cm groin incision, the neurovascular pedicle was visualized under a microscope (LW Scientific, Z2 Zoom Stereoscope) and the femoral nerve carefully dissected out. The femoral vein (located medially) was separated from the femoral artery (located laterally) allowing electrocoagulation of the left common femoral artery, proximal to the bifurcation of superficial and deep femoral artery while sparing the vein and nerve. Once the artery was occluded, the surgical site was inspected for any residual bleeding (Hoefer et al., 2004; Mirabella et al., 2011).

Laser Doppler perfusion imaging (LDPI) was performed as described previously (Hoefer et al., 2004; Mirabella et al., 2011). Briefly, mice were kept under isoflurane anaesthesia, and body temperature maintained on a circulating heated water pad. Blood flow recovery was monitored at d 0 (immediately post-surgery), d1, d3, and d10 using an LDPI analyzer (Moor Instruments, Inc. DE). The LDPI intensity of the ischemic foot was normalized to the contralateral foot and represented as relative blood flow of the ischemic limb (Ischemic/Non-ischemic ratio).

Mouse Exercise Training

12 wk old male 129/C57BL/6 WT and CGL KO mice were randomized into sedentary or exercise group. Mice were exercised on a Columbus Instruments 6 lane treadmill. Mice were acclimatized to the treadmill at 8 m/min for 5 min for 3d prior to exercise training. Mice ran 30min/d at 5° incline at 12 m/min for the first wk of training. Mice continued running 30min/d at 5° incline at 14 m/min for an additional 3 wk to reach 1 mo total of exercise training. Sedentary

controls and exercised animals were co-housed. Mice were euthanized 1 hr after the final exercise bout (Narkar et al., 2008; Narkar et al., 2011).

Gene expression analysis by qPCR

Total RNA was isolated from tissues and cells using RNeasy Mini Kit (Qiagen) and cDNA synthesized by random hexamer priming with the Verso cDNA kit (Thermo). qRT-PCR was performed with SYBR green dye (Lonza) and TaqPro DNA polymerase (Denville). Fold changes were calculated by the $\Delta\Delta C_t$ method using Hprt, 18S and/or b-Actin genes as standards, and normalized to the experimental control. Primer sequences are as follows:

mouse **CGL** F: TTGGATCGAAACACCCACAAA R: AGCCGACTATTGAGGTCATCA

mouse **HPRT** F: TTTCCCTGGTTAAGCAGTACAGCCC R:

TGGCCTGTATCCAACACTTCGAGA

mouse **Actin** F:AGCTTCTTTGCAGCTCCTTCGTTG R:TTCTGACCCATTCCCACCATCACA

mouse **18S** F: CATGCAGAACCCACGACAGTA R: CCTCACGCAGCTTGTTGTCTA

mouse **VEGF** F: CTGTAACGATGAAGCCCTGGAG R: TGGTGAGGTTTGATCCGCAT

mouse **ATF4** F: GAA ATG GCC GGC TAT GG R: TCC CGG AAA AGG CAT CCT

mouse **ASNS F:** GTCAAGAACTCCTGGTTCAAG R: GATCTGACGGTAGAAGTAGC

human **VEGF** F: AGCTGCGCTGATAGACATCC R: CTACCTCCACCATGCCAAGT

human **HIF1a** F: GAAGTGGCAACTGATGAGCA R: GCGCGAACGACAAGAAA

human **PGC1a** F: CTGCTAGCAAGTTTGCCTCA R: AGTGGTGCAGTGACCAATCA

human **CGL** F: CAACATCACTGTGGCCATTC R: AGAGGCAGCAATTACACCAGA

human **ATF4** F: CTATACCCAACAGGGCATCC R: GTCCCTCCAACAACAGCAAG

human **ASNS** F: GCGGAGTGCTTCAATGTAAC R: CCAATAAGAAAGTGTTCCTGGG

human **ACTIN** F: GTTGTCGACGACGAGCG R: GCACAGAGCCTCGCCTT

human **HPRT** F: ACCCTTTCCAAATCCTCAGC R: GTTATGGCGACCCGCAG

Immunoblotting

Cells were homogenized with passive lysis buffer (Promega), normalized for protein content, boiled with SDS loading buffer and separated by SDS-PAGE. Proteins were transferred to PVDF membrane (Whatman) and blotted for CGL (ab151769 Abcam), HIF1a (10006421 Cayman Chemical), p-eIF2a Ser51 (9712S Cell Signaling), total eIF2a (9722S Cell Signaling), ATF4 (11815 Cell Signaling), Actin (13E5 Cell Signaling) and Tubulin (2146S Cell Signaling) and secondarily with HPR conjugated anti-rabbit antibody (Dako).

VEGF ELISA

Mouse VEGF ELISA kit was purchased from Peprotech and the assay was performed as per manufacturer's instructions. 100 µl of plasma or cell culture media was used for each analysis.

Immunostaining

CD31 immunostaining was performed on 50 µm frozen sections of unfixed gastrocnemius muscle using the primary anti-mouse CD31 (17-0311-82, ebioscience), anti-mouse VEGF (Novus Biologicals) and Isolectin B4 (Life Technologies) at a dilution of 1:100. Sections were fixed for 5 min with PFA 4% and rinsed in PBS, the immunostaining was then performed as previously described (Longchamp et al., 2014). CD31 area was quantified from randomly photographed 10 µM stack sections (6 images per section, 4 sections per muscle per mouse) using Fiji software (http://fiji.sc/Fiji). All quantifications were performed blindly.

H_2S measurements

Lead sulfide method on live cells: For detection of H_2S production in live cells, growth media was supplemented with 10mM Cys and 10 µM Pyridoxal 5'-phosphate hydrate (PLP, Sigma), and a lead 6x4 inch pieces of lead acetate paper, made by soaking 703 size blotting paper (VWR) in 20 mM lead acetate (Sigma) and then vacuum drying, was placed over the plate for 2-24 hrs of further incubation in a CO_2 incubator at $37^{O}C$ until lead sulfide was detected but not saturated.

H_2S detection with fluorescent probe on live cells: For detection of endogenous H_2S production in live cells, growth media was supplemented with 10 μM P3 probe *(Singha et al., 2015)* for 30 min prior to fixation. Quantitative measurements were performed with a microplate reader (Biotek Synegy2) using a 360 nm excitation and 528 nm emission wavelength. Qualitative assessment was performed using a 2 photon microscope (Zeiss LSM780 w/ Mai Tai HP 2-photon laser (Spectra Physics) at 880 nm excitation and 520-550 emission *(Singha et al., 2015)*.

H_2S detection with fluorescent probe on tissue sections: 50 μm frozen sections of unfixed gastrocnemius muscle were incubated with 20 μM P3 probe *(Singha et al., 2015)* for 5 min and washed with PBS 2 times. Sections were then fixed for 5 min in 4% PFA prior to immunostaining as described above.

Cell culture conditions

Simulated in vitro MR: Pooled human umbilical vein endothelial cells (HUVECs) were obtained from Lonza (C2519A, Lonza) and used between passage 1 and 5. HUVECs were cultured in endothelial basal medium (EBM-2) supplemented with 2% FBS and endothelial growth medium SingleQuots (Clonetics, Lonza) at $37^{O}C$ in 5% O_2. Complete media are denoted as “control” (Ctrl) throughout the manuscript.

Primary hepatocytes were isolated by collagenase treatment (Liberase, Roche), Percoll (GE Healthcare) gradient centrifugation and initially cultured in William’s E media (Sigma) with 5% FBS for several hours.

Primary mouse endothelial cells were isolated from the lung by collagenase digestion (Liberase, Roche) followed by sequential affinity selection method using Dynabeads™ goat anti-rat conjugated to rat-anti mouse CD31 (BD Biosciences, San Jose, CA), and cultured in endothelial basal medium (EBM-2) supplemented with 2% FBS and endothelial growth medium SingleQuots (Clonetics, Lonza). At least three independent primary mouse EC cultures per genotype was tested per experiment.

When cultures reached confluence, the media was removed and replaced either with complete DMEM or DMEM lacking Met&Cys (Sigma) both supplemented with the same amount of dialysed FBS plus endothelial growth medium SingleQuots (Clonetics, Lonza) from 1 to 24 hrs.

Pharmacological interventions and hypoxia: L-NAME (100 μM), NaHS (100 μM), PAG (100 μM), SU5416 (20 μM), Axitinib (10 μM) and Ex527 (10 μM) were supplemented as previously described (Alonso et al., 2010; Hine et al., 2015; Price et al., 2012). Hypoxia was induced via oxygen displacement with nitrogen gas.

Transient transfection and siRNA knockdown in vitro: siRNA knockdown of human activating transcription factor 4 (ATF4), human endothelial nitric oxide synthase (eNOS), human hypoxia-inducible factor 1-alpha (HIF1a) and scrambled control was performed in HUVEC using lipofectamine RNAiMAX (Life Technologies) and 30nM siRNA purchased from Ambion (Ambion, Life Technologies) as described previously (Hine et al., 2015). All experiments were performed 2 d after transfection. Knockdown was confirmed by immunoblot and/or qPCR.

Adenoviral-mediated gene delivery in vitro: HUVEC were infected overnight in complete medium and collected 2 d later using Ad-m-CTH or the negative control virus Ad-CMV-Null adenovirus amplified and purified by Vector Biolabs (Philadelphia, PA, U.S.A.).

Spheroid capillary sprouting assay

Hanging drops of HUVEC or primary mouse ECs in EGM2 (De Bock et al., 2013) were embedded in Matrigel® (Corning) and cultured in the indicated media for 24 hrs to induce sprouting. Compounds were added at the indicated concentrations during the gel culture step, using corresponding vehicle concentrations as control. Images were captured with a Zeiss LSM 510 Meta NLO confocal microscope (oil objectives: x 40 with NA 1.3, x 63 with NA1.4, x 100 with NA 1.3; Carl Zeiss, Munich, Germany) or a Leica laser-scanning SP5 confocal microscope (Leica, Manheim, Germany). Analysis of the sprout length was performed using ImageJ software.

Wound healing assay

A single scratch wound was created using a sterile p200 pipette tip on a confluent field of ECs, 24 hrs after seeding (100,000 cells per well in 24-well plate) and after cells were mitotically arrested (1 µg/ml MitoC overnight). Repopulation across the scratch wound was recorded by phase-contrast microscopy every 4 hrs for up to 20 hrs using a digital camera. Wound closure (gap area at time = x hr relative to time = 0 hr) was determined at each time point from digital images using ImageJ software.

Glucose uptake

HUVEC were pretreated for 1 hr with VEGF (peprotech) 50ng/ml, NaHS 100µM or KCN 10µM. Cells were then depleted in Krebs-Ringer Bicarbonate Buffer (KRB; NaH2PO4/Na2HPO4 10mM, NaCl 136mM, KCl 4.7mM, MgSO4 1.25mM, CaCl2 1.25mM, pH7.4), without glucose and serum for 30 min and then incubated for 6 min in a solution containing 0.5µCi 2-DG. On ice, cells were then washed in cold PBS 3 times, lysed, and sample counted in a liquid scintillation counter. Samples were normalized to protein content as measured from the same cells by BCA.

Seahorse

Cellular oxygen consumption and extracellular acidification rate was measured using the Seahorse Cell Metabolism Analyzer XF96 (Seahorse Biosciences). Cells were plated at a density of 12,000 cells and untreated or pretreated with 100 µM NaHS, Cyanide 10 µM or Phenformin 500µM for 2 hrs. After 24 hrs, media was changed to unbuffered XF assay media with 0 or 11mM glucose, 0 or 2mM glutamine and pyruvate at pH7.4 and basal OCR and ECAR measured for 5 blocks of 2 min mixing and 5 min measuring. Glucose (10 mM final), 2-DG (50 mM final) and Oligomycin (2.5 µM final) were injected at indicated times. All plates were normalized to protein content as measured from the same cells after Seahorse by BCA.

Metabolite profiling for glucose flux analyses

To determine the relative levels of intracellular metabolites, extracts were prepared and analyzed by LC/MS/MS. Triplicate 15-cm confluent plates were incubated in EGM-2 media in

presence or absence of 100 μM NaHS 105 min prior to extraction. For D-[1,2-^{13}C]- glucose flux studies, cells were washed once with serum- and glucose free DMEM and then incubated in DMEM containing a 10 mM 1:1 mixture of D-[1,2-^{13}C]-glucose and unlabeled D-glucose for 15 min. Metabolites were extracted on dry ice with 4-mL 80% methanol (-80°C), as described previously (Ben-Sahra et al., 2013). Insoluble material was pelleted by centrifugation at 3000*g* for 5 min, followed by two subsequent extractions of the insoluble pellet with 0.5-ml 80% methanol, with centrifugation at 16000*g* for 5 min. The 5 ml metabolite extract from the pooled supernatants was dried down under nitrogen gas using an N-EVAP (Organomation Associates, Inc).

Dried pellets were resuspended using 20 μL HPLC grade water for mass spectrometry. 10 μL were injected and analyzed using a 5500 QTRAP triple quadrupole mass spectrometer (AB/SCIEX) coupled to a Prominence UFLC HPLC system (Shimadzu) via selected reaction monitoring (SRM). Some metabolites were targeted in both positive and negative ion mode for a total of 287 SRM transitions using pos/neg polarity switching. ESI voltage was +4900V in positive ion mode and –4500V in negative ion mode. The dwell time was 3 ms per SRM transition and the total cycle time was 1.55 seconds. Approximately 10-14 data points were acquired per detected metabolite. Samples were delivered to the MS via normal phase chromatography using a 4.6 mm i.d x 10 cm Amide Xbridge HILIC column (Waters Corp.) at 350 μL/min. Gradients were run starting from 85% buffer B (HPLC grade acetonitrile) to 42% B from 0-5 minutes; 42% B to 0% B from 5-16 minutes; 0% B was held from 16-24 minutes; 0% B to 85% B from 24-25 min; 85% B was held for 7 min to re-equilibrate the column. Buffer A was comprised of 20 mM ammonium hydroxide/20 mM ammonium acetate (pH=9.0) in 95:5 water:acetonitrile. Peak areas from the total ion current for each metabolite SRM transition were integrated using MultiQuant v2.0 software (AB/SCIEX). For stable isotope labeling experiments, custom SRMs were created for expected ^{13}C incorporation in various forms for targeted

LC/MS/MS. Peak areas of metabolites detected by mass spectrometry were normalized to median and then normalized to protein concentrations.

Statistical analyses

Data are displayed as means +/- standard error of the mean (SEM) and statistical significance assessed in GraphPad Prism using Student's t tests unless otherwise specified. A P-value of 0.05 or less was deemed statistically significant.

Author Contributions

A.L., T.M., A.D., C.H., L.E.B., I. B.S., P.M., M.T., G.S, C.C. and J.R.M. contributed to the performance of the experiments and/or analysis of the data; N.K., J.H.T.-V., R.W., J.-A.H., K.H.A., J.-M.C., K.H.A., B.D.M., C.-H.L. and D.A.S. advised on design and execution of experiments and/or provided critical expertise and reagents; A.L., T.M., A.D., C.H., C.C., C.K.O and J.R.M. designed the experiments; A.L. and J.R.M. wrote the paper; J.R.M. conceived and directed the study. All authors discussed the results and commented on the manuscript.

Acknowledgements

We thank Florant Allagnat for critical discussions and reading the manuscript; Andrew Thompson, Nandan Nurukar and Rohan Kulkarni for technical assistance; Gokhan Hotamisligil for the use of the Seahorse; and Constance Cepko for the use of the 2-photon microscope. This work was supported by grants from the Swiss National Science Foundation (P1LAP3_158895) to A.L.; National Science Foundation (NSF-DGE1144152) to L.E.B.; the Canadian Institutes of Health Sciences to R.W.; NIH (EB00262) to C.C.; American Heart Association (12GRNT9510001, 12GRNT1207025), Lea Carpenter du Pont Vascular Surgery Fund, and Carl and Ruth Shapiro Family Foundation to C.K.O.; and NIH (AG036712, DK090629) to J.R.M. The authors declare no competing financial interests.

References

Ahmet, I., Tae, H.J., de Cabo, R., Lakatta, E.G., and Talan, M.I. (2011). Effects of calorie restriction on cardioprotection and cardiovascular health. J Mol Cell Cardiol *51*, 263-271.
Alonso, F., Krattinger, N., Mazzolai, L., Simon, A., Waeber, G., Meda, P., and Haefliger, J.A. (2010). An angiotensin II- and NF-kappaB-dependent mechanism increases connexin 43 in murine arteries targeted by renin-dependent hypertension. Cardiovasc Res *87*, 166-176.
Altaany, Z., Ju, Y., Yang, G., and Wang, R. (2014). The coordination of S-sulfhydration, S-nitrosylation, and phosphorylation of endothelial nitric oxide synthase by hydrogen sulfide. Sci Signal *7*, ra87.
Arany, Z., Foo, S.Y., Ma, Y., Ruas, J.L., Bommi-Reddy, A., Girnun, G., Cooper, M., Laznik, D., Chinsomboon, J., Rangwala, S.M.*, et al.* (2008). HIF-independent regulation of VEGF and angiogenesis by the transcriptional coactivator PGC-1alpha. Nature *451*, 1008-1012.
Askew, C.D., Green, S., Walker, P.J., Kerr, G.K., Green, A.A., Williams, A.D., and Febbraio, M.A. (2005). Skeletal muscle phenotype is associated with exercise tolerance in patients with peripheral arterial disease. J Vasc Surg *41*, 802-807.
Ben-Sahra, I., Howell, J.J., Asara, J.M., and Manning, B.D. (2013). Stimulation of de novo pyrimidine synthesis by growth signaling through mTOR and S6K1. Science *339*, 1323-1328.
Bhattacharyya, S., Saha, S., Giri, K., Lanza, I.R., Nair, K.S., Jennings, N.B., Rodriguez-Aguayo, C., Lopez-Berestein, G., Basal, E., Weaver, A.L.*, et al.* (2013). Cystathionine beta-synthase (CBS) contributes to advanced ovarian cancer progression and drug resistance. PLoS One *8*, e79167.
Cantó, C., and Auwerx, J. (2009). Caloric restriction, SIRT1 and longevity. Trends Endocrinol Metab *20*, 325-331.
Chu, H., and Wang, Y. (2012). Therapeutic angiogenesis: controlled delivery of angiogenic factors. Ther Deliv *3*, 693-714.
Coletta, C., Papapetropoulos, A., Erdelyi, K., Olah, G., Módis, K., Panopoulos, P., Asimakopoulou, A., Gerö, D., Sharina, I., Martin, E.*, et al.* (2012). Hydrogen sulfide and nitric oxide are mutually dependent in the regulation of angiogenesis and endothelium-dependent vasorelaxation. Proc Natl Acad Sci U S A *109*, 9161-9166.
Colman, R.J., Anderson, R.M., Johnson, S.C., Kastman, E.K., Kosmatka, K.J., Beasley, T.M., Allison, D.B., Cruzen, C., Simmons, H.A., Kemnitz, J.W.*, et al.* (2009). Caloric restriction delays disease onset and mortality in rhesus monkeys. Science *325*, 201-204.
De Bock, K., Georgiadou, M., Schoors, S., Kuchnio, A., Wong, B.W., Cantelmo, A.R., Quaegebeur, A., Ghesquière, B., Cauwenberghs, S., Eelen, G.*, et al.* (2013). Role of PFKFB3-driven glycolysis in vessel sprouting. Cell *154*, 651-663.
Dillin, A., Hsu, A.L., Arantes-Oliveira, N., Lehrer-Graiwer, J., Hsin, H., Fraser, A.G., Kamath, R.S., Ahringer, J., and Kenyon, C. (2002). Rates of behavior and aging specified by mitochondrial function during development. Science *298*, 2398-2401.
Duscha, B.D., Kraus, W.E., Keteyian, S.J., Sullivan, M.J., Green, H.J., Schachat, F.H., Pippen, A.M., Brawner, C.A., Blank, J.M., and Annex, B.H. (1999). Capillary density of skeletal muscle: a contributing mechanism for exercise intolerance in class II-III chronic heart failure independent of other peripheral alterations. J Am Coll Cardiol *33*, 1956-1963.
Fontana, L., Partridge, L., and Longo, V.D. (2010). Extending healthy life span--from yeast to humans. Science *328*, 321-326.

Fukumura, D., Kashiwagi, S., and Jain, R.K. (2006). The role of nitric oxide in tumour progression. Nat Rev Cancer *6*, 521-534.
Haigis, M.C., and Sinclair, D.A. (2010). Mammalian sirtuins: biological insights and disease relevance. Annu Rev Pathol *5*, 253-295.
Hine, C., Harputlugil, E., Zhang, Y., Ruckenstuhl, C., Lee, B.C., Brace, L., Longchamp, A., Treviño-Villarreal, J.H., Mejia, P., Ozaki, C.K.*, et al.* (2015). Endogenous hydrogen sulfide production is essential for dietary restriction benefits. Cell *160*, 132-144.
Hoefer, I.E., van Royen, N., Rectenwald, J.E., Deindl, E., Hua, J., Jost, M., Grundmann, S., Voskuil, M., Ozaki, C.K., Piek, J.J.*, et al.* (2004). Arteriogenesis proceeds via ICAM-1/Mac-1-mediated mechanisms. Circ Res *94*, 1179-1185.
Hursting, S.D., Dunlap, S.M., Ford, N.A., Hursting, M.J., and Lashinger, L.M. (2013). Calorie restriction and cancer prevention: a mechanistic perspective. Cancer Metab *1*, 10.
Katsouda, A., Bibli, S.I., Pyriochou, A., Szabo, C., and Papapetropoulos, A. (2016). Regulation and role of endogenously produced hydrogen sulfide in angiogenesis. Pharmacol Res *113*, 175-185.
Kolluru, G.K., Bir, S.C., Yuan, S., Shen, X., Pardue, S., Wang, R., and Kevil, C.G. (2015). Cystathionine γ-lyase regulates arteriogenesis through NO dependent monocyte recruitment. Cardiovasc Res.
Kondo, M., Shibata, R., Miura, R., Shimano, M., Kondo, K., Li, P., Ohashi, T., Kihara, S., Maeda, N., Walsh, K.*, et al.* (2009). Caloric restriction stimulates revascularization in response to ischemia via adiponectin-mediated activation of endothelial nitric-oxide synthase. J Biol Chem *284*, 1718-1724.
Lee, J.I., Dominy, J.E., Sikalidis, A.K., Hirschberger, L.L., Wang, W., and Stipanuk, M.H. (2008). HepG2/C3A cells respond to cysteine deprivation by induction of the amino acid deprivation/integrated stress response pathway. Physiol Genomics *33*, 218-229.
Lee, S.S., Lee, R.Y., Fraser, A.G., Kamath, R.S., Ahringer, J., and Ruvkun, G. (2003). A systematic RNAi screen identifies a critical role for mitochondria in C. elegans longevity. Nat Genet *33*, 40-48.
Lehman, S.L., Ryeom, S., and Koumenis, C. (2015). Signaling through alternative Integrated Stress Response pathways compensates for GCN2 loss in a mouse model of soft tissue sarcoma. Sci Rep *5*, 11781.
Lin, V.S., Lippert, A.R., and Chang, C.J. (2013). Cell-trappable fluorescent probes for endogenous hydrogen sulfide signaling and imaging H2O2-dependent H2S production. Proc Natl Acad Sci U S A *110*, 7131-7135.
Liu, X., Jiang, N., Hughes, B., Bigras, E., Shoubridge, E., and Hekimi, S. (2005). Evolutionary conservation of the clk-1-dependent mechanism of longevity: loss of mclk1 increases cellular fitness and lifespan in mice. Genes Dev *19*, 2424-2434.
Liu, Y., Cox, S.R., Morita, T., and Kourembanas, S. (1995). Hypoxia regulates vascular endothelial growth factor gene expression in endothelial cells. Identification of a 5' enhancer. Circ Res *77*, 638-643.
Longchamp, A., Alonso, F., Dubuis, C., Allagnat, F., Berard, X., Meda, P., Saucy, F., Corpataux, J.M., Déglise, S., and Haefliger, J.A. (2014). The use of external mesh reinforcement to reduce intimal hyperplasia and preserve the structure of human saphenous veins. Biomaterials *35*, 2588-2599.
Ma, J., and Waxman, D.J. (2008). Modulation of the antitumor activity of metronomic cyclophosphamide by the angiogenesis inhibitor axitinib. Mol Cancer Ther *7*, 79-89.

Miller, R.A., Buehner, G., Chang, Y., Harper, J.M., Sigler, R., and Smith-Wheelock, M. (2005). Methionine-deficient diet extends mouse lifespan, slows immune and lens aging, alters glucose, T4, IGF-I and insulin levels, and increases hepatocyte MIF levels and stress resistance. Aging Cell *4*, 119-125.
Mirabella, T., Teodelinda, M., Cilli, M., Michele, C., Carlone, S., Sebastiano, C., Cancedda, R., Ranieri, C., Gentili, C., and Chiara, G. (2011). Amniotic liquid derived stem cells as reservoir of secreted angiogenic factors capable of stimulating neo-arteriogenesis in an ischemic model. Biomaterials *32*, 3689-3699.
Mishanina, T.V., Libiad, M., and Banerjee, R. (2015). Biogenesis of reactive sulfur species for signaling by hydrogen sulfide oxidation pathways. Nat Chem Biol *11*, 457-464.
Mustafa, A.K., Gadalla, M.M., Sen, N., Kim, S., Mu, W., Gazi, S.K., Barrow, R.K., Yang, G., Wang, R., and Snyder, S.H. (2009). H2S signals through protein S-sulfhydration. Sci Signal *2*, ra72.
Naiman, S., Kanfi, Y., and Cohen, H.Y. (2012). Sirtuins as regulators of mammalian aging. Aging (Albany NY) *4*, 521-522.
Narkar, V.A., Downes, M., Yu, R.T., Embler, E., Wang, Y.X., Banayo, E., Mihaylova, M.M., Nelson, M.C., Zou, Y., Juguilon, H.*, et al.* (2008). AMPK and PPARdelta agonists are exercise mimetics. Cell *134*, 405-415.
Narkar, V.A., Fan, W., Downes, M., Yu, R.T., Jonker, J.W., Alaynick, W.A., Banayo, E., Karunasiri, M.S., Lorca, S., and Evans, R.M. (2011). Exercise and PGC-1α-independent synchronization of type I muscle metabolism and vasculature by ERRγ. Cell Metab *13*, 283-293.
Nicholls, P., and Kim, J.K. (1982). Sulphide as an inhibitor and electron donor for the cytochrome c oxidase system. Can J Biochem *60*, 613-623.
Olsson, A.K., Dimberg, A., Kreuger, J., and Claesson-Welsh, L. (2006). VEGF receptor signalling - in control of vascular function. Nat Rev Mol Cell Biol *7*, 359-371.
Omodei, D., and Fontana, L. (2011). Calorie restriction and prevention of age-associated chronic disease. FEBS Lett *585*, 1537-1542.
Orentreich, N., Matias, J.R., DeFelice, A., and Zimmerman, J.A. (1993). Low methionine ingestion by rats extends life span. J Nutr *123*, 269-274.
Papapetropoulos, A., Pyriochou, A., Altaany, Z., Yang, G., Marazioti, A., Zhou, Z., Jeschke, M.G., Branski, L.K., Herndon, D.N., Wang, R.*, et al.* (2009). Hydrogen sulfide is an endogenous stimulator of angiogenesis. Proc Natl Acad Sci U S A *106*, 21972-21977.
Peng, W., Robertson, L., Gallinetti, J., Mejia, P., Vose, S., Charlip, A., Chu, T., and Mitchell, J.R. (2012). Surgical stress resistance induced by single amino acid deprivation requires Gcn2 in mice. Sci Transl Med *4*, 118ra111.
Perrone, C.E., Malloy, V.L., Orentreich, D.S., and Orentreich, N. (2013). Metabolic adaptations to methionine restriction that benefit health and lifespan in rodents. Exp Gerontol *48*, 654-660.
Potente, M., Ghaeni, L., Baldessari, D., Mostoslavsky, R., Rossig, L., Dequiedt, F., Haendeler, J., Mione, M., Dejana, E., Alt, F.W.*, et al.* (2007). SIRT1 controls endothelial angiogenic functions during vascular growth. Genes Dev *21*, 2644-2658.
Potente, M., Urbich, C., Sasaki, K., Hofmann, W.K., Heeschen, C., Aicher, A., Kollipara, R., DePinho, R.A., Zeiher, A.M., and Dimmeler, S. (2005). Involvement of Foxo transcription factors in angiogenesis and postnatal neovascularization. J Clin Invest *115*, 2382-2392.

Price, N.L., Gomes, A.P., Ling, A.J., Duarte, F.V., Martin-Montalvo, A., North, B.J., Agarwal, B., Ye, L., Ramadori, G., Teodoro, J.S*., et al.* (2012). SIRT1 is required for AMPK activation and the beneficial effects of resveratrol on mitochondrial function. Cell Metab *15*, 675-690.
Rea, S.L., Ventura, N., and Johnson, T.E. (2007). Relationship between mitochondrial electron transport chain dysfunction, development, and life extension in Caenorhabditis elegans. PLoS Biol *5*, e259.
Rivard, A., Fabre, J.E., Silver, M., Chen, D., Murohara, T., Kearney, M., Magner, M., Asahara, T., and Isner, J.M. (1999). Age-dependent impairment of angiogenesis. Circulation *99*, 111-120.
Rowe, G.C., Raghuram, S., Jang, C., Nagy, J.A., Patten, I.S., Goyal, A., Chan, M.C., Liu, L.X., Jiang, A., Spokes, K.C*., et al.* (2014). PGC-1α induces SPP1 to activate macrophages and orchestrate functional angiogenesis in skeletal muscle. Circ Res *115*, 504-517.
Ruckenstuhl, C., Netzberger, C., Entfellner, I., Carmona-Gutierrez, D., Kickenweiz, T., Stekovic, S., Gleixner, C., Schmid, C., Klug, L., Sorgo, A.G*., et al.* (2014). Lifespan extension by methionine restriction requires autophagy-dependent vacuolar acidification. PLoS Genet *10*, e1004347.
Satoh, A., Brace, C.S., Rensing, N., Cliften, P., Wozniak, D.F., Herzog, E.D., Yamada, K.A., and Imai, S. (2013). Sirt1 extends life span and delays aging in mice through the regulation of Nk2 homeobox 1 in the DMH and LH. Cell Metab *18*, 416-430.
Schoors, S., De Bock, K., Cantelmo, A.R., Georgiadou, M., Ghesquière, B., Cauwenberghs, S., Kuchnio, A., Wong, B.W., Quaegebeur, A., Goveia, J*., et al.* (2014). Partial and transient reduction of glycolysis by PFKFB3 blockade reduces pathological angiogenesis. Cell Metab *19*, 37-48.
Sen, S., Kawahara, B., Gupta, D., Tsai, R., Khachatryan, M., Roy-Chowdhuri, S., Bose, S., Yoon, A., Faull, K., Farias-Eisner, R*., et al.* (2015). Role of cystathionine β-synthase in human breast Cancer. Free Radic Biol Med *86*, 228-238.
Shestov, A.A., Liu, X., Ser, Z., Cluntun, A.A., Hung, Y.P., Huang, L., Kim, D., Le, A., Yellen, G., Albeck, J.G*., et al.* (2014). Quantitative determinants of aerobic glycolysis identify flux through the enzyme GAPDH as a limiting step. Elife *3*.
Short, K.R., Bigelow, M.L., Kahl, J., Singh, R., Coenen-Schimke, J., Raghavakaimal, S., and Nair, K.S. (2005). Decline in skeletal muscle mitochondrial function with aging in humans. Proc Natl Acad Sci U S A *102*, 5618-5623.
Singha, S., Kim, D., Moon, H., Wang, T., Kim, K.H., Shin, Y.H., Jung, J., Seo, E., Lee, S.J., and Ahn, K.H. (2015). Toward a selective, sensitive, fast-responsive, and biocompatible two-photon probe for hydrogen sulfide in live cells. Anal Chem *87*, 1188-1195.
Sonke, E., Verrydt, M., Postenka, C.O., Pardhan, S., Willie, C.J., Mazzola, C.R., Hammers, M.D., Pluth, M.D., Lobb, I., Power, N.E*., et al.* (2015). Inhibition of endogenous hydrogen sulfide production in clear-cell renal cell carcinoma cell lines and xenografts restricts their growth, survival and angiogenic potential. Nitric Oxide *49*, 26-39.
Stern, S., Behar, S., and Gottlieb, S. (2003). Cardiology patient pages. Aging and diseases of the heart. Circulation *108*, e99-101.
Szabo, C., Coletta, C., Chao, C., Módis, K., Szczesny, B., Papapetropoulos, A., and Hellmich, M.R. (2013). Tumor-derived hydrogen sulfide, produced by cystathionine-β-synthase, stimulates bioenergetics, cell proliferation, and angiogenesis in colon cancer. Proc Natl Acad Sci U S A *110*, 12474-12479.
Tao, B.B., Liu, S.Y., Zhang, C.C., Fu, W., Cai, W.J., Wang, Y., Shen, Q., Wang, M.J., Chen, Y., Zhang, L.J*., et al.* (2013). VEGFR2 functions as an H2S-targeting receptor protein kinase

with its novel Cys1045-Cys1024 disulfide bond serving as a specific molecular switch for hydrogen sulfide actions in vascular endothelial cells. Antioxid Redox Signal *19*, 448-464.
Trifunovic, A., Wredenberg, A., Falkenberg, M., Spelbrink, J.N., Rovio, A.T., Bruder, C.E., Bohlooly-Y, M., Gidlöf, S., Oldfors, A., Wibom, R.*, et al.* (2004). Premature ageing in mice expressing defective mitochondrial DNA polymerase. Nature *429*, 417-423.
Wang, R. (2012). Physiological implications of hydrogen sulfide: a whiff exploration that blossomed. Physiol Rev *92*, 791-896.
Wang, Y. (2014). Molecular Links between Caloric Restriction and Sir2/SIRT1 Activation. Diabetes Metab J *38*, 321-329.
Wang, Y., Ning, Y., Alam, G.N., Jankowski, B.M., Dong, Z., Nör, J.E., and Polverini, P.J. (2013). Amino acid deprivation promotes tumor angiogenesis through the GCN2/ATF4 pathway. Neoplasia *15*, 989-997.
Wek, S.A., Zhu, S., and Wek, R.C. (1995). The histidyl-tRNA synthetase-related sequence in the eIF-2 alpha protein kinase GCN2 interacts with tRNA and is required for activation in response to starvation for different amino acids. Mol Cell Biol *15*, 4497-4506.
Wheaton, W.W., Weinberg, S.E., Hamanaka, R.B., Soberanes, S., Sullivan, L.B., Anso, E., Glasauer, A., Dufour, E., Mutlu, G.M., Budigner, G.S.*, et al.* (2014). Metformin inhibits mitochondrial complex I of cancer cells to reduce tumorigenesis. Elife *3*, e02242.
Winnik, S., Auwerx, J., Sinclair, D.A., and Matter, C.M. (2015). Protective effects of sirtuins in cardiovascular diseases: from bench to bedside. Eur Heart J *36*, 3404-3412.
Yang, G., Wu, L., Jiang, B., Yang, W., Qi, J., Cao, K., Meng, Q., Mustafa, A.K., Mu, W., Zhang, S.*, et al.* (2008). H2S as a physiologic vasorelaxant: hypertension in mice with deletion of cystathionine gamma-lyase. Science *322*, 587-590.

Supplementary figures and Legends

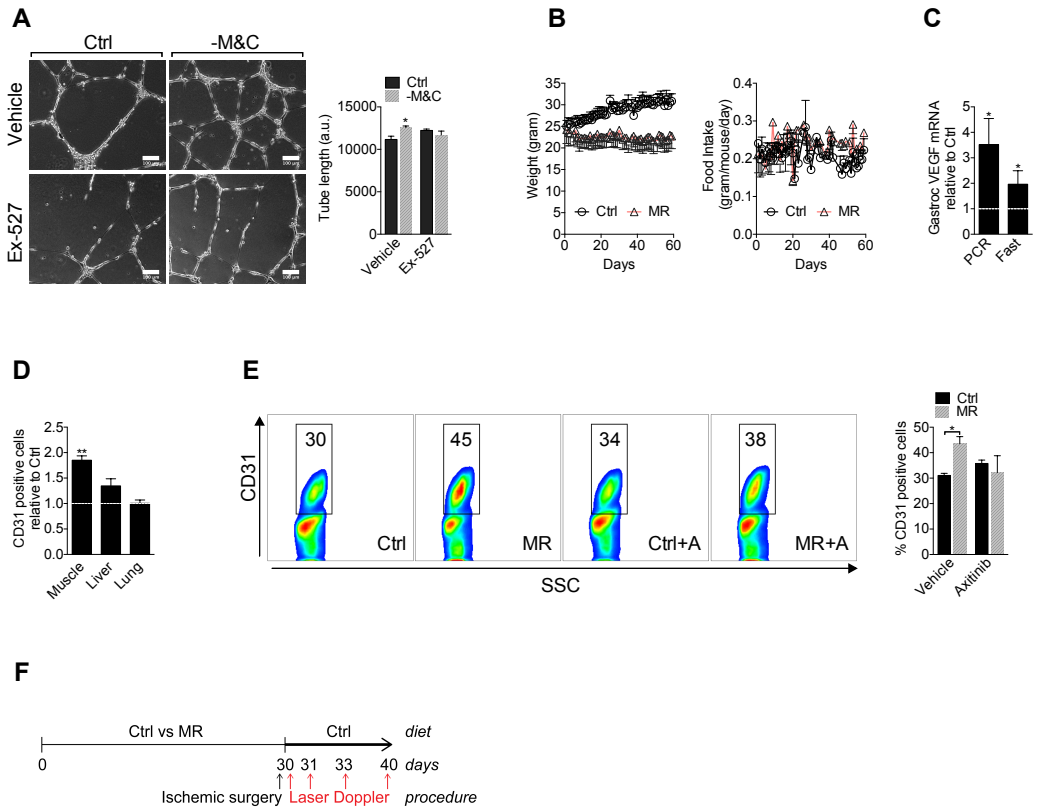

Figure S1

Figure S1.

(**A**) Representative capillary-like structures (left) and total tube length quantification (right) in HUVEC cultured in the indicated media in presence or absence of the SIRT1 inhibitor Ex-527 for 16 hrs. (**B**) Daily body weight (left) and food intake expressed as grams of food eaten per gram of mouse body weight (right) of mice given *ad libitum* access to methionine restricted (MR) vs. control (Ctrl) diet for 2 mo; n=10-15/group. (**B**) Expression of VEGF mRNA in gastrocnemius muscle of mice subject to 1 wk of 40% protein calorie restriction (PCR) or 3 d water-only fasting (Fast) expressed relative to Ctrl diet group; n=3-7/group. (**C**) Flow cytometric analysis of CD31 positive cells from the indicated organs of mice fed a Ctrl or MR diet for 2 mo and expressed as a ratio relative to Ctrl; n=3-4/group. (**D**) Flow cytometric analysis of CD31 positive cells from gastrocnemius muscle of mice fed for 2 wks on Ctrl or MR diets with or without VEGFR2 inhibition (Axitinib, +A); n=4-5/group. (**E**) Schematic representation of the hindlimb ischemia procedure. Error bars indicate SEM; **P* < 0.05, ***P* < 0.005 compared to Ctrl by Student's t test.

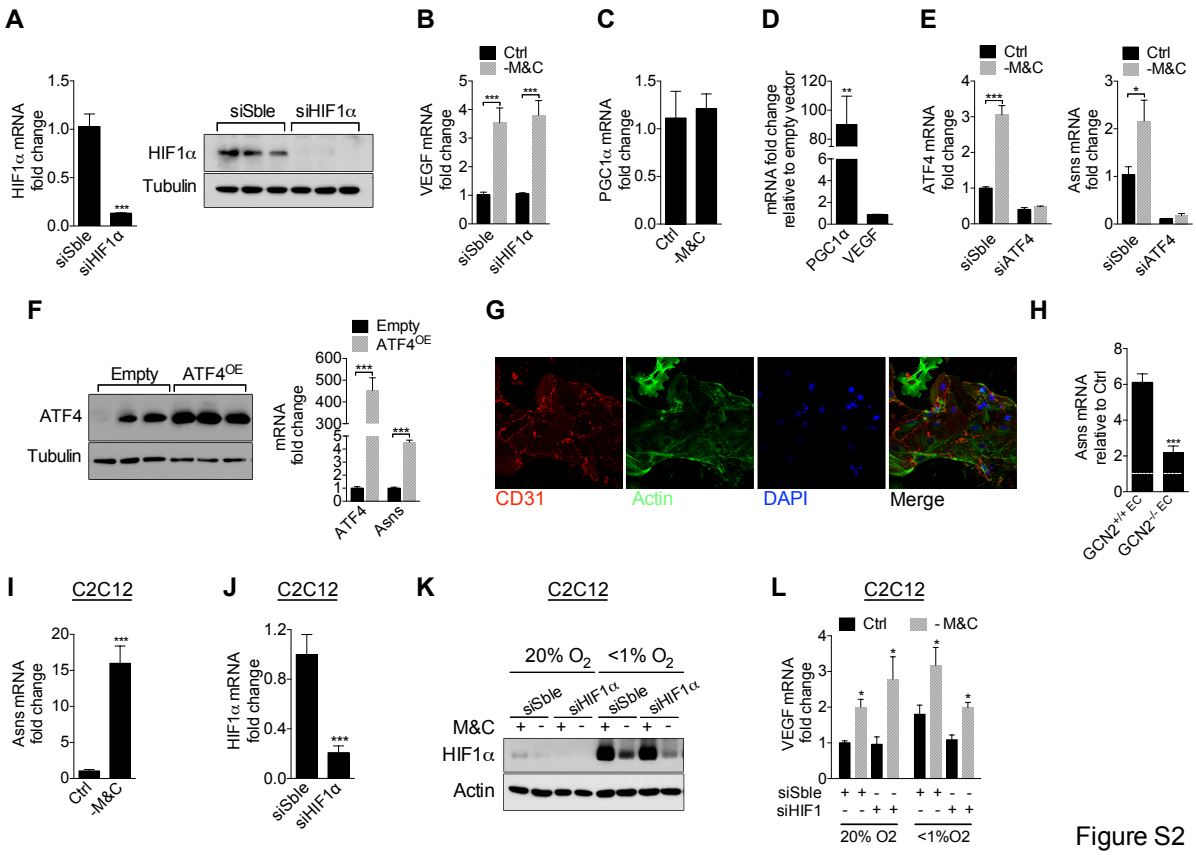

Figure S2

Figure S2.

(**A**) HIF1α mRNA expression (left) and protein level (right) in HUVEC 2 d after transfection with HIF1α siRNA or control scrambled (Sble) siRNA. (**B**) VEGF mRNA expression in HUVEC 2 d after transfection with HIF1α or control scrambled (Sble) siRNA and cultured in the indicated media for 16 hrs. (**C**) PGC1α mRNA levels of HUVEC cultured in the indicated media for 16 hrs. (**D**) PGC1α and VEGF mRNA levels in HUVEC, 2 d after transfection with a PGC1α overexpressing construct, and expressed relative to cells transfected with a control empty vector. (**E**) Relative ATF4 (left) and Asns (right) mRNA expression in HUVEC 2 d after transfection with ATF4 siRNA or control scrambled siRNA and cultured in the indicated media for 16 hrs. (**F**) Western blot of ATF4 (left) or ATF4 and Asns mRNA (right) expression in HUVEC 2 d after transfection with a CMV-driven ATF4 over-expressing construct ($ATF4^{OE}$) or empty vector (Empty). (**G**) Representative images of primary mouse ECs stained for CD31 (red), Actin (green) and DAPI (blue) at a 40X magnification. (**H**) Asns mRNA in $GCN2^{+/+}$ and $GCN2^{-/-}$ primary mouse EC cultured in M&C deficient media relative to control (Ctrl) media for 16 hrs. (**I**) Asns mRNA levels of C2C12 cultured in the indicated media for 16 hrs. (**J**) HIF1α mRNA expression in C2C12 cells 2 d after transfection with HIF1α or control scrambled (Sble) siRNA. (**K, L**) HIF1α protein level (**K**) and VEGF mRNA (**L**) in C2C12 2 d after transfection with HIF1α siRNA or control scrambled (Sble) siRNA under 20 or <1% oxygen in presence or absence of M&C. All cell-based assays were repeated at least three times. Error bars indicate SEM; $^{*}P < 0.05$, $^{**}P < 0.005$ $^{***}P < 0.001$ compared to Ctrl by Student's t test.

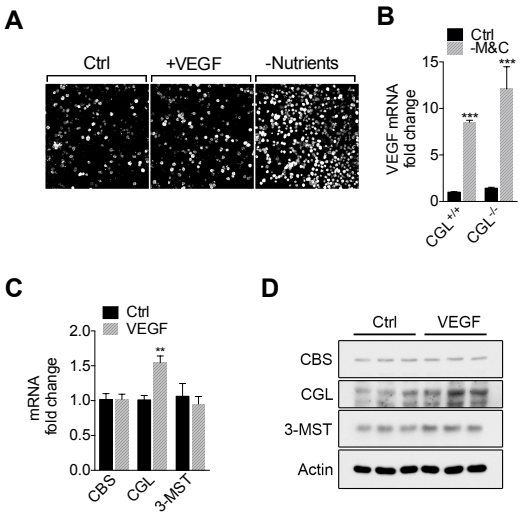

Figure S3

Figure S3.

(**A**) Representative images (10X magnification) of H_2S-specific probe fluorescence in primary mouse hepatocytes treated with VEGF (50 ng/ml) or deprived of all amino acids as well as serum (-Nutrients) for 16 hrs. (**B**) VEGF mRNA in $CGL^{+/+}$ and $CGL^{-/-}$ primary mouse EC cultured in M&C deficient media relative to control (Ctrl) media for 16 hrs. (**C, D**) CBS, CGL and 3-MST mRNA expression (left) and protein level (right) in HUVEC 16hrs after treatment with VEGF. All cell-based assays were repeated at least three times. Error bars indicate SEM; $^{**}P < 0.005$ $^{***}P < 0.001$ compared to Ctrl by Student's t test.

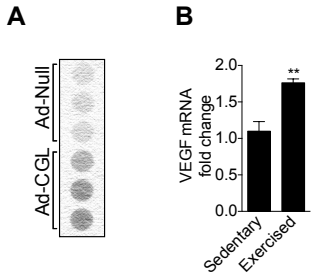

Figure S4

Figure S4.
(**A**) H_2S production capacity of gastrocnemius muscle extracts of Ad-Null or Ad-CGL infected mice 1 wk after i.m. injection; n=3/group. (**B**) Expression of VEGF mRNA in the gastrocnemius muscle of mice subjected to low intensity running (exercised) vs. control (sedentary) for 1mo; n=5-6/group.

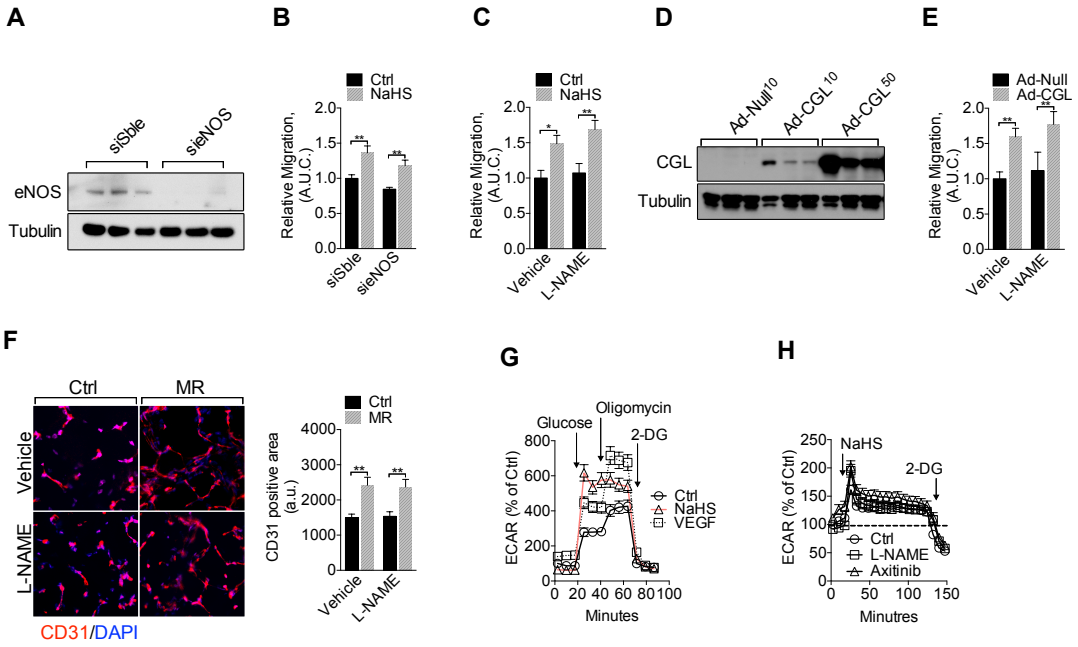

Figure S5

Figure S5.

(**A**) Western blotting of eNOS in HUVEC 2 d after transfection with eNOS or control scramble (Sble) siRNA. (**B**) Quantification of time-dependent wound closure (area under the curve, A.U.C.) in HUVEC scratch wound assays 2 d after transfection with eNOS siRNA or control scramble (Sble) siRNA +/- NaHS (100 μM) as indicated. (**C**) Quantification of wound closure (A.U.C.) in HUVEC scratch wound assays +/- NaHS (100 μM) or eNOS inhibitor L-NAME (100 μM). (**D**) Western blot of CGL in HUVEC 2 d after infection with a control (Ad-Null) or CGL-expressing adenovirus (Ad-CGL) at the indicated multiplicity of infection (MOI). (**E**) Quantification of wound closure (AUC) in HUVEC scratch wound assays 2 d after infection with control (Ad-Null) or CGL-expressing adenovirus (Ad-CGL) at multiplicity of infection 50 +/- L-NAME (100 μM) as indicated. (**F**) Representative transverse sections of gastrocnemius muscle stained for CD31 (left, 40X magnification) and quantification (right) from mice fed Ctrl or MR diets +/- L-NAME for 2 wks as indicated; n=4/group. (**G**) Extracellular acidification rate (ECAR) over time in HUVEC pretreated for 2 hrs with VEGF (50ng/ml) or NaHS (100 μM) and then treated with 10 mM Glucose, 2.5 μM Oligomycin and 50 mM 2-DG injection as indicated by the arrows. (**H**) Extracellular acidification rate (ECAR) over time in HUVEC pre-treated for 2 hrs with axitinib (10 μM) or L-NAME (100 μM) and then treated with NaHS or 2-DG as indicated by the arrows. All cell-based assays were repeated at least three times. Error bars indicate SEM; $*P < 0.05$, $**P < 0.005$, $***P < 0.001$ compared to Ctrl by Student's t test.

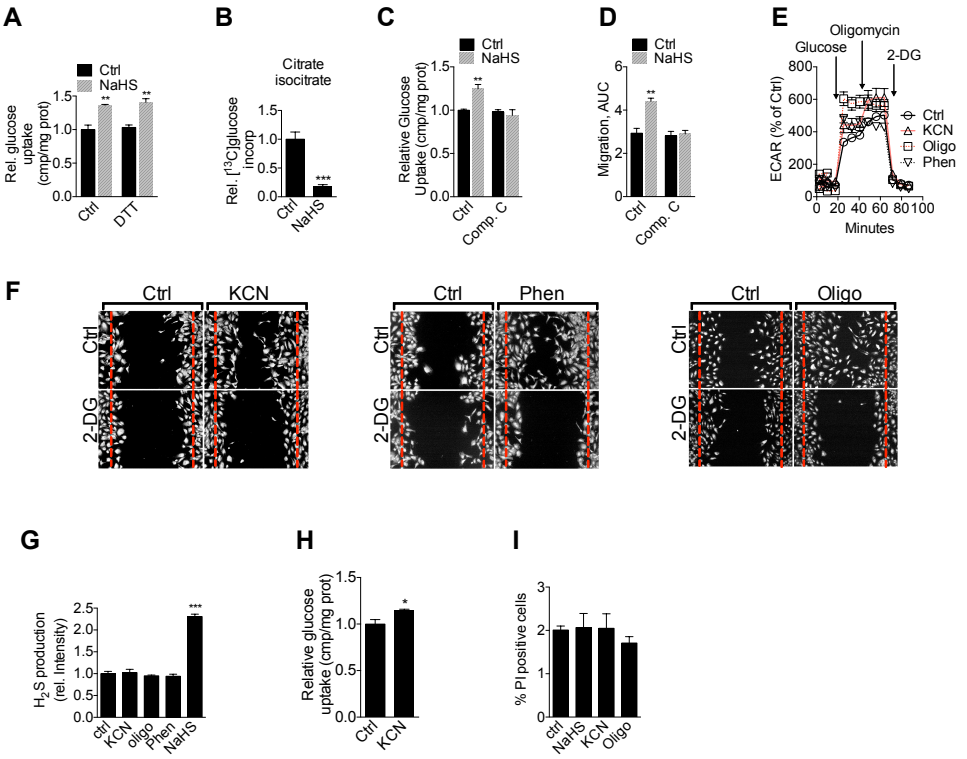

Figure S6

Figure S6.

(**A**) Relative 2-DG uptake in HUVEC treated with NaHS for 1 hr in presence or absence of dithiothreitol (DTT) to prevent sulfhydration. (**B**) C13-labeled metabolite levels measured by mass spectrometry-scaled intensity in C13 glucose pulsed HUVEC +/- NaHS. (**C**) Relative 2-DG uptake in HUVEC treated with NaHS for 1 hr in presence or absence of Compound C (Comp. C). (**D**) Wound closure quantification (A.U.C., area under the curve) in HUVEC treated with NaHS in presence or absence of Compound C (Comp. C). (**E**) Extracellular acidification rate (ECAR) over time in HUVEC pretreated for 2 hrs with cyanide 10μM, oligomycin 2μM (Oligo) or phenformin 500μM (Phen) and then treated with 10 mM glucose, 2.5 μM oligomycin and 50 mM 2-DG as indicated by the arrows. (**F**) Representative image of wound closure in MitoC-treated HUVEC scratch wound assays in the presence of 10 μM Cyanide (KCN, left), 500 μM Phenformin (Phen, middle) or 2 μM oligomycin (oligo, right) +/- 1 mM 2-DG. (**G**) Quantification of endogenous H_2S production by H_2S-specific fluorescent probe intensity in HUVEC treated for 2 hrs with cyanide (10μM), oligomycin (2μM, Oligo), phenformin (500μM, Phen) or NaHS (100 μM) as indicated. (**H**) Relative 2-DG uptake in HUVEC treated with KCN for 1 hr. (**I**) Quantification of HUVEC that fail to exclude PI dye after 2 hrs treatment with NaHS (100 μM), cyanide (10μM) or oligomycin (2μM) as indicated. All cell-based assays were repeated at least three times. Error bars indicate SEM; ***P* < 0.05, ****P* < 0.005, compared within genotype to Ctrl by Student's t test.

Chapter 3: Association of Serum Hydrogen Sulfide Production with Post-operative Mortality in Patients Undergoing Surgical Revascularization

Alban Longchamp[1,2], Gaurav Sharma[1], Christopher Hine[1], William W. King[2], Ming Tao[2], Peter Nagy[3], C. Keith Ozaki[2]*, and James R. Mitchell[1]*

[1]Department of Genetics & Complex Diseases, Harvard T. H. Chan School of Public Health, Boston, MA, USA; [2]Department of Surgery and the Heart and Vascular Center, Brigham & Women's Hospital and Harvard Medical School, Boston, MA, USA; [3]Department of Physical Chemistry and Materials Science, Budapest University of Technology and Economics, Budapest, Hungary.

Running title: Serum H_2S and Mortality

***Address correspondence to:**

CKOzaki@partners.org

75 Francis Street, Boston, MA 02115

Telephone: (857)307-1920

Fax: (857)307-1922

jmitchel@hsph.harvard.edu

655 Huntington Ave. Building 2-121, Boston, MA 02115

Telephone: (617) 432-7286

Fax: (617) 432-5368

Abstract

Background – Hydrogen Sulfide (H_2S) is an endogenously produced gas with broad protective effects on the vascular system. Circulating H_2S levels correlate positively with vascular health, but are difficult to measure quantitatively. Activities of enzymes that produce H_2S can also be measured in blood serum, however the biological significance or predictive value with regard to vascular health is unknown.

Methods – Clinical history and blood were prospectively collected from patients undergoing vascular surgery (mean age 69 years, male 67%), including carotid endarterectomy (n=49), open lower extremity arterial revascularization (n=44) or major leg amputation (n=22) as well as in 20 control patients (mean age 68.4 years, male 65%). H_2S production, was measured using the lead acetate method. Free sulfur, CBS and CGL activity was quantified using mass spectrometry and compared in patient with vascular disease versus control. Given the Gaussian distribution of serum H_2S, we divided high (n=57) versus low (n=58) H_2S producing patients to examine if serum H2S was associated with 1 and 2-year mortality following surgery. For comparison of continuous clinical, demographic variables, and H_2S, either Pearson or Spearman correlation testing was used depending upon the normality of distribution.

Results – Control patients that did not require cardiovascular surgery had the highest serum H_2S production capacity [mean±SD (81±13)]. Among patients that underwent surgery for vascular disease, preoperative serum H_2S production capacity was significantly lower in patients with mortality [mean±SD (53±7); n= 20 all-cause mortality events during a 2 year follow up] than those alive [mean±SD (57± 8)]. Furthermore, the percentage of survival in the low H_2S (defined as <median) was lower [6 months, 2 years (78 and 74)] compared to high H_2S (defined as >median), [6 months, 2 years (93, 91)].

Conclusions – Serum H_2S production capacity was linearly correlated with mortality following surgical revascularization and may serve as an easily quantified measure with biological significance with regards to vascular health.

Introduction

Hydrogen sulfide (H_2S) is a colorless gas with a characteristic rotten-egg odor found in various natural and industrial sources (1). Although toxic at high levels, H_2S produced at low concentrations by degradation of Cys or homocysteine by CGL or CBS acts on the vasculature and the brain as a signaling molecule to prevent neurodegeneration (2), reduce blood pressure (3), protect from hear failure (4, 5), promote angiogenesis (6, 7) and protect from limb ischemia (8) Exogenous H_2S can also extend lifespan of worms (9) and induce suspended animation in mammals (10).

Results

Circulating H_2S has previously been inversely correlated with reduced cardiovascular health (8, 11), however the absolute values of these measurements and the source of H_2S remain controversial (12). We thus chose to use the lead sulfide method to test H_2S production capacity in serum (rather than actual free or bound H_2S) of rodents on the most effective pro-longevity intervention (13-16), calorie restriction (CR). One week of CR significantly increased serum H_2S production ($p<0,05$; Fig. 1), providing proof of principle that serum H_2S production capacity is plastic.

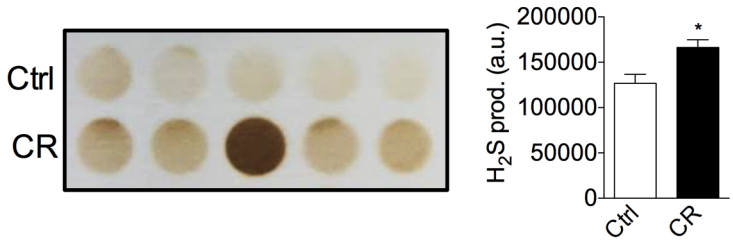

Figure 1: Circulating H_2S is increased by Caloric restriction.
Representative plasma H_2S production capacity (**left**) and quantification (**right**) in mice fed for 1 week on control (Ctrl) or 50% caloric restricted (CR) diets. Error bars indicate SEM; $p<0.05$ by Student *t* test.

In human ischemic heart disease and stroke, underlying atherosclerosis, are the world's leading cause of death, accounting for a combined 30% (15 million) of the mortality worldwide. Therefore, we measured H_2S production capacity in patients suffering chronic

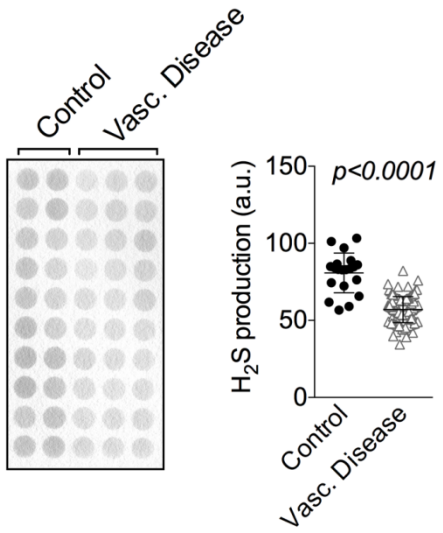

Figure 2: Circulating H_2S production is reduced in patients with vascular disease and correlates with survival.
Representative plasma H_2S production capacity (**left**) and quantification (**right**) from human patients suffering vascular occlusive disease (Disease, n=115), versus healthy age-matched individuals (Healthy, n=20) as detected by the lead sulfide method. Error bars indicate SD; p<0.0001 by Mann-Whitney (Wilcoxon rank sum).

ischemia, underlying advanced atherosclerosis (vascular cohort) compared a control cohort (ctrl, table 1). The vascular and control population consisted of 115 and 20 patients, respectively. Both group were similar in terms of age, sex and BMI. Although the prevalence of hypertension (HTN) was similar in both group (3), other cardiovascular risk factors and disease (diabetes, hyperlipidemia, renal insufficiency, stroke, PAD, MI) as well as antiplatelet therapy, statin use and anti-hypertensive medication were more prevalent in the vascular cohort (Table 1).

Comparison of control versus vascular patients revealed 1.4 fold higher serum H2S (p<0.0001; Fig. 2 and S1). Given the Gaussian distribution of serum H_2S among patients that underwent surgery (vascular cohort, Fig 3A), we divided high (n=57) versus low (n=58) H_2S producing patients to examine if serum H_2S was associated with clinical 1 and 2-year mortality following surgery. Among patients that underwent surgery for vascular disease, preoperative serum H_2S production capacity was significantly lower in patients with mortality [mean±SD (53±7); n= 20 all-cause mortality events during a 2 year follow up] than those alive [mean±SD (57± 8)]. Furthermore, the percentage of survival in the low H_2S (defined as <median) was lower [6 months, 2 years (78 and 74)] compared to high H_2S (defined as >median), [6 months, 2 years (93, 91)].

Interestingly, using LC-MS, we found that in the CBS activity was reduced but that free Sulfur was increase in plasma level in patients undergoing vascular surgery procedure, consistnat with the observation that H2S protects from cardiovascular disease (Fig. 4)

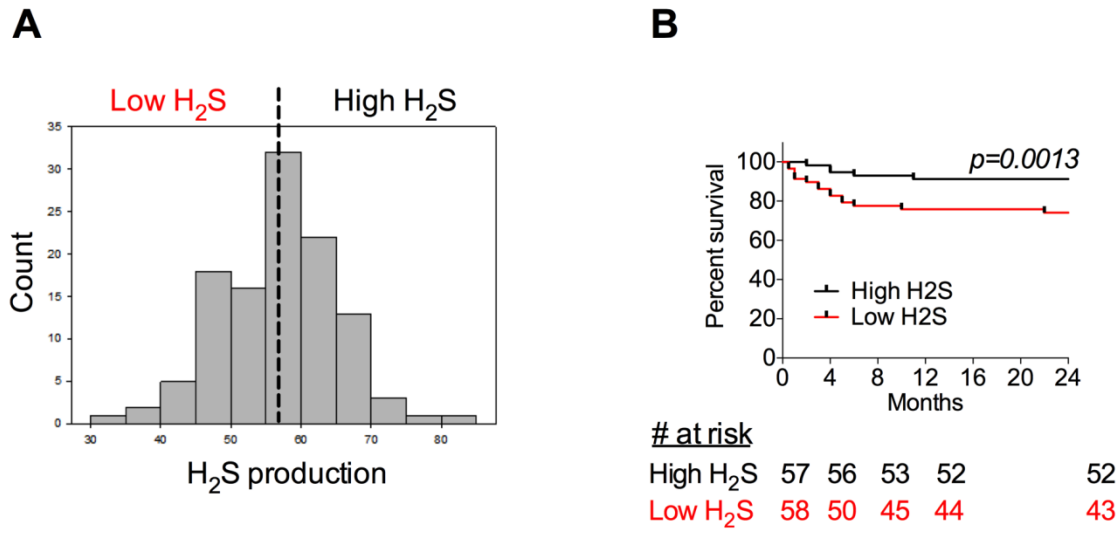

Figure 3: Pre-operative serum H_2S correlates with survival.
(**A**) Distribution of H_2S plasma level in patients undergoing vascular surgery procedure. (**B**) Kaplan-Meier survival curve for patients with low (n=58) and high (n=57) plasma H_2S before undergoing vascular surgery procedure. P value is derived from log-rank calculation.

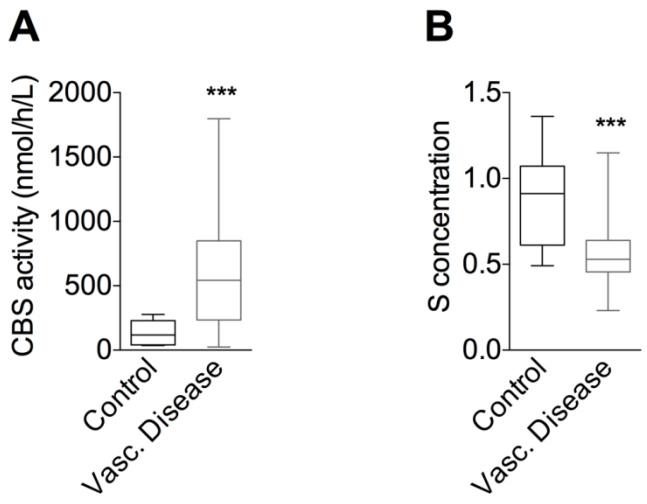

Figure 4: CBS activity and sulfide levels.
CBS activity (**A**) and free Sulfur (**B**) in plasma level in patients undergoing vascular surgery procedure

Discussion

Here we find that serum H_2S increased H_2S production capacity is detectable in serum upon nutrient restriction in rodents, and correlates with survival in patients suffering vascular disease.

Caloric restriction represents the best-studied anti-aging model in rodents. To date, molecular mechanism underlying pleiotropic benefits on health and lifespan are not completely understood. Previously we found that in mouse liver, endogenous H_2S increased upon CR. H_2S production was necessary and sufficient for surgical stress resistance, using model of hepatic ischemia reperfusion injury in mice. Furthermore, H_2S was associated with extended longevity in fly, worm and yeast models (17). Here we found increased serum H_2S production in mice fed with a CR for 1 week compared to ad-libitum fed animals (Ctrl).

Circulating proteins that change in abundance across the lifespan have the potential to serve as instructive biomarkers and, potentially, targetable modifiers of aging conditions (18-20). In a small study including 57 patients, total plasma sulfide is negatively related to severity of congestive heart failure and predict mortality. (21). In mice with heart failure, H_2S levels are decreased in the heart and blood. Additionally, systemic H_2S supplementation in mice lacking the H_2S producing enzyme CGL (CGL KO) restored H_2S blood levels and prevented heart failure (4). In our study, we found H_2S to be an important predictive marker of survival in patient following vascular surgery. Interestingly, H_2S levels affected 8-mo mortality but benefit was lost after. Taken together, these data are consistent with increased serum H_2S as a marker of health, and pro-longevity factor. These findings also further support a role for the clinical utility of measuring H_2S in the context of vascular surgery.

Material and Methods

Mice

All experiments were performed with the approval of the Harvard Medical Area or Boston University Institutional Animal Care and Use Committee (IACUC). 8-12 weeks old male and female C56/BL6 (The Jackson Laboratory, Bar Harbor, ME) were used for all experiments unless otherwise indicated.

Dietary regimens: Mice were given *ad libitum* (AL) access to food and water unless otherwise indicated. Experimental diets were based on Research Diets D12450B with approximately 18% of calories from protein (hydrolyzed casein or individual crystalline amino acids (Ajinomoto) in the proportions present in casein), 10% from fat and 72% from carbohydrate. AL food intake per gram of body weight was monitored daily for several days and used to calculate 50% dietary restriction (CR) based on initial animal weights. Animals were fed daily with fresh food between 6pm and 7pm. Fasting was applied by transferring mice to a fresh cage without food for 3 days.

Human Study Participants and Serum Collection

Patients undergoing carotid endarterectomy for symptomatic or asymptomatic stenosis and patients undergoing lower limb amputation or bypass following critical limb ischemia at a single institution in 2013 provided written informed consent for prospective collection of demographic, clinical, and duplex ultrasonography data under a Partners Human Research Committee institutional review board–approved protocol. Fifteen milliliters of peripheral blood were obtained at the time of the surgery from peripheral intravenous line placement. Serum was isolated by centrifugation for 15 min at 2000g at room temperature. All samples were immediately snap frozen in liquid nitrogen then stored at -80°C until the time of analysis.

H_2S measurements

Lead sulphide method: 20 μl of serum was diluted 150 μl of PBS containing 100 mM Cys and 3 mM PLP. 6x4 inch pieces of lead acetate paper, made by soaking 703 size blotting paper (VWR) in 20 mM lead acetate (Sigma) and then vacuum drying, were placed over the 96-well dish and incubated for 2-24 hrs at 37^{O}C until lead sulphide was detected but not saturated. Quantification of lead sulfide H_2S production capacity assays was done using the IntDen measurement in ImageJ software as previously published(13, 17).

Statistical Analyses

Data are displayed as means +/- Standard error of the mean (SEM) if not specified and statistical significance assessed in GraphPad Prism using Student's t tests to compare values and one-sample t test to compare means to a hypothetical value of 1 or 100 when data was normalized to the average value of the control group. Non-Gaussian distributed data were compared using the Mann Whitney t-test. Continuous clinical and demographic variables Pearson or Spearman correlation testing was utilized depending upon the normality of distribution. A P-value of 0.05 or less was deemed statistically significant.

References

1. Wang R. Two's company, three's a crowd: can H2S be the third endogenous gaseous transmitter? FASEB J. 2002;16(13):1792-8.
2. Paul BD, Snyder SH. H_2S signalling through protein sulfhydration and beyond. Nat Rev Mol Cell Biol. 2012;13(8):499-507.
3. Yang G, Wu L, Jiang B, Yang W, Qi J, Cao K, et al. H2S as a physiologic vasorelaxant: hypertension in mice with deletion of cystathionine gamma-lyase. Science. 2008;322(5901):587-90.
4. Kondo K, Bhushan S, King AL, Prabhu SD, Hamid T, Koenig S, et al. H_2S protects against pressure overload-induced heart failure via upregulation of endothelial nitric oxide synthase. Circulation. 2013;127(10):1116-27.
5. Polhemus DJ, Kondo K, Bhushan S, Bir SC, Kevil CG, Murohara T, et al. Hydrogen sulfide attenuates cardiac dysfunction after heart failure via induction of angiogenesis. Circ Heart Fail. 2013;6(5):1077-86.
6. Tao BB, Liu SY, Zhang CC, Fu W, Cai WJ, Wang Y, et al. VEGFR2 functions as an H2S-targeting receptor protein kinase with its novel Cys1045-Cys1024 disulfide bond serving as a specific molecular switch for hydrogen sulfide actions in vascular endothelial cells. Antioxid Redox Signal. 2013;19(5):448-64.
7. Papapetropoulos A, Pyriochou A, Altaany Z, Yang G, Marazioti A, Zhou Z, et al. Hydrogen sulfide is an endogenous stimulator of angiogenesis. Proc Natl Acad Sci U S A. 2009;106(51):21972-7.
8. Islam KN, Polhemus DJ, Donnarumma E, Brewster LP, Lefer DJ. Hydrogen Sulfide Levels and Nuclear Factor-Erythroid 2-Related Factor 2 (NRF2) Activity Are Attenuated in the Setting of Critical Limb Ischemia (CLI). J Am Heart Assoc. 2015;4(5).
9. Miller DL, Roth MB. Hydrogen sulfide increases thermotolerance and lifespan in Caenorhabditis elegans. Proc Natl Acad Sci U S A. 2007;104(51):20618-22.
10. Blackstone E, Morrison M, Roth MB. H2S induces a suspended animation-like state in mice. Science. 2005;308(5721):518.
11. Alshorafa AK, Guo Q, Zeng F, Chen M, Tan G, Tang Z, et al. Psoriasis is associated with low serum levels of hydrogen sulfide, a potential anti-inflammatory molecule. Tohoku J Exp Med. 2012;228(4):325-32.
12. Olson KR, DeLeon ER, Liu F. Controversies and conundrums in hydrogen sulfide biology. Nitric Oxide. 2014;41:11-26.
13. Mitchell SJ, Madrigal-Matute J, Scheibye-Knudsen M, Fang E, Aon M, González-Reyes JA, et al. Effects of Sex, Strain, and Energy Intake on Hallmarks of Aging in Mice. Cell Metab. 2016;23(6):1093-112.
14. Hine C, Mitchell JR. Calorie restriction and methionine restriction in control of endogenous hydrogen sulfide production by the transsulfuration pathway. Exp Gerontol. 2015;68:26-32.
15. Hine C, Mitchell JR. Saying no to drugs: fasting protects hematopoietic stem cells from chemotherapy and aging. Cell Stem Cell. 2014;14(6):704-5.
16. McCay CM, Crowell MF, Maynard LA. The effect of retarded growth upon the length of life span and upon the ultimate body size. 1935. Nutrition. 1989;5(3):155-71; discussion 72.

17. Hine C, Harputlugil E, Zhang Y, Ruckenstuhl C, Lee BC, Brace L, et al. Endogenous hydrogen sulfide production is essential for dietary restriction benefits. Cell. 2015;160(1-2):132-44.
18. Schafer MJ, Atkinson EJ, Vanderboom PM, Kotajarvi B, White TA, Moore MM, et al. Quantification of GDF11 and Myostatin in Human Aging and Cardiovascular Disease. Cell Metab. 2016;23(6):1207-15.
19. Loffredo FS, Steinhauser ML, Jay SM, Gannon J, Pancoast JR, Yalamanchi P, et al. Growth differentiation factor 11 is a circulating factor that reverses age-related cardiac hypertrophy. Cell. 2013;153(4):828-39.
20. Lees EK, Król E, Grant L, Shearer K, Wyse C, Moncur E, et al. Methionine restriction restores a younger metabolic phenotype in adult mice with alterations in fibroblast growth factor 21. Aging Cell. 2014;13(5):817-27.
21. Kovačić D, Glavnik N, Marinšek M, Zagožen P, Rovan K, Goslar T, et al. Total plasma sulfide in congestive heart failure. J Card Fail. 2012;18(7):541-8.

Supplemental Materials

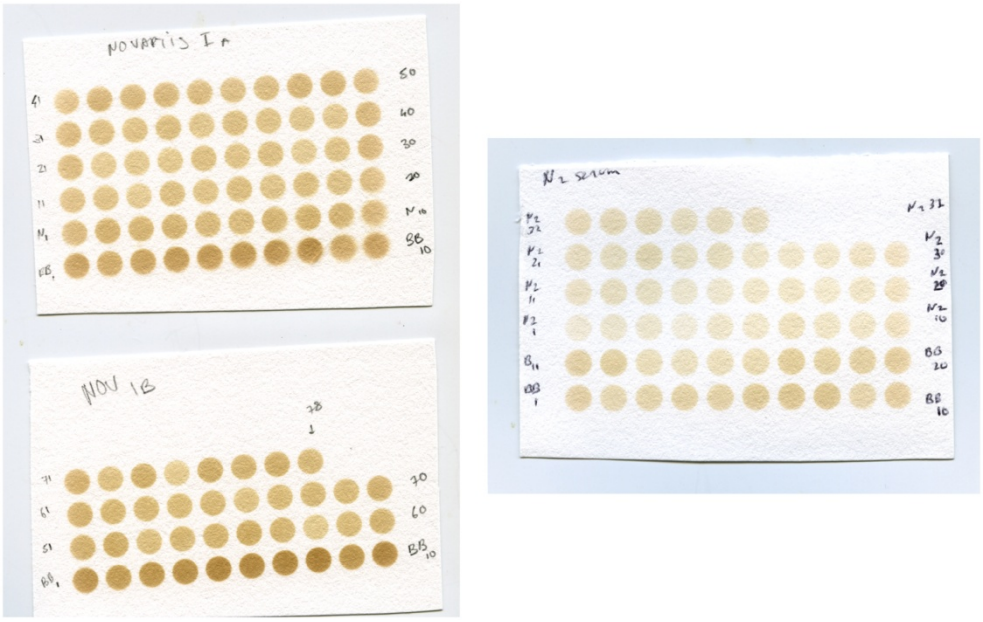

Supplemental Figure 1:
Plasma H_2S production capacity from human patients suffering vascular occlusive disease (Disease, n=115), versus healthy age-matched individuals (Healthy, n=20) as detected by the lead sulfide method.

Supplemental table 1: Baseline Study Population Characteristics.

Variable	*Vascular Cohort (n=115)*	*Control Cohort (n=20)*
Mean age, years (SD)	69 (9)	68 (2.3)
Sex		
Male (%)	73 (63)	13 (65)
Female (%)	42 (37)	7 (35)
Race		
White (%)	97 (84)	18 (90)
Hispanic (%)	10 (9)	0
Black (%)	4 (3.5)	0
Other (%)	4 (3.5)	2 (10)
Mean BMI (SD)	28.3 (5.3)	28.7 (7.2)
Comorbidities		
Prior stroke (%)	24 (21)	0
Peripheral arterial disease (%)	75 (65)	0
Prior MI (%)	30 (26)	0
Prior coronary intervention (%)	44 (38)	0
Heart failure (%)	19 (17)	0
HTN (%)	106 (92)	19 (95)
Hyperlipidaemia (%)	98 (85)	6 (30)
Diabetes mellitus (%)	45 (39)	2 (10)
COPD (%)	7 (6)	0
Renal insufficiency (%)	16 (14)	5 (1)
Malignancy	23 (20)	4 (20)
Smoking status		
Never	25 (22)	9 (45)
Former	60 (52)	11 (55)
Current	30 (26)	0
Preoperative medications		
Aspirin (%)	102 (89)	6 (30)
Clopidogrel (%)	28 (24)	0
Warfarin (%)	11 (10)	2 (10)
Low molecular weight heparin (%)	6 (5)	0
Unfractionated heparin (%)	14 (12)	0
Statin (%)	99 (86)	7 (35)
Beta blocker (%)	89 (77)	10 (50)
Calcium channel blocker (%)	37 (32)	3 (15)
ACE-inhibitor (%)	49 (43)	8 (40)
ARB (%)	13 (11)	0
Procedure		

Carotid endarterectomy (%)	49 (43)	0
Infrainguinal revascularization (%)	44 (38)	0
Lower extremity amputation (%)	22 (19)	0

SD, standard deviation; N.A., not available; BMI, body mass index; MI, myocardial infarction; HTN, hypertension; COPD, chronic obstructive pulmonary disease; ACE, angiotensin converting enzyme; ARB, angiotensin receptor blocker; HDL, high density lipoprotein; LDL, low density lipoprotein; CRP, C-reactive protein; Cr, creatinine

CONCLUSION AND PERSPECTIVES

The aim of this work was to investigate the role of nutrients in vascular homeostasis, especially following surgery.

The first chapter, provides an update on the nutritional basis, nutrient sensing mechanisms, and downstream effectors of protection by short-term DR in preclinical models of surgical stress. While DR clearly protects from oxidative stress, ionizing irradiation and chemotherapy (1), we have used mouse models of surgical stress, in particular ischemia-reperfusion injury to the liver and kidney (2-5), as well as stroke (6) not only understand the underlying mechanisms of DR but to demonstrate that in the context of surgery, DR works rapidly (2 days in rodents) (7) and that protein restriction alone, especially restriction of the sulfur amino acids methionine and cysteine are sufficient for the benefits of DR (2, 3). These and other observations (8), have strengthened the translational potential of "pre-surgical short-term DR". Although the implementation of these dietary measures in human is appealing, the immediate challenge is to define the timing and examine if DR would be applicable to everyone (9) or identify the patients or procedure(s) that might benefits the most and those at risk of adverse effects.

In the second aim we tested the potential of isolated nutrient restriction independent of hypoxia to impact the formation of new vessels (angiogenesis). Previously we found that CGL as well as hepatic H_2S production capacity are increased upon DR, and repressed by dietary sulfur amino acids, but the molecular requirements for dietary control of H_2S production were not elucidated (2). Here, we revealed a requirement for the AASR in the coordinate regulation of CGL as well as VEGF upon nutrient restriction. In all cells tested, sulfur amino acid deprivation increased CGL and VEGF gene expression via the integrated stress response through GCN2 activation and ATF4 stabilization (10). Interestingly, additional regulation of H_2S production appeared to occur in ECs on a post-translational level, as evidenced by rapidly increased H_2S

production upon VEGF addition, possibly via calcium-calmodulin stimulation of CGL (11). Future studies will determine the relative importance of each pathway.

More importantly, we identified an unrecognized pro-angiogenic pathway activated by dietary amino acid restriction and controlled by the GCN2/ATF4-dependent AASR. These findings reveal the AASR as a new target for modulation of angiogenesis by pharmacological or even dietary manipulations. This has therapeutic value for example in the context of limb ischemia, a major complication of cardiovascular disease and diabetes that is not amenable to treatment by exercise. In the context of cancer chemotherapy, where inhibition of angiogenesis is desired, it is also important to recognize the AASR as an independent pathway with the ability to contribute to tumor vascularization.

The discovery that H_2S boosts glycolytic ATP production by inhibiting mitochondrial electron transport in ECs, especially complex I and IV provides a novel mechanism of H_2S action in biology, not only for its toxicity at high H_2S concentrations. It further demonstrates the H_2S ability to alter cellular oxidative/glycolytic energy balance at physiological levels. EC generate 85% of their ATP via glycolysis (12). Despite the significantly lower energy yield per molecule of glucose via glycolysis anaerobic glucose metabolism enables ECs to vascularize avascular anoxic tissues, an activity that would not be possible if they would rely primarily on oxidative glucose metabolism. The effects of H_2S on cellular energy metabolism may also have important implications for cancer, both in terms of therapeutic inhibition of angiogenesis (13) as well as in energy metabolism of the tumor itself. Interestingly, a number of tumors and cancer cells lines upregulate GCN2 (14, 15) or H_2S production (16-19), and thus possibly contributing to the Warburg effect through inhibition of mitochondrial respiration.

In human, ischemic heart disease and stroke, are the world's leading cause of death, accounting for a combined 30% (15 million) of the mortality worldwide. In the last chapter, we hypothesized that circulating H_2S production was a relevant marker of vascular health. Clinical history and blood were prospectively collected from patients undergoing vascular surgery as

well as 20 controls, healthy patients. Consistent with our hypothesis, serum H_2S was significantly higher in healthy individuals. Furthermore, among patients that underwent surgery for vascular disease, preoperative serum H_2S production was linearly correlated with survival. Consistently, in another study, including 57 patients, total plasma sulfides are negatively related to severity of congestive heart failure and predict mortality (21). In mice with heart failure, H_2S levels are decreased in the heart and blood. Taken together, these data are consistent with increased serum H_2S as a marker of health. These findings also further support a role for the clinical utility of measuring H_2S in the context of vascular surgery.

FUTURE DIRECTIONS

Basic research

ECs are plastic cells, located at the interface between blood and organs, that can switch between growth states(12), and undergo multiple developmental and functional transitions during fetal, neonatal and adult life. This plasticity is crucial to maintain a healthy microvascular network, providing adequate blood supply to organs throughout life and during metabolic stresses(20). In the latest stages of life, impaired EC regenerative potential leads to progressive organ failure throughout the body, suggesting that improved understanding of the fundamental mechanisms underlying EC plasticity and aging would have tremendous impact on lifespan and quality of life. Aging itself is associated with reduced capillary density; reduced new vessel formation; reduced number and function of endothelial precursor cells; and increased EC senescence. Extensive published and preliminary data indicate that H_2S has a key role in regulating well as vascular remodeling/angiogenesis. However the role of CGL/H_2S in vascular homeostasis with advancing age, its role in the vascular benefits of DR or the relevant cellular source of H_2S in this context are unknown. In addition, the H_2S generating enzymes circulate at high level in healthy individuals, but declines dramatically with vascular diseases in concert with the emergence of multiple age-associated pathologies in muscle and other tissues. Based on these data, we propose that **H_2S represent a new endothelial-derived circulating anti-aging molecule, which holds therapeutic promise to restore more youthful function to aging tissues** (appendix 1). In this project, we will use DR as well as transgenic models to stimulate endogenous H_2S production from endothelial cells. We will define H_2S therapeutic relevance in the prevention and treatment of age-related disease, especially skeletal muscle dysfunction and hypertension, central elements of the vascular aging process.

Clinical translation

1. Circulating H_2S levels correlate positively with vascular health (e.g. blood pressure, muscle function(21-23) and dietary restriction (24) in mice. In human, single nucleotide polymorphism (SNP) in CGL is linked to variation in serum homocysteine(25). Our preliminary data indicates that in PAD patients, serum H_2S is significantly reduced compared to healthy control and inversely correlates with metabolic health (Chapter 3). Importantly, in PAD patients undergoing open surgical revascularization, pre-operative serum H_2S linearly correlates with 2-years survival following surgery (Chapter 3). Thus, we propose to expand our analysis in humans, and **determine the relationship between serum H_2S production and cardiovascular health in human, using the Cohort study of Lausanne (CoLaus,** Appendix 1**,** 26-29).

2. In rodent, removing protein from thee diet for about a week dramatically protects from injury such as ischemia reperfusion and other surgical related injury. In human, there is currently no pre-operative dietary consensus nor guidelines that aim to reduce surgical mortality or complications. To prevent bronchoaspiration, general anesthesia and sedation require stomach emptying via fasting 2 hrs after clear fluids, 4 hrs after ingestion of breast milk or 6 hrs in the case of non human milk and 8 hrs after a meal containing fat or meat. Enhanced recovery after surgery (ERAS) protocols are increasingly used multimodal perioperative care pathways designed to achieve early recovery after surgical procedures. The key components of ERAS protocols include preoperative counseling, optimization of nutrition, standardized analgesic and anesthetic regimens and early mobilization. Interestingly, pre-operative 12.6% oral carbohydrate loading is one cornerstone of ERAS. 100g of carbohydrate administered the day before, and 50g the day of the surgery are thought to alleviate surgical induced insulin resistance, “reduce catabolism”, and thirst. Several studies report shorter length of stay

and a reduction in patient discomfort. While non-mutually exclusive, we aim to **determine the safety and feasibility of implementing a defined protein-calorie restriction regimen as a nutriceutical intervention to improve recovery after surgery**. Ongoing Clinical trial, in collaboration with with Prof. C.-K. Ozaki at Brigham Women's Hospital in Boston (USA) is currently evaluating the safety of a 3-day diet reduced in both total calories (1000 kcal/daily) and total protein before carotid endarterectomy. Future work will help us to define what is the most effective diet and for how long. Will the diet need to be individualized to clinical parameters such as age, body mass index, diabetes, etc.? The challenge of voluntary reduced food intake scales with the severity and duration of food restriction. We aim for maximal efficacy within the shortest time frame and with the least restrictive diet. In these early phase clinical trials, safety will be measured using clinical observation and blood glucose measurement. Weight loss will be recorded, with a drop over 7% of body mass during the pre-conditioning period considered as dangerous. Systemic adverse effects to evaluate will include fatigue, malaise and neuromuscular weakness. On the other hand, will primary endpoint for efficacy will be length of hospital stay and complication rate, surrogates efficacy can be assessed in the serum using H_2S production capacity and available commercial ELISA kits for determine changes in insulin, IGF-1, leptin, adiponectin and FGF21 following diet.

References

1. de Groot S, Vreeswijk MP, Welters MJ, Gravesteijn G, Boei JJ, Jochems A, et al. The effects of short-term fasting on tolerance to (neo) adjuvant chemotherapy in HER2-negative breast cancer patients: a randomized pilot study. BMC Cancer. 2015;15:652.
2. Hine C, Harputlugil E, Zhang Y, Ruckenstuhl C, Lee BC, Brace L, et al. Endogenous hydrogen sulfide production is essential for dietary restriction benefits. Cell. 2015;160(1-2):132-44.
3. Robertson LT, Treviño-Villarreal JH, Mejia P, Grondin Y, Harputlugil E, Hine C, et al. Protein and Calorie Restriction Contribute Additively to Protection from Renal Ischemia Reperfusion Injury Partly via Leptin Reduction in Male Mice. J Nutr. 2015.
4. Harputlugil E, Hine C, Vargas D, Robertson L, Manning BD, Mitchell JR. The TSC complex is required for the benefits of dietary protein restriction on stress resistance in vivo. Cell Rep. 2014;8(4):1160-70.
5. Peng W, Robertson L, Gallinetti J, Mejia P, Vose S, Charlip A, et al. Surgical stress resistance induced by single amino acid deprivation requires Gcn2 in mice. Sci Transl Med. 2012;4(118):118ra11.
6. Varendi K, Airavaara M, Anttila J, Vose S, Planken A, Saarma M, et al. Short-term preoperative dietary restriction is neuroprotective in a rat focal stroke model. PLoS One. 2014;9(4):e93911.
7. Mitchell JR, Verweij M, Brand K, van de Ven M, Goemaere N, van den Engel S, et al. Short-term dietary restriction and fasting precondition against ischemia reperfusion injury in mice. Aging Cell. 2010;9(1):40-53.
8. Jongbloed F, de Bruin RW, Klaassen RA, Beekhof P, van Steeg H, Dor FJ, et al. Short-Term Preoperative Calorie and Protein Restriction Is Feasible in Healthy Kidney Donors and Morbidly Obese Patients Scheduled for Surgery. Nutrients. 2016;8(5).
9. Levine ME, Suarez JA, Brandhorst S, Balasubramanian P, Cheng CW, Madia F, et al. Low protein intake is associated with a major reduction in IGF-1, cancer, and overall mortality in the 65 and younger but not older population. Cell Metab. 2014;19(3):407-17.
10. Lee JI, Dominy JE, Sikalidis AK, Hirschberger LL, Wang W, Stipanuk MH. HepG2/C3A cells respond to cysteine deprivation by induction of the amino acid deprivation/integrated stress response pathway. Physiol Genomics. 2008;33(2):218-29.
11. Yang G, Wu L, Jiang B, Yang W, Qi J, Cao K, et al. H2S as a physiologic vasorelaxant: hypertension in mice with deletion of cystathionine gamma-lyase. Science. 2008;322(5901):587-90.
12. De Bock K, Georgiadou M, Schoors S, Kuchnio A, Wong BW, Cantelmo AR, et al. Role of PFKFB3-driven glycolysis in vessel sprouting. Cell. 2013;154(3):651-63.
13. Schoors S, De Bock K, Cantelmo AR, Georgiadou M, Ghesquière B, Cauwenberghs S, et al. Partial and transient reduction of glycolysis by PFKFB3 blockade reduces pathological angiogenesis. Cell Metab. 2014;19(1):37-48.
14. Wang Y, Ning Y, Alam GN, Jankowski BM, Dong Z, Nör JE, et al. Amino acid deprivation promotes tumor angiogenesis through the GCN2/ATF4 pathway. Neoplasia. 2013;15(8):989-97.
15. Lehman SL, Ryeom S, Koumenis C. Signaling through alternative Integrated Stress Response pathways compensates for GCN2 loss in a mouse model of soft tissue sarcoma. Sci Rep. 2015;5:11781.

16. Bhattacharyya S, Saha S, Giri K, Lanza IR, Nair KS, Jennings NB, et al. Cystathionine beta-synthase (CBS) contributes to advanced ovarian cancer progression and drug resistance. PLoS One. 2013;8(11):e79167.
17. Szabo C, Coletta C, Chao C, Módis K, Szczesny B, Papapetropoulos A, et al. Tumor-derived hydrogen sulfide, produced by cystathionine-β-synthase, stimulates bioenergetics, cell proliferation, and angiogenesis in colon cancer. Proc Natl Acad Sci U S A. 2013;110(30):12474-9.
18. Sen S, Kawahara B, Gupta D, Tsai R, Khachatryan M, Roy-Chowdhuri S, et al. Role of cystathionine β-synthase in human breast Cancer. Free Radic Biol Med. 2015;86:228-38.
19. Sonke E, Verrydt M, Postenka CO, Pardhan S, Willie CJ, Mazzola CR, et al. Inhibition of endogenous hydrogen sulfide production in clear-cell renal cell carcinoma cell lines and xenografts restricts their growth, survival and angiogenic potential. Nitric Oxide. 2015;49:26-39.
20. Rivard A, Fabre JE, Silver M, Chen D, Murohara T, Kearney M, et al. Age-dependent impairment of angiogenesis. Circulation. 1999;99(1):111-20.
21. Islam KN, Polhemus DJ, Donnarumma E, Brewster LP, Lefer DJ. Hydrogen Sulfide Levels and Nuclear Factor-Erythroid 2-Related Factor 2 (NRF2) Activity Are Attenuated in the Setting of Critical Limb Ischemia (CLI). J Am Heart Assoc. 2015;4(5).
22. Kondo K, Bhushan S, King AL, Prabhu SD, Hamid T, Koenig S, et al. H_2S protects against pressure overload-induced heart failure via upregulation of endothelial nitric oxide synthase. Circulation. 2013;127(10):1116-27.
23. Polhemus DJ, Kondo K, Bhushan S, Bir SC, Kevil CG, Murohara T, et al. Hydrogen sulfide attenuates cardiac dysfunction after heart failure via induction of angiogenesis. Circ Heart Fail. 2013;6(5):1077-86.
24. Young JB, Mullen D, Landsberg L. Caloric restriction lowers blood pressure in the spontaneously hypertensive rat. Metabolism. 1978;27(12):1711-4.
25. Wang J, Huff AM, Spence JD, Hegele RA. Single nucleotide polymorphism in CTH associated with variation in plasma homocysteine concentration. Clin Genet. 2004;65(6):483-6.
26. Christe V, Waeber G, Vollenweider P, Marques-Vidal P. Antihypertensive drug treatment changes in the general population: the CoLaus study. BMC Pharmacol Toxicol. 2014;15:20.
27. Pruijm M, Vollenweider P, Mooser V, Paccaud F, Preisig M, Waeber G, et al. Inflammatory markers and blood pressure: sex differences and the effect of fat mass in the CoLaus Study. J Hum Hypertens. 2013;27(3):169-75.
28. Danon-Hersch N, Marques-Vidal P, Bovet P, Chiolero A, Paccaud F, Pécoud A, et al. Prevalence, awareness, treatment and control of high blood pressure in a Swiss city general population: the CoLaus study. Eur J Cardiovasc Prev Rehabil. 2009;16(1):66-72.
29. Firmann M, Mayor V, Vidal PM, Bochud M, Pécoud A, Hayoz D, et al. The CoLaus study: a population-based study to investigate the epidemiology and genetic determinants of cardiovascular risk factors and metabolic syndrome. BMC Cardiovasc Disord. 2008;8:6.

APPENDIXES

Appendix 1
Role of endogenous hydrogen sulfide in the control of vascular aging.
This was submitted to the Swiss National Science Foundation (SNSF) 2016 research grant.
Principal Investigator: **Longchamp A**.

Appendix 2
Longchamp A, Alonso F, Dubuis C, Allagnat F, Berard X, Meda P, Saucy F, Corpataux JM, Déglise S, Haefliger JA. **The use of external mesh reinforcement to reduce intimal hyperplasia and preserve the structure of human saphenous veins.**
Biomaterials 2014

Appendix 3
Longchamp A, Allagnat F, Berard X, Alonso F, Haefliger JA, Deglise S, Corpataux JM. **Procedure for Human Saphenous Vein Ex-vivo Perfusion and External Reinforcement.**
JoVE 2014.

Appendix 4
Longchamp A, Allagnat F, Alonso F, Kuppler C, Dubuis C, Ozaki CK, Mitchell JR, Berceli S, Corpataux JM, Déglise S, Haefliger JA.
Connexin43 Inhibition Prevents Human Vein Grafts Intimal Hyperplasia.
PlosOne 2015.

Appendix 5
Mauro CR, Tao M, Yu P, Treviño-Villerreal JH, **Longchamp A**, Kristal BS, Ozaki CK, Mitchell JR.
Preoperative dietary restriction reduces intimal hyperplasia and protects from ischemia-reperfusion injury.
JVS 2016.

SUMMARY

Human aging and age-associated diseases represent one of the biggest health challenges faced by developed and developing countries. As the body ages, one of the most dramatic and threatening changes is a decline in the function of endothelial cells that line the vasculature, resulting in a failure in most physiological systems. The clinical manifestations are multiple, including hypertension, myocardial infarction, stroke, dementia, critical limb ischemia, muscle decline and exercise intolerance, vascular dementia, impaired wound healing, and erectile dysfunction. Importantly, vascular dysfunction in the elderly is one of the strongest predictors of imminent death. This suggests that a better mechanistic understanding underlying vascular aging, and novel strategies to intervene in this process could tremendously impact lifespan and the quality of life in this growing population of aged (>65 years old) individuals.

Dietary Restriction (DR), defined as reduced food intake without malnutrition, was first described nearly a century ago by McCay and colleagues to extend lifespan in rats. Since then, DR has been extensively studied, in a multitude of organisms, and evidence supports that DR increases lifespan and confers protection against age-associated diseases such as hypertension and ischemia of the limbs, heart, or brain. However, despite DR's health benefits, it would be extremely difficult to achieve adherence to such a stringent diet in humans. To this end, extensive efforts have been made towards the identification of the nutritional, cellular and molecular mechanisms that underlie DR benefits, and could prime pharmacological "DR-mimetics". One step closer to this goal, we recently reported that DR increases endogenous hydrogen sulfide production (H_2S) in the liver, via upregulation specifically of the enzyme cystathionine γ-lyase (CGL), but not other H_2S producing enzymes. In this context, the increase in CGL/H_2S was necessary and sufficient for DR-mediated protection from ischemic injury to the liver and for lifespan extension in worms.

Extensive published and preliminary data indicate that H_2S has a key role in regulating blood pressure as well as vascular remodeling/angiogenesis during muscle ischemia. However the role of CGL/H_2S in vascular homeostasis with advancing age, its role in the vascular benefits of DR or the relevant cellular source of H_2S in this context are unknown. In addition, the H_2S generating enzymes circulate at high level in healthy individuals, but declines dramatically with vascular diseases in concert with the emergence of multiple age-associated pathologies in muscle and other tissues. Based on these data, we propose that **H_2S represent a new endothelial-derived circulating anti-aging molecule, which holds therapeutic promise to restore more youthful function to aging tissues**. In this project, we will use DR as well as transgenic models to stimulate endogenous H_2S production from endothelial cells. We will define H_2S therapeutic relevance in the prevention and treatment of age-related disease, especially skeletal muscle dysfunction and hypertension, central elements of the vascular aging process, according to the following **specific aims** (Figure 1):

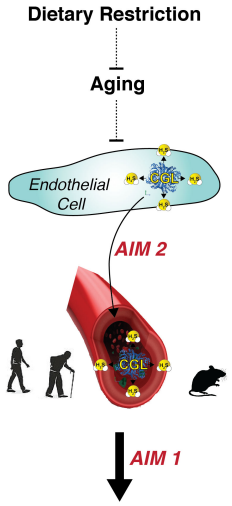

Figure 1: Role of H_2S in vascular aging

Aim 1. **Evaluate the function of H_2S in endothelial cells growth and plasticity, and clarify the basis for the age- and ischemia-dependent effects on muscle function.**

Aim 2. **Determine the relationship between serum H_2S production and cardiovascular health in mice and in human, using the Cohort study of Lausanne (CoLaus).**

Together these studies will lend important insights into the basic science of vascular aging, especially endothelial cells dysfunction, as well as open new avenues for the rapid development of therapeutics of age-related diseases, specifically skeletal muscle dysfunction and hypertension.

2. RESEARCH PLAN

2.1 Current state of research in the field

2.1.1 Aging and dietary restriction

The population aged 65 and over is projected to grow from 40 million in 2012 to 80 million in 2050 in the United State alone. According to the vascular theory of aging[1], the progressive decline in endothelial function is one of the major causes of aging and age-related diseases, manifesting in diverse ways, from cardiac infarctions and strokes, to peripheral artery disease (PAD), exercise intolerance and sarcopenia to hypertension, erectile dysfunction, liver failure, osteoporosis, impaired wound healing, and frailty[2-5]. Despite the importance of endothelial function to human health and longevity, it is surprising how little we understand about its underlying causes [1].

In 1935, Clive McCay discovered that dietary restriction (DR), or reduced food intake without malnutrition, extends lifespan in rats[6,7], a finding later confirmed in in a multitude of organisms from yeast[8] to worms[9] to flies[10,11], fish[12], rodents [13,14] and rhesus monkeys[15,16]. Notably, DR remains the only non-genetic method to increase longevity in every species studied. In humans, DR reduces risk factors for diabetes, cardiovascular disease, and cancer[17,18]. In the past years we and others demonstrated that short-term DR (2 days in rodents) improves the outcome of preclinical mouse models of acute and chronic vascular disease model such as ischemia-reperfusion injury to the liver and kidney[19-23], stroke[24] and vascular restenosis[25]. Importantly, our recent data implicate H_2S produced by CGL (discussed below) in DR-mediated protection from ischemia reperfusion injury and lifespan extension[19,26,27].

2.1.2. Hydrogen sulfide

Hydrogen sulfide (H_2S) is a gas easily identified by its distinctive odor of rotten eggs. While toxic at high levels, H_2S produced endogenously by CGL or CBS (Figure 2) acts on the vasculature and the brain as a signaling molecule to reduce blood pressure[28] and prevent neurodegeneration[29]. Low levels of exogenous H_2S also extends lifespan of worms[19,27] and induce suspended animation in mammals[30]. H_2S has numerous other cardiovascular benefits, including pro-angiogenesis in vitro and in vivo[31,32], reduced vascular restenosis (intimal hyperplasia)[33,34], anti-atherosclerotic activity[35], and reduced binding of neutrophils to the wall of blood vessel[36]. On the other hand, in humans, serum H_2S concentration declines with age[37] and the levels of the H_2S producing enzymes are reduced in patients suffering vascular diseases[38,39]. We have recently demonstrated that mice lacking the H_2S-producing enzyme CGL fail to gain the protective effects of DR, while adenoviral overexpression of CGL in the liver, or delivery of H_2S itself, recapitulate DR-like benefits without the need for any dietary intervention[19]. Whether free H_2S is a circulating gasotransmitter that acts as a paracrine, or autocrine molecule is still being debated and difficult to address[40,41]. However, the enzyme CGL secreted by endothelial cells (EC)s and hepatocytes circulates in the plasma/serum, and actively produces H_2S in human blood[42], which may be critical for the systemic vascular benefits of H_2S[43]. H_2S has many potential mechanisms of action, including sulfhydration, or formation of –SSH moieties on surface-exposed Cys residues, of an ever-growing list of protein targets[29,40,44-47]. In ECs, for example, such targets include the Kir6.2 regulatory subunit of the K_{ATP} channel and the VEGF receptor leading to vessel relaxation and angiogenesis, respectively[45,47]. H_2S also has

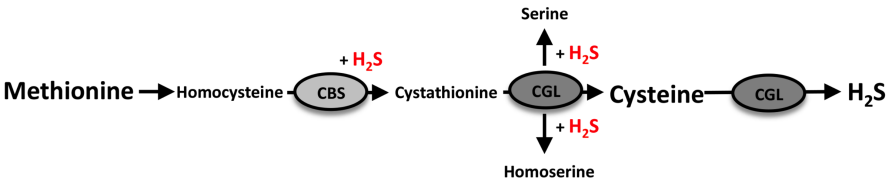

Figure 2: Model of the Cysteine and Methionine metabolism, specifically the transsulfuration pathway. Arrows trace sulfur from Met to Cys and downstream cellular processes via cystathionine beta-synthase (CBS) and cystathionine gamma-lyase (CGL).

direct antioxidant properties, and can participate in mitochondrial energy production by donating electrons to the mitochondrial electron transport chain protein SQR, with a potential role in protection from organ ischemia[48,49].

2.1.3. Contribution of endothelial cells to organismal aging

ECs are plastic cells, located at the interface between blood and organs, that can switch between growth states[50], and undergo multiple developmental and functional transitions during fetal, neonatal and adult life. This plasticity is crucial to maintain a healthy microvascular network, providing adequate blood supply to organs throughout life and during metabolic stresses[51]. In the latest stages of life, impaired EC regenerative potential leads to progressive organ failure throughout the body, suggesting that improved understanding of the fundamental mechanisms underlying EC plasticity and aging would have tremendous impact on lifespan and quality of life. Aging itself is associated with reduced capillary density; reduced new vessel formation; reduced number and function of endothelial precursor cells; and increased EC senescence[52]. Systolic blood pressure continuously increases with age[5,53] as well as the occurrence of vascular diseases, even in populations without other major risk factors[54-56]. Besides prevalence, mortality due to ischemia is higher in the elderly[55,57]. Mechanisms of age-associated decline in vascular function are complicated and poorly understood, but appear in many cases to be initiated by EC dysfunction[58,59]. While the mechanisms are currently unknown, in human and rodents, DR dramatically reduces endothelial dysfunction[60], blood pressure[61,62] and promotes angiogenesis as well as functional muscle recovery following femoral artery ligation[63]. Similarly, blood pressure is increased in CGL knockout mice[28], and can be reduced by exogenous H_2S[64].

2.1.4. H_2S and vascular diseases

The benefit of generating new blood vessels to the ischemic tissues is obvious[40,65-67]. In this regards, exogenous H_2S promotes collateral vessel growth, capillary density, and blood flow in ischemic muscles following femoral artery ligation[68], in the heart during heart failure[32] and in wound healing[69]. Mice lacking endogenous CGL/H_2S (CGL knockout / CGL^{KO} mice), have decreased blood flow and vascular density, following limb and heart ischemia[65,70], while cardiac-specific overexpression of CGL[71] or exogenous H_2S limits ischemia-reperfusion damage[72,73]. Similarly, H_2S protects from ischemic in injury in the liver[19], the brain[74,75], and the kidney[76]. The growth of new blood vessels (angiogenesis) involves coordinate EC proliferation, migration and sprouting. In vitro, the absence of CGL reduces ECs sprouting[77,78], while exogenous H_2S increases EC proliferation, adhesion, migration, formation of tube-like structure and sprouting[31,78].

2.2 Current state of our research

In the past 4 years spent between the Service of Vascular Surgery (CHUV, Lausanne) and the laboratories of Professors James R. Mitchell and C. Keith Ozaki at Harvard University (Boston, USA), including the funded period (**SNSF, P1LAP3_158895**, 01.12.2014 – 31.05.2016), I have contributed to a total of 11 peer-reviewed publications, including 10 original research papers and 1 review. As a clinician-scientist, I will devote 50% of my time to this project (please see accompanying letter from Prof. J-M. Corpataux).

The proposed 4-year project will be carried out in Lausanne, Switzerland, at the CHUV in the laboratory of vascular surgery (see “Resources” and letter of support Prof. J.-M. Corpataux). Beside our cutting edge laboratory of molecular and cellular biology, we benefit from a modern surgical suite in the animal facility. Importantly, we will continue our close local collaboration with Professors Jacques-Antoine Haefliger (with whom we share the laboratory space), as well as international collaboration with James R. Mitchell and C.- Keith Ozaki at the Harvard University (Boston, USA), both world experts in aging/DR and vascular biology, and Massimo Santoro at Leuven University (Leuven, Belgium), an

expert on metabolism and angiogenesis (see letters of support). In addition, we are closely collaborating with Prof. Peter Vollenweider in the CHUV (Lausanne, Switzerland) for the handling and analysis of the CoLaus samples (Aim 2, see letter of support).

Together with additional preliminary data presented below, this proposal builds on published expertise in vascular biology[19,25,79-120], aging[19,26,121-124], dietary interventions[7,19-26,101,114,120-134] and hydrogen sulfide[19,26,121]. In Aim 1, we will test the functionality of H_2S/CGL in preventing/reversing age-related vascular dysfunction using murine models in which improvement in endothelial function gives a measurable benefit. These models include i) longitudinal blood pressure measurement[113,135-143] and ii) neovascularization and muscle function following femoral ligation, a validated pre-clinical model of peripheral artery disease (Figure 1, 6 and [113,135-143]). In Aim 2, with Prof. Peter Vollenweider and the CoLaus team, we will examine the association between serum CGL/H_2S and cardiovascular disease in human.

Below I present the recent work that is directly related to this research proposal.

2.2.1. Vascular density and skeletal muscle function decreases with age

As the body ages, there is senescence and apoptosis of muscle ECs, leading to blood vessel loss, decreased muscle perfusion, reduced muscle mass (sarcopenia) and a steady decline in strength, endurance and regenerative capacity[51,56,144-146]. However, the exact mechanism underlying the switch from young to old muscle is currently unknown. Our preliminary data indicates that aging reduces angiogenic potential, as shown by decreased ECs sprouting using the aortic-ring assay (Figure 3a). Similarly, vascular density as measured by CD31 immunostaining of ECs was reduced in the skeletal muscle of aged (12 month-old), compared to young (10 week-old) mice (Figure 3b). Reduced vascular density in aged mice was associated with reduction in muscle fiber size as well as decreased oxidative capacity (Figure 3c). At a functional level, these histological changes imparted running endurance as shown by significantly reduced running time and distance in aged mice (Figure 3d), using the treadmill assay as published[147,148]. Together, these findings demonstrate that muscle function is reduced by age, which could be facilitated by a decrease in vascular function.

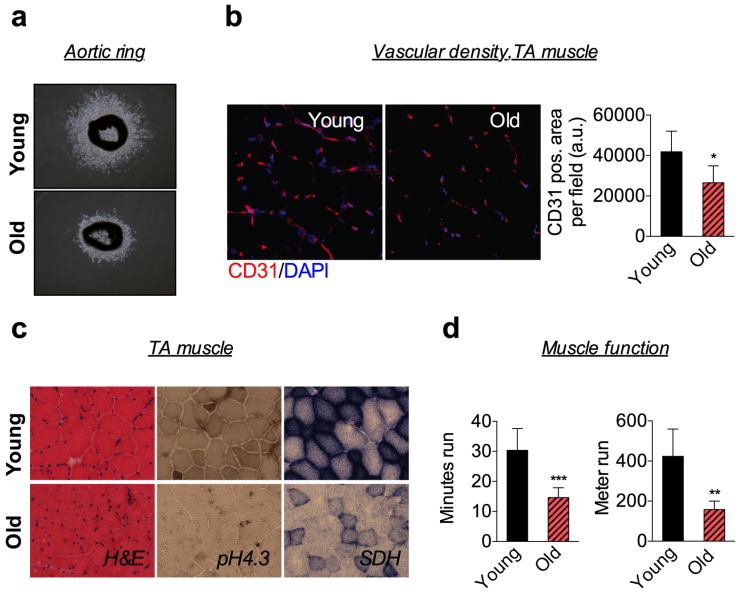

Figure 3. Decrease in endothelial function and exercise capacity with age. (**a**) Representative phase-contrast images of aortic rings from young (10 weeks) and old (12 months) WT mice (n=6 per age) (**b**) Representative transverse sections (40X magnification) of baseline TA muscle from young (10 weeks) and old (12 months) WT mice stained for CD31. (**c**) Representative transverse sections (40X magnification) of baseline TA muscle from young (10 weeks) and old (12 months) WT mice stained for H&E, mATPase (indicating type I and II fibers) and SDH activity (from left to right). (**d**) Time spent and distance run until exhaustion in treadmill exercise test in young (10 weeks) and old (12 months) mice (n = 6 per age). Error bars indicate SD. *p<0.05, ***p<0.001 compared to young by Student's t test .

2.2.2. Hydrogen sulfide produced via CGL decreases with age and vascular diseases

The importance of CGL-derived H_2S to maintain vascular health is unequivocal[19,28,31,32,38,40,65,70,71,78,149,150]. Recently, we found that H_2S is crucial in the benefits of DR on lifespan and protection from ischemia[19]. Furthermore, H_2S/CGL is decreased by vascular diseases[38,39] and in the elderly[37]. Therefore, we hypothesized that H_2S is critically linked to vascular aging. In our preliminary data, we took advantage of publically available data sets from aged versus young mice, and demonstrated down-regulation of CGL (but not CBS or 3-MST, data not shown) in multiple organs of aged mice, including the muscle (Figure 4a) and the heart (Figure 4b). Furthermore, "vasculo-protective interventions" such as exercise and DR, consistently increased CGL (Figure 4a and b, accession number GSE6323, 38063, 7640, 6718 and 68646). CGL is decreased in the muscle of patients suffering from limb ischemia[38]. Similarly, CGL is significantly reduced in human carotid atheroma of the plaque compared to distant macroscopically intact tissue (Figure 4c). Finally, serum H_2S production is significantly lower in patients suffering arterial occlusive disease (defined as requiring surgical revascularization), compared to similar patients without arterial lesion (Figure 4d). Altogether, these preliminary data are consistent with a progressive decline in H_2S production with age, and suggest an important interplay between H_2S levels and vascular health (Figure 4).

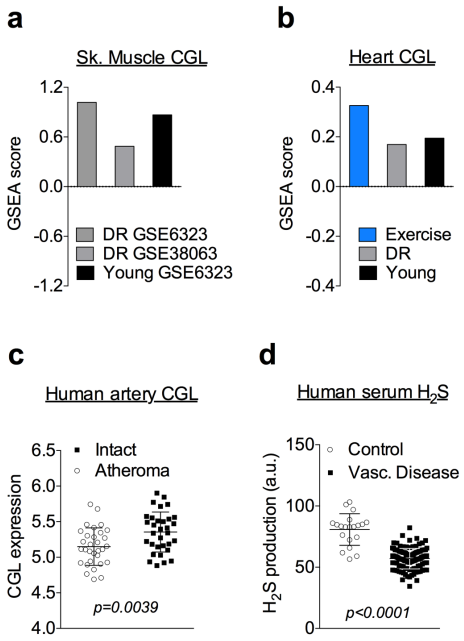

Figure 4: Beneficiary interventions such as running, DR and youth increase CGL in vascular tissues and in the serum. (**a-c**) Muscle (**a**), heart (**b**) and carotid (**c**) CGL expression using microarray data from the publicly available GEO data sets (accession number GSE6323, 38063, 7640, 6718, 68646 and 43292) (**d**) Serum H_2S production from human patients suffering vascular occlusive disease (Disease, n=115), versus healthy age-matched individuals (Healthy, n=20) as detected by the lead sulfide method. Error bars indicate SD; $p<0.0001$ by Mann-Whitney (Wilcoxon rank sum).

2.2.3. In endothelial cells, hydrogen sulfide is induced by DR and is required for vascular growth

We previously demonstrated that DR induces H_2S production via CGL (but not CBS and 3-MST), and protects from ischemic injury in vivo[19]. Exogenous H_2S promotes EC migration, proliferation and formation of capillary-like structure[31,40], while endogenous CGL promotes EC sprouting[78]. Here we propose that DR induction of endogenous H_2S is fundamental to the growth of new blood vessels (see Longchamp et al., appendix 1). According to our preliminary data, in ECs, DR[19], and the pro-angiogenic vascular endothelial growth factor (VEGF)[151,152] stimulate H_2S enzymatic production (measured using the lead acetate method, Figure 5a) and CGL, but not CBS and 3-MST, expression (Figure 5b). H_2S production in ECs is also abrogated by specific inhibition of CGL with DL-Propargylglycine (PAG, Figure 5a). Increased endothelial H_2S production correlated with increased vascular growth in models such wound healing assay (Figure 5c),

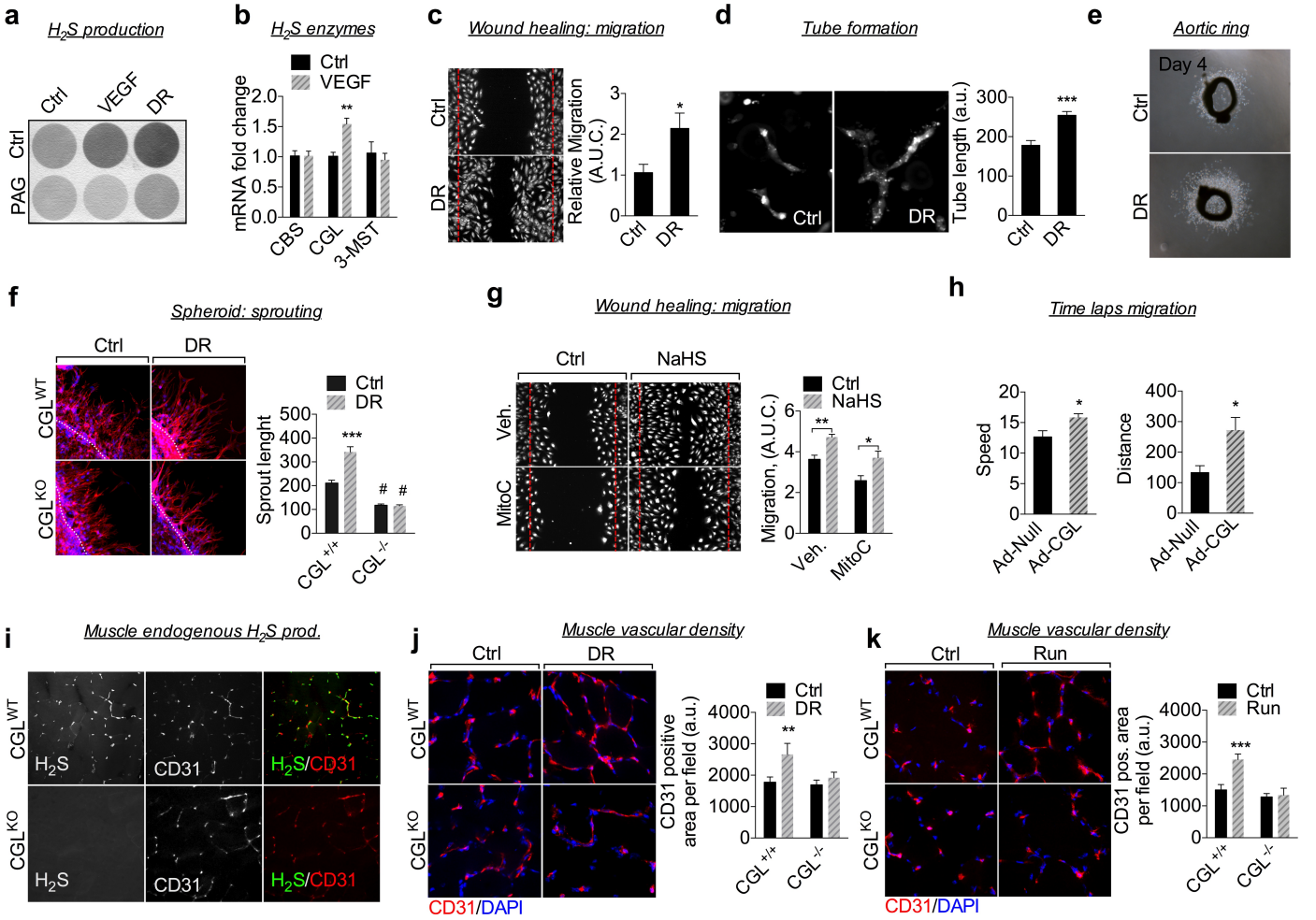

Figure 5: H_2S produced via CGL promotes angiogenesis *in-vitro* and in the skeletal muscle *in-vivo*. (**a**) Representative H_2S production capacity as indicated by black lead sulfide formation from EC in absence of methionine and cysteine (DR) for 16 hours or treated with VEGF (50 ng/ml) in the presence or absence of the CGL inhibitor propargylglycine (PAG, 100 μM) as indicated. (**b**) CBS, CGL and 3-MST mRNA expression in HUVEC 16 hours after treatment with VEGF. (**c**) Representative wound closure (left, 10X magnification at time = 20 hours; dotted lines indicate boundary of the scratch wound at time = 0 hour) and area under the curve (A.U.C., right) from HUVEC in the indicated media. (**d**) Representative capillary-like structures (left, tube formation at 40X magnification) and mean tube length quantification (right) in HUVEC cultured in the indicated media for 24 hours. (**e**) Representative phase-contrast images of aortic rings from mice fed for 2 weeks on the indicated diet. (**f**) Representative images (left, 40X magnification) and quantification (right) of CGL^{KO} primary EC sprouts in control media (Ctrl) or media lacking methionine and cysteine (DR) for 24 hours. (**g**) Time-dependent wound closure (left) and quantification (right, A.U.C., area under the curve) in HUVEC +/- 100μM NaHS in the presence of vehicle or mitomycin C (MitoC) to inhibit proliferation. (**h**) Quantification of migration speed (left) and distance (right) from time-lapse video imaging of GFP+ HUVEC infected with control (Ad-Null) or CGL adenovirus (Ad-CGL) as indicated. (**i**) Representative transverse sections (20X magnification) of gastrocnemius muscle from CGL^{WT} and CGL^{KO} mice stained for CD31 and endogenous H_2S. (**j**, **k**) Representative transverse section (left, 40X magnification) and quantification (right) of gastrocnemius muscle stained for CD31 from CGL^{WT} and CGL^{KO} mice fed for 2 weeks on Ctrl or DR diets (**i**) or subjected to low intensity running (exercised) vs. control (sedentary) for 1 month (**k**); n=5-6/group. Error bars indicate SEM; **P* < 0.05, ***P* < 0.005, ****P* < 0.001 compared within genotype to Ctrl by Student's t test.

formation of capillary-like structures (tube formation, Figure 5d) and aortic ring sprouting (Figure 5e). Similarly, increased sprout length of EC spheroids upon DR was prevented by CGL inhibition with PAG in HUVECs (data not shown) and by genetic CGL ablation (CGL^{KO}) in mouse ECs (Figure 5f). CGL is a promiscuous enzyme that can convert cystathionine to cysteine as part of the transsulfuration pathway, but that can also use cysteine to produce H_2S, serine and glutathione (Figure 2). Importantly, DR reduces glutathione and cysteine levels (Figure 3D of [19]), we thus directly tested H_2S as the CGL metabolite relevant to angiogenesis. H_2S delivery in the form of NaHS promoted EC proliferation/migration indicative of increased angiogenic potential in the wound closure assay (Figure 5g). Blocking proliferation with mitomycinC (MitoC) only partially reduced H_2S-induced wound closure (Figure 5g), suggesting that migration is a critical factor in H_2S-induced angiogenic potential. To confirm the effects of CGL on migration, time-lapse video imaging of GFP^+ HUVECs revealed that cells overexpressing CGL (Ad-CGL) formed lamellipodial projections over larger areas (data not shown) coincident with increased migration speed and greater cell body displacement (Figure 5h).

As illustrated above (Figure 3), skeletal muscle function relies on a abundant, fully functional vascular network upon physiological (e.g. exercise) or pathological condition (e.g. ischemia – vessel occlusion)[153]. Consistent with our findings using in-vitro models, in-vivo in skeletal muscle sections, P3 fluorescence, indicative of endogenous H_2S production[154], co-localized with $CD31^+$ ECs in CGL^{WT} but not CGL^{KO} mice, further suggesting endothelial CGL (and not CBS or 3-MST) as the major producer of endogenous H_2S in the skeletal muscle (Figure 5j). Coincident with a failure to increase H_2S, CGL^{KO} mice demonstrated no increase in vascular density upon 1 month of DR or following exercise as in the WT group (Figure 5j, k). CGL^{KO} in a C57BL/6 background are a kind gift of Prof. James R. Mitchell, and are currently in the Lausanne vascular laboratory breeding colony. Taken together, CGL-derived H_2S is required for angiogenesis triggered by nutrient deprivation or exercise (Figure 5, 4b and [19]).

2.2.4. Dietary or genetically induced CGL/H_2S promotes vascular growth and muscle recovery following femoral ligation

To further study in vivo the role of CGL/H_2S in vascular growth we used a mouse model of PAD via ligation of the femoral artery as published (Figure 6a and [66,67]). This results in limb muscle ischemia, followed by progressive neovascularization (quantified as the relative blood flow of the ischemic limb to the contralateral non ischemic limb, using laser doppler imaging, Figure 6b) and muscle regeneration (Figure 6c). In this context, aging results in impaired angiogenesis and more severe muscle injury[51,55,56]. Consistent with our hypothesis that dietary induction of CGL/H_2S promotes functional muscle recovery after ischemic injury, PAG treatment (a specific inhibitor of CGL), which blocks endothelial H_2S production (Figure 5a) abrogated the

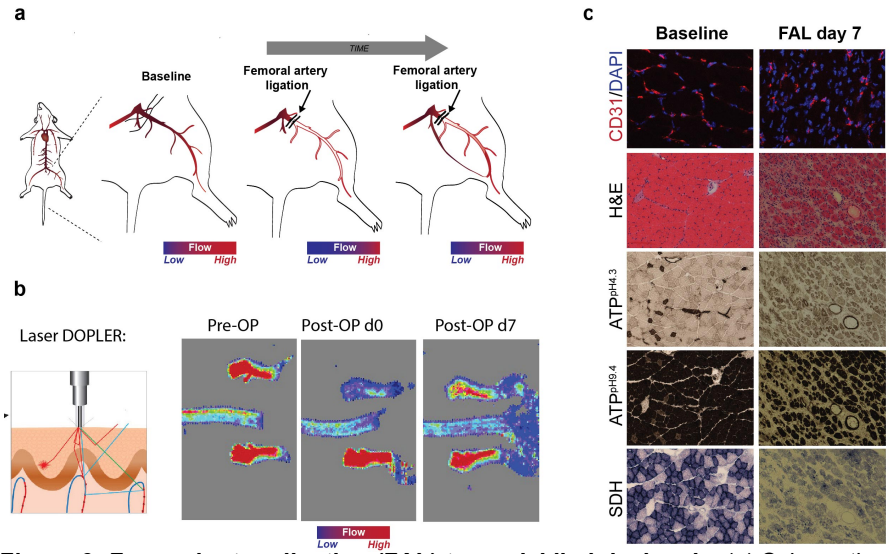

Figure 6: Femoral artery ligation (FAL) to model limb ischemia. (a) Schematic representation of the FAL model. (**b**) Representative Laser Doppler Imaging of the ischemic and non ischemic limb at the indicated time. (**c**) Representative transverse sections of gastrocnemius muscle from WT mice stained for CD31, H&E, mATPase (indicating type I and II fibers) and SDH activity (from top to bottom).

neovascularization induced by DR (Figure 7a). At a functional level, these changes in vascularization imparted running endurance as shown by significantly increased running time and distance in DR animals compared to *ad libitum* (AL)-fed control, which was abrogated by PAG (Figure 7b). To examine the importance of H_2S produced via CGL, in absence of dietary intervention, we recently generated CGL overexpressing mice (CGL^{Tg}, Figure 7c-f) by inserting 157 kb fragment of genomic DNA containing the CGL-encoding gene, resulting in a duplication of the complete CGL gene (a kind gift of Prof. James R. Mitchell, and currently in the Lausanne vascular laboratory breeding colony). CGL^{Tg} mice are on a C57BL/6 background. As predicted, Western blot analyses of multiple tissues confirmed that CGL was overexpressed in CGL^{Tg} mice compared to littermate controls (see CGL overexpression in liver extracts in Figure 7c). This correlated with increased H_2S production (Figure 7d) and importantly, improved recovery following femoral ligation in vivo (Figure 7e). Finally, the functional benefits of CGL overexpression were demonstrated by significantly increased running time and distance in CGL^{Tg} mice compared to CGL^{WT} controls, 4 and 14 days following femoral artery ligation (Figure 7f).

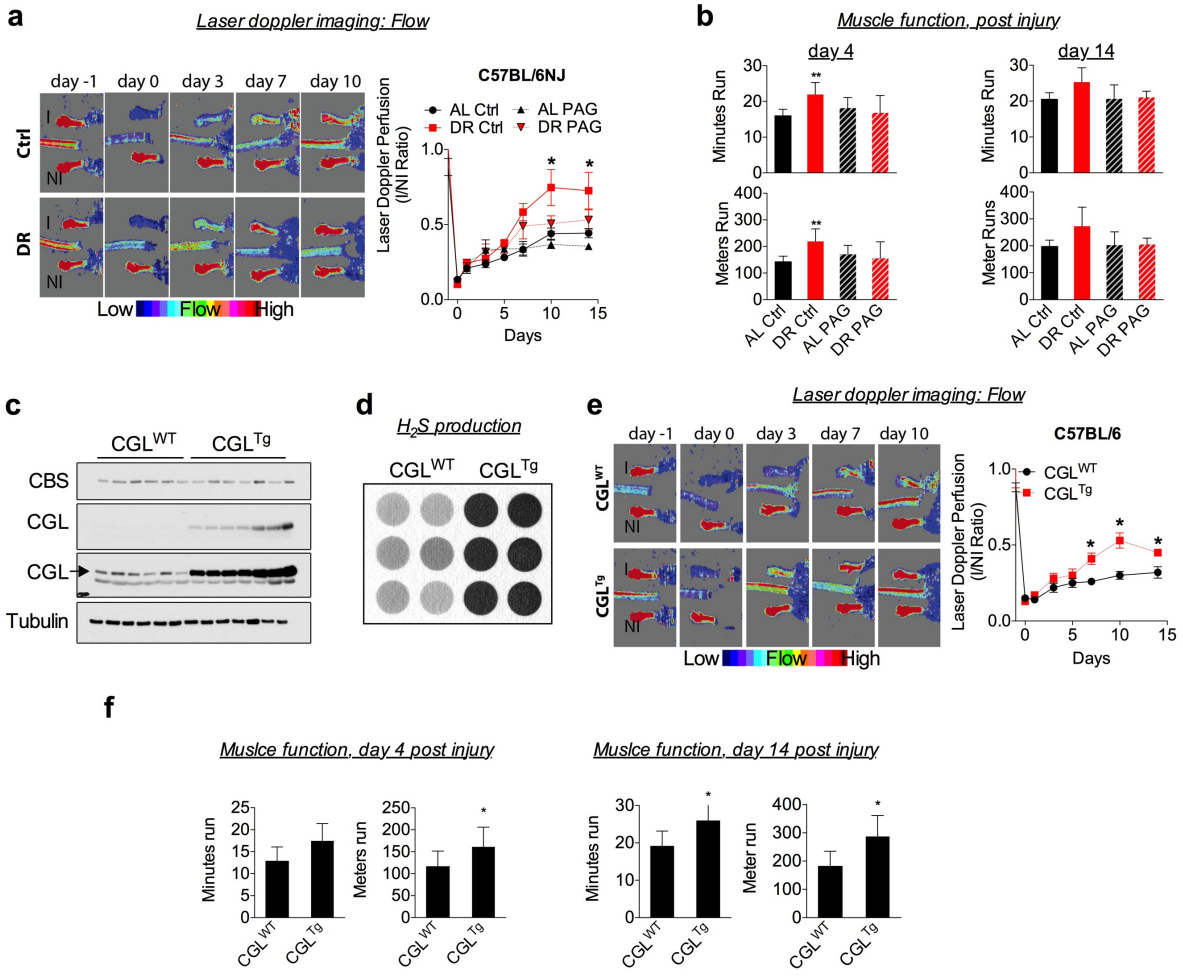

Figure 7. Role of H_2S following ischemic muscle injury (**a**) Longitudinal Doppler imaging of blood flow in WT mice preconditioned on Ctrl or DR diets as indicated for 2 weeks prior to femoral artery occlusion, in presence or absence of PAG (20mg/kg/day, a specific inhibitor of CGL) as indicated. I=ischemic; NI, non-ischemic. Left: representative infrared images on the indicated day after occlusion. Right: quantification of blood-flow recovery; n=6/group. (**b**) Time spent and distance run until exhaustion in treadmill exercise test 4 and 14 days after femoral artery occlusion, in mice preconditioned on Ctrl or DR diets for 2 wks, in presence or absence of PAG (n=6/group). (**c-d**) Immunoblot for the indicated protein (**c**) and H_2S production (**d**) in liver extracts of CGL^{WT} or CGL^{Tg} mice as indicated. (**e**) Longitudinal Doppler imaging of blood flow in in CGL^{WT} or CGL^{Tg} as indicated. I=ischemic; NI, non-ischemic. Left: representative infrared images on the indicated day after occlusion. Right: quantification of blood-flow recovery; n=8/genotype. (**f**) Time spent and distance run until exhaustion in treadmill exercise test 4 and 14 days after femoral artery occlusion, in CGL^{WT} or CGL^{Tg}; n=8/genotype. Error bars indicate SD. **p*<0.05, ***p*<0.0 compared to Ctrl or WT by Student's t test or two-way ANOVA.

2.2.5. CGL/H_2S regulates blood pressure

In human, systolic blood pressure (SBP) continuously increases with age[53,155]. In addition mice lacking CGL display pronounced hypertension and diminished endothelium-dependent vasorelaxation[28]. Preliminary results demonstrated that 1 week of DR significantly decreased blood pressure (Figure 8a), measured as published[113]. Importantly, mice treated with the CGL inhibitor PAG had higher blood pressure, which was not reduced by DR (Figure 8a). In accordance with the role of H_2S as a physiologic vasodilator, preliminary data suggest that SBP is lower in mice overexpressing CGL (CGL Tg) than in their WT counterpart (Figure 8b).

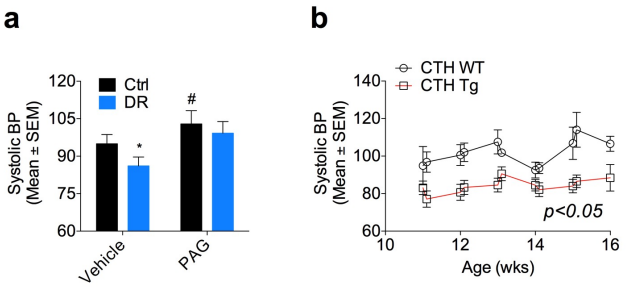

Figure 8 CGL/H_2S regulates blood pressure in-vivo. (**a**) Systolic blood pressure in mice fed ad libitum (AL) or 50% restricted (DR) with or without specific inhibition of CGL with PAG (20mg/kg/day), as indicated. (**b**) Systolic blood pressure in CGL^{WT} or CGL^{Tg}, at the indicated age. n=7-8/group. Error bars indicate SEM. *p<0.05, #p<0.05 compared to Ctrl, or vehicle respectively by two-way ANOVA.

2.2.6. CGL is a circulating enzyme producing systemic H_2S, which predicts survival in human patients undergoing surgical revascularization

The enzyme CGL, secreted by EC and hepatocyte, circulates in the plasma/serum, and actively produces H_2S in human blood[42]. Parabiosis experiments, in which two mice are surgically joined together and develop a single, shared circulatory system[156], indicate that young blood containing humoral "rejuvenating" factors can ameliorate the function of aged tissues[157-161]. We hypothesized that CGL is a circulatory enzyme, important in the support of vascular health. Consitent with enzymatic H_2S production in the serum, our prelimary data indicate that in human and mice, serum H_2S production, using the lead acetate methods[19], requires pyridoxal phosphate (PLP, Figure 9a) a coenzyme for CBS and CGL (but not 3-MST). Furthermore, we observed that 1 week of DR (Figure 9b) and intravenous overexpression of CGL using adenovirus (ad-CGL), without any dietary intervention (Figure 9c) greatly increased serum H_2S. This observation is consistent with our hypothesis that CGL is a circulating enzyme producing systemic H_2S.

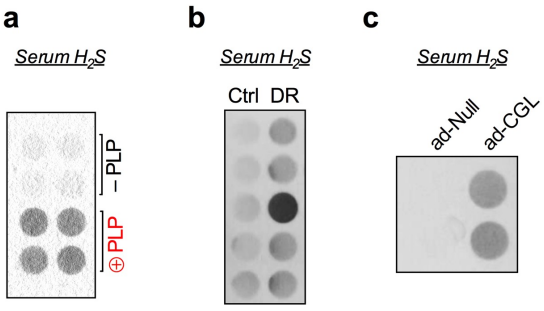

Figure 9. Serum CGL/H_2S is a circulating factor. (**a**) Human serum H_2S production, in presence of absence of pyridoxal phosphate (PLP, as indicated) a coenzyme for CBS and CGL (but not 3-MST). (**b**,**c**) Mouse serum H_2S production capacity in mice under 50% dietary restriction (DR, **b**) or one week after i.v. injection of an adenovirus overexpressing CGL (ad-CGL, **c**). Error bars indicate SEM. *p<0.05 compared to Ctrl-IP by two-way ANOVA.

Using the same assay described in Figure 5a, 9a-c and [19], our preliminary data in 115 vascular surgery patients with PAD reveal that the percentage of survival in the low H_2S group (defined as <median) was lower [6 months, 2 years (78 and 74)] compared to the high H_2S group (defined as >median), [6 months, 2 years (93, 91)], (Figure 10a). Interestingly, in the same patients, H_2S production was inversely correlated with cholesterol and total triglyceride (Figure 10b), well-described cardiovascular risk factors[5,164,165]. Thus, we propose that CGL is a circulating enzyme producing H_2S, with biological impact in human vascular health.

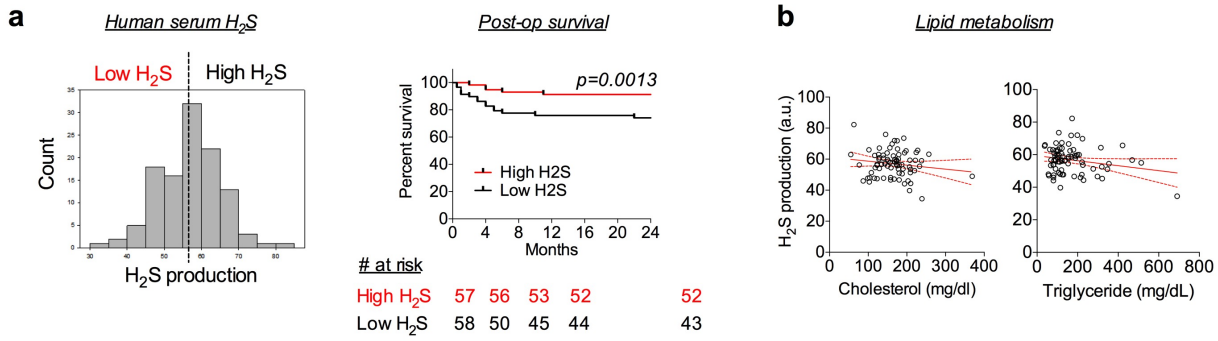

Figure 10: Circulating H_2S production correlates with survival in human
(**a**) Kaplan-Meier survival curve for patients with low (n=58) and high (n=57) serum H_2S before undergoing vascular surgery procedure. P value is derived from log-rank calculation. Error bars indicate SD; p<0.0001 by Mann-Whitney (Wilcoxon rank sum). (**b**) Total serum cholesterol (left) and triglyceride (right) as a function of circulating H_2S. Bars indicate estimate and 95% confidence bands.

2.3 Detailed research plan

Aim 1. Evaluate the function of H_2S in endothelial cells growth and plasticity, and clarify the basis for the age-and ischemia-dependent effects on muscle function.

Aim 1A. Evaluate the role of endothelial CGL/H_2S on vascular homeostasis as a function of age and oxidative stress.

Rationale: ECs are plastic cells that can switch between growth states[50]. In the latest stages of life, impaired ECs regenerative potential and senescence lead to progressive organ failure throughout the body[166,167]. Our preliminary data indicate that endogenous H_2S induced by DR (Figure 5a, appendix 1 and [19,26]), exogenous H_2S (NaHS), and CGL overexpression increases angiogenesis (the formation of new blood vessel), as measured by increased ECs migration, migration speed, tube formation and sprouting both in-vitro and ex-vivo in young ECs (Figure 5). These data in normal "young" ECs will be first be confirmed, then angiogenesis will be further tested in-vitro, using the assays described above, in primary human and mouse ECs exposed to metabolic or oxidative stress, or in senescent EC[166,167]. Further ex-vivo experiment will be performed using aortic rings from young vs. old mice (see Figure 5 and appendix 1). These experiments will provide fundamental insight into the specific role of CGL/H_2S to prevent and/or restore more youthful function to aging ECs. We predict that ablation of CGL/H_2S production in ECs will accelerate senescence and reduce angiogenesis, while overexpression of CGL will delay ECs aging and/or restore ECs youth.

Experimental Approach:

To confirm and extend our preliminary results, ex-vivo aortic ring assays (as in Figure 3a and 5e) will be performed using the following mice models:

1. Young (10 weeks) and old (12 months) CGL^{WT} and CGL^{Tg} aortas (n=7 per group, total 28). The number and total area of sprouts originating from aortic rings will be quantified at day 0, 3 and every day up to day 10. In addition, primary ECs will be isolated from the lung by collagenase digestion followed by sequential affinity selection method using positive selection of CD31 (as in Figure 5f and appendix 1), ECs sprouting will be assayed as described below.
2. Young (10 weeks) and aging (6 months) CGL^{WT} and CGL^{KO} aortas (n=7 per group, total 28) and primary ECs isolated (as above in 1. and appendix 1). We note that for the age effect, 6 month-old mice (versus 12 month-old) will be used, allowing the **detection of premature aging**.

To model the effect of age *in-vitro*, we will also compare the "angiogenic potential" (as in Figure 5 and appendix 1) in several models of stress/age-induced senescence in vitro.

1. **Young** normal HUVECs (passages 1-5, Lonza) vs. **old replicative senescent** HUVECs (passages 21-16[166]).
2. **Young** HUVECs exposed or not to chronic low-dose **H_2O_2 to induce senescence**-like phenotype. To mimic the age-related oxidative environment, HUVECs will be treated with H_2O_2 (40, 60 and 80μM for 1 hour and then cultured for another 24 hours as published[168-170].
3. **Young** HUVECs exposed or not to chronic high glucose and low dose palmitate. To model **age-related metabolic** stress HUVECs will be treated with high glucose (25 mM) and palmitate (1-200 μM) for 48 hours as published[171,172].

The "angiogenic potential" will be studied as follows:

i. To assess **migration**, wound healing assay will be used in serum-starved (over night), mitotically arrested cells (1 μg/ml Mitomycin C overnight). Migration will be quantified every 4 hours up to 16 hours, and expressed as the migrated area over the total area of the wound.

ii. To assess **proliferation**, HUVECs will be seeded at a low density, serum starved overnight then incubated for 24 hours in media containing 2% serum and 100 *μ*M BrdU in presence or absence of 100ng/ml of VEGF. Results will be expressed as a the ratio of BrdU positive cells per total (DAPI positive) cells, in multiples random fields, as published[117].

iii. To assess **tube formation** serum-starved (over night) HUVECs will be seeded in media with or without 100ng/ml of VEGF in a 24-well plate coated with 150 μL Matrigel® reduced growth factor basement membrane extract (Corning). Following an 18 hour-incubation, the number of branch points and total length of tubule networks will be quantified.

iv. To assess **senescence** and DNA damage Senescence-associated beta-galactosidase (SA-β-Gal) and phosphorylated histone H2AX (γH2AX) will be quantified. Results will be expressed as ratio of SA-β-Gal or γH2AX positive cells to total number of cells[171,172].

v. To asses oxidative stress and apoptosis, Mitosox and Annexin V staining assays will be used, respectively. Single cell suspension will be stained with MitoSox (ThermoFischer) and with Annexin V kit (Pharmingen). H_2O_2 (500*μ*M) will be used a positive control. Results will be expressed as fluorescence intensity (MitoSox) or as the ratio of Annexin V positive / total number cells alive[171,172].

The ability of CGL/H_2S to restore angiogenic potential in "old/stressed" ECs (using the best model of aging defined above) will be tested in the following conditions:

1. HUVECs will be infected with a control adenovirus (ad-Null, Ctrl) or an adenovirus overexpressing CGL (ad-CGL, Figure 5h). 48 hours post infection, cells will be assayed as described above.
2. HUVECs will be treated 24 hours before and throughout the assay or not (Ctrl) with 200μM GYY413 (Sigma-Aldrich, long acting H_2S releasing drug) or 10μM NaHS (Sigma-Aldrich, short acting H_2S releasing drug).

Aim 1B: Evaluate the impact of CGL/H_2S on endothelial health and skeletal muscle function.

Rationale: Skeletal muscle is an ideal tissue to study the effects of aging on the vascular system, with clearly documented reductions in capillary density and function, contributing to a loss of muscle mass (sarcopenia), exercise and regenerative capabilities (Figure 3 and [145,149,160,173,174 175-177]). DR stimulates angiogenesis via endogenous H_2S (Figure 4, 5), and muscle regeneration in young and old mice (Figure 7 and [63,178]). ECs are the principal source of H_2S in the muscle, and require CGL (Figure 5i). Here, we propose to examine if CGL/H_2S can prevent and/or restore more youthful function to aging ECs *in-vivo*. We predict that overexpression of CGL in transgenic mice (CGL^{Tg}) will delay aging. In addition, we hypothesized that in old mice, 2-week DR will induce endothelial H_2S production and restore the functions of ECs.

Experimental Approach:

1. To examine if CGL/H_2S can prevent and/or delay the age-dependant reduction in vascular density and muscle function, male, **young** (10 week-old) and **old** (12 month-old) CGL^{WT} and CGL^{Tg} (n=10 per group) will undergo unilateral femoral artery ligation; a clinically relevant model of age-related vascular injury (Figure 6 and [149,160,179,180]). Prior to femoral ligation, longitudinal non-invasive tail cuff blood pressure measures will be taken on all the mice over two weeks (Figure 11) in the awake, conscious animal using the BP-2000 Blood Pressure Analysis System™ in the Cardiovascular Assessment Facility (CAF) in the University of Lausanne (www.unil.ch/caf) as published[113].

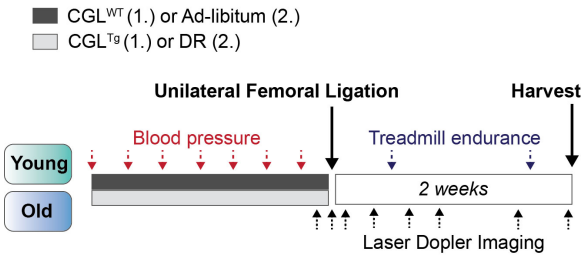

Figure 11: Aim 1B experimental design

In each of these experiments, the contralateral, uninjured limb will be used as the baseline (control). All the animals will return to a normal control chow diet after surgery. Longitudinal non-invasive limb and foot flow will be measured using Laser Doppler perfusion imaging (LDPI, Moor Instruments, Inc. DE) pre-and post-operatively at day (POD) 0, 1, 3, 5, 7 10, 14 in mice kept under isoflurane anaesthesia, and body temperature maintained on a circulating heated water pad (Figure 11). Blood flow will be expressed as Ischemic/Non-ischemic ratio by measuring the ratio of LDPI intensity of the ischemic foot to the contralateral foot. Muscle functionality will be examined using treadmill endurance test (Figure 3, 7 and appendix 1) pre-operatively and at POD 4 and 10. Endurance is measured as the function of time and distance ran. At POD14, animals will be euthanized and muscles (gastrocnemius, tibialis anterior (TA) and popliteal) from the control and ischemic limb harvested. The TA muscle and the upper half of the gastrocnemius will be OCT embedded, frozen and sectioned (7-10μm) for CD31, H_2S (using the fluorescent probe[154], H&E, myosin(m)ATPase assay, Succinate dehydrogenase histochemistry (as in Figure 3, 5, 6 and appendix 1). Vascular density will be expressed as the number and area of CD31+ cells per muscle fiber. Fibers size, number and type will be measured as described[146,181,182]. The distal/lower half of the gastrocnemius and the

popliteal muscle will be snap frozen for molecular analyses, including gene (qPCR) and protein expression (western blot) of VEGF, CBS and CGL as published[19,114,117,119].

In addition, cardiac hypertrophy is a prominent pathological feature of age-related vascular dysfunction, that can be reversed by circulating factors[161]. Thus, we will weights the hearts at the time of sacrifice. Hearts will be fixed embedded, sectioned at midventricle and Masson Trichrome-stained to evaluate fibrosis and hypertrophy as published[119,161]. Heart weight will be normalized to tibia length, a standard method that corrects for differences in body frame size and that is more appropriate than normalization to body weight when using older mice[161].

2. To test if endogenous CGL/H_2S can restore ECs youth, male, young (10 week-old) and old (12 month-old), C57BL/6 WT will be randomly assigned into 2 preconditioning groups (n=10 per group) prior to surgery: 1) Control chow 2) 2-week DR. The complete control diet purchased from Research Diets consists of semipurified ingredients with 72% calories in the form of carbohydrate (sucrose, maltodextrin); 10% calories as fat (lard, soybean oil); and 18% as protein from hydrolyzed casein). The DR regimens tested: 50% DR (50% of *ad libitum* fed control group, or ~0.11 g food/g mouse/day based on average consumption of ~0.22 g food/g mouse/day) as described previously[183]. All groups will then be subjected to the same Experimental Approach as in *1. from Aim 1B*).

Anticipated Results: Aim 1A. Ablation of CGL/H_2S production should reduce sprouting in young but not in old, senescent ECs (Figure 5f). Acute overexpression of CGL (ad-CGL) and exogenous H_2S should rescue age-dependent impairment in angiogenesis (Figure 5g, h) and prevent ECs senescence. Chronic overexpression of CGL (CGL^{Tg}) will prevent ECs aging. Aim 1B. Overexpression of CGL in transgenic mice (CGL^{Tg} Figure 7c-f) should **delay** EC aging and stimulate the formation of new blood vessels, muscle regeneration and muscle function in both young and old animals (Figure 5). Short-term DR/endogenous H_2S should promote angiogenesis and **restore** muscle function after injury in both young and old mice.

Data Analysis and Statistical Considerations: Descriptive statistics (e.g. mean, median, standard deviation) will be calculated for each endpoint. Students t-test will be utilized for the primary endpoint when comparing between two groups, and 2-way-ANOVA for multiple comparisons. We will analyze each of the primary endpoints separately and adjust for multiple comparisons using False Discovery Rate (FDR)[184]. Based on prior reports and extensive experience with the femoral ligation model[66,67] utilizing a detectable difference of 20% (LDI flow or running time/distance), a standard deviation of 12%, a desired power (1-beta) of 0.8, and p value of 0.05 (alpha =0.05), a total of 9 animals in each group are necessary to reach statistically meaningful conclusions[185]. Based on our preliminary and published results, in mice fed ad-libitum, SBP is 15% higher than in littermates mice under DR. If we consider a standard deviation of 10% [28], a desired power (1-beta) of 0.8 and a p value of 0.05 (alpha =0.05), a total of 9 animals in each group are necessary to reach statistically meaningful conclusions[185]. For the aortic ring assay, our preliminary data suggest a detectable difference of 50%. Using standard deviation of 30%, a desired power of 80% and an alpha of 5%, a total of 6 animals in each group are necessary to reach statistically meaningful conclusions[185]. Thus, for Aim 1 a total of 120 mice are needed. We also included an animal and specimen loss rate of 10 percent in determination of the resources necessary to complete this work, leading to a final total of 136 mice.

Potential Problems, Limitations, Alternative Approaches: Aim 1A, Senescent ECs (defined here and elsewhere[167] as cells that seized to proliferate for >2 wks and >50% are positive for SA-β-Gal and γH2AX). These characteristics are usually

observed after passage 20. Depending on the HUVECs and murine ECs isolation this might vary. If so, we will consider defining the time course of senescence, using the molecular markers defined above. It is possible that *in-vitro* CBS is the predominant enzyme generating H_2S, as it has been demonstrated that CBS expression is increased *in-vitro* under conditions of stress whereas in-vivo, our preliminary data consistently suggest that endothelial-H_2S is mostly produced by CGL[186]. As an alternative strategy, we have experience using aminooxyacetic acid (AOAA, 100μM, Sigma-Aldrich), which inhibit both CBS and CGL as published[187]. In addition, CBS can be knocked-down using siRNAs in addition to CGL knock-down. Aim 1B. Aged mice may take longer for maximal effect than young healthy mice. If so, we will consider placing mice for longer periods of time on DR or using alternating regimens (such as methionine restriction, a diet that shares many of the benefits of DR but is given ad-libitum). In addition, the biological function of senescent ECs might differ in aged laboratory rodents than in humans, despite the many similarities in their vascular aging phenotypes[188]. If so, we will consider using a mouse model of premature aging (Cockayne syndrome (CS), lacking DNA repair genes *Csa* and *Xpa* (CX), as published (Brace et al, in press). These mice are currently in the Mitchell lab breeding colony.

Aim 2. Determine the relationship between serum H_2S production and cardiovascular health in mice and in human, using the Cohort study of Lausanne (CoLaus).

Rationale: Circulating H_2S levels correlate positively with vascular health (e.g. blood pressure, muscle function)[32,38,70] and dietary restriction (Figure 4, 8, 9 and [62]) in mice. In human, single nucleotide polymorphism (SNP) in CGL is linked to variation in serum homocysteine[189]. Published and preliminary data indicate that the enzyme CGL, secreted by ECs and hepatocytes, circulates in the serum, and actively produces H_2S in human blood (Figure 4d, 10 and [42]). Our preliminary data indicates that in PAD patients, serum H_2S is significantly reduced compared to healthy control (Figure 4d) and inversely correlates with metabolic health (Figure 10b). Importantly, in PAD patients undergoing open surgical revascularization, pre-operative serum H_2S linearly correlates with 2-years survival following surgery (Figure 10a). Here we propose 1) Characterize the association between H_2S and the function of ECs in the mice from Aim 1B. , and 2). Expand our analysis (Figure 10) in humans, and define the association between serum CGL/H_2S and cardiovascular diseases in the CoLaus cohort[164,165,190,191].

Experimental Approach:

Aim 2A. Establish the importance of circulating/systemic H_2S production in mice throughout life.

1. First, to characterize serum H_2S production, serum will be collected in male, **young** (10 week-old) and **old** (12 month-old) CGL^{WT} and CGL^{Tg} (n=10 per group) from Aim 1B. Small volume of tail blood (~150 microliter) will be collected 2d before surgery. Serum will be prepared from blood centrifugation as published[114]. Serum H_2S production will be measured using the lead acetate assay. Briefly 20 microliter of serum will be incubated with 10mM Cysteine and 1 mM Pyridoxal 5'-phosphate hydrate (PLP, Sigma) until lead sulfide darkening is visible, but not oversaturated (as in [19,26] and Figure 5a, 9). Mean $intensity^{-1}$ of the darkening will be used to quantify the activity of H_2S producing enzymes[26,121].
2. Serum will be collected in male, young (10 week-old) and old (12 month-old), fed with 1) Control chow 2) 2-week DR (n=10 per group) from Aim 1B. Serum H_2S production will be assessed as in *1. from Aim 2A*
3. H_2S production using lead acetate method is an indirect readout of the associated presence of CGL. In order to gain further insight into the exact level of circulating H_2S-producing enzyme, large volume of serum will be collected in **young** (10 week-old) and **old** (12 month-old) C57BL/6 WT (n=10 per group). Blood will be collected by cardiac puncture (0.5 to 1 ml) under general anesthesia. Serum H_2S production will be assessed as in *1. from Aim 2A*. The exact level of circulating H_2S-producing enzyme, CGL, CBS and 3-MST will be assessed by western blot, after clearing the samples of IgG and albumin (Albumin & IgG Depletion SpinTrap™, Sigma-Aldrich) and quantified as published[117,119].

Aim 2B: Determine the relationship between serum H_2S and cardiovascular traits in CoLaus, a large human cohort.

The CoLaus study, initiated in 2003, is a large population-based monocentric study in Lausanne, including 6738 extensively phenotyped subjects at baseline and during a 5-years follow-up. All of the subjects were genotyped using Affymetrix 500K SNP chip. Designed to identify novel epidemiology and genetic determinants of cardiovascular health, the CoLaus cohort led to almost 100 original articles, and novel links between cardiovascular risk factor and disease with socioecomnomic status, mental disorders, dietary habits, biological mediators and single-nucleotide polymorphism (SNP)[164,165,190-194]. These experiments will be performed in collaboration with Prof. Peter Vollenweider and his team of bioinformaticians (please see accompanying letter of support).

To examine the importance of serum H_2S in human cardiovascular disease, serum H_2S production will be assessed as in *1. from Aim 2A*. Serum H_2S will be primarily correlated with major adverse cardiac events (MACE, defined as death, Q-wave myocardial infarction and the need for repeat revascularization by redo-CABG or repeat percutaneous intervention). MACE was chosen as the primary endpoint as it provides greater statistical power than PAD for example, that occurs with a lower frequency. Secondary endpoints will include PAD and cardiovascular risk factors obtained at the somatic baseline assessment (http://www.colaus.ch/en/tableau_1.pdf). All statistically significant associations will be further tested for confounders using multivariate analysis[195].

Aim 2C: Determine the relationship between H_2S producing enzymes and cardiovascular traits in the CoLaus study.
We will further test for potential associations between 5 annotated SNPs for CBS (chr 21), 4 annotated SNPs for CGL (chr 1) with MACE and H_2S production (from Aim 2B). We note that there is no annotated SNP for 3-MST in the CoLaus cohort. In addition, we propose to confirm the SNP1364G>T (S403I) in exon 12 of CGL[189] as a candidate causal mutation for high total serum homocysteine concentration. This work will be performed by Prof. Peter Vollenweider and his team of bioinformaticians (please see accompanying letter of support).

Aim 2D: Uncover novel genetic determinants of serum H_2S production using the CoLaus study.
From a discovery cohort in the CoLaus study, we will test all possible SNP – serum H_2S pairs for association. After pruning according to SNP linkage and feature correlation, pairs indicating suggestively significant association (defined here as p-value below 5×10^{-8}) in CoLaus will be considered for replication (two-stage GWAS design). This work will be performed by Prof. Peter Vollenweider and his team of Bioinformaticians (please see accompanying letter of support).

Anticipated Results: Aim 2A. Serum CGL/H_2S, will be boosted by CGL overexpression (CGL^{Tg}) and by DR in both young and old mice (Figure 9b, c). From a retrospective analysis of Aim1B, we predict that serum H_2S will be correlated with reduction in blood pressure and muscle damage following femoral ligation. Aim 2B. We predict that serum H_2S production will be reduced in patients with documented MACE and inversely correlate with systolic blood pressure, total triglyceride and cholesterol levels (Figure 9 and 10). Aim 2C, D We anticipate that annotated SNPs in CBS and/or CGL and/or regulating serum H_2S will be associated with or predict the occurrence of MACE.

Data Analysis and Statistical Considerations: For Aim 2A only, 20 mice are needed to reach statistically meaningful conclusions[185], taking into account an animal and specimen loss rate of 10 percent (see Aim 1B for the analysis). The total number of mice needed to complete this work is 156 (Aim 1 and 2). For Aim 2B-D descriptive results will be expressed as number of participants and percentage or as mean ± standard deviation. Bivariate analysis will be conducted using Chi square test for categorical variables and using Student's t test or one-way analysis of variance (ANOVA) for quantitative values. For continuous variables, post hoc pairwise comparisons using the method of Scheffe will be performed when the results of the ANOVA are statistically significant. Multivariable analysis will be conducted using logistic regression for binary dependent variables, and the results expressed as odds-ratio and (95 % confidence interval); for quantitative variables, multivariable ANOVA will be used and the results will be expressed as adjusted mean ± standard error. Logarithmic transformation will be applied to skewed traits. For Aim 2B, our preliminary data suggest a 1.4 fold decrease in serum H_2S levels among patients suffering PAD compared to healthy control. Using a p value of 0.01 (alpha =0.01), desired power (1-beta) of 0.9 and common standard deviation of 25%, the sample size that

will detect a statistically significant difference is 46. For biologically relevant linear variable (e.g. blood pressure, lipids, age), we anticipate a Pearson (R square) value of 0.1. Using a p value of 0.01 (alpha =0.01), the estimate sample size is 272, which can be extracted from the cohort via simple randomization. Statistical analyses were conducted using SAS software (v9.3; SAS Institute, Inc, Cary, NC.). For Aim 2C, D. Upon completion of Aim 2 we plan to meet with Prof. Peter Vollenweider and the CoLaus team to determine the appropriate additional confirmatory cohorts based on preliminary data provided by the CoLaus study.

Potential Problems, Limitations, Alternative Approaches: Aim 2A. Same as Aim 1B. Aim 2A. The effects of H_2S produced by CGL in the serum on vascular health may be difficult to separate from the benefits of free H_2S or sulfur species. Thus, we might measure H_2S and sulfane sulfur levels using gas chromatography chemilumunescence (Agilent 7890 GC gas chromatography system and G660XA Series chemiluminescence detector)[38]. This can be easily accomplished in collaboration with Prof. James Mitchell in Boston. Aim 2B-D. Our primary endpoint (MACE) was chosen to increase statistical power. However, due to variation amongst humans with very different genetic backgrounds and diets, we may need to significantly increase the number of samples (see *Data Analysis and Statistical Considerations)* to detect a significant association between H_2S and any MACE (primary endpoint).

2.4 Schedule and milestones

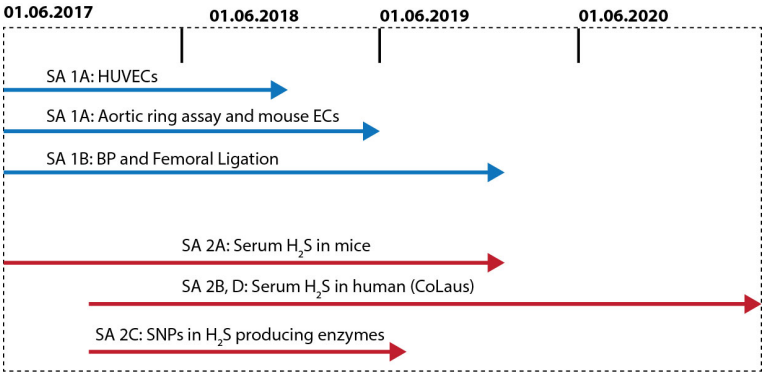

The experiments in Aim 1 and 2 can be accomplished within 4 years given that all of the mouse lines, models and human samples are available. General benchmarks for success beyond rigorous peer review and publication include access to cutting edge facilities and technical assistance available in Lausanne or Harvard University in Boston.

2.5 Relevance and impact

The progressive decline in vascular ECs function is one of the major causes of aging and age-related diseases including heart and cerebrovascular diseases, exercise intolerance, hypertension, impaired wound healing, and sarcopenia. The number of people of advanced age is going to double in the next 35 years, further compounding the problem. Yet the underlying cause of vascular decline with age is not known and there is little that can be done for frail patients. Although the implementation of health and social measures is necessary to improve the quality of life of older adults, the immediate challenge for medical gerontology is to identify pharmacological strategies to promote healthy aging "healthspan". Next year, Metformin (an oral anti-diabetic molecule) will be the world first anti-aging molecule tested on humans in trials (*https://clinicaltrials.gov/ct2/show/NCT02432287)*. This proposal will provide important mechanistic insight into the potential of endothelial H_2S to improve vascular health in the context of aging and aging-related diseases such as hypertension and peripheral artery disease. Within this age group, cardiovascular disease is the leading cause of death, and the cost associated with treatment will continue to increase. The role of ECs, and the potential of endothelial-targeted therapies to promote vascular health in the context of aging remain mostly unexplored. The knowledge to be obtained

through this research proposal will provide the basis for new translational research of DR and H_2S-based therapies in humans.

2.5.1. Future directions – Basic research

1. Based on published[42] and the data generated from Aim 1-2, we anticipate that ECs are the source of serum CGL. ECs as the source of H_2S vascular benefits opens up a number questions, including whether autocrine, paracrine or endocrine signaling is mediating the benefits of H_2S (e.g. protection from ischemia, neurodegeneration, etc). Furthermore, it questions whether some of the DR benefits (e.g. increase lifespan, stress resistance) require endothelial-derived circulating CGL/H_2S. In the future, we may need to develop a model such as parabiosis in which two mice are surgically joined together and develop a single, shared circulatory system (Figure 9 and [156]) using hetero-parabionts of mice lacking or not CGL specifically in ECs (CGL^{ECKO}).
2. The data generated form Aim 2D, may provide a novel gene implicated in the regulation of H_2S production, and relevant to the biology of aging, and beyond in the treatment and prevention of ischemia, metabolic syndrome, cancer or hypoxia.

2.5.2. Future directions – Clinical translation

1. The knowledge to be obtained from Aim 2 might validate the use of circulating H_2S as a novel biomarker of vascular dysfunction or/and potential target for H_2S based therapies in the treatment and prevention myocardial infarction, stroke, peripheral artery disease and aging.
2. In addition, patients with artery disease undergoing surgery (e.g. vein graft) experience a number of surgical complications including poor wound healing, heart attack/stroke, and/or revascularization failure in the period of up to one year following surgery at a relatively high rate[196]. Although a number of risk factors for poor surgical outcome have been identified, no single risk factor or group of risk factors can accurately predict postoperative outcome, nor are there any interventional strategies to mitigate surgical risk [197]. We propose that serum H_2S could be a novel marker of surgical outcome, which could improve patient diagnosis, care and overall outcome. Importantly, we are currently evaluating the use of short-term DR preconditioning (with Prof. Ozaki at Brigham Women's Hospital) in patients undergoing endovascular interventions.

3. BIBLIOGRAPHY

1 Le Couteur, D. G. & Lakatta, E. G. A vascular theory of aging. *J Gerontol A Biol Sci Med Sci* **65**, 1025-1027, doi:10.1093/gerona/glq135 (2010).

2 Duscha, B. D. *et al.* Capillary density of skeletal muscle: a contributing mechanism for exercise intolerance in class II-III chronic heart failure independent of other peripheral alterations. *J Am Coll Cardiol* **33**, 1956-1963 (1999).

3 Askew, C. D. *et al.* Skeletal muscle phenotype is associated with exercise tolerance in patients with peripheral arterial disease. *J Vasc Surg* **41**, 802-807, doi:10.1016/j.jvs.2005.01.037 (2005).

4 Costa, C. & Virag, R. The endothelial-erectile dysfunction connection: an essential update. *J Sex Med* **6**, 2390-2404, doi:10.1111/j.1743-6109.2009.01356.x (2009).

5 Mozaffarian, D. *et al.* Heart Disease and Stroke Statistics-2016 Update: A Report From the American Heart Association. *Circulation* **133**, e38-360, doi:10.1161/CIR.0000000000000350 (2016).

6 McCay, C. M., Crowell, M. F. & Maynard, L. A. The effect of retarded growth upon the length of life span and upon the ultimate body size. 1935. *Nutrition* **5**, 155-171; discussion 172 (1989).

7 Speakman, J. R. & Mitchell, S. E. Caloric restriction. *Mol Aspects Med* **32**, 159-221, doi:10.1016/j.mam.2011.07.001 (2011).

8 Johnson, J. E. & Johnson, F. B. Methionine restriction activates the retrograde response and confers both stress tolerance and lifespan extension to yeast, mouse and human cells. *PLoS One* **9**, e97729, doi:10.1371/journal.pone.0097729 (2014).

9 Cabreiro, F. *et al.* Metformin retards aging in C. elegans by altering microbial folate and methionine metabolism. *Cell* **153**, 228-239, doi:10.1016/j.cell.2013.02.035 (2013).

10 Grandison, R. C., Piper, M. D. & Partridge, L. Amino-acid imbalance explains extension of lifespan by dietary restriction in Drosophila. *Nature* **462**, 1061-1064, doi:10.1038/nature08619 (2009).

11 Troen, A. M. *et al.* Lifespan modification by glucose and methionine in Drosophila melanogaster fed a chemically defined diet. *Age (Dordr)* **29**, 29-39, doi:10.1007/s11357-006-9018-4 (2007).

12 Heilbronn, L. K. & Ravussin, E. Calorie restriction and aging: review of the literature and implications for studies in humans. *Am J Clin Nutr* **78**, 361-369 (2003).

13 Miller, R. A. *et al.* Methionine-deficient diet extends mouse lifespan, slows immune and lens aging, alters glucose, T4, IGF-I and insulin levels, and increases hepatocyte MIF levels and stress resistance. *Aging Cell* **4**, 119-125, doi:10.1111/j.1474-9726.2005.00152.x (2005).

14 Orentreich, N., Matias, J. R., DeFelice, A. & Zimmerman, J. A. Low methionine ingestion by rats extends life span. *J Nutr* **123**, 269-274 (1993).

15 Mattison, J. A. *et al.* Impact of caloric restriction on health and survival in rhesus monkeys from the NIA study. *Nature* **489**, 318-321, doi:10.1038/nature11432 (2012).

16 Colman, R. J. *et al.* Caloric restriction delays disease onset and mortality in rhesus monkeys. *Science* **325**, 201-204, doi:10.1126/science.1173635 (2009).

17 Fontana, L., Partridge, L. & Longo, V. D. Extending healthy life span--from yeast to humans. *Science* **328**, 321-326, doi:10.1126/science.1172539 (2010).

18 Fontana, L. & Klein, S. Aging, adiposity, and calorie restriction. *JAMA* **297**, 986-994, doi:10.1001/jama.297.9.986 (2007).

19 Hine, C. *et al.* Endogenous hydrogen sulfide production is essential for dietary restriction benefits. *Cell* **160**, 132-144, doi:10.1016/j.cell.2014.11.048 (2015).

20 Robertson, L. T. *et al.* Protein and Calorie Restriction Contribute Additively to Protection from Renal Ischemia Reperfusion Injury Partly via Leptin Reduction in Male Mice. *J Nutr*, doi:10.3945/jn.114.199380 (2015).

21 Harputlugil, E. *et al.* The TSC complex is required for the benefits of dietary protein restriction on stress resistance in vivo. *Cell Rep* **8**, 1160-1170, doi:10.1016/j.celrep.2014.07.018 (2014).

22 Peng, W. *et al.* Surgical stress resistance induced by single amino acid deprivation requires Gcn2 in mice. *Sci Transl Med* **4**, 118ra111, doi:10.1126/scitranslmed.3002629 (2012).

23 Verweij, M. *et al.* Preoperative fasting protects mice against hepatic ischemia/reperfusion injury: mechanisms and effects on liver regeneration. *Liver Transpl* **17**, 695-704, doi:10.1002/lt.22243 (2011).

24 Varendi, K. *et al.* Short-term preoperative dietary restriction is neuroprotective in a rat focal stroke model. *PLoS One* **9**, e93911, doi:10.1371/journal.pone.0093911 (2014).

25 Mauro, C. R. *et al.* Preoperative dietary restriction reduces intimal hyperplasia and protects from ischemia-reperfusion injury. *J Vasc Surg*, doi:10.1016/j.jvs.2014.07.004 (2014).

26 Mitchell, S. J. *et al.* Effects of Sex, Strain, and Energy Intake on Hallmarks of Aging in Mice. *Cell Metab* **23**, 1093-1112, doi:10.1016/j.cmet.2016.05.027 (2016).

27 Miller, D. L. & Roth, M. B. Hydrogen sulfide increases thermotolerance and lifespan in Caenorhabditis elegans. *Proc Natl Acad Sci U S A* **104**, 20618-20622, doi:10.1073/pnas.0710191104 (2007).

28 Yang, G. *et al.* H2S as a physiologic vasorelaxant: hypertension in mice with deletion of cystathionine gamma-lyase. *Science* **322**, 587-590, doi:10.1126/science.1162667 (2008).

29 Paul, B. D. & Snyder, S. H. H_2S signalling through protein sulfhydration and beyond. *Nat Rev Mol Cell Biol* **13**, 499-507, doi:10.1038/nrm3391 (2012).
30 Blackstone, E., Morrison, M. & Roth, M. B. H2S induces a suspended animation-like state in mice. *Science* **308**, 518, doi:10.1126/science.1108581 (2005).
31 Cai, W. J. *et al.* The novel proangiogenic effect of hydrogen sulfide is dependent on Akt phosphorylation. *Cardiovasc Res* **76**, 29-40, doi:10.1016/j.cardiores.2007.05.026 (2007).
32 Polhemus, D. J. *et al.* Hydrogen sulfide attenuates cardiac dysfunction after heart failure via induction of angiogenesis. *Circ Heart Fail* **6**, 1077-1086, doi:10.1161/CIRCHEARTFAILURE.113.000299 (2013).
33 Shi, Y. X. *et al.* Chronic sodium hydrosulfide treatment decreases medial thickening of intramyocardial coronary arterioles, interstitial fibrosis, and ROS production in spontaneously hypertensive rats. *Am J Physiol Heart Circ Physiol* **293**, H2093-2100, doi:10.1152/ajpheart.00088.2007 (2007).
34 Zhao, X. *et al.* Regulatory effect of hydrogen sulfide on vascular collagen content in spontaneously hypertensive rats. *Hypertens Res* **31**, 1619-1630, doi:10.1291/hypres.31.1619 (2008).
35 Wang, Y. *et al.* Role of hydrogen sulfide in the development of atherosclerotic lesions in apolipoprotein E knockout mice. *Arterioscler Thromb Vasc Biol* **29**, 173-179, doi:10.1161/ATVBAHA.108.179333 (2009).
36 Zanardo, R. C. *et al.* Hydrogen sulfide is an endogenous modulator of leukocyte-mediated inflammation. *FASEB J* **20**, 2118-2120, doi:10.1096/fj.06-6270fje (2006).
37 Chen, Y. H. *et al.* Endogenous hydrogen sulfide in patients with COPD. *Chest* **128**, 3205-3211, doi:10.1378/chest.128.5.3205 (2005).
38 Islam, K. N., Polhemus, D. J., Donnarumma, E., Brewster, L. P. & Lefer, D. J. Hydrogen Sulfide Levels and Nuclear Factor-Erythroid 2-Related Factor 2 (NRF2) Activity Are Attenuated in the Setting of Critical Limb Ischemia (CLI). *J Am Heart Assoc* **4**, doi:10.1161/JAHA.115.001986 (2015).
39 Beard, R. S. & Bearden, S. E. Vascular complications of cystathionine β-synthase deficiency: future directions for homocysteine-to-hydrogen sulfide research. *Am J Physiol Heart Circ Physiol* **300**, H13-26, doi:10.1152/ajpheart.00598.2010 (2011).
40 Wang, R. Physiological implications of hydrogen sulfide: a whiff exploration that blossomed. *Physiol Rev* **92**, 791-896, doi:10.1152/physrev.00017.2011 (2012).
41 Olson, K. R. Is hydrogen sulfide a circulating "gasotransmitter" in vertebrate blood? *Biochim Biophys Acta* **1787**, 856-863, doi:10.1016/j.bbabio.2009.03.019 (2009).
42 Bearden, S. E., Beard, R. S. & Pfau, J. C. Extracellular transsulfuration generates hydrogen sulfide from homocysteine and protects endothelium from redox stress. *Am J Physiol Heart Circ Physiol* **299**, H1568-1576, doi:10.1152/ajpheart.00555.2010 (2010).
43 Bian, J. S. *et al.* Role of hydrogen sulfide in the cardioprotection caused by ischemic preconditioning in the rat heart and cardiac myocytes. *J Pharmacol Exp Ther* **316**, 670-678, doi:10.1124/jpet.105.092023 (2006).
44 Altaany, Z., Ju, Y., Yang, G. & Wang, R. The coordination of S-sulfhydration, S-nitrosylation, and phosphorylation of endothelial nitric oxide synthase by hydrogen sulfide. *Sci Signal* **7**, ra87, doi:10.1126/scisignal.2005478 (2014).
45 Tao, B. B. *et al.* VEGFR2 functions as an H2S-targeting receptor protein kinase with its novel Cys1045-Cys1024 disulfide bond serving as a specific molecular switch for hydrogen sulfide actions in vascular endothelial cells. *Antioxid Redox Signal* **19**, 448-464, doi:10.1089/ars.2012.4565 (2013).
46 Gao, X. H. *et al.* Quantitative H2S-mediated protein sulfhydration reveals metabolic reprogramming during the integrated stress response. *Elife* **4**, e10067, doi:10.7554/eLife.10067 (2015).
47 Mustafa, A. K. *et al.* H2S signals through protein S-sulfhydration. *Sci Signal* **2**, ra72, doi:10.1126/scisignal.2000464 (2009).
48 Módis, K., Coletta, C., Erdélyi, K., Papapetropoulos, A. & Szabo, C. Intramitochondrial hydrogen sulfide production by 3-mercaptopyruvate sulfurtransferase maintains mitochondrial electron flow and supports cellular bioenergetics. *FASEB J* **27**, 601-611, doi:10.1096/fj.12-216507 (2013).
49 Olson, K. R. *et al.* Thiosulfate: a readily accessible source of hydrogen sulfide in oxygen sensing. *Am J Physiol Regul Integr Comp Physiol* **305**, R592-603, doi:10.1152/ajpregu.00421.2012 (2013).
50 De Bock, K. *et al.* Role of PFKFB3-driven glycolysis in vessel sprouting. *Cell* **154**, 651-663, doi:10.1016/j.cell.2013.06.037 (2013).
51 Rivard, A. *et al.* Age-dependent impairment of angiogenesis. *Circulation* **99**, 111-120 (1999).
52 Lahteenvuo, J. & Rosenzweig, A. Effects of aging on angiogenesis. *Circ Res* **110**, 1252-1264, doi:10.1161/CIRCRESAHA.111.246116 (2012).
53 Lerner, D. J. & Kannel, W. B. Patterns of coronary heart disease morbidity and mortality in the sexes: a 26-year follow-up of the Framingham population. *Am Heart J* **111**, 383-390 (1986).
54 Mozaffarian, D. *et al.* Heart disease and stroke statistics--2015 update: a report from the American Heart Association. *Circulation* **131**, e29-322, doi:10.1161/CIR.0000000000000152 (2015).
55 Faber, J. E. *et al.* Aging causes collateral rarefaction and increased severity of ischemic injury in multiple tissues. *Arteriosclerosis, thrombosis, and vascular biology* **31**, 1748-1756, doi:10.1161/ATVBAHA.111.227314 (2011).

56 Epstein, S. E., Lassance-Soares, R. M., Faber, J. E. & Burnett, M. S. Effects of aging on the collateral circulation, and therapeutic implications. *Circulation* **125**, 3211-3219, doi:10.1161/CIRCULATIONAHA.111.079038 (2012).

57 Fonarow, G. C. *et al.* Age-related differences in characteristics, performance measures, treatment trends, and outcomes in patients with ischemic stroke. *Circulation* **121**, 879-891, doi:10.1161/CIRCULATIONAHA.109.892497 (2010).

58 Ungvari, Z., Kaley, G., de Cabo, R., Sonntag, W. E. & Csiszar, A. Mechanisms of vascular aging: new perspectives. *J Gerontol A Biol Sci Med Sci* **65**, 1028-1041, doi:10.1093/gerona/glq113 (2010).

59 Nguyen, A., Thorin-Trescases, N. & Thorin, E. Working under pressure: coronary arteries and the endothelin system. *Am J Physiol Regul Integr Comp Physiol* **298**, R1188-1194, doi:10.1152/ajpregu.00653.2009 (2010).

60 Csiszar, A. *et al.* Aging-induced phenotypic changes and oxidative stress impair coronary arteriolar function. *Circ Res* **90**, 1159-1166 (2002).

61 Fontana, L., Meyer, T. E., Klein, S. & Holloszy, J. O. Long-term calorie restriction is highly effective in reducing the risk for atherosclerosis in humans. *Proc Natl Acad Sci U S A* **101**, 6659-6663, doi:10.1073/pnas.0308291101 (2004).

62 Young, J. B., Mullen, D. & Landsberg, L. Caloric restriction lowers blood pressure in the spontaneously hypertensive rat. *Metabolism* **27**, 1711-1714 (1978).

63 Kondo, M. *et al.* Caloric restriction stimulates revascularization in response to ischemia via adiponectin-mediated activation of endothelial nitric-oxide synthase. *J Biol Chem* **284**, 1718-1724, doi:10.1074/jbc.M805301200 (2009).

64 Al-Magableh, M. R., Kemp-Harper, B. K. & Hart, J. L. Hydrogen sulfide treatment reduces blood pressure and oxidative stress in angiotensin II-induced hypertensive mice. *Hypertens Res* **38**, 13-20, doi:10.1038/hr.2014.125 (2015).

65 Kolluru, G. K. *et al.* Cystathionine γ-lyase regulates arteriogenesis through NO dependent monocyte recruitment. *Cardiovasc Res*, doi:10.1093/cvr/cvv198 (2015).

66 Hoefer, I. E. *et al.* Arteriogenesis proceeds via ICAM-1/Mac-1- mediated mechanisms. *Circ Res* **94**, 1179-1185, doi:10.1161/01.RES.0000126922.18222.F0 (2004).

67 Hoefer, I. E. *et al.* Direct evidence for tumor necrosis factor-alpha signaling in arteriogenesis. *Circulation* **105**, 1639-1641 (2002).

68 Wang, M. J. *et al.* The hydrogen sulfide donor NaHS promotes angiogenesis in a rat model of hind limb ischemia. *Antioxid Redox Signal* **12**, 1065-1077, doi:10.1089/ars.2009.2945 (2010).

69 Liu, F. *et al.* Hydrogen sulfide improves wound healing via restoration of endothelial progenitor cell functions and activation of angiopoietin-1 in type 2 diabetes. *Diabetes* **63**, 1763-1778, doi:10.2337/db13-0483 (2014).

70 Kondo, K. *et al.* H_2S protects against pressure overload-induced heart failure via upregulation of endothelial nitric oxide synthase. *Circulation* **127**, 1116-1127, doi:10.1161/CIRCULATIONAHA.112.000855 (2013).

71 Elrod, J. W. *et al.* Hydrogen sulfide attenuates myocardial ischemia-reperfusion injury by preservation of mitochondrial function. *Proc Natl Acad Sci U S A* **104**, 15560-15565, doi:10.1073/pnas.0705891104 (2007).

72 Sivarajah, A. *et al.* Anti-apoptotic and anti-inflammatory effects of hydrogen sulfide in a rat model of regional myocardial I/R. *Shock* **31**, 267-274, doi:10.1097/SHK.0b013e318180ff89 (2009).

73 Osipov, R. M. *et al.* Effect of hydrogen sulfide in a porcine model of myocardial ischemia-reperfusion: comparison of different administration regimens and characterization of the cellular mechanisms of protection. *J Cardiovasc Pharmacol* **54**, 287-297, doi:10.1097/FJC.0b013e3181b2b72b (2009).

74 Wei, X. *et al.* Hydrogen sulfide induces neuroprotection against experimental stroke in rats by down-regulation of AQP4 via activating PKC. *Brain Res* **1622**, 292-299, doi:10.1016/j.brainres.2015.07.001 (2015).

75 Qu, K., Chen, C. P., Halliwell, B., Moore, P. K. & Wong, P. T. Hydrogen sulfide is a mediator of cerebral ischemic damage. *Stroke* **37**, 889-893, doi:10.1161/01.STR.0000204184.34946.41 (2006).

76 Han, S. J., Kim, J. I., Park, J. W. & Park, K. M. Hydrogen sulfide accelerates the recovery of kidney tubules after renal ischemia/reperfusion injury. *Nephrol Dial Transplant* **30**, 1497-1506, doi:10.1093/ndt/gfv226 (2015).

77 Katsouda, A., Bibli, S. I., Pyriochou, A., Szabo, C. & Papapetropoulos, A. Regulation and role of endogenously produced hydrogen sulfide in angiogenesis. *Pharmacol Res* **113**, 175-185, doi:10.1016/j.phrs.2016.08.026 (2016).

78 Papapetropoulos, A. *et al.* Hydrogen sulfide is an endogenous stimulator of angiogenesis. *Proc Natl Acad Sci U S A* **106**, 21972-21977, doi:10.1073/pnas.0908047106 (2009).

79 Neu, J., Ozaki, C. K. & Angelides, K. J. Glucocorticoid-mediated alteration of fluidity of brush border membrane in rat small intestine. *Pediatr.Res.* **20**, 79-82 (1986).

80 Farrehi, P. M., Ozaki, C. K., Carmeliet, P. & Fay, W. P. Regulation of arterial thrombolysis by plasminogen activator inhibitor- 1 in mice. *Circulation* **97**, 1002-1008 (1998).

81 Rectenwald, J. E., Moldawer, L. L., Huber, T. S., Seeger, J. M. & Ozaki, C. K. Direct evidence for cytokine involvement in neointimal hyperplasia. *Circulation* **102**, 1697-1702 (2000).

82 Hoefer, I. E. *et al.* Direct evidence for tumor necrosis factor-alpha signaling in arteriogenesis. *Circulation* **105**, 1639-1641 (2002).

83 Rectenwald, J. E. *et al.* Interleukin-10 fails to modulate low shear stress-induced neointimal hyperplasia. *J.Surg.Res.* **102**, 110-118 (2002).

84 Berceli, S. A. *et al.* Differential expression and activity of matrix metalloproteinases during flow-modulated vein graft remodeling. *J Vasc.Surg.* **39**, 1084-1090 (2004).

85 Hoefer, I. E. *et al.* Arteriogenesis proceeds via ICAM-1/Mac-1- mediated mechanisms. *Circ.Res.* **94**, 1179-1185 (2004).
86 Jiang, Z. *et al.* Wall shear modulation of cytokines in early vein grafts. *J Vasc Surg* **40**, 345-350 (2004).
87 Jiang, Z. *et al.* Impact of IL-1beta on flow-induced outward arterial remodeling. *Surgery* **136**, 478-482 (2004).
88 Jiang, Z. *et al.* A novel vein graft model: adaptation to differential flow environments. *American journal of physiology* **286**, H240-245 (2004).
89 Berceli, S. A., Jiang, Z., Klingman, N. V., Schultz, G. S. & Ozaki, C. K. Early differential MMP-2 and -9 dynamics during flow-induced arterial and vein graft adaptations. *J Surg Res.* **134**, 327-334 (2006).
90 Jiang, Z. *et al.* Tumor necrosis factor-alpha and the early vein graft. *J Vasc Surg.* **45**, 169-176 (2007).
91 Jiang, Z. *et al.* TGF-beta- and CTGF-mediated fibroblast recruitment influences early outward vein graft remodeling. *American journal of physiology* **293**, H482-488 (2007).
92 Ozaki, C. K. Cytokines and the early vein graft: strategies to enhance durability. *J Vasc Surg* **45** A92-98 (2007).
93 Zacharski, L. R. *et al.* Reduction of iron stores and cardiovascular outcomes in patients with peripheral arterial disease: a randomized controlled trial. *Jama* **297**, 603-610 (2007).
94 Jiang, Z. *et al.* Interplay of CCR2 signaling and local shear force determines vein graft neointimal hyperplasia in vivo. *FEBS letters* **583**, 3536-3540 (2009).
95 Jiang, Z. *et al.* Established neointimal hyperplasia in vein grafts expands via TGF-beta-mediated progressive fibrosis. *American journal of physiology* **297**, H1200-1207 (2009).
96 Yu, P., Nguyen, B. T., Tao, M., Campagna, C. & Ozaki, C. K. Rationale and practical techniques for mouse models of early vein graft adaptations. *J Vasc Surg* **52**, 444-452 (2010).
97 Nguyen, B. T. *et al.* Immobilization of iron oxide magnetic nanoparticles for enhancement of vessel wall magnetic resonance imaging--an ex vivo feasibility study. *Bioconjugate chemistry* **21**, 1408-1412 (2010).
98 Yu, P., Nguyen, B. T., Tao, M., Bai, Y. & Ozaki, C. K. Mouse vein graft hemodynamic manipulations to enhance experimental utility. *The American journal of pathology* **178**, 2910-2919 (2011).
99 Tao, M. *et al.* Locally Applied Leptin Induces Regional Aortic Wall Degeneration Preceding Aneurysm Formation in Apolipoprotein E-Deficient Mice. *Arterioscler Thromb Vasc Biol*, doi:10.1161/ATVBAHA.112.300543 (2012).
100 Favreau, J. T. *et al.* Murine ultrasound imaging for circumferential strain analyses in the angiotensin II abdominal aortic aneurysm model. *J Vasc Surg* **56**, 462-469, doi:10.1016/j.jvs.2012.01.056 (2012).
101 Mitchell, J. R., Beckman, J. A., Nguyen, L. L. & Ozaki, C. K. Reducing elective vascular surgery perioperative risk with brief preoperative dietary restriction. *Surgery*, doi:10.1016/j.surg.2012.09.007 (2013).
102 Nguyen, B. T. *et al.* Perivascular innate immune events modulate early murine vein graft adaptations. *J Vasc Surg* **57**, 486-492, doi:10.1016/j.jvs.2012.07.007 (2013).
103 Yu, P. *et al.* Lack of interleukin-1 signaling results in perturbed early vein graft wall adaptations. *Surgery* **153**, 63-69 (2013).
104 Tao, M. *et al.* A simplified murine intimal hyperplasia model founded on a focal carotid stenosis. *The American journal of pathology* **182**, 277-287 (2013).
105 Ozaki, C. K., Sobieszczyk, P. S., Ho, K. J., McPhee, J. T. & Gravereaux, E. C. Evidence-based carotid artery-based interventions for stroke risk reduction. *Current problems in surgery* **51**, 198-242, doi:10.1067/j.cpsurg.2014.01.002 (2014).
106 Ozaki, C. K. In brief. *Current problems in surgery* **51**, 194-196, doi:10.1067/j.cpsurg.2014.02.003 (2014).
107 Ho, K. J. *et al.* Predictors and consequences of unplanned hospital readmission within 30 days of carotid endarterectomy. *J Vasc Surg* **60**, 77-84, doi:10.1016/j.jvs.2014.01.055 (2014).
108 Barshes, N. R., Kougias, P., Ozaki, C. K., Goodney, P. P. & Belkin, M. Cost-effectiveness of revascularization for limb preservation in patients with end-stage renal disease. *J Vasc Surg*, doi:10.1016/j.jvs.2014.02.003 (2014).
109 Kalwa, H. *et al.* Central role for hydrogen peroxide in P2Y1 ADP receptor-mediated cellular responses in vascular endothelium. *Proceedings of the National Academy of Sciences of the United States of America* **111**, 3383-3388, doi:10.1073/pnas.1320854111 (2014).
110 Ho, K. J. *et al.* Contemporary predictors of extended postoperative hospital length of stay after carotid endarterectomy. *J Vasc Surg* **59**, 1282-1290, doi:10.1016/j.jvs.2013.11.090 (2014).
111 Barshes, N. R. *et al.* Cost-effectiveness of revascularization for limb preservation in patients with marginal functional status. *Annals of vascular surgery* **28**, 10-17, doi:10.1016/j.avsg.2013.08.004 (2014).
112 Yu, P., Nguyen, B. T., Tao, M., Jiang, T. & Ozaki, C. K. Diet-induced obesity drives negative mouse vein graft wall remodeling. *J Vasc Surg* **59**, 1670-1676, doi:10.1016/j.jvs.2013.05.033 (2014).
113 Allagnat, F. *et al.* Nitric Oxide Deficit Drives Intimal Hyperplasia in Mouse Models of Hypertension. *Eur J Vasc Endovasc Surg* **51**, 733-742, doi:10.1016/j.ejvs.2016.01.024 (2016).
114 Longchamp, A. *et al.* Surgical injury induces local and distant adipose tissue browning. *Adipocyte* **5**, 163-174, doi:10.1080/21623945.2015.1111971 (2016).
115 Mauro, C. R. *et al.* Adipose phenotype predicts early human autogenous arteriovenous hemodialysis remodeling. *J Vasc Surg* **63**, 171-176.e171, doi:10.1016/j.jvs.2014.06.110 (2016).

116 Sharma, G. *et al.* Local perivascular adiponectin associates with lower extremity vascular operative wound complications. *Surgery* **160**, 204-210, doi:10.1016/j.surg.2016.01.024 (2016).
117 Longchamp, A. *et al.* Connexin43 Inhibition Prevents Human Vein Grafts Intimal Hyperplasia. *PLoS One* **10**, e0138847, doi:10.1371/journal.pone.0138847 (2015).
118 Sharma, G. *et al.* Perivascular adipose adiponectin correlates with symptom status of patients undergoing carotid endarterectomy. *Stroke* **46**, 1696-1699, doi:10.1161/STROKEAHA.114.008468 (2015).
119 Longchamp, A. *et al.* The use of external mesh reinforcement to reduce intimal hyperplasia and preserve the structure of human saphenous veins. *Biomaterials* **35**, 2588-2599, doi:10.1016/j.biomaterials.2013.12.041 (2014).
120 Mauro, C. *et al.* Pre-Operative Dietary Restriction Reduces Intimal Hyperpalsia and Protects from Ischemia Reperfusion. *Journal of Vascular Surgery* (in press).
121 Hine, C. & Mitchell, J. R. Calorie restriction and methionine restriction in control of endogenous hydrogen sulfide production by the transsulfuration pathway. *Exp Gerontol* **68**, 26-32, doi:10.1016/j.exger.2014.12.010 (2015).
122 Longo, V. D. *et al.* Interventions to Slow Aging in Humans: Are We Ready? *Aging Cell*, doi:10.1111/acel.12338 (2015).
123 Brace, L. E. *et al.* Lifespan extension by dietary intervention in a mouse model of Cockayne syndrome uncouples early postnatal development from segmental progeria. *Aging Cell* **12**, 1144-1147, doi:10.1111/acel.12142 (2013).
124 Gallinetti, J., Harputlugil, E. & Mitchell, J. R. Amino acid sensing in dietary-restriction-mediated longevity: roles of signal-transducing kinases GCN2 and TOR. *Biochem J* **449**, 1-10, doi:10.1042/BJ20121098 (2013).
125 Mejia, P. *et al.* Dietary restriction protects against experimental cerebral malaria via leptin modulation and T-cell mTORC1 suppression. *Nat Commun* **6**, 6050, doi:10.1038/ncomms7050 (2015).
126 Hine, C. & Mitchell, J. R. Calorie restriction and methionine restriction in control of endogenous hydrogen sulfide production by the transsulfuration pathway. *Exp Gerontol*, doi:10.1016/j.exger.2014.12.010 (2014).
127 Hine, C. & Mitchell, J. R. Saying no to drugs: fasting protects hematopoietic stem cells from chemotherapy and aging. *Cell Stem Cell* **14**, 704-705, doi:10.1016/j.stem.2014.05.016 (2014).
128 Nguyen, B. *et al.* Preoperative diet impacts the adipose tissue response to surgical trauma. *Surgery* **153**, 584-593, doi:10.1016/j.surg.2012.11.001 (2013).
129 Robertson, L. T. & Mitchell, J. R. Benefits of short-term dietary restriction in mammals. *Exp Gerontol* **48**, 1043-1048, doi:10.1016/j.exger.2013.01.009 (2013).
130 van Ginhoven, T. M. *et al.* Dietary restriction modifies certain aspects of the postoperative acute phase response. *J Surg Res* **171**, 582-589, doi:10.1016/j.jss.2010.03.038 (2011).
131 Verweij, M. *et al.* Glucose supplementation does not interfere with fasting-induced protection against renal ischemia/reperfusion injury in mice. *Transplantation* **92**, 752-758, doi:10.1097/TP.0b013e31822c6ed7 (2011).
132 Mitchell, J. R. *et al.* Short-term dietary restriction and fasting precondition against ischemia reperfusion injury in mice. *Aging Cell* **9**, 40-53, doi:10.1111/j.1474-9726.2009.00532.x (2010).
133 van Ginhoven, T. M. *et al.* Pre-operative dietary restriction is feasible in live-kidney donors. *Clinical transplantation* **25**, 486-494 (2010).
134 Harputlugil, E. *et al.* Tsc1 required for benefits of dietary protein restriction on hepatic insulin sensitivity and stress resistance. *Cell reports* (in press).
135 Le Gal, L., Alonso, F., Mazzolai, L., Meda, P. & Haefliger, J. A. Interplay between connexin40 and nitric oxide signaling during hypertension. *Hypertension* **65**, 910-915, doi:10.1161/HYPERTENSIONAHA.114.04775 (2015).
136 Le Gal, L. *et al.* Restoration of connexin 40 (Cx40) in Renin-producing cells reduces the hypertension of Cx40 null mice. *Hypertension* **63**, 1198-1204, doi:10.1161/HYPERTENSIONAHA.113.02976 (2014).
137 Bosco, D., Haefliger, J. A. & Meda, P. Connexins: key mediators of endocrine function. *Physiol Rev* **91**, 1393-1445, doi:10.1152/physrev.00027.2010 (2011).
138 Alonso, F. *et al.* An angiotensin II- and NF-kappaB-dependent mechanism increases connexin 43 in murine arteries targeted by renin-dependent hypertension. *Cardiovasc Res* **87**, 166-176, doi:10.1093/cvr/cvq031 (2010).
139 Alonso, F., Boittin, F. X., Bény, J. L. & Haefliger, J. A. Loss of connexin40 is associated with decreased endothelium-dependent relaxations and eNOS levels in the mouse aorta. *Am J Physiol Heart Circ Physiol* **299**, H1365-1373, doi:10.1152/ajpheart.00029.2010 (2010).
140 Krattinger, N. *et al.* Connexin40 regulates renin production and blood pressure. *Kidney Int* **72**, 814-822, doi:10.1038/sj.ki.5002423 (2007).
141 Haefliger, J. A., Nicod, P. & Meda, P. Contribution of connexins to the function of the vascular wall. *Cardiovasc Res* **62**, 345-356, doi:10.1016/j.cardiores.2003.11.015 (2004).
142 Haefliger, J. A. & Meda, P. Chronic hypertension alters the expression of Cx43 in cardiovascular muscle cells. *Braz J Med Biol Res* **33**, 431-438 (2000).
143 Haefliger, J. A. *et al.* Hypertension differentially affects the expression of the gap junction protein connexin43 in cardiac myocytes and aortic smooth muscle cells. *Adv Exp Med Biol* **432**, 71-82 (1997).
144 Jang, Y. C., Sinha, M., Cerletti, M., Dall'Osso, C. & Wagers, A. J. Skeletal muscle stem cells: effects of aging and metabolism on muscle regenerative function. *Cold Spring Harb Symp Quant Biol* **76**, 101-111, doi:10.1101/sqb.2011.76.010652 (2011).

145 Groen, B. B. *et al.* Skeletal muscle capillary density and microvascular function are compromised with aging and type 2 diabetes. *J Appl Physiol (1985)* **116**, 998-1005, doi:10.1152/japplphysiol.00919.2013 (2014).
146 Nilwik, R. *et al.* The decline in skeletal muscle mass with aging is mainly attributed to a reduction in type II muscle fiber size. *Exp Gerontol* **48**, 492-498, doi:10.1016/j.exger.2013.02.012 (2013).
147 Narkar, V. A. *et al.* Exercise and PGC-1α-independent synchronization of type I muscle metabolism and vasculature by ERRγ. *Cell Metab* **13**, 283-293, doi:10.1016/j.cmet.2011.01.019 (2011).
148 Narkar, V. A. *et al.* AMPK and PPARdelta agonists are exercise mimetics. *Cell* **134**, 405-415, doi:10.1016/j.cell.2008.06.051 (2008).
149 Kuswanto, W. *et al.* Poor Repair of Skeletal Muscle in Aging Mice Reflects a Defect in Local, Interleukin-33-Dependent Accumulation of Regulatory T Cells. *Immunity* **44**, 355-367, doi:10.1016/j.immuni.2016.01.009 (2016).
150 Wallace, J. L. & Wang, R. Hydrogen sulfide-based therapeutics: exploiting a unique but ubiquitous gasotransmitter. *Nat Rev Drug Discov* **14**, 329-345, doi:10.1038/nrd4433 (2015).
151 Arany, Z. *et al.* HIF-independent regulation of VEGF and angiogenesis by the transcriptional coactivator PGC-1alpha. *Nature* **451**, 1008-1012, doi:10.1038/nature06613 (2008).
152 Liu, Y., Cox, S. R., Morita, T. & Kourembanas, S. Hypoxia regulates vascular endothelial growth factor gene expression in endothelial cells. Identification of a 5' enhancer. *Circ Res* **77**, 638-643 (1995).
153 Poole, D. C., Copp, S. W., Ferguson, S. K. & Musch, T. I. Skeletal muscle capillary function: contemporary observations and novel hypotheses. *Exp Physiol* **98**, 1645-1658, doi:10.1113/expphysiol.2013.073874 (2013).
154 Singha, S. *et al.* Toward a selective, sensitive, fast-responsive, and biocompatible two-photon probe for hydrogen sulfide in live cells. *Anal Chem* **87**, 1188-1195, doi:10.1021/ac503806w (2015).
155 Franklin, S. S. *et al.* Hemodynamic patterns of age-related changes in blood pressure. The Framingham Heart Study. *Circulation* **96**, 308-315 (1997).
156 Lynch, L. *et al.* Regulatory iNKT cells lack expression of the transcription factor PLZF and control the homeostasis of T(reg) cells and macrophages in adipose tissue. *Nat Immunol* **16**, 85-95, doi:10.1038/ni.3047 (2015).
157 Mei, W. *et al.* GDF11 Protects against Endothelial Injury and Reduces Atherosclerotic Lesion Formation in Apolipoprotein E-Null Mice. *Mol Ther*, doi:10.1038/mt.2016.160 (2016).
158 Schafer, M. J. *et al.* Quantification of GDF11 and Myostatin in Human Aging and Cardiovascular Disease. *Cell Metab* **23**, 1207-1215, doi:10.1016/j.cmet.2016.05.023 (2016).
159 Katsimpardi, L. *et al.* Vascular and neurogenic rejuvenation of the aging mouse brain by young systemic factors. *Science* **344**, 630-634, doi:10.1126/science.1251141 (2014).
160 Sinha, M. *et al.* Restoring systemic GDF11 levels reverses age-related dysfunction in mouse skeletal muscle. *Science* **344**, 649-652, doi:10.1126/science.1251152 (2014).
161 Loffredo, F. S. *et al.* Growth differentiation factor 11 is a circulating factor that reverses age-related cardiac hypertrophy. *Cell* **153**, 828-839, doi:10.1016/j.cell.2013.04.015 (2013).
162 Gibney, B. C. *et al.* Cross-circulation and cell distribution kinetics in parabiotic mice. *J Cell Physiol* **227**, 821-828, doi:10.1002/jcp.22796 (2012).
163 Kamran, P. *et al.* Parabiosis in mice: a detailed protocol. *J Vis Exp*, doi:10.3791/50556 (2013).
164 Danon-Hersch, N. *et al.* Prevalence, awareness, treatment and control of high blood pressure in a Swiss city general population: the CoLaus study. *Eur J Cardiovasc Prev Rehabil* **16**, 66-72, doi:10.1097/HJR.0b013e32831e9511 (2009).
165 Firmann, M. *et al.* The CoLaus study: a population-based study to investigate the epidemiology and genetic determinants of cardiovascular risk factors and metabolic syndrome. *BMC Cardiovasc Disord* **8**, 6, doi:10.1186/1471-2261-8-6 (2008).
166 Krouwer, V. J., Hekking, L. H., Langelaar-Makkinje, M., Regan-Klapisz, E. & Post, J. A. Endothelial cell senescence is associated with disrupted cell-cell junctions and increased monolayer permeability. *Vasc Cell* **4**, 12, doi:10.1186/2045-824X-4-12 (2012).
167 Wagner, M. *et al.* Replicative senescence of human endothelial cells in vitro involves G1 arrest, polyploidization and senescence-associated apoptosis. *Exp Gerontol* **36**, 1327-1347 (2001).
168 Song, Z. *et al.* Ginsenoside Rb1 prevents H2O2-induced HUVEC senescence by stimulating sirtuin-1 pathway. *PLoS One* **9**, e112699, doi:10.1371/journal.pone.0112699 (2014).
169 Sun, Y., Hu, X., Hu, G., Xu, C. & Jiang, H. Curcumin Attenuates Hydrogen Peroxide-Induced Premature Senescence via the Activation of SIRT1 in Human Umbilical Vein Endothelial Cells. *Biol Pharm Bull* **38**, 1134-1141, doi:10.1248/bpb.b15-00012 (2015).
170 Ruan, Y., Wu, S., Zhang, L., Chen, G. & Lai, W. Retarding the senescence of human vascular endothelial cells induced by hydrogen peroxide: effects of 17beta-estradiol (E2) mediated mitochondria protection. *Biogerontology* **15**, 367-375, doi:10.1007/s10522-014-9507-2 (2014).
171 Liu, J. *et al.* Hydrogen sulfide decreases high glucose/palmitate-induced autophagy in endothelial cells by the Nrf2-ROS-AMPK signaling pathway. *Cell Biosci* **6**, 33, doi:10.1186/s13578-016-0099-1 (2016).
172 Ido, Y., Carling, D. & Ruderman, N. Hyperglycemia-induced apoptosis in human umbilical vein endothelial cells: inhibition by the AMP-activated protein kinase activation. *Diabetes* **51**, 159-167 (2002).

173 Wang, H. *et al.* Apoptosis in capillary endothelial cells in ageing skeletal muscle. *Aging Cell* **13**, 254-262, doi:10.1111/acel.12169 (2014).
174 Degens, H. Age-related changes in the microcirculation of skeletal muscle. *Adv Exp Med Biol* **454**, 343-348 (1998).
175 Croley, A. N. *et al.* Lower capillarization, VEGF protein, and VEGF mRNA response to acute exercise in the vastus lateralis muscle of aged vs. young women. *J Appl Physiol (1985)* **99**, 1872-1879, doi:10.1152/japplphysiol.00498.2005 (2005).
176 Ryan, N. A. *et al.* Lower skeletal muscle capillarization and VEGF expression in aged vs. young men. *J Appl Physiol (1985)* **100**, 178-185, doi:10.1152/japplphysiol.00827.2005 (2006).
177 Denis, C. *et al.* Effects of endurance training on capillary supply of human skeletal muscle on two age groups (20 and 60 years). *J Physiol (Paris)* **81**, 379-383 (1986).
178 Cerletti, M., Jang, Y. C., Finley, L. W., Haigis, M. C. & Wagers, A. J. Short-term calorie restriction enhances skeletal muscle stem cell function. *Cell Stem Cell* **10**, 515-519, doi:10.1016/j.stem.2012.04.002 (2012).
179 Tabebordbar, M. *et al.* In vivo gene editing in dystrophic mouse muscle and muscle stem cells. *Science* **351**, 407-411, doi:10.1126/science.aad5177 (2016).
180 Castiglioni, A. *et al.* FOXP3+ T Cells Recruited to Sites of Sterile Skeletal Muscle Injury Regulate the Fate of Satellite Cells and Guide Effective Tissue Regeneration. *PLoS One* **10**, e0128094, doi:10.1371/journal.pone.0128094 (2015).
181 Fry, C. S. *et al.* Inducible depletion of satellite cells in adult, sedentary mice impairs muscle regenerative capacity without affecting sarcopenia. *Nat Med* **21**, 76-80, doi:10.1038/nm.3710 (2015).
182 Ge, X. *et al.* Lack of Smad3 signaling leads to impaired skeletal muscle regeneration. *Am J Physiol Endocrinol Metab* **303**, E90-102, doi:10.1152/ajpendo.00113.2012 (2012).
183 Hine, C. *et al.* Endogenous hydrogen sulfide production is essential for dietary restriction benefits. *Cell* **160**, 132-144, doi:10.1016/j.cell.2014.11.048 (2015).
184 Benjamini, Y. & Hochberg, Y. Controlling the false discovery rate: a practical and powerful approach to multiple testing. *Journal of the Royal Statistical Society* **57**, 289-300 (1995).
185 SigmaPlot for Windows Version 11.0 v. 11.0 (Systat Software, Inc., 2008).
186 Kabil, O., Yadav, V. & Banerjee, R. Heme-dependent Metabolite Switching Regulates H2S Synthesis in Response to Endoplasmic Reticulum (ER) Stress. *J Biol Chem* **291**, 16418-16423, doi:10.1074/jbc.C116.742213 (2016).
187 Szabo, C. *et al.* Tumor-derived hydrogen sulfide, produced by cystathionine-β-synthase, stimulates bioenergetics, cell proliferation, and angiogenesis in colon cancer. *Proc Natl Acad Sci U S A* **110**, 12474-12479, doi:10.1073/pnas.1306241110 (2013).
188 Dantas, A. P. *et al.* Western diet consumption promotes vascular remodeling in non-senescent mice consistent with accelerated senescence, but does not modify vascular morphology in senescent ones. *Exp Gerontol* **55**, 1-11, doi:10.1016/j.exger.2014.03.004 (2014).
189 Wang, J., Huff, A. M., Spence, J. D. & Hegele, R. A. Single nucleotide polymorphism in CTH associated with variation in plasma homocysteine concentration. *Clin Genet* **65**, 483-486, doi:10.1111/j.1399-0004.2004.00250.x (2004).
190 Christe, V., Waeber, G., Vollenweider, P. & Marques-Vidal, P. Antihypertensive drug treatment changes in the general population: the CoLaus study. *BMC Pharmacol Toxicol* **15**, 20, doi:10.1186/2050-6511-15-20 (2014).
191 Pruijm, M. *et al.* Inflammatory markers and blood pressure: sex differences and the effect of fat mass in the CoLaus Study. *J Hum Hypertens* **27**, 169-175, doi:10.1038/jhh.2012.12 (2013).
192 Rueedi, R. *et al.* Genome-wide association study of metabolic traits reveals novel gene-metabolite-disease links. *PLoS Genet* **10**, e1004132, doi:10.1371/journal.pgen.1004132 (2014).
193 Bender, N. *et al.* Association between variants of the leptin receptor gene (LEPR) and overweight: a systematic review and an analysis of the CoLaus study. *PLoS One* **6**, e26157, doi:10.1371/journal.pone.0026157 (2011).
194 Lin, X. *et al.* Risk prediction of prevalent diabetes in a Swiss population using a weighted genetic score--the CoLaus Study. *Diabetologia* **52**, 600-608, doi:10.1007/s00125-008-1254-y (2009).
195 Neter, J. E., Stam, B. E., Kok, F. J., Grobbee, D. E. & Geleijnse, J. M. Influence of weight reduction on blood pressure: a meta-analysis of randomized controlled trials. *Hypertension* **42**, 878-884, doi:10.1161/01.HYP.0000094221.86888.AE (2003).
196 Ozaki, C. K. *et al.* Prospective, randomized, multi-institutional clinical trial of a silver alginate dressing to reduce lower extremity vascular surgery wound complications. *Journal of vascular surgery* **61**, 419-427 e411, doi:10.1016/j.jvs.2014.07.034 (2015).
197 Mitchell, J. R., Beckman, J. A., Nguyen, L. L. & Ozaki, C. K. Reducing elective vascular surgery perioperative risk with brief preoperative dietary restriction. *Surgery* **153**, 594-598 (2013).

Biomaterials 35 (2014) 2588–2599

Contents lists available at ScienceDirect

Biomaterials

journal homepage: www.elsevier.com/locate/biomaterials

The use of external mesh reinforcement to reduce intimal hyperplasia and preserve the structure of human saphenous veins

Alban Longchamp [a,1], Florian Alonso [a,1], Céline Dubuis [a], Florent Allagnat [a], Xavier Berard [b], Paolo Meda [c], François Saucy [a], Jean-Marc Corpataux [a], Sébastien Déglise [a,1], Jacques-Antoine Haefliger [a,*,1]

[a] Department of Thoracic and Vascular Surgery, University Hospital, Laboratory of Experimental Medicine, Bugnon 21, 1011 Lausanne, Switzerland
[b] Department of Vascular Surgery, Pellegrin Hospital, Univ. Bordeaux, Place Amelie Raba Leon, 33000 Bordeaux, France
[c] Department of Cell Physiology and Metabolism, University of Geneva, School of Medicine, CMU, 1211 Genève 4, Switzerland

ARTICLE INFO

Article history:
Received 1 October 2013
Accepted 18 December 2013
Available online 13 January 2014

Keywords:
Intimal hyperplasia
External polyester mesh reinforcement
Caspase-3
MMPs
Shear stress
Vein graft

ABSTRACT

The saphenous vein is the conduit of choice in bypass graft procedures. Haemodynamic factors play a major role in the development of intimal hyperplasia (IH), and subsequent bypass failure. To evaluate the potential protective effect of external reinforcement on such a failure, we developed an *ex vivo* model for the perfusion of segments of human saphenous veins under arterial shear stress. In veins submitted to pulsatile high pressure (mean pressure at 100 mmHg) for 3 or 7 days, the use of an external macroporous polyester mesh 1) prevented the dilatation of the vessel, 2) decreased the development of IH, 3) reduced the apoptosis of smooth muscle cells, and the subsequent fibrosis of the media layer, 4) prevented the remodelling of extracellular matrix through the up-regulation of matrix metalloproteinases (MMP-2, MMP-9) and plasminogen activator type I. The data show that, in an experimental *ex vivo* setting, an external scaffold decreases IH and maintains the integrity of veins exposed to arterial pressure, via increase in shear stress and decrease wall tension, that likely contribute to trigger selective molecular and cellular changes.

1. Introduction

About one million vascular reconstructions are performed annually worldwide, and the great saphenous vein remains the most widely used conduit [1]. Still, 30–50% of the saphenous grafts fail 1–18 months after the implantation [2]. The main reason for this failure is intimal hyperplasia (IH), which reflects the adaptation of a vein to the injuries caused by an arterial environment [3]. Insertion into the arterial circulation is associated with proliferation and migration of smooth muscle cells (SMCs) into the intima layer [4,5], leading to wall thickening, vessel stenosis and, eventually, graft failure. Among the proteins involved in the development of IH, selected matrix metalloproteinases (MMP-2 and MMP-9) [6], tissue inhibitors of these enzymes (TIMP) [7], and possibly the plasminogen activator inhibitor-1 (PAI-1) [8], play a major role, due to their ability to selectively degrade components of the extracellular matrix, to release SMCs and to promote SMCs migration [3]. Mechanical forces, and particularly low shear stress and high wall tension, contribute to the development of these changes [9]. Following implantation, the vein graft is immediately subjected to arterial pressure as well as to circumferential, radial and pulsatile deformations [10]. Further haemodynamic disturbances occur at the site of anastomoses, because of compliance mismatches [11–13].

Mammalian studies suggest the utility of an external support to prevent the over-distension of grafts, increasing shear stress and reducing wall tension [14–19]. However, the molecular and cellular events affected by such a reinforcement have not yet been investigated under rigorous experimental conditions. We hypothesised that a mesh reinforcement could preserve the architecture of veins exposed to arterial haemodynamic conditions and limit the development of IH through selective molecular modulations. To compare the behaviour of human saphenous veins in the absence and presence of an external macroporous

* Corresponding author. Department of Thoracic and Vascular Surgery C/O Department of Physiology, Bugnon 7a, 1005 Lausanne, Switzerland. Tel.: +41 79 556 85 96.
E-mail address: Jacques-Antoine.Haefliger@chuv.ch (J.-A. Haefliger).
[1] These authors contributed equally to this work.

0142-9612/$ – see front matter © 2013 Elsevier Ltd. All rights reserved.
http://dx.doi.org/10.1016/j.biomaterials.2013.12.041

polyester tubular mesh, we have developed an *ex vivo* vein perfusion system (EVPS), which allows for the independent control of the major haemodynamic forces affecting a venous graft, thus permitting to differentiate their selective effect on specific molecular and cellular parameters [8,20].

2. Material and methods

2.1. Human saphenous veins

Twenty seven surplus segments of non varicose human saphenous veins, hereafter referred to as veins, were obtained from of 27 randomly selected patients (15 men and 12 women) with a median age of 72 years (interquartile range 51–82), who underwent lower limb bypass surgery for critical ischaemia. A 9 cm long segment of the greater saphenous vein, considered to be suitable for bypass surgery, with an external diameter of 2.5–4 mm, was harvested and stored at 4 °C in a RPMI-1640 Glutamax medium, supplemented with 12.5% fetal calf serum (Gibco). All sampled veins were used, whichever the native thickness of their intima layer. Within 1 h after the surgery, the segment was divided in 3 equal parts. One part was fixed in either formalin for immunohistochemistry or rapidly frozen in liquid nitrogen for molecular analyses. A second part was reinforced with an external macroporous polyester tubular mesh (ProVena, B.Braun Medical SA), hereafter referred to as mesh, which covered the entire vein segment (Fig. 1), and whose diameter (4 mm) was chosen to obtain a cross-sectional area quotient Qc > 0.45, where $Qc = a_h/a_g$ (a_h being the cross-sectional area of the host vessel, and a_g that of the interposition graft) (Fig. 1B and C). This part and the third segment of the very same vein, which had not been reinforced by a mesh (control), were perfused in parallel in the EVPS (Fig. 1A and B) for 3 or 7 days, at either low or high pressure. The Ethical Committee of the University of Lausanne approved the experiments, which are in accordance with the principles outlined in the Declaration of Helsinki of 1975, as revised in 1983 for the use of human tissues.

2.2. Ex vivo perfusion system

The EVPS [8,20–22] was modified for the simultaneous perfusion of two vein segments, one of which was reinforced with the mesh (Fig. 1). The 2 segments were connected to the perfusion pump by a peroxide-treated silicone tubing (internal diameter 3.2 mm; Ismatec®, Switzerland), and maintained at 37 ± 0.1 °C in two distinct perfusion chambers, which were placed inside a cell culture incubator (Fig. 1A). In all the experiments, the medium of both the chambers (250 ml each) and the perfusate (150 ml) was RPMI-1640, supplemented with Glutamax, 12.5% fetal calf serum (Gibco), 8% 70 kDa dextran (Sigma), and 1% antibiotic-antimycotic solution (10,000 U/ml penicillin G, 10 mg/ml streptomycin sulphate, 25 mg/ml amphotericin B, and 0.5 μg/ml gentamycin). This medium was changed every 2 days. The conditions of the perfusion were set to obtain a shear stress (SS) of 9–15 dyn/cm^2, as expected in the femoral artery [8], given by $SS = 4\mu Q/\pi r^3$, where μ is the viscosity of the perfusion medium set to $3.73 \cdot 10^{-2}$ dyn s/cm^2, as measured in a Coulter viscometer (Coulter Electronics, High Wycombe, UK), Q the flow rate (mL/s), and r the radius (cm) of the vein segment.

Veins were exposed for 3 or 7 days to a pulsatile biphasic flow of 60 pulses/min under either low (MP = 7 mmHg; systolic/diastolic pressure = 8 ± 1/6 ± 1 mmHg) or high perfusion pressure (MP = 100 mmHg; systolic/diastolic pressure = 120 ± 5/90 ± 5 mmHg). Upon completion of the perfusion, the 5 mm proximal and distal ends, which attached the vein to the equipment, were discarded. A central, 5 mm-thick ring was cut from the remaining segment and fixed in formalin for morphometry. The remaining fragments were frozen and reduced into powder for RT-PCR and Western blot analysis.

2.3. Morphometry

Morphometric analysis was performed on vein sections processed for Van Gieson-elastin (VGEL) staining, using the Leica Qwin® software (Leica, Switzerland). Twenty-four measurements of the thickness of the intima and media layers, as well as of the perimeter of the internal (IEL) and external elastic laminae (EEL) were made in each sample at a magnification of ×100 and ×2, respectively.

2.4. Image processing and cleaved-caspase-3 staining quantification

For the assessment of caspase-3 cleavage, images of human veins were converted using the Fiji software (http://fiji.sc/Fiji), to provide a binary image with a consistent threshold method. After application of the "open" binary operation, particles with an area >50 pixels were summed, and related to the area of the region of interest (one region per vein). At least 5 veins from different patients were analysed in the 5 experimental groups which we compared.

2.5. Quantitative real-time PCR

Quantitative real-time PCR analysis was, performed on vein RNA as previously described [23,24], using the primers given in Table 1. All experiments included negative controls (amplification of distilled water or RNA samples that had not been reversed transcribed). Levels of expression were determined relative to those of GAPDH.

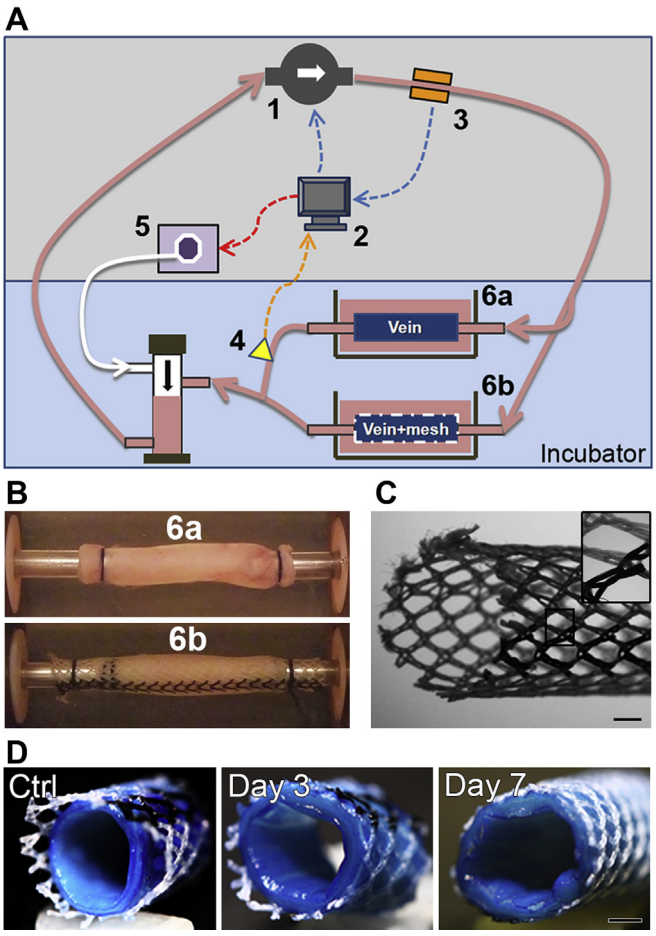

Fig. 1. The *ex vivo* perfusion system, A: A gearing pump (1) generates a pulsatile signal controlled by a computer (2), which monitors the pressure (3) and flow velocity (4), and controls the minimal diastolic pressure (5). B: Two segments of a very same saphenous vein were connected in parallel to the perfusion pump inside separate perfusion chambers (6a and 6b in A), which were placed in a cell culture incubator. C: View of the tubular mesh of 4 mm diameter, made of a polyester wire defining pores of 750 μm, and which was tested as external reinforcement. The insets show enlargements of the boxed area, that highlight the honeycomb structure. Bar, 500 μm. D: Views of a same vein (stained with 2% Evan's blue) inside the mesh reinforcement, immediately before the perfusion (Ctrl) and after 3 and 7 days of perfusion at a mean pressure of 100 mmHg. Bar, 500 μm. (For interpretation of the references to colour in this figure legend, the reader is referred to the web version of this article.)

2.6. Western blots

Veins were reduced to powder and processed for Western blotting as previously reported [23,24] using the following primary antibodies: rabbit polyclonal against MMP2 (Abcam); rabbit polyclonal against MMP-9 (Abcam); mouse monoclonal against TGFβ$_2$ (Abcam); rabbit polyclonal against PAI-1 (Novus Biologicals); mouse monoclonal against eNOS (BD Biosciences); mouse monoclonal against HO-1 (Abcam); goat polyclonal against TIMP-1 (R&D systems), at dilutions 1:400–1000. To evaluate total protein levels, membranes were probed with a mouse monoclonal against α-Tubulin (Sigma), diluted 1:1000.

2.7. Immunostaining

Paraffin sections of veins were immunostained using the primary antibodies mentioned above and an avidin-biotinylated horseradish peroxidase complex (Vectastain Elite ABC Kit, USA), and counterstained with hemalun.

Frozen sections of unfixed veins were immunostained as previously described [20,21], using the same antibodies at a dilution of 1:100–1:3000, a relevant secondary Alexa Fluor 488-labelled antibody (Dako), diluted 1:500 and counterstained with 0.02% Evans Blue.

Table 1
Human primers used for the quantitative reverse transcription polymerase chain reaction (RT-PCR).

Gene	Sense primer (5′–3′)	Antisense primer (5′–3′)
PAI-1	GGCTGGTGCTGGTGAATG	ATCGGGCGTGGTGAACTC
$TGF\beta_2$	GTGGAAACCCACAACGAAAT	CACGTGCTGCTCCACTTTTA
MMP2	CAGAGCCACCCCTAAAGAGA	TGTGAAAGGAGAAGAGCCTGA
MMP9	GCCACTTCCCCTTCATCTTC	GTCGTCGGTGTCGTAGTTGG
TIMP1	TGACATCCGGTTCGTCTACA	TGCAGTTTTCCAGCAATGAG
TIMP2	AAGCGGTCAGTGAGAAGGAA	TCTCAGGCCCTTTGAACATC
Ephrin-B2	CTTTGGAGGGCCTGGATAAC	CTGTTGCCGTCTGTGCTAGA
Eph-B4	CGCAGACCAAAGAGAGTGTG	GGGACTACAAACCCCAATGA
Notch1	CACTGTGAGAACAACACGCC	TGACATCGTGCTGGCAGTAG
Notch4	TACGACTGTGAGACCCCTCC	TTTCTCACAGTGCCCGTTGT
eNOS	GACGCTACGAGGAGTGGAAG	CTGGGTGAGGAGCAGTGG
HO-1	AGGAGGTCATCCCCTACACA	GGGGTAGAGCTGCTTGAACT
SM22α	TTCCAGACTGTTGACCTCTTTG	CAAAGCCATCAGGGTCCTC
Calponin	GCTGTCAGCCGAGGTTAAGA	CCCCTCGATCCACTCTCTC
GAPDH	AACTTTGGTATCGTGGAAGG	CAGTAGAGGCAGGGATGATGT

2.8. Statistical analysis

Student's *t* test and two-way analysis of variance with post hoc Bonferonni correction (Statistical Package for the Social Sciences (SPSS 17.0, Chicago, Ill., USA)) were run to compare mean values between groups.

3. Results

3.1. Intimal hyperplasia and mesh reinforcement

We first studied the morphometry of human saphenous veins subjected or not (Ctrl) to a pulsatile flow under arterial shear stress at low (7 mmHg) or high (100 mmHg) pressure. Masson's trichrome staining, which differentiates smooth muscle cells (SMCs) (red) and connective tissues (blue), revealed that SMCs were equally distributed in three layers, comprising an inner longitudinal, a middle circular and an outer longitudinal layer in freshly isolated veins (Ctrl). In absence of an external support, veins subjected to 100 mmHg perfusion for 7 days displayed thinning of the media layer with persistence of only one of the three muscle layers. The external reinforcement preserved the distribution of the SMCs and media structure (Fig. 2, upper row). Immunostaining showed that von Willebrand factor (vWf)-positive endothelial cells lined the lumen of all veins (Fig. 2 middle row). In contrast, in veins submitted to high pressure for 7 days, immunostaining for alpha smooth muscle actin, revealed a reduced number of SMCs in the media layer and the redistribution of these cells in the intima layer (Fig. 2 lower row). This change was largely prevented by the mesh support (Fig. 2 lower row). Quantitative assessment of the intima and media thickness after VGEL staining revealed that the morphology of the vein grafts was unchanged in veins exposed to 7 mmHg. In contrast, the intima thickness was increased 3 fold in vessels exposed for 7 days to 100 mmHg, whereas the media thickness was decreased by 50% (Fig. 3A and B). The intima and the media alteration were prevented in veins reinforced with the external mesh (Fig. 3A and B). As a result, the mesh reduced by 50% the intima-to-media ratio, compared to that of non-reinforced veins (Fig. 3B).

The perimeters of both internal and external elastic laminae were increased in veins exposed for 7 days to both 7 or 100 mmHg, indicating a significant outward remodelling (Fig. 3C and D). This change was fully (7 mmHg) or partially (100 mmHg) prevented by the mesh reinforcement (Fig. 3C and D). Further analysis revealed that the alteration of the intima, media and internal elastic lamina, but not that of the external elastic lamina, were already evident

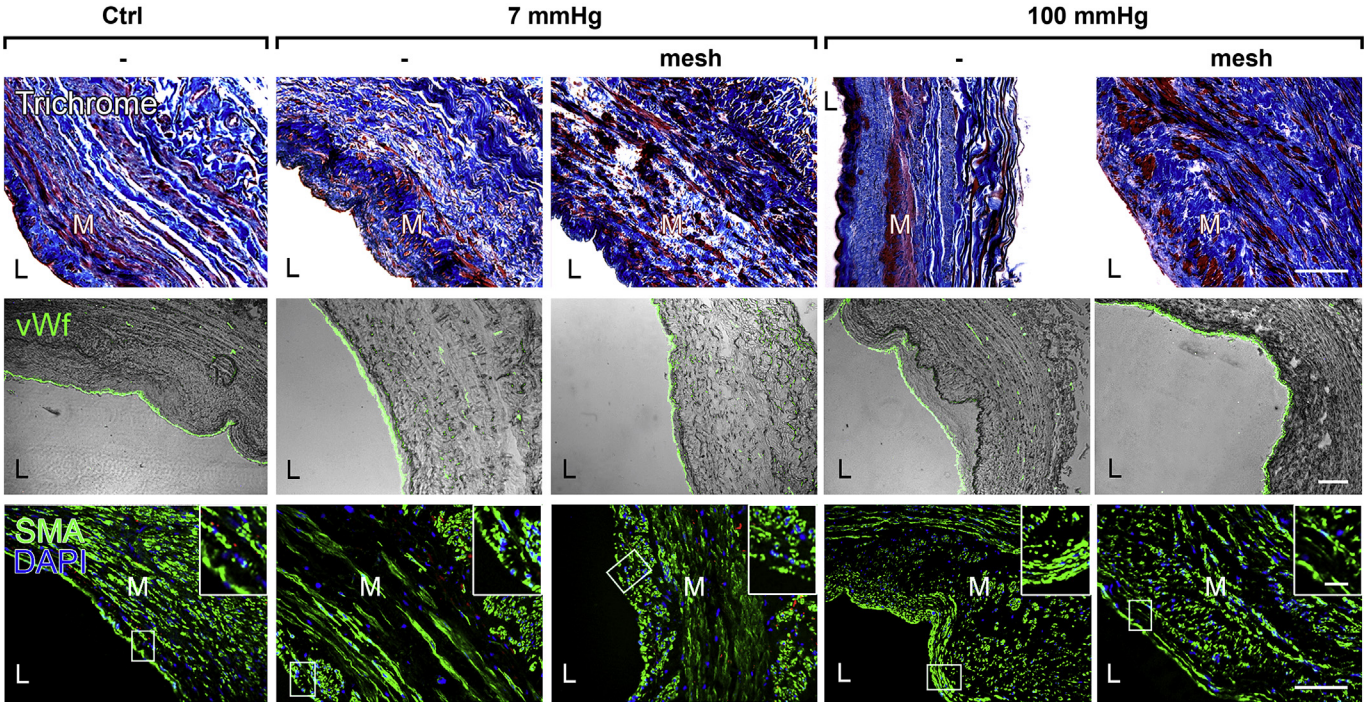

Fig. 2. The external mesh reinforcement prevents most alteration of the vessel wall induced by high pressure, Upper panel: Masson's trichrome staining differentiates SMCs (red) and connective tissue (blue). In control veins, SMCs are equally distributed in 3 distinct layers of the vein. These layers were much reduced in veins exposed to 100 mmHg for 7 days, but not in veins exposed to the same conditions after the mesh wrapping. Middle panel: Antibodies against von Willebrand factor show the lining of endothelial cells at the luminal surface of all vessels. Lower panel: Antibodies against alpha smooth muscle actin, together with a nuclear staining by DAPI, reveal an accumulation of SMCs in the intima layer of the veins exposed to 100 mmHg. This alteration was prevented in veins with the external mesh. Insets are higher magnification views of the framed areas. L, lumen; M, media. Bars represent 100 μm in figures and 400 μm in the insets. (For interpretation of the references to colour in this figure legend, the reader is referred to the web version of this article.)

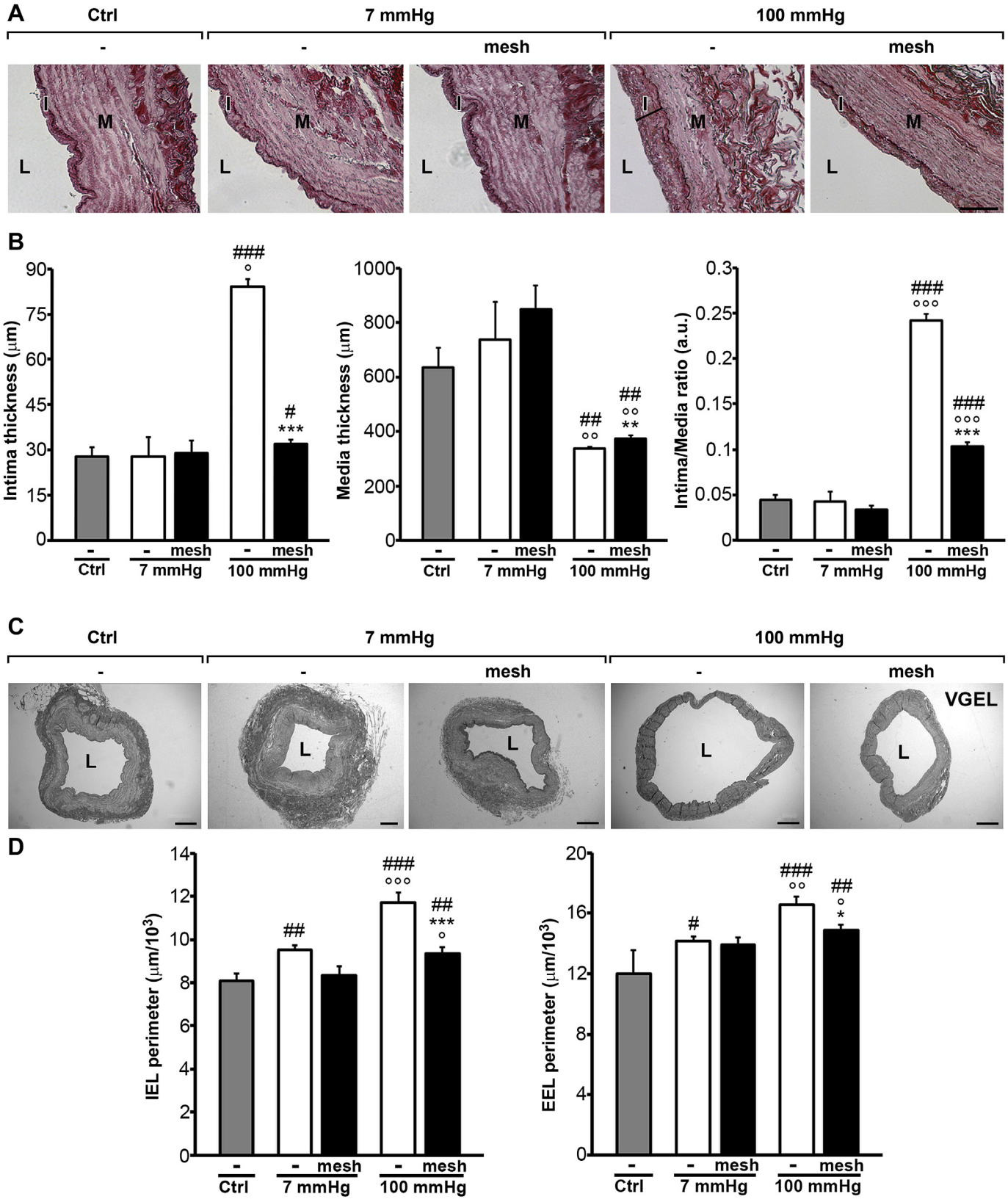

Fig. 3. The external reinforcement prevents the thickening of the intima layer and the outward remodelling of veins, A: Representative histological sections stained for elastin show a similar intima thickness in control, non perfused veins and in veins exposed to a low pressure perfusion (7 mmHg). In contrast, IH is seen in veins perfused at high pressure (100 mmHg), and is largely decreased in the presence of the external mesh. M = media, I = intima and L = lumen. Bar represents 100 μm. B: Morphometric measurements show that high pressure perfusion induced IH and thinning of the media layer. IH was inhibited in the presence of the mesh, which also partially prevented the reduction of the media layer. C: Representative histological sections stained for elastin show marked dilatation and wall thinning of veins exposed to high pressure for 7 days. These changes were prevented by the mesh. L = lumen. Bar represents 500 μm. D: Measurements show increased perimeter of both internal (IEL) and external elastic membranes (EEL) of veins perfused at high pressure (100 mmHg). This change is partially prevented in the presence of the external mesh. E and F: The changes of intima, media, internal and external lamina were already apparent after 3 days of perfusion. While the two former changes were already prevented by the mesh, the latter was not. Data represent mean + SEM of 8–9 experiments. $^{\#}p < 0.05$, $^{\#\#}p < 0.01$ and $^{\#\#\#}p < 0.001$ versus the non perfused segment (Ctrl); $^{\circ}p < 0.05$, $^{\circ\circ}p < 0.01$ and $^{\circ\circ\circ}p < 0.001$ versus the respective 7 mmHg perfused veins $^{*}p < 0.05$, $^{**}p < 0.01$ and $^{***}p < 0.001$ versus the non-reinforced veins (mesh).

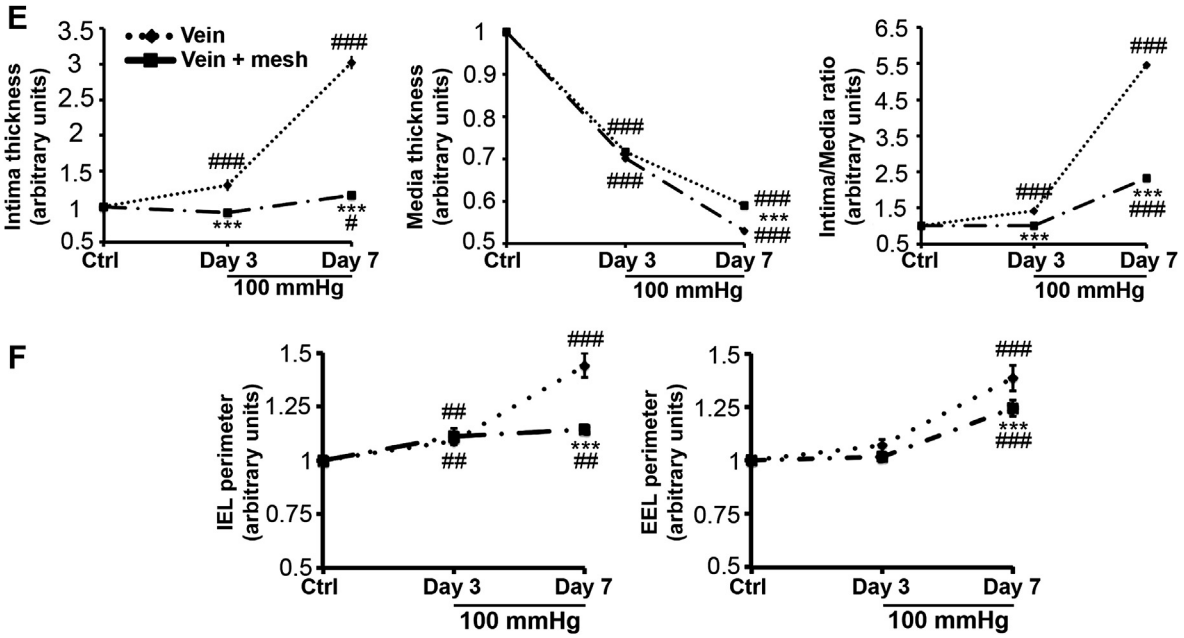

Fig. 3. (*continued*).

after 3 days of perfusion (Fig. 3E and Suppl. Fig. 1). The mesh prevented these early intima and media changes, but not the modest outward remodelling (Fig. 3F and Suppl. Fig. 2).

3.2. Cellular and molecular changes

The media layer of control veins showed a minimal staining for the cleaved form of caspase-3 (Fig. 4). In contrast, this staining was markedly increased after either 3 or 7 days of perfusion at high pressure (100 mmHg). The mesh reinforcement strongly diminished this alteration (Fig. 4). As compared to non perfused veins, the levels of MMP-2 mRNA were decreased after 3 days of perfusion at high pressure, and increased after 7 days (Fig. 5A). These alterations were averted by the mesh, which also partially prevented the elevation in the levels of pro- and mature-MMP-2 proteins (Fig. 5A and B). The levels of the MMP-9 transcript were greatly induced

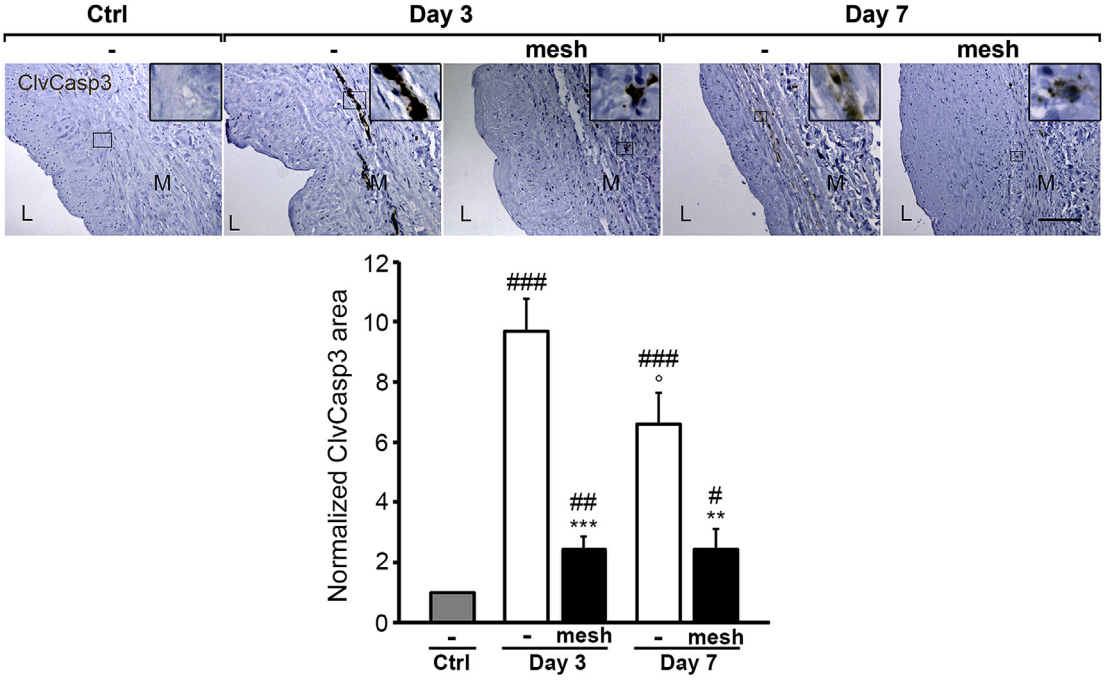

Fig. 4. The mesh reinforcement inhibits the cleavage of caspase-3 induced by exposure to high pressure, Top: Immunostaining revealed minimal cleaved caspase-3 (ClvCasp3) in non perfused veins (Ctrl), and a sizable increase of the staining (brown) in veins perfused at high pressure for 3 or 7 days. Insets are higher magnification views of the framed areas. L, lumen; M, media. Bar represent 100 μm. Bottom: Quantification of ClvCasp3 staining demonstrates a 10- and 7-fold increase in apoptosis after 3 and 7 days of perfusion, respectively. The external reinforcement markedly prevented this alteration. Data represent mean + SEM of 5 experiments. $^{\#}p < 0.05$, $^{\#\#}p < 0.01$ and $^{\#\#\#}p < 0.001$ versus non-perfused veins (Ctrl); $^{**}p < 0.01$ and $^{***}p < 0.001$ versus non-reinforced veins. $^{\circ}p < 0.05$ versus veins perfused for 3 days. (For interpretation of the references to colour in this figure legend, the reader is referred to the web version of this article.)

after 3 days of vein perfusion (Fig. 5C). The levels of the mature MMP-9 protein were similarly regulated, whereas those of the pro-MMP-9 protein were only increased after 7 days (Fig. 5D). The mesh had little impact on the levels of MMP-9, at both mRNA and protein levels. However, it impeded the up-regulation of mature MMP-9, both after 3 and 7 days of perfusion (Fig. 5C and D). The mRNA expression of the tissue inhibitor of metalloproteinases, TIMP-1, was similarly enhanced in veins exposed to high pressure for either 3 or 7 days, and was not affected by the mesh reinforcement (Fig. 5E). The expression of the TIMP-2 transcript was markedly

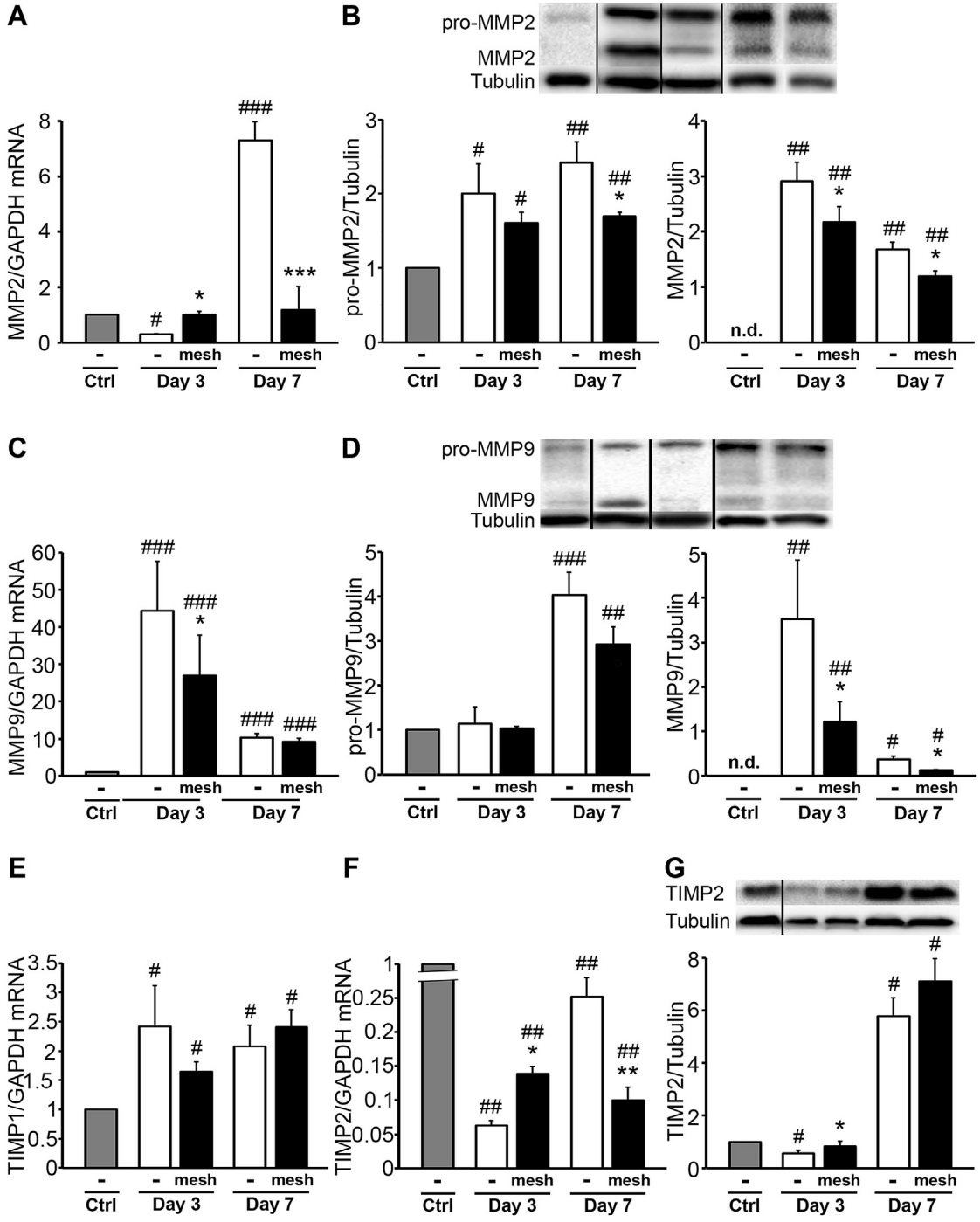

Fig. 5. The external mesh reinforcement attenuates the increased expression of MMP-2 and MMP-9 induced by high pression, A: Compared to the control level (Ctrl), the MMP-2 transcript was decreased after a high pression perfusion for 3 days, and increased when the perfusion lasted 7 days. Both changes were prevented in the presence of the mesh. B: Western blots demonstrate that the high pression perfusion increased both the proactive (middle panel) and active (right panel) forms of the MMP-2 protein. This effect was prevented in reinforced veins. C and D: the MMP-9 transcript (C), as well as the pro- and active forms of the cognate protein (D) were up-regulated as a function of the duration of the perfusion. These effects were partially prevented in reinforced veins. E: Veins exposed to arterial shear stress for 3 and 7 days featured increased expression of TIMP-1 mRNA, which was not prevented by the external reinforcement. F and G: High pressure perfusion decreased the levels of the TIMP-2 transcript (F) and protein (G) after 3 days, 2 effects which were partially prevented by the mesh. In contrast, the expression of the TIMP-2 protein (G) was increased after 7 days of perfusion, an effect which was not prevented by the mesh. Data represent mean + SEM of 8–9 experiments. $^{\#}p < 0.05$, $^{\#\#}p < 0.01$ and $^{\#\#\#}p < 0.001$ versus the non perfused control veins (Ctrl); $^{*}p < 0.05$, $^{**}p < 0.01$ and $^{***}p < 0.001$ versus the non-reinforced veins.

decreased after both 3 and 7 days of perfusion at high pressure, and the mesh had little effect on this regulation (Fig. 5F). The levels of the cognate protein were also slightly decreased after 3 days of perfusion, and the mesh counteracted this down-regulation. However after 7 days, the high pressure perfusion resulted in a 6 fold increase in the TIMP-2 protein levels in both control and reinforced veins (Fig. 5G). Compared to the levels observed in non perfused controls, both PAI-1 transcript and protein levels were elevated after 3 and 7 days of perfusion at high pressure (Fig. 6A and B). The mesh reinforcement partially prevented the increase of PAI-1 mRNA expression at 7 days (Fig. 6A), and fully normalized the levels of the cognate protein both after 3 or 7 days of perfusion (Fig. 6B). Immunohistochemistry further demonstrated an increase in PAI-1 expression in the media layer, which was reduced in reinforced veins (Fig. 6C). The expression of the TGFβ_2 transcript was decreased after 3 days of perfusion, and up-regulated after 7 days and the mesh partially prevented these alterations (Fig. 6D). The levels of the cognate protein markedly decreased after 3 days of perfusion at high pressure, an effect which was partly avoided upon mesh reinforcement (Fig. 6E).

We then studied the expression of the venous Eph-B4 and the arterial Ephrin-B2 markers and their respective transcription factors Notch 1 and 4, known to regulate vessel fate [25]. Compared to controls, the levels of Notch 1, Notch 4, Ephrin-B2 and Eph-B4 mRNA were decreased after 3 and 7 days of perfusion at high pressure (Fig. 7A–D). The mesh did not prevent this changes for Notch 1 and Notch 4 (Fig. 7A and B), whereas it partially counteracted the down-regulation of Ephrin-B2 and Eph-B4, at both transcript and protein levels (Fig. 7C–E). We next investigated the regulation of the vasculoprotective genes endothelial nitric oxide synthase (eNOS) and heme oxygenase-1 (HO-1), which have both been shown to inhibit neointimal hyperplasia [26]. The expression

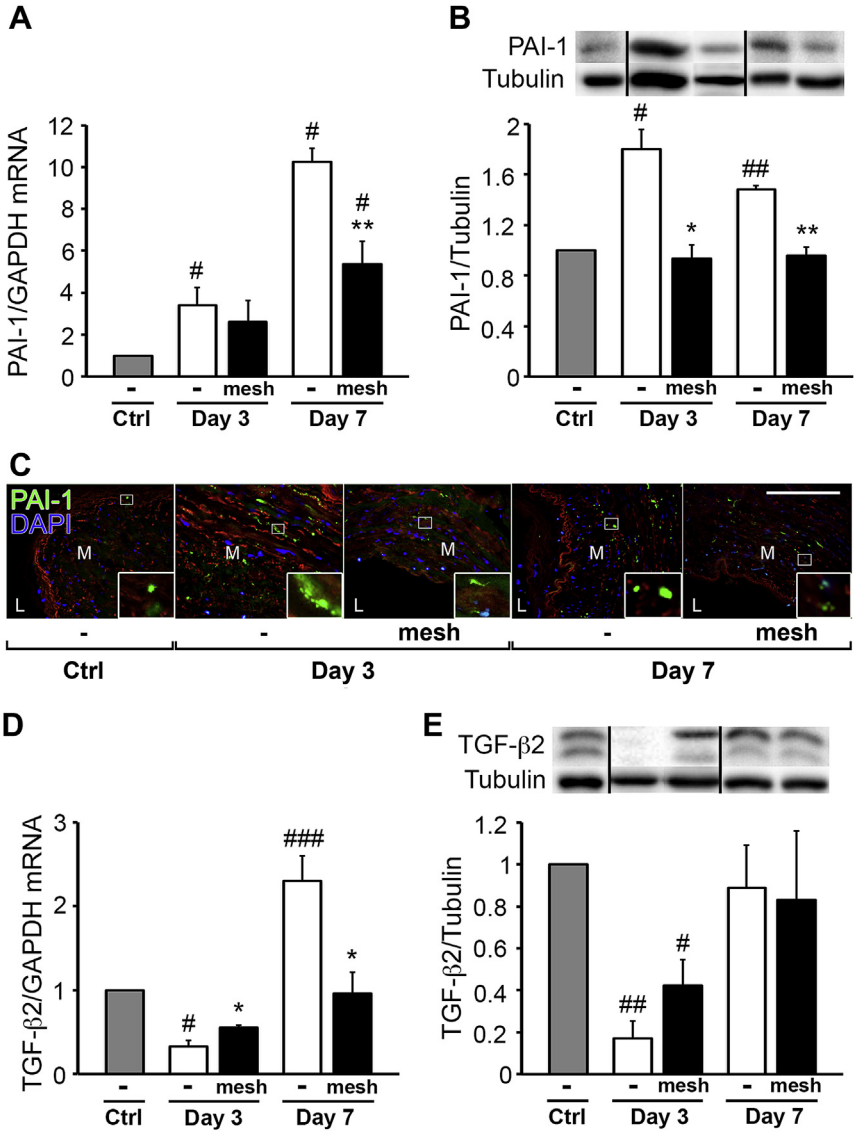

Fig. 6. The external mesh reinforcement differentially modulates the increased expression of plasminogen activator inhibitor and transforming growth factor induced by high pressure, A and B: Compared to control levels (Ctrl), those of the PAI-1 transcript (A) and protein (B) were increased in veins perfused at high pressure for 3 and 7 days. A significant reduction of these changes was observed in reinforced veins. C: immunohistochemistry further revealed that PAI-1 mostly increased in the media layer. The insets show higher magnifications of the boxed areas. Bar represent 100 μm. D: Veins exposed to high pressure featured a down- and up-regulation in the levels of transforming growth factor beta type II (TGFβ_2) mRNA after 3 and 7 days of perfusion, respectively. E: The cognate protein was decreased after 3, but not 7 days of perfusion. The mesh prevented most of the transcript and protein alterations. Data represent mean + SEM of 8–9 experiments. $^{\#}p < 0.05$, $^{\#\#}p < 0.01$ and $^{\#\#\#}p < 0.001$ versus the non perfused control veins; $^{*}p < 0.05$ and $^{**}p < 0.01$ versus the non-reinforced segment.

of endothelial nitric oxide synthase (eNOS) was also decreased after 7 days of perfusion at high pressure, and this down regulation was not affected by the mesh reinforcement (Fig. 8A and B). In contrast, the expression of the heme oxygenase-1 (HO-1) transcript was up regulated after 3 and 7 days of perfusion at high pressure, an alteration which was markedly reduced by the mesh (Fig. 8C). Exposure of veins to high pressure perfusion dramatically reduced the transcript levels of the contractile SMCs markers SM22α and calponin, whether the mesh was present or not (Fig. 9A and B).

4. Discussion

We show that wrapping saphenous veins with a macroporous tubular polyester mesh, markedly reduces the development of IH and the thinning of the media layer, two alterations which are otherwise observed after 3–7 days of a pulsatile perfusion mimicking the conditions prevailing in the arterial compartment. We further demonstrate that the structural alterations induced by high pressure are associated with changes in SMCs survival, and in the expression of several genes and proteins involved in the development of IH [4], documenting that the mesh resulted in a marked protection against most of these changes (Fig. 10).

Animal studies of venous bypass surgery have demonstrated that the presence of a constrictive external support could efficiently limit the dilation of venous walls, improving blood flow, and that the association of increased shear stress, decreased wall tension and better size match between the host and the grafted vessels prevent the development of IH [15–19]. Here, we show that a

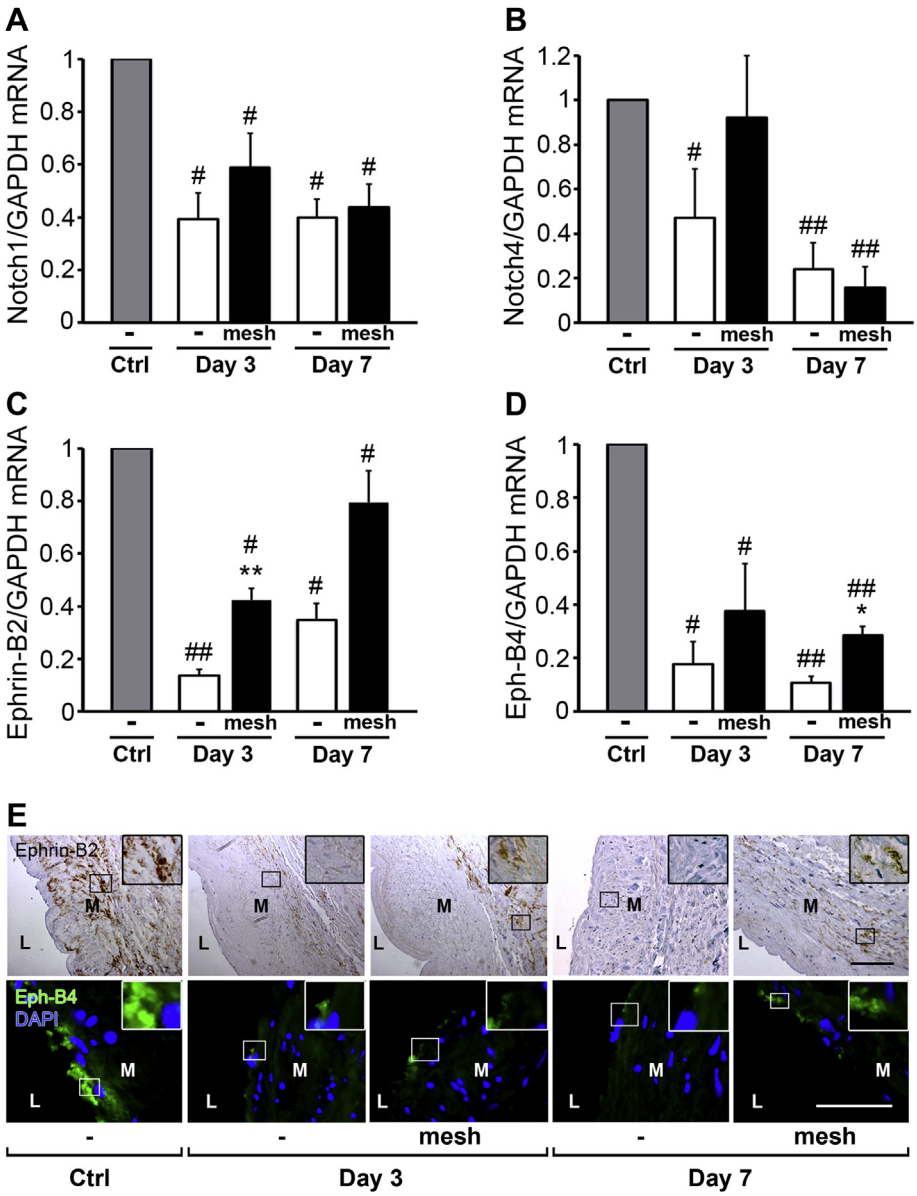

Fig. 7. The external mesh reinforcement prevents the down-regulation of Ephrin-B2 and Eph-B4, A and B: The transcripts levels of Notch1 (A) and Notch4 (B) were decreased in veins submitted to high pressure for 3 and 7 days. The mesh failed to prevent these down regulations. C and E: The transcript (C) and protein (E, upper panel) levels of Ephrin-B2 were significantly reduced after a high pressure perfusion for 3 and 7 days. This down-regulation was prevented by the mesh only in veins perfused for 3 days. Insets show the box area at higher magnifications. L, lumen; M, media. Bar represents 100 μm. Data are mean + SEM of 8–9 experiments. $^{\#}p < 0.05$ and $^{\#\#}p < 0.01$ versus the non perfused veins (Ctrl); $^{*}p < 0.05$ and $^{**}p < 0.01$ versus the non-reinforced veins. D and E: The expression of Eph-B4 also decreased, at both transcript (D) and protein levels (E, lower panel), after 3 and 7 days of high pressure perfusion. These changes were partially prevented by the mesh reinforcement in veins perfused for 7 days. Insets show higher magnifications of the boxed areas. L, lumen; M, media. Bar represent 100 μm. Data represent mean + SEM of 8–9 experiments. $^{\#}p < 0.05$ and $^{\#\#}p < 0.01$ versus non perfused veins (Ctrl); $^{*}p < 0.01$ and $^{**}p < 0.01$ versus the non-reinforced veins.

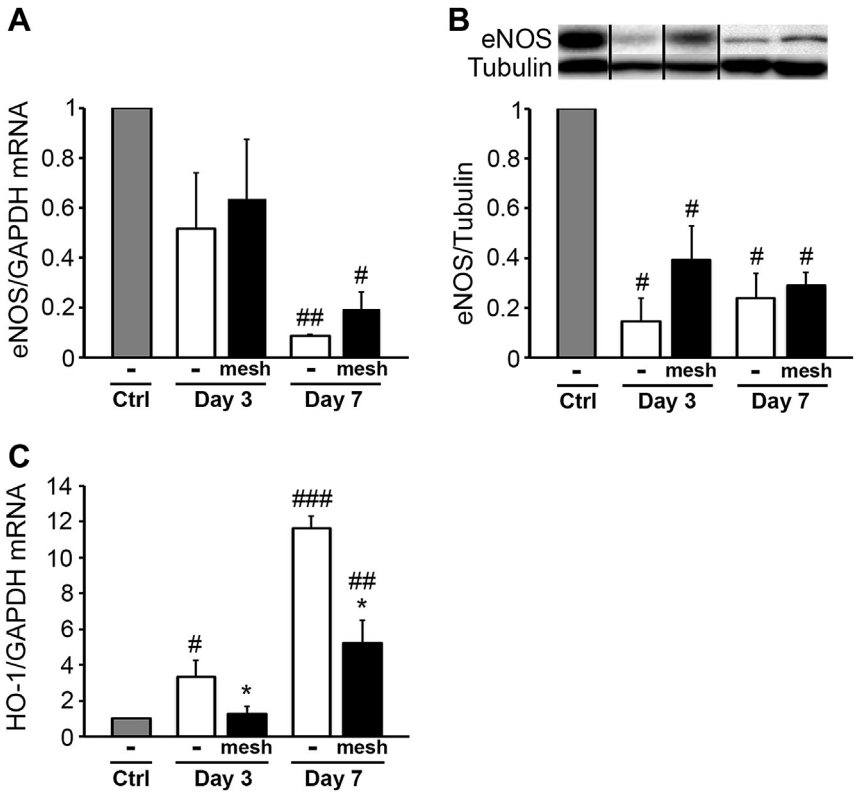

Fig. 8. The mesh reinforcement differentially affects the pressure-induced changes in endothelial nitric oxide synthase and heme oxygenase, A and B: High pressure perfusion down regulated the levels of eNOS transcript (A) and protein (B). The presence of the external mesh reinforcement failed to prevent these changes. C: The transcript of HO-1 was increased after 3 and 7 days of high pressure perfusion, two effects which were significantly reduced in reinforced veins. Data represent mean + SEM of 8–9 experiments. $^{\#}p < 0.05$, $^{\#\#}p < 0.01$ and $^{\#\#\#}p < 0.001$ versus non perfused controls (Ctrl); $^{*}p < 0.01$ versus the non-reinforced veins.

similar mesh is also efficient in preventing the dilatation and media remodelling of human great saphenous veins exposed *ex vivo* to arterial conditions. Interestingly, this study demonstrates that IH develops rapidly upon perfusion under an arterial regimen, even in the absence of aggravating inflammatory and growth factors released by circulating cells *in vivo*, thus supporting a major role for haemodynamic forces in the development of IH. We conclude that, by preserving the structure of the vein graft, the external support increases shear stress and decreases wall tension, thereby preventing IH.

Our study provides cellular and molecular evidence on how the mechanical effects of the mesh reinforcement are translated into protective tissue effects. First, the alterations in the organization of the vein wall induced by high pressure perfusion are associated with a marked increase in the apoptosis of SMCs within the media layer. Disruption of the balance between SMCs proliferation and apoptosis is a key event in the injury-induced IH [27]. Our data support the view that this balance is mostly controlled by apoptosis, whose importance in the thickening of the intima has so far remained a matter of debate [28,29]. Second, our study shows that, under conditions mimicking those of an arterial bed, there is a rapid and marked decrease in SM22α and calponin, two markers of contractile SMCs, consistent with a switch of these cells from a contractile to a synthetic phenotype, as observed under several pathological conditions [30,31], and after exposure to an arterial environment [32]. We further observed a marked decrease in the

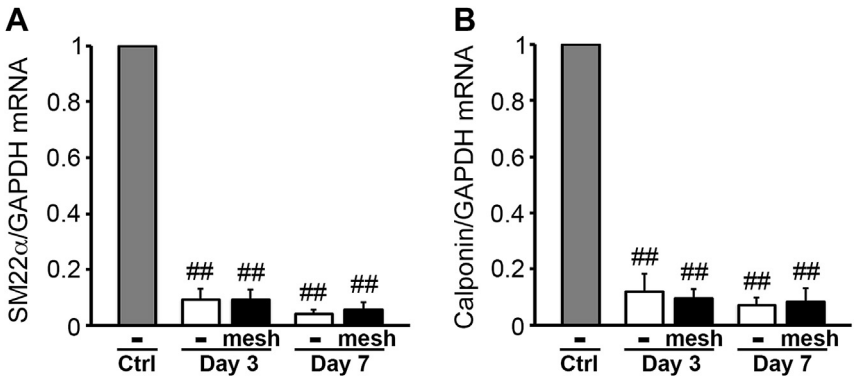

Fig. 9. Early decrease of the contractile smooth muscle cells markers Smooth muscle 22 alpha (SM22α) and Calponin, A and B: A 3 and 7 day-long high pressure perfusion decreased the transcripts of SM22α (A) and calponin (B). The presence of the mesh did not prevent these down-regulations. Data represent mean + SEM of 8–9 experiments. $^{\#\#}p < 0.01$ the non perfused control veins (Ctrl).

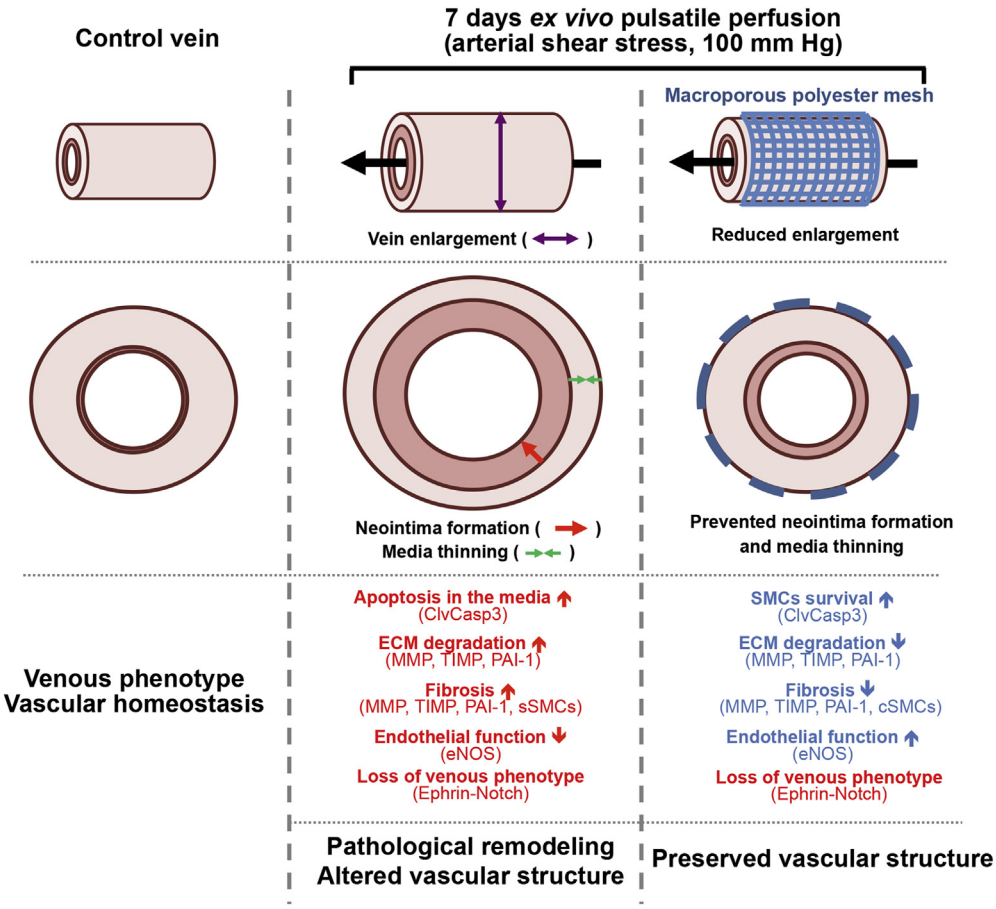

Fig. 10. Schematic representation of the mechanisms involved in the mesh-dependent preservation of a vein graft structure. Vein submitted to an arterial pressure for 7 days showed significant IH and media thinning. These changes are associated with 1) increased SMCs apoptosis, 2) increased ECM degradation and fibrosis, 3) altered endothelial function, 4) loss of venous phenotype. The presence of a mesh limited the vein dilatation, prevented the development of IH, and preserved the architecture of the media layer by 1) reducing SMCs apoptosis, 2) preventing the ECM degradation and the fibrosis, 3) reducing the endothelial alterations, and 4) regulating the expression of key proteins involved in the development of IH.

expression of Ephrin-B2 and Eph-B4, as previously reported [25], but also of Notch 1 and Notch 4, consistent with a loss of differentiation and higher proliferative phenotype of the "arterialised" vein. Still, and in spite of its efficient protection against the development of IH, the mesh did not fully preserve the normal vein phenotype, as indicated by the persistent down-regulation of eNOS, a marker of endothelial function, which is consistent with a down-regulation of the Notch/Ephrin pathway [33]. We further observed that the mesh reinforcement prevented the over-expression of HO-1, which counteracts cell growth in vascular diseases, and protects against oxidative stress and intimal thickening [34,35]. Although HO-1 has been demonstrated to be increased by shear stress and pulsatile flow [36], the exact mechanism underlying HO-1 regulation remains to be elucidated. In our model, HO-1 is likely over-expressed in response to SMCs proliferation and increased oxidative stress, as a way to counteract the development of IH.

We also provide evidence that the external mesh prevents the induction of both MMP-2 and MMP-9, which is observed under high pressure perfusion [8]. Matrix metalloproteases play a crucial role in the remodelling of the extracellular matrix (ECM) which, in turn, contributes to the proliferation and migration of SMCs [37]. *In situ*, the activity of MMP-2 and MMP-9 is modulated by tissue inhibitors of the TIMP family [37]. In veins exposed to arterial haemodynamic conditions, we observed that TIMP1 was rapidly up-regulated with its MMP-9 substrate, whereas TIMP2 expression was initially decreased and later increased with the continuation of the perfusion. The data thus reveal a complex temporal regulation of both MMPs and their regulators during the development of IH. The mesh efficiently dampened these changes, consistent with a protective effect on ECM remodelling. Accordingly, PAI-1 expression, a key regulator of ECM remodelling, as well as of SMCs adhesion and migration [38], was found increased under arterial conditions that trigger IH [20,21], and this alteration was fully prevented by the mesh reinforcement.

Although the mechanisms whereby external mesh reinforcements protect veins exposed to arterial haemodynamic conditions remain to be fully unravelled, our data clearly suggest that external scaffolding may prevent IH in vein grafts. Several clinical studies have already documented the usefulness of rigid polytetrafluoroethylene reinforcement [15–19,39,40] or ProVena mesh support [41,42], enabling the use of suboptimal autologous ectatic or varicose veins in lower limb grafts. However, the only published trial addressing the effectiveness of an external support to improve healthy vein patency during coronary artery bypass reported the thrombosis of all veins reinforced with an external Dacron stent, or Extent. This dramatic outcome was most likely due to the rigidity and design of this external support, which probably resulted in graft kinking and thrombosis [43]. Together with previous animal studies [15–19] and clinical evidence [41,42,44], our data suggest that the ProVena, given its flexible, honeycomb structure, will not cause kinking and thrombosis and may reduce the development of IH in vein graft bypass surgery. The majority of

bypasses are connected using end-to-side anastomosis, which disrupt laminar flow [3]. As a result, most graft stenoses due to IH occur in the perianastomotic regions. This could not be tested in the EVPS, since veins are attached in an end-to-end fashion, which preserves a laminar flow. Hopefully, future studies will demonstrate that the flexible structure of the ProVena mesh, which allows complete mesh wrapping of the veins, including at the anastomosis [44], will prove efficient in reducing IH at these specifics sites.

5. Conclusions

In summary we provide morphological and molecular evidence that an external mesh reinforcement is effective in preventing the pathological alterations that saphenous veins face once exposed to arterial haemodynamic conditions. *Ex vivo*, such reinforcement prevented the dilatation of the vessel, decreased the development of IH and preserved the architecture of the media layer by reducing the apoptosis of SMCs and subsequent fibrosis. At the molecular level, the mesh prevented the up-regulation of matrix metalloproteinases (MMP-2, MMP-9) and plasminogen activator type I, which are involved in the remodelling of the extracellular matrix. Together with previous animal studies, our experimental, *ex vivo* data on human veins now call for revisiting this efficacy in a large randomized multicenter clinical study, which could provide for a proper *in vivo* comparison of reinforced and non-reinforced grafts.

Acknowledgements

This work was supported by grants from the SNF [31003A-138528; 310030_141162; CR32I3_129987], the JDRF [40-2011-11; 5-2012-281; 1-2011-589], the EU [BETAIMAGE 222980; IMIDIA, C2008-T7; BETATRAIN 289932], NIH HL64232, the Octav and The Marcella Botnar Foundation, the Novartis Foundation and the Emma Muschamp Foundation.

Appendix A. Supplementary data

Supplementary data related to this article can be found at http://dx.doi.org/10.1016/j.biomaterials.2013.12.041.

References

[1] Osgood MJ, Hocking KM, Voskresensky IV, Li FD, Komalavilas P, Cheung-Flynn J, et al. Surgical vein graft preparation promotes cellular dysfunction, oxidative stress, and intimal hyperplasia in human saphenous vein. J Vasc Surg 2013 Jul; 30. [Epub ahead of print].
[2] Owens CD. Adaptive changes in autogenous vein grafts for arterial reconstruction: clinical implications. J Vasc Surg 2010 Mar;51(3):736–46.
[3] Davies MG, Hagen PO. Reprinted article "pathophysiology of vein graft failure: a review". Eur J Vasc Endovasc Surg 2011 Sep;42(Suppl. 1):S19–29.
[4] Mitra AK, Gangahar DM, Agrawal DK. Cellular, molecular and immunological mechanisms in the pathophysiology of vein graft intimal hyperplasia. Immunol Cell Biol. 2006 Apr;84(2):115–24.
[5] Newby AC, Zaltsman AB. Molecular mechanisms in intimal hyperplasia. J Pathol 2000 Feb;190(3):300–9.
[6] Berceli SA, Jiang Z, Klingman NV, Schultz GS, Ozaki CK. Early differential MMP-2 and -9 dynamics during flow-induced arterial and vein graft adaptations. J Surg Res. 2006 Aug;134(2):327–34.
[7] Mountain DJ, Kirkpatrick SS, Freeman MB, Stevens SL, Goldman MH, Grandas OH. Role of MT1-MMP in estrogen-mediated cellular processes of intimal hyperplasia. J Surg Res. 2012 Apr;173(2):224–31.
[8] Berard X, Deglise S, Alonso F, Saucy F, Meda P, Bordenave L, et al. Role of hemodynamic forces in the ex vivo arterialization of human saphenous veins. J Vasc Surg 2013 May;57(5):1371–82.
[9] Morrow D, Sweeney C, Birney YA, Guha S, Collins N, Cummins PM, et al. Biomechanical regulation of hedgehog signaling in vascular smooth muscle cells in vitro and in vivo. Am J Physiol Cell Physiol 2007 Jan;292(1):C488–96.
[10] Dobrin PB, Littooy FN, Endean ED. Mechanical factors predisposing to intimal hyperplasia and medial thickening in autogenous vein grafts. Surgery 1989 Mar;105(3):393–400.
[11] Gusic RJ, Myung R, Petko M, Gaynor JW, Gooch KJ. Shear stress and pressure modulate saphenous vein remodeling ex vivo. J Biomech 2005 Sep;38(9):1760–9.
[12] Gusic RJ, Petko M, Myung R, William Gaynor J, Gooch KJ. Mechanical properties of native and ex vivo remodeled porcine saphenous veins. J Biomech 2005 Sep;38(9):1770–9.
[13] Desai M, Mirzay-Razzaz J, von Delft D, Sarkar S, Hamilton G, Seifalian AM. Inhibition of neointimal formation and hyperplasia in vein grafts by external stent/sheath. Vasc Med 2010 Aug;15(4):287–97.
[14] Vijayan V, Shukla N, Johnson JL, Gadsdon P, Angelini GD, Smith FC, et al. Long-term reduction of medial and intimal thickening in porcine saphenous vein grafts with a polyglactin biodegradable external sheath. J Vasc Surg 2004 Nov;40(5):1011–9.
[15] Jeremy JY, Gadsdon P, Shukla N, Vijayan V, Wyatt M, Newby AC, et al. On the biology of saphenous vein grafts fitted with external synthetic sheaths and stents. Biomaterials 2007 Feb;28(6):895–908.
[16] Zilla P, Human P, Wolf M, Lichtenberg W, Rafiee N, Bezuidenhout D, et al. Constrictive external nitinol meshes inhibit vein graft intimal hyperplasia in nonhuman primates. J Thorac Cardiovasc Surg 2008 Sep;136(3):717–25.
[17] Zilla P, Wolf M, Rafiee N, Moodley L, Bezuidenhout D, Black M, et al. Utilization of shape memory in external vein-graft meshes allows extreme diameter constriction for suppressing intimal hyperplasia: a non-human primate study. J Vasc Surg 2009 Jun;49(6):1532–42.
[18] Yeoman MS, Reddy D, Bowles HC, Bezuidenhout D, Zilla P, Franz T. A constitutive model for the warp-weft coupled non-linear behavior of knitted biomedical textiles. Biomaterials 2010 Nov;31(32):8484–93.
[19] Zilla P, Moodley L, Wolf MF, Bezuidenhout D, Sirry MS, Rafiee N, et al. Knitted nitinol represents a new generation of constrictive external vein graft meshes. J Vasc Surg 2011 Nov;54(5):1439–50.
[20] Saucy F, Probst H, Alonso F, Berard X, Deglise S, Dunoyer-Geindre S, et al. Ex vivo pulsatile perfusion of human saphenous veins induces intimal hyperplasia and increased levels of the plasminogen activator inhibitor 1. Eur Surg Res. 2010;45(1):50–9.
[21] Paroz A, Probst H, Saucy F, Mazzolai L, Rizzo E, Ris HB, et al. Comparison of morphological and functional alterations of human saphenous veins after seven and fourteen days of ex vivo perfusion. Eur Surg Res. 2004 Sep-Oct;36(5):274–81.
[22] Rey J, Probst H, Mazzolai L, Bosman FT, Pusztaszeri M, Stergiopulos N, et al. Comparative assessment of intimal hyperplasia development after 14 days in two different experimental settings: tissue culture versus ex vivo continuous perfusion of human saphenous vein. J Surg Res. 2004 Sep;121(1):42–9.
[23] Alonso F, Boittin FX, Beny JL, Haefliger JA. Loss of connexin40 is associated with decreased endothelium-dependent relaxations and eNOS levels in the mouse aorta. Am J Physiol Heart Circ Physiol 2010 Nov;299(5):H1365–73.
[24] Alonso F, Krattinger N, Mazzolai L, Simon A, Waeber G, Meda P, et al. An angiotensin II- and NF-kappaB-dependent mechanism increases connexin 43 in murine arteries targeted by renin-dependent hypertension. Cardiovascular research 2010 Jul 1;87(1):166–76.
[25] Kudo FA, Muto A, Maloney SP, Pimiento JM, Bergaya S, Fitzgerald TN, et al. Venous identity is lost but arterial identity is not gained during vein graft adaptation. Arterioscler Thromb Vasc Biol. 2007 Jul;27(7):1562–71.
[26] Sugimoto M, Yamanouchi D, Komori K. Therapeutic approach against intimal hyperplasia of vein grafts through endothelial nitric oxide synthase/nitric oxide (eNOS/NO) and the Rho/Rho-kinase pathway. Surg Today 2009;39(6):459–65.
[27] Si Y, Ren J, Wang P, Rateri DL, Daugherty A, Shi XD, et al. Protein kinase C-delta mediates adventitial cell migration through regulation of monocyte chemoattractant protein-1 expression in a rat angioplasty model. Arterioscler Thromb Vasc Biol. 2012 Apr;32(4):943–54.
[28] Tasaki T, Yamada S, Guo X, Tanimoto A, Wang KY, Nabeshima A, et al. Apoptosis signal-regulating kinase 1 deficiency attenuates vascular injury-induced neointimal hyperplasia by suppressing apoptosis in smooth muscle cells. Am J Pathol 2013 Feb;182(2):597–609.
[29] Bechler SL, Si Y, Yu Y, Ren J, Liu B, Lynn DM. Reduction of intimal hyperplasia in injured rat arteries promoted by catheter balloons coated with polyelectrolyte multilayers that contain plasmid DNA encoding PKCdelta. Biomaterials 2013 Jan;34(1):226–36.
[30] Mano T, Luo Z, Malendowicz SL, Evans T, Walsh K. Reversal of GATA-6 downregulation promotes smooth muscle differentiation and inhibits intimal hyperplasia in balloon-injured rat carotid artery. Circ Res 1999 Apr 2;84(6):647–54.
[31] Schachner T, Zou Y, Oberhuber A, Tzankov A, Mairinger T, Laufer G, et al. Local application of rapamycin inhibits neointimal hyperplasia in experimental vein grafts. Ann Thorac Surg 2004 May;77(5):1580–5.
[32] Rzucidlo EM, Martin KA, Powell RJ. Regulation of vascular smooth muscle cell differentiation. J Vasc Surg 2007 Jun;45(Suppl. A):A25–32.
[33] Brown DJ, Rzucidlo EM, Merenick BL, Wagner RJ, Martin KA, Powell RJ. Endothelial cell activation of the smooth muscle cell phosphoinositide 3-kinase/Akt pathway promotes differentiation. J Vasc Surg 2005 Mar;41(3):509–16.
[34] Beck K, Wu BJ, Ni J, Santiago FS, Malabanan KP, Li C, et al. Interplay between heme oxygenase-1 and the multifunctional transcription factor yin yang 1 in the inhibition of intimal hyperplasia. Circ Res 2010 Dec 10;107(12):1490–7.
[35] Cerrito MG, Scagliarini A, Froio A, Liloia A, Busnelli M, Giovannoni R, et al. Heme oxygenase-1 inhibition prevents intimal hyperplasia enhancing nitric oxide-dependent apoptosis of vascular smooth muscle cells. Biol Pharm Bull. 2011;34(8):1204–14.

[36] Freidja ML, Toutain B, Caillon A, Desquiret V, Lambert D, Loufrani L, et al. Heme oxygenase 1 is differentially involved in blood flow-dependent arterial remodeling: role of inflammation, oxidative stress, and nitric oxide. Hypertension 2011 Aug;58(2):225–31.
[37] Turner NA, Hall KT, Ball SG, Porter KE. Selective gene silencing of either MMP-2 or MMP-9 inhibits invasion of human saphenous vein smooth muscle cells. Atherosclerosis 2007 Jul;193(1):36–43.
[38] Fay WP, Garg N, Sunkar M. Vascular functions of the plasminogen activation system. Arterioscler Thromb Vasc Biol 2007 Jun;27(6):1231–7.
[39] Melliere D, Desgrange P, Allaire E, Becquemin JP. Long-term results of venous bypass for lower extremity arteries with selective short segment prosthetic reinforcement of varicose dilatations. Ann Vasc Surg 2007 Jan;21(1):45–9.
[40] Lundgren F, Swedish External Support S. External support of a polytetrafluoroethylene graft improves patency for bypass to below-knee arteries. Ann Vasc Surg 2013 Aug;27(8):1124–33.
[41] Arvela E, Kauhanen P, Alback A, Lepantalo M, Neufang A, Adili F, et al. Initial experience with a new method of external polyester scaffolding for infrainguinal vein grafts. Eur J Vasc Endovasc Surg 2009 Oct;38(4):456–62.
[42] Carella GS, Stilo F, Benedetto F, David A, Risitano DC, Buemi M, et al. Femorodistal bypass with varicose veins covered by prosthetic mesh. J Surg Res. 2011 Jun 15;168(2):e189–94.
[43] Murphy GJ, Newby AC, Jeremy JY, Baumbach A, Angelini GD. A randomized trial of an external Dacron sheath for the prevention of vein graft disease: the extent study. J Thorac Cardiovasc Surg 2007 Aug;134(2):504–5.
[44] Berard X, Brizzi V, Mayeux S, Sassoust G, Biscay D, Ducasse E, et al. Salvage treatment for venous aneurysm complicating vascular access arteriovenous fistula: use of an exoprosthesis to reinforce the vein after aneurysmorrhaphy. Eur J Vasc Endovasc Surg 2010 Jul;40(1):100–6.

Video Article

Procedure for Human Saphenous Veins *Ex Vivo* Perfusion and External Reinforcement

Alban Longchamp*[1], Florent Allagnat*[2], Xavier Berard[3], Florian Alonso[2], Jacques-Antoine Haefliger[2], Sébastien Deglise*[4], Jean-Marc Corpataux*[4]

[1]Department of Surgery, Brigham and Women's Hospital/Harvard Medical School

[2]Laboratory of Experimental Medicine, Department of Medicine, CHUV University Hospital

[3]Department of Vascular Surgery, Pellegrin Hospital, University of Bordeaux

[4]Department of Thoracic and Vascular Surgery, CHUV University Hospital

*These authors contributed equally

Correspondence to: Alban Longchamp at alban.longchamp@gmail.com

URL: http://www.jove.com/video/52079
DOI: doi:10.3791/52079

Keywords: Medicine, Issue 92, vein, human, intimal hyperplasia, neointima, perfusion, mesh, pressure, *ex vivo*

Date Published: 10/1/2014

Citation: Longchamp, A., Allagnat, F., Berard, X., Alonso, F., Haefliger, J.A., Deglise, S., Corpataux, J.M. Procedure for Human Saphenous Veins *Ex Vivo* Perfusion and External Reinforcement. *J. Vis. Exp.* (92), e52079, doi:10.3791/52079 (2014).

Abstract

The mainstay of contemporary therapies for extensive occlusive arterial disease is venous bypass graft. However, its durability is threatened by intimal hyperplasia (IH) that eventually leads to vessel occlusion and graft failure. Mechanical forces, particularly low shear stress and high wall tension, are thought to initiate and to sustain these cellular and molecular changes, but their exact contribution remains to be unraveled. To selectively evaluate the role of pressure and shear stress on the biology of IH, an *ex vivo* perfusion system (EVPS) was created to perfuse segments of human saphenous veins under arterial regimen (high shear stress and high pressure). Further technical innovations allowed the simultaneous perfusion of two segments from the same vein, one reinforced with an external mesh. Veins were harvested using a no-touch technique and immediately transferred to the laboratory for assembly in the EVPS. One segment of the freshly isolated vein was not perfused (control, day 0). The two others segments were perfused for up to 7 days, one being completely sheltered with a 4 mm (diameter) external mesh. The pressure, flow velocity, and pulse rate were continuously monitored and adjusted to mimic the hemodynamic conditions prevailing in the femoral artery. Upon completion of the perfusion, veins were dismounted and used for histological and molecular analysis. Under *ex vivo* conditions, high pressure perfusion (arterial, mean = 100 mm Hg) is sufficient to generate IH and remodeling of human veins. These alterations are reduced in the presence of an external polyester mesh.

Video Link

The video component of this article can be found at http://www.jove.com/video/52079/

Introduction

Cardiovascular diseases are the leading cause of morbidity and mortality in Western countries[1]. Despite advances made in endovascular treatments, bypass surgery remains the mainstay of contemporary therapies, thus over half a million vein grafts are performed annually in the United States. However, despite decades of research, 30-60% of lower extremity vein grafts fail within the first years due to intimal hyperplasia (IH)[2]. Mechanical forces, particularly low shear stress (SS) and high wall tension, are pivotal in the initiation and development of this hyperplastic response[3,4]. To address this issue, an *ex vivo* veins perfusion system (EVPS) was generated to study, under strictly controlled hemodynamic conditions (pressure and shear stress), the behavior of human saphenous veins. In this study, following insertion into the arterial-like circulation, high pressure (mean = 100 mm Hg) was sufficient to stimulate proliferation and migration of smooth muscle cells into the intimal layer (IH)[5].

Mammalian studies have suggested the use of external reinforcement as an efficient method to support the “arterialized vein” and counteract the acute hemodynamic changes the vein faces once implanted into an arterial milieu. The mesh prevented over-distension, increased shear stress, and reduced wall tension and consequently IH[6-10]. However, the underlying mechanisms and its applicability to human veins in improving bypass patency have not been fully characterized. Our EVPS was used to compare, in condition mimicking the alterations a vein faces once inserted into an arterial regimen (high shear stress and pressure), the behavior of human saphenous veins in the absence and presence of an external macroporous polyester tubular mesh. By preventing pathological remodeling and IH, the mesh provided evidence of its potential clinical efficiency[11].

This study 1) introduces a model of *ex vivo* human saphenous veins perfusion under controlled pressure and shear stress 2) demonstrates that external macro-porous polyester mesh reduces IH and provides crucial information for its potential clinical application.

Protocol

The Ethical Committee of the University of Lausanne approved the experiments, which are in accordance with the principles outlined in the Declaration of Helsinki of 1975, as revised in 1983 for the use of human tissues.

1. Human Great Saphenous Vein Harvest

1. Obtain surplus segments of non-varicose human saphenous veins from patients undergoing lower limb bypass surgery for ischemia. In the operating room, disinfect the entire leg with an iodine solution and drape the patient to expose the leg from the groin to the foot.
2. Make a median incision from the groin to the knee (leaving the interrupted skin portion).
3. Harvest the great saphenous vein with a pedicle of surrounding tissue (no-touch technique). Secure side branches of the veins with 4-0 silk ties. Immediately store a minimum of 9 cm long surplus segment of the greater saphenous vein, with an external diameter of 2.5-4 mm at 4 °C in a RPMI-1640 Glutamax medium, supplemented with 12.5% fetal calf serum and bring it to the laboratory.

2. EVPS Design

1. Assemble the general equipment shown in **Figure 1**. Autoclave all equipment and keep all components under sterile conditions. In addition, ensure that the system is waterproof and does not leak chemicals into the medium. Use polymethacrylate methyl (PMMA-GS) for the cover. Steel (X5 Cr Ni 18 10) and polyoxymethylene plastic (POM) as the vein support.
2. Design the perfusion chamber to the desired geometry to allow the placement of the vein and its connection. Make sure the depth (or radius if using cylindrical construction) is at least 2.5 cm so it allows minimal flexion and dilatation of the vessel along with constant coverage by the culture media (**Figure 1**). Sealing is a major issue and is the reason rectangular PMMA-GS construction is used.
3. Design the vein support to the desired geometry. To avoid vein kinking or over distension, allow length adjustment by pushing or pulling (screw cannot be used to that purpose, as the vein would be twisted along with the screw).
   NOTE: A full steel rod connected by 2 sliding L-shaped pieces that support the 2 vein cylinders (5 mm diameter to fit the vessel) and the vein (**Figure 1B** and **Figure 2**) is used here.
4. Design the pressure column, such that the “resting pressure” applied to the system is: p = 0-10 = h x ρ x g, where p = pressure (N/m^2, Pa) h = height of fluid column (m) ρ = density of liquid (kg/m^3) and g = the gravitational constant (9.81 m/sec^2). Design four connection ducts, from top to bottom: to apply pressure, for the outflow (from the vein), the inflow (to the vein) and to allow medium change.
5. Prepare the medium. Based on previous studies[5,11-14], choose RPMI-1640, supplemented with Glutamax, 12.5% fetal calf serum, and 1% antibiotic-antimycotic solution (10,000 U/ml penicillin G, plus 10 mg/ml streptomycin sulfate, plus 25 mg/ml amphotericin B, plus 0.5 µg/ml: gentamycin). Shear stress (SS) is given by $SS= 4 \mu Q/\pi * r^3$ Q is the flow rate (ml/sec), r the radius (cm) of the vein segment, and µ is the viscosity of the perfusion medium.
   1. Modulate SS by adjusting the viscosity through addition of 70 kDa dextran. Measure the viscosity with a viscometer. Here, add 8% 70 kDa dextran to set SS to 9-15 dyn/cm^2.
6. Set the gearing pump to induce a pulsatile cardioid signal of 60 pulses/min and constant amplitude generating a unidirectional flow of 150 ± 15 ml/min, independent from the pressure applied in the system and controlled by a computer. Ensure that the driving software integrates constant acquisition and monitoring of pressures, flow velocity, pulse rate, and signal. If desired, use a second pump (non synchronized) to produce a non-laminar, turbulent flow.

3. EVPS Assembly (Figure 1)

1. Before starting, make sure all the equipment is sterile. Perform all the following steps under asepsis in a laminar flow hood.
2. Place the vein in a Petri dish filled with medium. Use a surgical blade and divide the vein into 3 equal segments.
3. Immediately rinse one segment in PBS. Divide the segment in 3 parts, fix one in formalin for morphometry. Freeze the other two for quantitative transcript (RT-PCR) and protein (western blot) analysis. Consider these segments as a control, non-perfused vein.
4. Use the 2 remaining segments for perfusion.
   1. Very gently inject medium into the vein and determine the normal flow direction; in presence of valves the vein is reversed.
   2. Sealing the veins is of utmost importance to experimental success. Check for leaks through collaterals. Secure any leaks with 6-0 silk sutures.
5. Connect the vein segment between the two metallic cylinders, one end at a time (2.3, **Figure 1**). Secure the cylinders with Ethibon 3-0 around the indentations (**Figure 1A and B**).
   1. Place the entire venous segment into the perfusion chamber previously filled with medium. Repeat the same procedure for the second segment.
      NOTE: Failure to properly seal the vein to the cylinder will be a source of leak, require reintervention, and significantly increase the risk of infection and experimental failure.
6. To reinforce (mesh) the second segment, release the two cylinders (with the vein attached) from the L-shaped pieces (2.3 and **Figure 1**).
   1. Be gentle and do not touch the vein with any instruments. Slide the mesh first on the cylinder then onto the vein. A push/pull jostling will get the mesh on the vein.
   2. Once the mesh covers the entire surface of the vein secure the jacketed vein to the cylinders with Ethibon 3-0.
   3. Reassemble the vein/cylinder compound to the L-shaped support and transfer it to the perfusion chamber, previously filled with medium.
7. Connect each metallic cylinder (in-and outflow) to a Y-splitter using peroxide-treated silicone tubing with an internal diameter of 3.2 mm.

8. Connect the outflow splitter to a second Y-splitter using the same type of tubing. From this Y-splitter, use one tube to measure the perfusion pressure through both vessels. Connect the other one back to the column to form a closed loop system (**Figure 2**).
9. Inside the incubator, use a long (one-meter length) tube to connect the pressure column to the pump head.
10. Complete the set up by connecting the pump head to the inflow Y-splitter with another long length tube (**Figure 1**).

4. Veins Perfusion

1. After the EVPS assembly has been completed, fill the column with medium (stay below the vein outflow duct to allow refilling). Add more medium into the column until the system is full. Move all the system into the incubator maintained at 37 ± 0.1 °C with a pH kept constant at 7.40 ± 0.01 (using a CO_2/pH algorithm based on the Henderson-Hasselbach equation).
2. Bring the gear pump head outside the incubator and connect it to the gear pump drive. Screw the rods to secure the assembly.
3. Switch on the pump power, make sure it is activated on the driving software and allow 5 min for the medium to be equally distributed in every compartment.
4. To monitor the pressure, use an arterial line monitoring. Connect the EVPS pressure output (it corresponds to the arterial catheter) to the pressure transducer linked to the computer.
    1. Make sure the tube is entirely filled with medium and does not contain any bubbles. De-bubble the culture system through the “arterial line” tube (**Figure 2**). Pay attention to the display and look for a pulsatile cardioid signal of 60 pulses/min of constant amplitude. At this point, the average pressure is between 0-10 mm Hg. If the pressure is < 0 and the column progressively empties look for a leak (vein collateral or inadequate seal between the vein and the tube).
5. Set the minimal pressure to 6 mm Hg for a venous test or at 90 mm Hg for an arterial test. Under these conditions, an air injector applies the required pressure to the column and system.
6. Change the medium every 2 days by using the tube connected to the pressure column. To prevent pressure change damage, open the column plug first.

5. Completion of the Perfusion

1. After 3 or 7 days of perfusion: take the EVPS out of the incubator and dismount the veins. Discard the 5 mm proximal and distal vein ends attached to the equipment. Cut a central, 5 mm thick rings from the remaining segment and fix in formalin (morphometry). Freeze the remaining fragments and reduce into powder for further molecular analyses.

Representative Results

The EVPS provides a valuable tool to independently assess the hemodynamic forces on human saphenous vein grafts remodeling and IH.

Figure 1 shows the perfusion chamber and the vein support. In **Figures 1A** and **B**, the vein support before (**Figure 1A**) and after (**Figure 1B**) assembly, respectively, is pictured. It is composed (from the top to the bottom) of 1 plain stainless steel tube measuring 9 cm, which serves as a support for 2 L-shaped pieces that can easily slide (from the left to the right) and provides a reliable technique to adjust the support size to the vein. Each of these pieces holds a POM disc to fit a steel cylinder (vein connector) fixed in place by integrated screw (arrowhead). **Figure 1C-D** shows the perfusion chamber alone (C) and after insertion of the vein support (D). On the perfusion chamber, depressions are designed to hold the vein support in place (top) and to avoid kinking of the connecting tube coming in and out from the vein (bottom).

Figure 2 shows real time pictures (**Figure 2A**) and a schematic representation (**Figure 2B**) of the EVPS. The perfusion chamber, veins and its supports, as well as the pressure column, are maintained in a controlled environment (temperature, CO_2 and O_2) whereas the pump, pressure injector, and control devices all remain outside the incubator. The figure illustrates the gearing pump (1) that generates a pulsatile signal controlled by a computer (2), which monitors the flow velocity (3), pressure (4), and controls the minimal diastolic pressure (5); two segments of a same saphenous vein are connected in parallel to the perfusion pump inside separate perfusion chambers (6a and 6b) placed in a cell culture incubator.

In **Figure 3**, histomorphometric analysis shows that external reinforcement prevents intimal hyperplasia and pathological media remodeling otherwise observed after 7 days under high pressure (arterial regimen, mean = 100 mm Hg) perfusion. In **Figure 3A**, representative histological sections stained for Hematoxylin-eosin (HE) reveals the lining of the lumen by nuclei of endothelial cells and the nuclei of SMCs in the media layer in all conditions. **Figures 3B-C** shows representative Van Gieson Elastic Lamina (VGEL) stained sections. In **Figure 3B**, the intima is thickened (IH) in veins perfused at high pressure (mean = 100 mm Hg) for 7 days compared to control non-perfused veins, a phenomenon largely decreased in the presence of an external mesh. **Figure 3C** illustrates the pathological outward remodeling and media thinning in veins subjected to 7 days of arterial pressure. This is largely prevented by the external reinforcement. Furthermore, in **Figure 3D**, Masson’s trichrome staining (blue=connective tissue, red=muscle) associates this pathological remodeling with the persistence of only one of the three muscle layers and accumulation of smooth muscle cells in the inner layer (intima). The external reinforcement preserves the distribution of the SMCs and media structure.

Figure 4 illustrates a current clinical application of the external mesh. An illustrative example is provided by external reinforcement of an aneurysmal arterio-venous fistula (hemodialysis access). **Figure 4A** shows a time-course representation of the vein reinforcement (from the top to the bottom). First, the mesh was placed around a rigid tube while the vein’s extremity is fixed to a mandrel (upper panel). Then, the vein was pulled through the tube thanks to the mandrel. Once the vein was in place, the tube was slowly retracted, leaving the mesh around the vein (upper and middle panel). In this particular case, the procedure was repeated on both sides of the veins, and the veins segments and mesh reinforcements were assembled by an end-to-end anastomosis (lower panel). **Figure 4B** provides a larger view of the arterio-venous end-to-side anastomosis, showing that the mesh is wrapped around the anastomosis by tying it along the posterior wall of the artery.

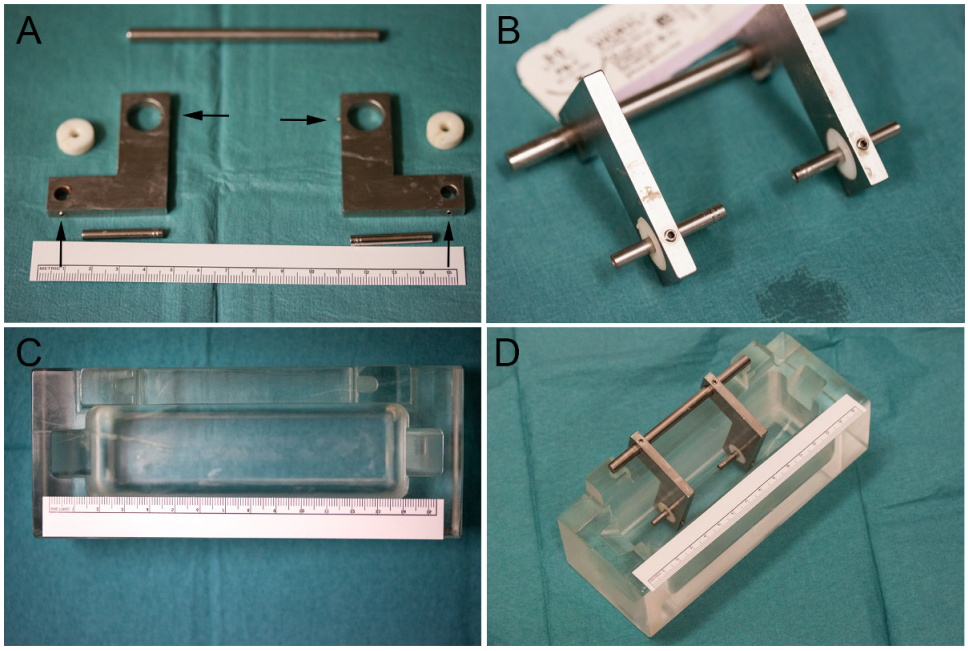

Figure 1. The vein support and perfusion chamber. A. The vein support is composed of 1 plain tube, 2 L-shaped pieces, discs and cylinders (form the top to the bottom). **B.** The vein support once assembled. **C.** View of the perfusion chamber. **D.** The perfusion chamber is designed to hold in place the vein support and allows its connection to the vein and connecting tubes.

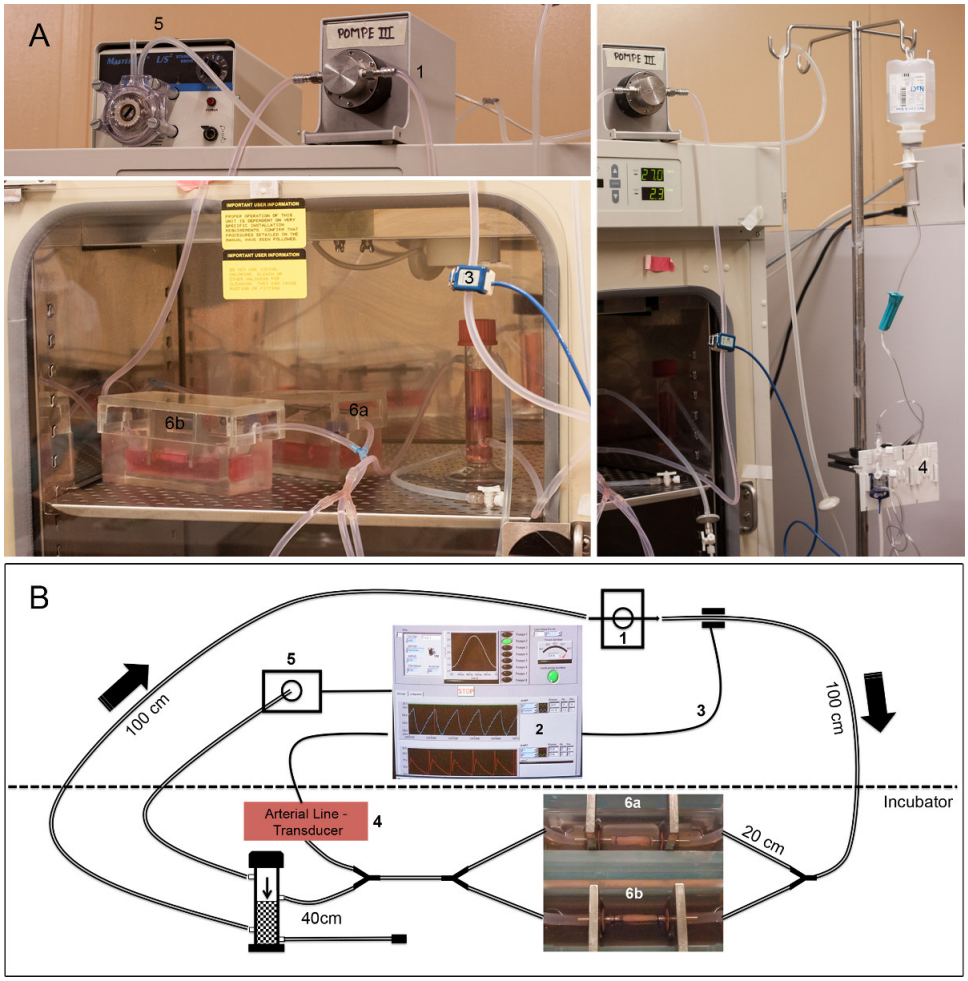

Figure 2. The *ex vivo* perfusion system. A. The completely assemble EVPS in the cell-culture incubator. **B.** Schematic representation. 1) the pump generating a pulsatile cardioid wave; 2) the computer controlling the pressure, flow (type, rate and amplitude); 3) the flow meter; 4) the pressure transducer – arterial line; 5) the pressure injector; 6) two segments of a very same saphenous vein are perfused without (6a) or with external mesh reinforcement (6b).

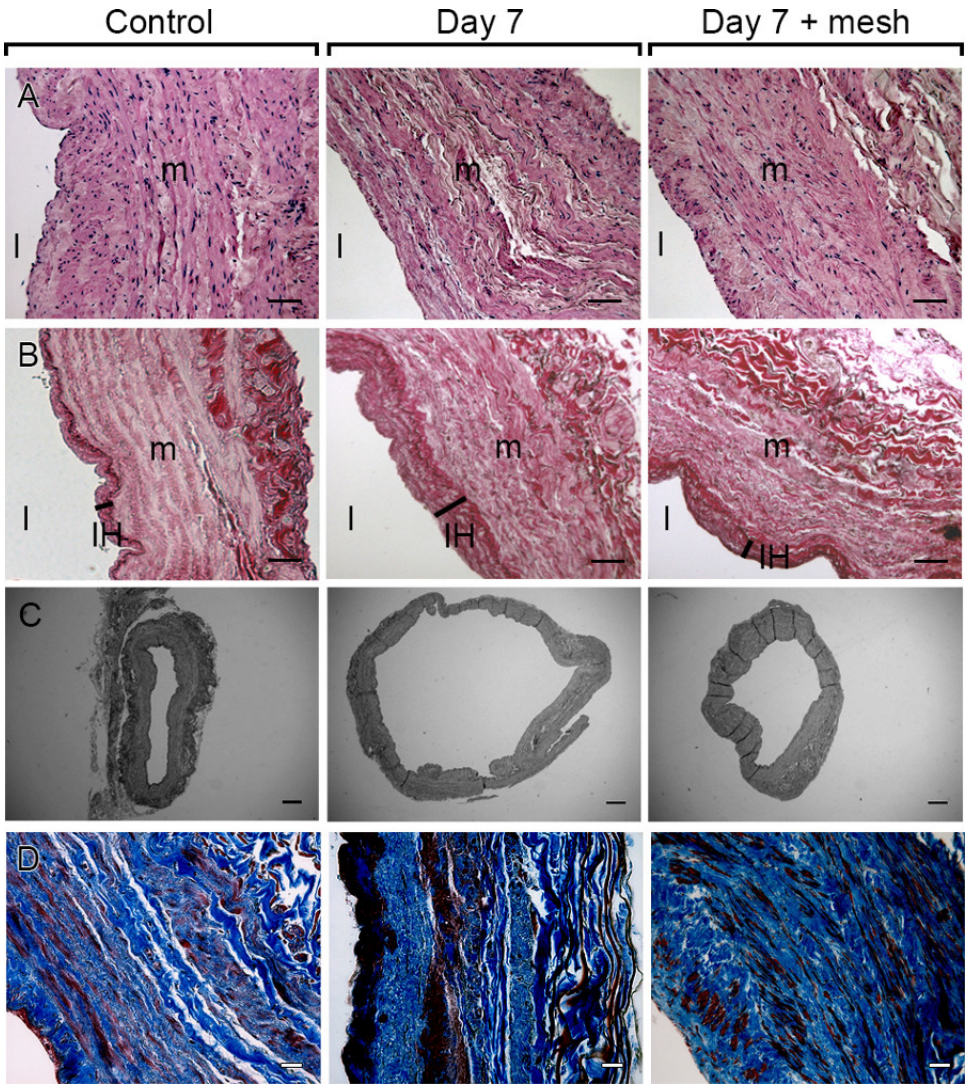

Figure 3. The external reinforcement prevents intimal hyperplasia. A. Representative histological sections stained with Hematoxylin-eosin (HE). Bar represents 50 µm. **B-C.** Representative histological sections stained for elastin (VGEL). l = lumen m = media, IH = intimal hyperplasia. Bar represents 50 µm. **D.** Representative histological sections stained with Masson's trichrome. Bar represents 50 µm.

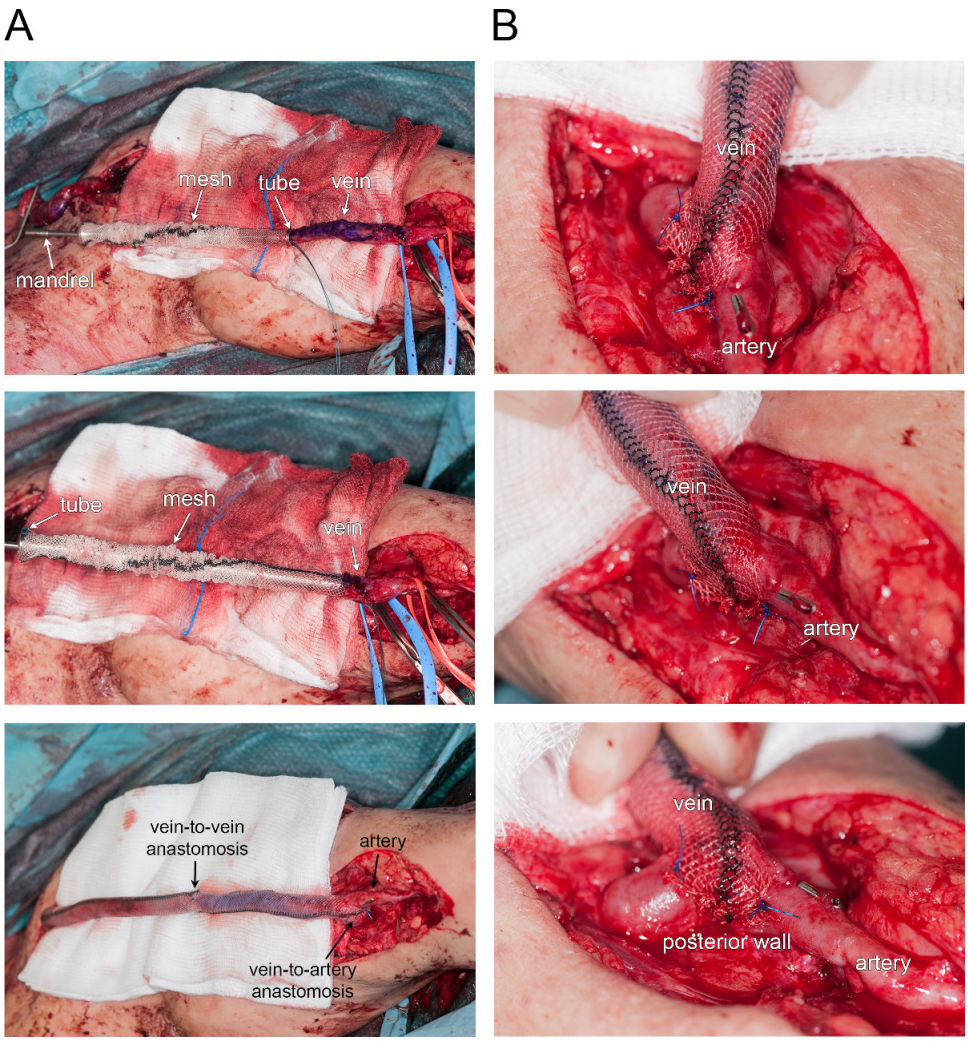

Figure 4. External reinforcement of an aneurysmal fistula. A. Time-course photographs of vein reinforcement (from top to bottom). **B.** Larger view of the arterio-venous end-to-side anastomosis.

Discussion

This study uncovers an *ex vivo* vein perfusion system (EVPS) to perform extensive hemodynamic studies in human veins. This system allows saphenous veins perfusion under defined hemodynamic parameters in the absence of aggravating inflammatory and growth factors released by circulating cells *in vivo*. Thus, it provides a better understanding of the underlying pathways involved in the control of IH in human veins grafts[5,11,12,15].

Reproducible and quantifiable hemodynamic perturbations are limited *in vivo*. Several complex murine microsurgical procedures have been described. Using a bypass isograft model via interposition of a vena cava from a donor mouse into the right common carotid artery and the additional creation of an outflow branch ligation, mid graft or common carotid stenosis, flow and SS acutely decreased and enhanced IH[3]. Outward versus inward remodeling can further be interrogated using a mid-focal versus distal common carotid stenosis[16]. In large animals (sheep, pig, and baboon), bypass grafts are technically easier and represent an attractive approach to test pre-clinical human sized devices such as the mesh used in the present study[8-10]. However, its cost and the paucity of validated molecular tools limit the use of these strategies. Finally, these flow manipulations constantly alter wall tension and fail to interrogate one single constituent. In addition, the intricate relationships between the hemodynamics and the immune and endocrine systems further limit the analysis of a single actor.

Several issues arise with the use of the EVPS. 1) Low-grade bacterial contamination often accompanied human vein harvest and the *ex-vivo* absence of circulating cells stand as an important cause of infection. This is mainly prevented by hand washing the pieces separately then autoclaving all material prior to use. Furthermore the assembly is performed in less than 90 minutes and under rigorous asepsis. 2) Sealing that endures repeated sterilization. For this reason, a rectangular PMMA-GS construction was used, avoiding the use of joints and limiting deformation. 3) SS and wall tension are calculated at defined time points, based on the vessel lumen radius (histology), the flow and viscosity being constant. The integration of a longitudinal imaging (high definition camera, laser or Doppler) that continuously monitors the vein diameter and/or flow will provide more detailed information on local flow variations and allow cyclic strain calculations. 4) The two parallel vein segments may have uncontrolled differences in their wall compliance and radius. Thus, we only compare segments from a same vein and assume that under the same pressure, the flow rate pattern is similar in both segments.

In this study, veins were submitted to pulsatile laminar flow; however, 50% of intimal hyperplastic lesions occur in the end-to-side perianastomotic areas of the vein graft, where laminar flow is disrupted. Turbulent conditions can be modeled with the addition of a second pump, non-synchronized with the first pump. Future studies will be performed to specifically assess the impact of laminar flow disruption on IH and the potentially beneficial effect of mesh reinforcement. Interestingly, the flexible structure of the mesh allows circumferential wrapping at the anastomosis sites, as already performed to repair aneurysmal fistulas[17] (**Figure 4**). Thus, the mesh could prove useful to limit perianastomotic dilatation, laminar flow disruption and consequently reduce IH at the anastomosis sites. This may be particularly beneficial in distal bypass graft, frequently affected by diameter mismatch between the vein and the tibial or peroneal artery.

In summary, the setup shown here allows parallel perfusion of human veins, under identical hemodynamic conditions. These data demonstrate that the use of an external macroporous tubular polyester mesh is an efficient method to limit the development of IH in vein grafts inserted into an arterial environment[11]. This system can profit several areas of research. Especially, it emerges as a powerful tool to perform pre-clinical studies testing the feasibility and efficiency of various approaches to reduce IH in human material, and is a valuable addition to *in vivo* animal models. Other prosthetic supports or meshes coated with pharmaceutical agents will be evaluated using this method[6-10]. In addition, one could envision to test locally applied pharmacological molecules to prevent IH in human tissue, under near physiological state. Gene therapy interventions are also achievable, transducing a vein segment to overexpress or silence target genes of interest.

In conclusion, our system will increase our understanding of the hemodynamic contribution to human vein graft diseases. It provides an innovative platform to test new therapeutic strategies and may arise as a “bench to beside translation tool.”

Disclosures

The authors have nothing to disclose.

Acknowledgements

This work was supported by grants from the SNF [31003A-138528], the Octav and the Marcella Botnar Foundation, the Novartis Foundation and the Emma Muschamp Foundation. We thank Martine Lambelet, and Jean-Christophe Stehle for their excellent technical assistance.

References

1. Sal Go, A., *et al.* Executive summary: heart disease and stroke statistics--2014 update: a report from the american heart association. *Circulation*. **129**, 399-410 (2014).
2. Sal Conte, M., *et al.* Results of PREVENT III: a multicenter, randomized trial of edifoligide for the prevention of vein graft failure in lower extremity bypass surgery. *Journal of Vascular Surgery*. **43**, 742-751 (2006).
3. Yu, P., Nguyen, B. T., Tao, M., Bai, Y., Ozaki, C. K. Mouse vein graft hemodynamic manipulations to enhance experimental utility. *The American Journal of Pathology*. **178**, 2910-2919 (2011).
4. Davies, M. G., Hagen, P. O. Reprinted article "Pathophysiology of vein graft failure: a review". *European journal of vascular and endovascular surgery : the official journal of the European Society for Vascular Surgery*. **42**, Suppl 1. S19-S29 (2011).
5. Berard, X., *et al.* Role of hemodynamic forces in the ex vivo arterialization of human saphenous veins.*Journal of Vascular Surgery*. **57**, 1371-1382 (2013).
6. Vijayan, V., *et al.* Long-term reduction of medial and intimal thickening in porcine saphenous vein grafts with a polyglactin biodegradable external sheath. *Journal of Vascular Surgery*. **40**, 1011-1019 (2004).
7. Jeremy, J. Y., *et al.* On the biology of saphenous vein grafts fitted with external synthetic sheaths and stents. *Biomaterials*. **28**, 895-908 (2007).
8. Zilla, P., *et al.* Constrictive external nitinol meshes inhibit vein graft intimal hyperplasia in nonhuman primates. *The Journal of Thoracic and Cardiovascular Surgery*. **136**, 717-725 (2008).
9. Zilla, P., *et al.* Utilization of shape memory in external vein-graft meshes allows extreme diameter constriction for suppressing intimal hyperplasia: a non-human primate study. *Journal of Vascular Surgery*.**49**, 1532-1542 (2009).
10. Yeoman, M. S., *et al.* A constitutive model for the warp-weft coupled non-linear behavior of knitted biomedical textiles. *Biomaterials*. **31**, 8484-8493 (2010).
11. Longchamp, A., *et al.* The use of external mesh reinforcement to reduce intimal hyperplasia and preserve the structure of human saphenous veins. *Biomaterials*. **35**, 2588-2599 (2014).
12. Saucy, F., *et al.* Ex vivo pulsatile perfusion of human saphenous veins induces intimal hyperplasia and increased levels of the plasminogen activator inhibitor 1. *European Surgical Research. Europaische Chirurgische Forschung. Recherches Chirurgicales Europeennes*. **45**, 50-59 (2010).
13. Dubuis, C., *et al.* Atorvastatin-loaded hydrogel affects the smooth muscle cells of human veins. *The Journal of pharmacology and experimental*. **347**, 574-581 (2013).
14. Deglise, S., *et al.* Increased connexin43 expression in human saphenous veins in culture is associated with intimal hyperplasia. *Journal of Vascular Surgery*. **41**, 1043-1052 (2005).
15. Muto, A., Model, L., Ziegler, K., Eghbalieh, S. D., Dardik, A. Mechanisms of vein graft adaptation to the arterial circulation: insights into the neointimal algorithm and management strategies. *Circulation Journal : Official Journal of the Japanese Circulation Society*. **74**, 1501-1512 (2010).
16. Tao, M., *et al.* A simplified murine intimal hyperplasia model founded on a focal carotid stenosis. *The American Journal of Pathology*. **182**, 277-287 (2013).

17. Berard, X., *et al.* Salvage treatment for venous aneurysm complicating vascular access arteriovenous fistula: use of an exoprosthesis to reinforce the vein after aneurysmorrhaphy. *European Journal of Vascular and Endovascular Surgery : the Official Journal of the European Society for Vascular Surgery*. **40**, 100-106 (2010).

PLOS ONE

RESEARCH ARTICLE

Connexin43 Inhibition Prevents Human Vein Grafts Intimal Hyperplasia

Alban Longchamp[1,2,4‡], Florent Allagnat[1‡], Florian Alonso[1], Christopher Kuppler[3], Céline Dubuis[1], Charles-Keith Ozaki[2], James R. Mitchell[4], Scott Berceli[3], Jean-Marc Corpataux[1], Sébastien Déglise[1☯], Jacques-Antoine Haefliger[1☯*]

1 Department of Vascular Surgery, Centre Hospitalier Universitaire Vaudois, Laboratory of Experimental Medicine, Lausanne, Switzerland, **2** Department of Surgery, Brigham and Women's Hospital, Harvard Medical School, Boston, Massachusetts, United States of America, **3** Malcom Randall Veterans Affairs Medical Center and the Division of Vascular and Endovascular Surgery, University of Florida College of Medicine, Gainesville, Florida, United States of America, **4** Department of Genetics and Complex Diseases, Harvard School of Public Health, Boston, Massachusetts, United States of America

☯ These authors contributed equally to this work as senior authors.
‡ These authors contributed equally to this work as first authors.
* Jacques-Antoine.Haefliger@chuv.ch

Citation: Longchamp A, Allagnat F, Alonso F, Kuppler C, Dubuis C, Ozaki C-K, et al. (2015) Connexin43 Inhibition Prevents Human Vein Grafts Intimal Hyperplasia. PLoS ONE 10(9): e0138847. doi:10.1371/journal.pone.0138847

Editor: Christos E. Chadjichristos, National Institute of Health and Medical Research, FRANCE

Received: May 27, 2015

Accepted: September 4, 2015

Published: September 23, 2015

Data Availability Statement: All relevant data are within the paper and its Supporting Information files.

Funding: This work was supported by grants from the Swiss National Science Foundation (SNSF, www.snf.ch) 31003A-155897 to JAH; the Octav and the Marcella Botnar Foundation to JAH; the Muschamp Foundation (http://www.s-a-v.org/-Fondations-associees-.html) to SD; The American Heart Association (http://www.heart.org) 12GRNT9510001 and 12GRNT1207025 to CKO; and the Swiss National Science Foundation (SNSF, www.snf.ch) P1LAP3_158895 to AL.

Abstract

Venous bypass grafts often fail following arterial implantation due to excessive smooth muscle cells (VSMC) proliferation and consequent intimal hyperplasia (IH). Intercellular communication mediated by Connexins (Cx) regulates differentiation, growth and proliferation in various cell types. Microarray analysis of vein grafts in a model of bilateral rabbit jugular vein graft revealed Cx43 as an early upregulated gene. Additional experiments conducted using an *ex-vivo* human saphenous veins perfusion system (EVPS) confirmed that Cx43 was rapidly increased in human veins subjected *ex-vivo* to arterial hemodynamics. Cx43 knock-down by RNA interference, or adenoviral-mediated overexpression, respectively inhibited or stimulated the proliferation of primary human VSMC *in vitro*. Furthermore, Cx blockade with carbenoxolone or the specific Cx43 inhibitory peptide ^{43}gap26 prevented the burst in myointimal proliferation and IH formation in human saphenous veins. Our data demonstrated that Cx43 controls proliferation and the formation of IH after arterial engraftment.

Introduction

Bypass of stenotic arteries with autologous saphenous vein is an established treatment for ischemic vascular disease. However its long-term success is limited, with 30–50% of the saphenous grafts failing within 5 years post implantation [1]. Vein graft failure is due to intimal hyperplasia (IH), a process whereby the vein wall thickens and expands to adapt to the high arterial pressure and flow.

Several studies suggest that intercellular signaling regulates VSMC's phenotypic switch [2, 3] and proliferation [4–7]. However gap junction's response to flow, pressure and their contribution to IH remains poorly delineated. The direct intercellular exchange of small molecule (<1kDa) through gap junctions is critical to integrate individual cells into coordinated

Competing Interests: The authors have declared that no competing interests exist.

Abbreviations: VSMC, vascular smooth muscle cells; EC, endothelial cells; Cx, connexin; GJ, gap junction protein; IH, intimal hyperplasia; VGEL, Van Gieson elastic lamina; RNAi, RNA interference; EVPS, ex vivo perfusion system.

multicellular units, allowing maintenance of cellular homeostasis and regulation of cellular functions including proliferation, migration and differentiation [8–10]. Endothelial cells (EC) predominantly express Cx37, Cx40 and some Cx43, whereas vascular smooth muscle cells (VSMC) are mostly coupled by Cx43 and Cx45, albeit minimal levels of Cx37 and Cx40 have been reported [8–10].

To determine the contribution of hemodynamic forces in the development of IH, we previously developed a model of bilateral rabbit carotid artery interposition grafts plus a unilateral distal outflow ligation to model differential flow states [11, 12]. In this setting, we identified divergent patterns of vein graft remodeling under low versus high flow and shear stress [12]. To further study the impact of hemodynamic forces after human vein arterial engraftment, we developed an *ex-vivo* human vein perfusion system (EVPS) [13, 14] and observed a 7-day high-pressure perfusion (mean = 100 mmHg) to be sufficient for IH formation. The VSMC forming the media layer of the vessels are highly specialized contractile cells featuring a very low proliferation rate under physiological conditions [15]. Following injury, VSMC integrate signals that promote their phenotypic switch from a quiescent contractile to a proliferative and motile state. The proliferation and migration of VSMC from the media toward the intimal layer are keys component to IH.

The aim of this study was to characterize the regulation of vascular connexins flowing arterial implantation of vein grafts. We observed that endothelial connexins Cx37 and Cx40 are rapidly down-regulated while VSMC connexin Cx43 is strongly and rapidly up-regulated in response to pulsatile arterial perfusion in rabbit vein grafts *in-vivo* and in human veins grafts *ex-vivo*. We further demonstrate, using primary human VSMC, that Cx43 controlled proliferation and show for the first time that specific Cx43 blockade partially prevented IH formation in human veins *ex-vivo*.

Materials and Methods

Animal vein graft

Male New Zealand White rabbits (3.0–3.5 kg; n = 56) were anesthetized through an intramuscular injection with ketamine hydrochloride (30.0 mg/kg). Anesthesia was maintained with endotracheal intubation and continuous isoflurane inhalant anesthesia (2% during painful stimuli, and 1% at latent periods). Vein bypass grafts were constructed with an anastomotic cuff technique as previously as described [11, 12]. Bilateral carotid artery interposition grafting with jugular vein and unilateral distal carotid artery branch ligation were performed to create two distinct flow states. Briefly, differential flow states between the right and left vein grafts were accomplished by ligation of the internal carotid artery and three of the four primary branches of the external carotid artery, resulting in an immediate six fold difference in mean shear stress [11, 12]. Routine daily postoperative care and analgesia was provided, including daily neurologic assessment up to day 5 post surgery to identify any or all of head tilt, ear droop, or extremity weakness. Graft flow rates were determined at the time of implantation and harvest with an ultrasonic flow meter (VisualSonics Inc, Toronto, Ontario, Canada). Vein grafts harvest was performed under general anesthesia through an intramuscular injection with ketamine hydrochloride (30.0 mg/kg). Then the recipient rabbit was whole-body blood flushed with saline via intravascular access through the left ventricle, leading to exsanguination and death. Vein grafts were harvested after implantation at 2 hours (0.08 days) (high-flow, n = 4; low-flow, n = 4) and 1 day (high-flow, n = 5; low-flow, n = 4), 3 days (high-flow, n = 4; low-flow, n = 5), 7 days (high-flow, n = 5; low-flow, n = 5), 14 days (high-flow, n = 4; low-flow, n = 5), and 28 days (high-flow, n = 6; low-flow, n = 6). Normal rabbit jugular vein served as the control (n = 5). The perianastomotic regions for each vein graft were removed, and the mid-

portion of the graft was divided into two segments, one for histological and immunohistochemical analyses and the other for total RNA extraction using the RNeasyMiniKit (Qiagen) as previously described [12].

Microarray analysis

Microarray analysis was performed as previously described [12]. Briefly Complementary DNA form rabbit vein was generated using Ovation Pico WT kit (NuGEN, San Carlos, Calif) and labeled using GeneChip WT Terminal Labeling (Affymetrix, Santa Clara, Calif). Samples were hybridized to a proprietary rabbit array (Affymetrix). The resulting expression data were normalized with the Partek Genomics Suite (Partek, St. Louis, Mo).

Human saphenous veins culture

After informed consents, 27 surplus segments of non-varicose human saphenous veins were obtained from 27 patients (15 men and 12 women) with a median age of 72 years (interquartile range 51–82), who underwent lower limb bypass surgery for critical ischemia. A 7 to 9 cm long segment of the greater saphenous vein, with an external diameter of 2.5–4 mm, was harvested and immediately stored at 4°C in a RPMI-1640 Glutamax medium, supplemented with 12.5% fetal calf serum (Life Technologies Europe B.V.). The segment was divided in 3 equal parts. One part was immediately fixed in either formalin (one half) or rapidly frozen in liquid nitrogen (the other half). The two others parts from the same vein were perfused using an *ex-vivo* perfusion system (EVPS) [13, 14, 16], with or without an external mesh reinforcement (ProVena, B.Braun Medical SA) to model and control (mesh) the development of IH as previously described [13] (more details on the method can be found at: http://www.jove.com/video/52079/procedure-for-human-saphenous-veins-ex-vivo-perfusion-external). A pulsatile, cardioid signal at 60 pulses per minute with constant amplitude was setup up via the computer software which independently pilots the gearing pump. The resulting flow was about 160 milliliters per minute. The conditions of the perfusion were set to obtain a shear stress (SS) of 9–15 dyn/cm^2, as expected in the femoral artery [14], given by $SS = 4\ \mu Q / \pi r^3$, where μ is the viscosity of the perfusion medium set to was 3.73 10^{-2} dyn·s/cm^2, as measured in a Coulter viscometer (Coulter Electronics, High Wycombe, UK), Q the flow rate (mL/s), and r the radius (cm) of the vein segment. Mean pressure (MP) = 100 mmHg, as given by MP = (systolic pressure + 2 x diastolic pressure)/3. Upon completion of the perfusion period, the vein segments were dismounted and the 5 mm proximal and distal ends, which attached the vessel to the perfusion equipment, were discarded.

Static vein cultures were performed as previously described [17]. Briefly, 5 mm segments of vein were opened longitudinally and pinned on a layer of Sylgard 184 resin (Dow Corning, Seneffe, Belgium) in a Pyrex dish and kept in culture for 10 days in RPMI-1640 Glutamax supplemented with 10% FBS and and 1% antibiotic solution (10,000 U/mL penicillin G, 10,000 U/mL streptomycin sulphate). 100 μM Carbenoxolone (Sigma-Aldrich), 200 μM of the Cx-mimetic peptides ^{43}Gap26 (VCYDKSFPISHVR, Tocris Bioscience Bristol, UK) and the control scrambled peptide (PSFDSRHCIVKYV) (Severn Biotech, UK) were prepared in SMC culture media. 5-mm segments of vein were harvested after culture. The vein segments were either frozen for molecular analysis or fixed in 4% formalin and paraffin-embedded for histological analysis.

Morphometry

Hematoxylin-eosin and Van Gieson-elastin (VGEL) stainings were used for histological and morphometric analysis, respectively. All morphometric measurements were done by 2 independent

researchers, one of them blind to the experimental groups using the Leica Qwin® software (Leica, Switzerland). Twenty-four measurements of the thickness of the intima and media layers were made in each sample at a magnification of x100 as previously described [14, 16].

Cell culture

The human smooth muscle cells were prepared from explants culture, as previously described [18–20]. Briefly, primary smooth muscle cells were cultured from human saphenous veins from a similar cohort used for *ex-vivo* perfusion. Veins explants of 1–2 mm were plated, luminal side down, on the dry surface of a 24-well culture plate, previously coated with 1.5% Gelatin type B (Sigma-Aldrich). Explants were gently covered with one drop of RPMI, 10%FBS medium, and placed overnight in a 37°C, 5% CO2. The next day, culture medium was carefully added to the wells, taking care not to detach the explants. VSMC were identified by immunostaining using antibodies to smooth muscle actin (abcam, ab5694) and desmin (Dako, M 0760). Passages 1 to 4 were used for the experiments.

RNA interference

Smooth muscle cells were transiently transfected using lipofectamine RNAiMAX (Life Technologies Europe B.V.) and 30nM siRNA. Cx43 siRNAs 1 and 2 (s5758 and s5759) were purchased from Ambion (Ambion, Life Technologies Europe B.V., Zug, Switzerland). Briefly, confluent cells were transfected using antibiotics free Optimem medium (Life Technologies Europe B.V.), according to the manufacturer's indications. Cells were kept 48 hours in culture before the experiments. The Allstars Negative Control siRNA (Qiagen, Hombrechtikon, Switzerland) was used as a control. The efficiency of transfection was above 90% as evaluated using the Thermo Scientific™ Dharmacon™ siGLO™ Green Transfection Indicator (Thermo Fisher Scientific Inc. Waltham, MA, USA).

Adenoviral transfer

The Control Ad-GFP virus were generated as previously described [21, 22]. Ad-Cx43 was a kind gift from Professor Viviana Berthoud and Eric Bayer (University of Chicago, Illinois, U.S.A.). All viral vectors were amplified and purified by Vector Biolabs, (Philadelphia, PA, U.S.A.). Human VSMC were infected overnight in complete medium and collected 48 hours later.

Quantitative real-time PCR

Quantitative real-time PCR analysis was performed on total RNA extracted from human saphenous veins using the TriPure isolation reagent (Roche) as previously described [14, 20]. The primers used to amplify specific cDNAs are given in S1 Table, and were designed using the free online software Primer3Plus (http://primer3plus.com/cgi-bin/dev/primer3plus.cgi) [23]. Levels of expression were determined relative to those of GAPDH, which were not significantly altered by the experimental conditions tested here.

Western Blots

Segments of saphenous veins were reduced to powder in liquid nitrogen, and homogenized in lysis buffer as published [23, 24]. Immunoblot analyses were performed as previously described [16, 23, 25] using the following antibodies: rabbit polyclonal against Cx43 (Millipore) diluted 1:1000; rabbit polyclonal against Cx40 (InVitrogen) diluted 1:2000; rabbit polyclonal against Cx37 (kindly provided by Pr. A. Simon [23]) diluted 1:2500; mouse monoclonal against α-

Tubulin (Sigma-Aldrich), diluted 1:1000 and horseradish peroxidase-conjugated goat anti-rabbit or anti-mouse IgG (Sigma-Aldrich), diluted 1: 5000.

Immunohistochemistry and immunocytochemistry

The Proliferating Cell Nuclear Antigen (PCNA) and alpha smooth muscle actin (α-SMA) immunostaining were performed on paraffin-embedded tissue slides using the monoclonal mouse anti-human PCNA (Clone PC10 1/200; Dako Schweiz AG, Baar, Switzerland), and anti-SMA (Abcam, ab5697, Lucerna chem. AG, Luzern, Switzerland) antibodies. Slides were subjected to standard protocol of antigen retrieval prior to antibody incubation. PCNA staining was revealed either using DAKO envision^{TM}+-HRP-DAB staining or using secondary biotin-steptavidin antibodies coupled to AlexaFluor 594. The PCNA positive signal was evaluated automatically using the ImageJ software on 10 slides per vein and 3 to 5 veins per conditions [16]. PCNA/DAB^{+} signal were quantified as follows: images were converted into 16 bit and a color threshholding based on red hue was applied to select only the brown staining. The selected staining was processed into a binary image and the number of positive pixels determined. This signal was normalized to the total pixel number composing the vein section and expressed as a PCNA positive pixels/total vein pixels ratio. PCNA fluorescent signal were quantified as follows: images were converted to a 32 bit format and the signal to noise ratio was determined by applying the Yen thresholding method. A binary image was then created and the number PCNA^{+} nuclei automatically detected. Data were normalized to the number of cells (nuclei imaged by DAPI staining) in each image. Cx immunostainings were performed using frozen sections of unfixed veins as previously described [23], using the primary antibodies used for Western blotting at a dilution of 1:100, except those against Connexin43 (Millipore), which was diluted 1:200. Vein sections were rinsed in PBS, counterstained with 0,02% Evans Blue and coverslipped. BrdU and Cx43 immunostaining were performed as previously described [20, 26] on SMC grown on glass coverslips and fixed for 5 min in −20°C acetone, air-dried, rinsed in PBS and permeabilized for 1 h in PBS supplemented with 2% BSA and 0.1% Triton X-100 (full PBS). Brdu positive nuclei were automatically detected using the ImageJ software and normalized to the total number of DAPI-positive nuclei.

Cell cycle analysis

To measure the cellular DNA content, transfected cells were kept under 0% FBS for 48 hours, and then supplemented with 10 ng/mL Platelet-Derived Growth Factor (PDGF-BB, Pepro-Tech) for an additional 24 hours. Adherent cells were collected by trypsinization. Cells were pelleted, rand washed in PBS/EDTA and fixed in 70% ethanol overnight at 4°C. Cells were pelleted and resuspended 15 min at 37° in 1ml PBS 0.1% Triton X-100 with 0.1 mg RNase (Sigma-Aldrich) and 0.2 mg propidium iodide as previously described [27]. Samples were analyzed on BD FACS Scan. The percentage of cells in different phases was calculated using FlowJo software (Tree Star, Inc).

Scratch wound assay

Two perpendicular scratch wounds were created on confluent cells using a sterile p200 pipette tip. Repopulation of the wounded areas was recorded by phase-contrast microscopy connected to a digital camera every 2 hours and for 24 hours. The size of the denuded area was determined at each time point from digital images using the ImageJ software. The area of each experiment, measured immediately after the wounding was used to standardize quantitative analysis.

Statistical Analysis

All experiments were quantitatively analyzed and results shown as mean + SEM. One or two-way analysis of variance (ANOVA) were performed to compare mean values between groups, using post hoc t-tests with Bonferroni correction, as provided by the Statistical Package for the Social Sciences (SPSS 17.0, Chicago, Ill., USA). Statistical significance was set at $p < 0.05$.

Ethics Statement

Written, informed consent was obtained from all vein donors who underwent lower limb bypass surgery for critical ischemia. The study protocols for organ collection and use were reviewed and approved by the Centre Hospitalier Universitaire Vaudois (CHUV) and the Cantonal Human Research Ethics Committee (http://www.cer-vd.ch/, no IRB number, Protocol Number 170/02), and are in accordance with the principles outlined in the Declaration of Helsinki of 1975, as revised in 1983 for the use of human tissues.

Rabbit care, surgery and euthanasia procedures were approved by the Institutional Animal Care and Use Committee of the University of Florida (https://iacuc.ufl.edu) and conforms to the Guide for the Care and Use of Laboratory Animals (NIH Publication, Revised 2011, Animal Welfare Assurance Number A3377-01).

Results

Arterial engraftment induces vein intimal hyperplasia and time-dependent regulation of the vascular connexins

As previously described [11, 12, 28], bilateral rabbit vein grafting caused a robust hyperplastic response beginning at 7 days after vein graft implantation, and progressing to 28 days. Microarray analysis of both vein grafts demonstrated that flow did not impact the gene expression of Cx37 (GJA4), Cx40 (GJA5) and 43 (GJA1), as assessed by ANOVA for fixed effects with flow and time as the two variables (Fig 1 and S1 Fig). Temporal changes in gene expression after vein graft placement were then analyzed from 2 hours (0.08 days) following grafting and up to 28 days. At a p value < 0.05, 57 genes were differentially expressed over time (S1 Fig). Unsupervised genes cluster analysis revealed that individual vein grafts cluster by time point rather than by flow state, indicating time from implantation as the dominant effect on gene expression (S1A Fig). A supervised hierarchal clustering analysis using averaged expression data further revealed that among the early upregulated genes (S1B Fig), Cx43 was the most differentially expressed, with a fivefold upregulation 2 hours after implantation, which persisted over time (Fig 1A and 1B). In the cluster of downregulated genes, despite an early downregulation, the Cx37 and Cx40 transcript levels did not significantly change over time (Fig 1A and 1B).

Myointimal proliferation and Cx43 are increased in human veins exposed to arterial hemodynamic

Using our validated *ex-vivo* vein perfusion model [13, 16], human saphenous veins grafts were exposed to high-pressure (mean = 100mmHg) and high flow (180-200ml/min), mimicking the femoral artery hemodynamic. As previously established [16], 3 and 7 days of arterial perfusion resulted in neointima formation (Fig 2A upper panel and 2B) and reduced media thickness (Fig 2A upper panel and 2C). Von Willebrand factor (vWF) immunostaining revealed intact endothelial cells lining the lumen of native vein and vein subjected to a 3 or 7 days high pressure pulsatile perfusion (Fig 2A, **lower panel**).

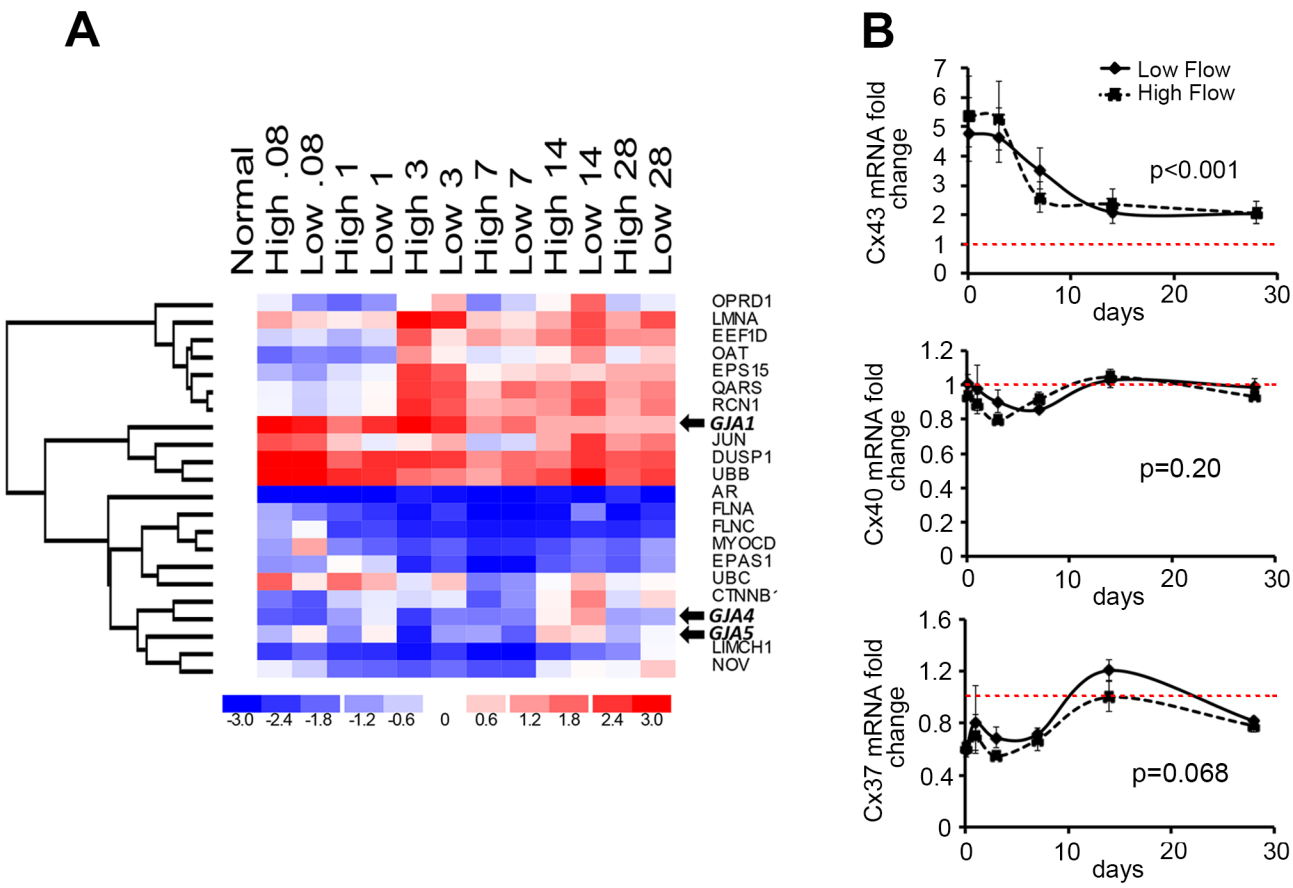

Fig 1. Probe sets analysis demonstrate changes in Cx transcripts levels over time after rabbit vein graft. A) Supervised hierarchal clustering analysis of selected time-dependent probe sets (false discovery rate = .05) reveals GJA1 (Cx43), GJA4 (Cx37) and GJA5 (Cx40) to cluster with differential expression patterns. Mean expression data at each time point (expressed as day) and flow condition are presented across the x-axis, with red representing upregulation and blue representing downregulation compared to normal vein. **B)** Mean expression fold change from baseline (normal vein) of Cx43 (**top**), Cx40 (**middle**) and Cx37 (**bottom**) at each time point under high and low flow conditions. Dotted red line represents the mean value observed in control normal vein. Data represent mean ± SEM of 5 experiments.

doi:10.1371/journal.pone.0138847.g001

Further analysis of cell growth dynamics, showed reduced media cellularity and a concomitant increase in proliferative activity within the myointima after 3 and 7 days (Fig 3), as assessed by PCNA immunostaining. The addition of an external reinforcement preserved the structure but not the cellularity of the media layer, reduced the number of PCNA-positive nuclei, and prevented the development of IH (Fig 3).

In human saphenous vein, Cx37 and Cx40 are specifically expressed in ECs, whereas Cx43 is mainly expressed in VSMC [17, 29]. Both Cx37 and Cx40 transcripts (Fig 4A and 4C) and protein (Fig 4B and 4D) levels decreased after 3 and 7 days of arterial hemodynamic exposure. In contrast, Cx43 mRNA (Fig 4E) and protein (Fig 4F) levels were both increased after 3 and 7 days.

External vein support did not prevent Cx37 mRNA (Fig 5A) and protein decrease (Fig 5B). The external mesh had a tendency to reverse Cx40 mRNA (Fig 5B) and significantly prevented Cx40 protein drop (Fig 5D). In contrast, the mesh support dampened Cx43 mRNA (Fig 5E) and protein (Fig 5F) upregulation.

Further immunofluorescent staining of connexins after 7 days of perfusion confirmed that endothelial Cx37 and 40 remained decreased in presence of the mesh, whereas Cx43 overexpression was attenuated (Fig 6).

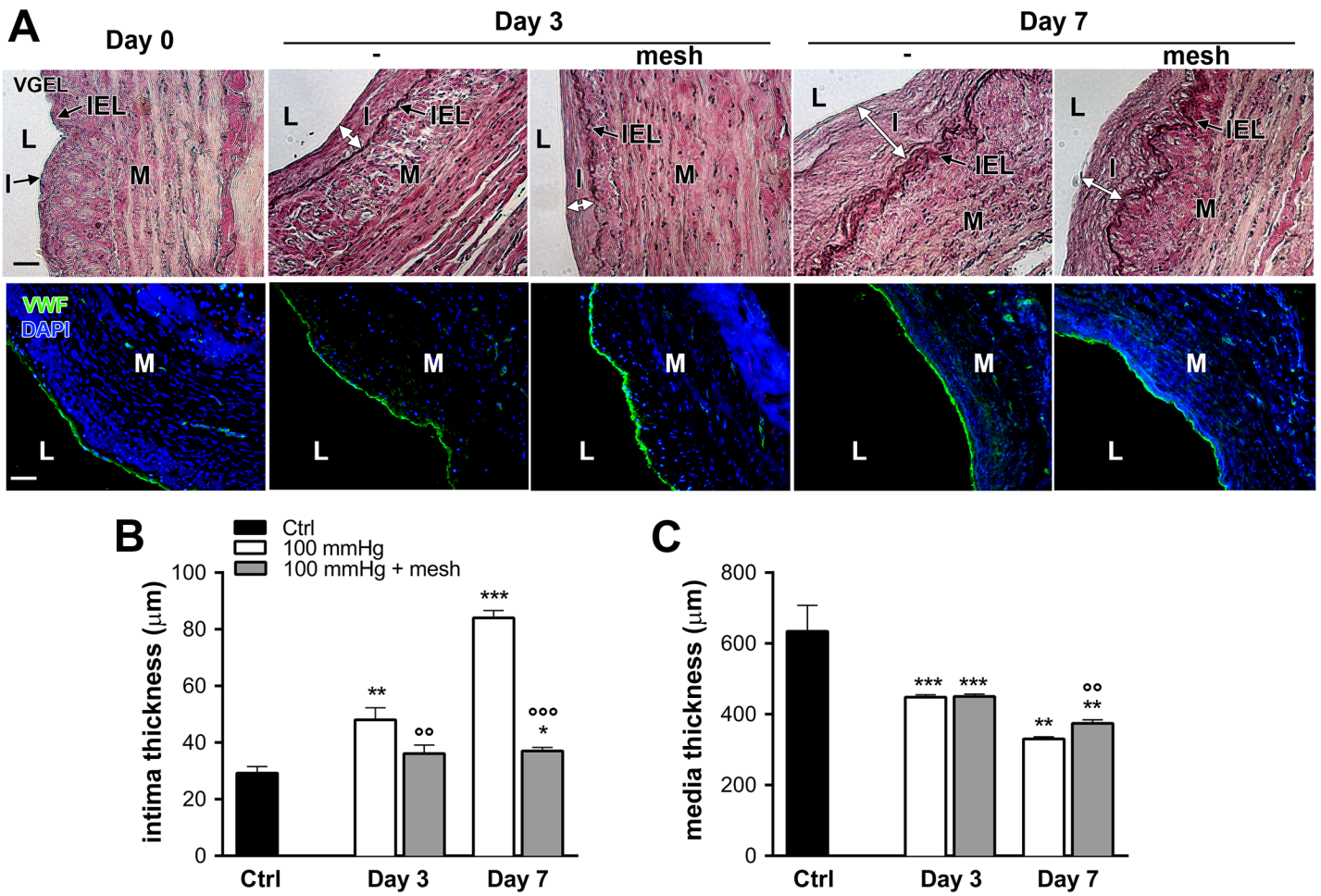

Fig 2. Intimal hyperplasia formation in *ex-vivo* human vein perfusion. Human veins were subjected to arterial pressure and flow (mean pressure = 100, high flow) for 3 and 7 days using an *ex-vivo* perfusion model. **A)** Representative Van Gieson Elastic Laminae staining (VGEL, **upper panel**) and vWf (green) and nuclei (DAPI blue) (**lower panel**) staining. I: intimal hyperplasia; L: lumen; M: media; IEL: internal elastic lamina. Bar represents 100 µm. Data are representative of 8–9 experiments. **B-C)** Morphometric measurements of human veins subjected to a 3- and 7-day pulsatile high pressure perfusion, with or without external mesh reinforcement. Data represent mean ± SEM of 4–9 experiments. *p<0.05, **p<0.01 and ***p<0.001 versus the non-perfused veins (ctrl). °°p<0.01 and °°°p<0.001 versus the unsupported vein segment.

doi:10.1371/journal.pone.0138847.g002

Cx43 controls smooth muscle cell proliferation

To determine the role of Cx43 in VSMC phenotypic switch, Cx43 was knocked-down in primary human VSMC using two distinct siRNAs, which both decreased Cx43 protein levels by 90% (Fig 7A). Loss of Cx43 (siCx43$^{1 \text{ and } 2}$) did not alter VSMC migration, as compared to VSMC transfected with a control siRNA (siCtrl) (Fig 7B and 7C). However, the absence of Cx43 reduced by 40% the number of Brdu positive cells over a 24h treatment with 10 ng/mL PDGF-BB (Fig 8A). Flow cytometry analysis of DNA content further revealed that the absence of Cx43 arrested VSMC in G0/G1 cell cycle phase (76% vs 68%) (Fig 8B). Conversely, the adenoviral-mediated overexpression of human Cx43, which resulted in a dose-dependent increase in Cx43 protein levels (Fig 9A) at the cell-cell membrane contacts (Fig 9B), increased VSMC proliferation by 30% over a period of 24 hours in presence of 10 ng/mL PDGF-BB (Fig 9C and 9D).

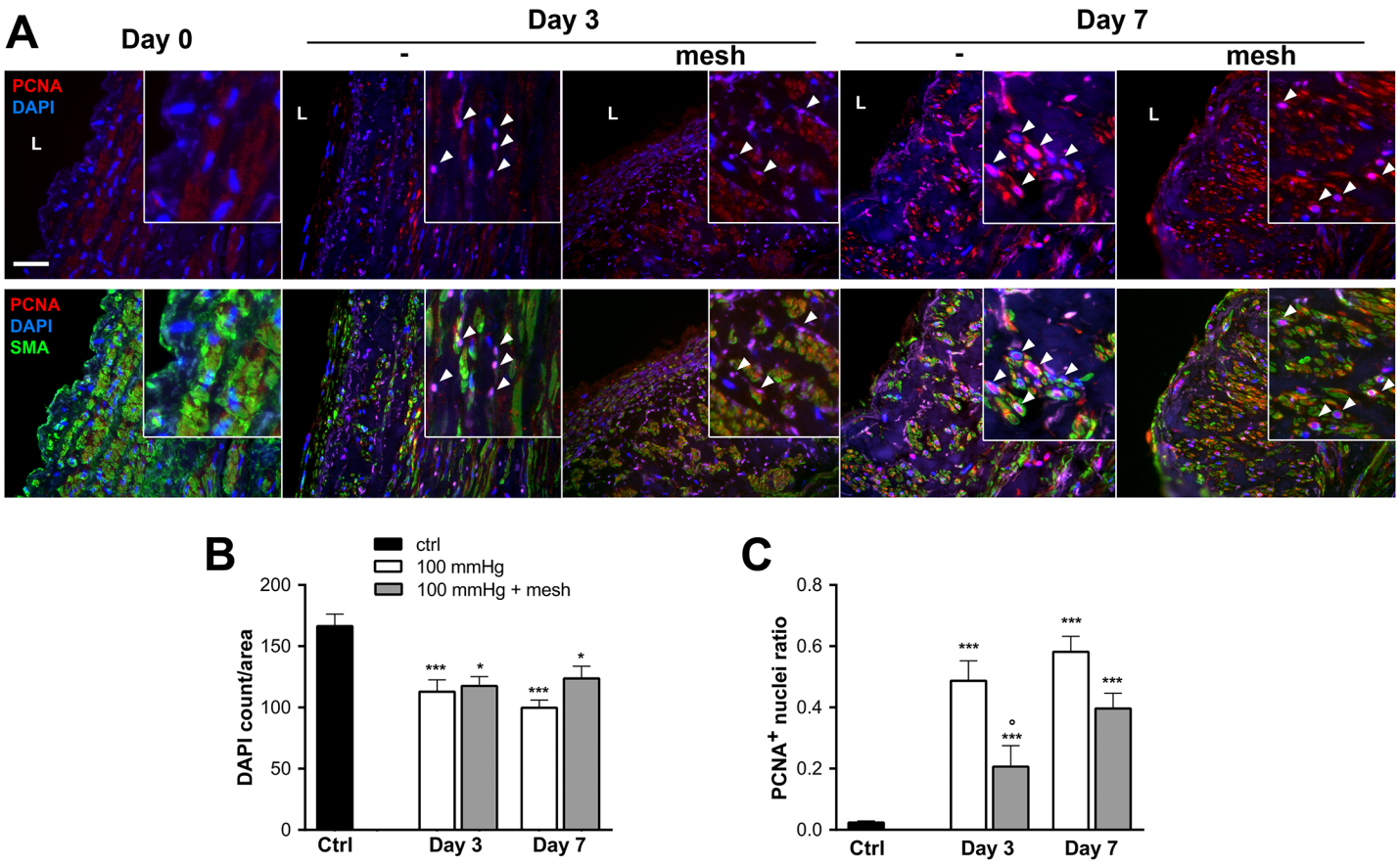

Fig 3. Growth dynamics in *ex-vivo* human vein perfusion. Human veins were subjected to arterial pressure and flow (mean pressure = 100, high flow) for 3 and 7 days using an *ex-vivo* perfusion model. **A)** Representative PCNA (red) and DAPI (blue) and smooth muscle actin (SMA; green). Arrowheads point to PCNA positive nuclei. L: lumen, Bar represents 50 μm. Data are representative of 8–9 experiments. Square insets represent a 4 fold magnification of images. Quantitative assessment of nuclei (DAPI) over section area (**B**) and PCNA positive nuclei over total DAPI positive nuclei (**C**). Data represent mean ± SEM of 4–9 experiments. *p<0.05 and ***p<0.001 versus the non-perfused veins (ctrl). °p<0.05 versus the unsupported vein segment.

doi:10.1371/journal.pone.0138847.g003

Connexins blockade prevents intimal hyperplasia

The potential vasculoprotective effect of Cx43 blockade was then tested in human saphenous vein, using the pan-Cx inhibitor carbenoxolone (100 μM) or the specific Cx43 inhibiting peptide ^{43}Gap26 (200 μM) [30, 31]. Both strategies reduced the development of IH (Fig 10) and myointimal proliferation (PCNA staining) (Fig 10) observed after 10 days of static culture, suggesting that Cx43 is the main Cx involved in VSMC proliferation and IH.

Discussion

The data here show that arterial engraftment rapidly increased rabbit Cx43 gene expression *in-vivo*. Consistently, Cx43 transcript and protein levels were upregulated in human veins exposed to arterial hemodynamics *ex-vivo*. Cx43 genetic inactivation or chemical inhibition reduced VSMC proliferation in vitro and in vivo, reducing myointimal proliferation and IH formation.

Cx43 was rapidly and consistently increased in all our experimental models, which supports findings from previous studies showing higher Cx43 levels in vascular occlusive disorders, including rabbit iliac and rat carotid restenosis models [32, 33], or atherosclerotic lesion in rabbit aorta [34, 35]. We further observed that flow, which play a key role in intimal expansion

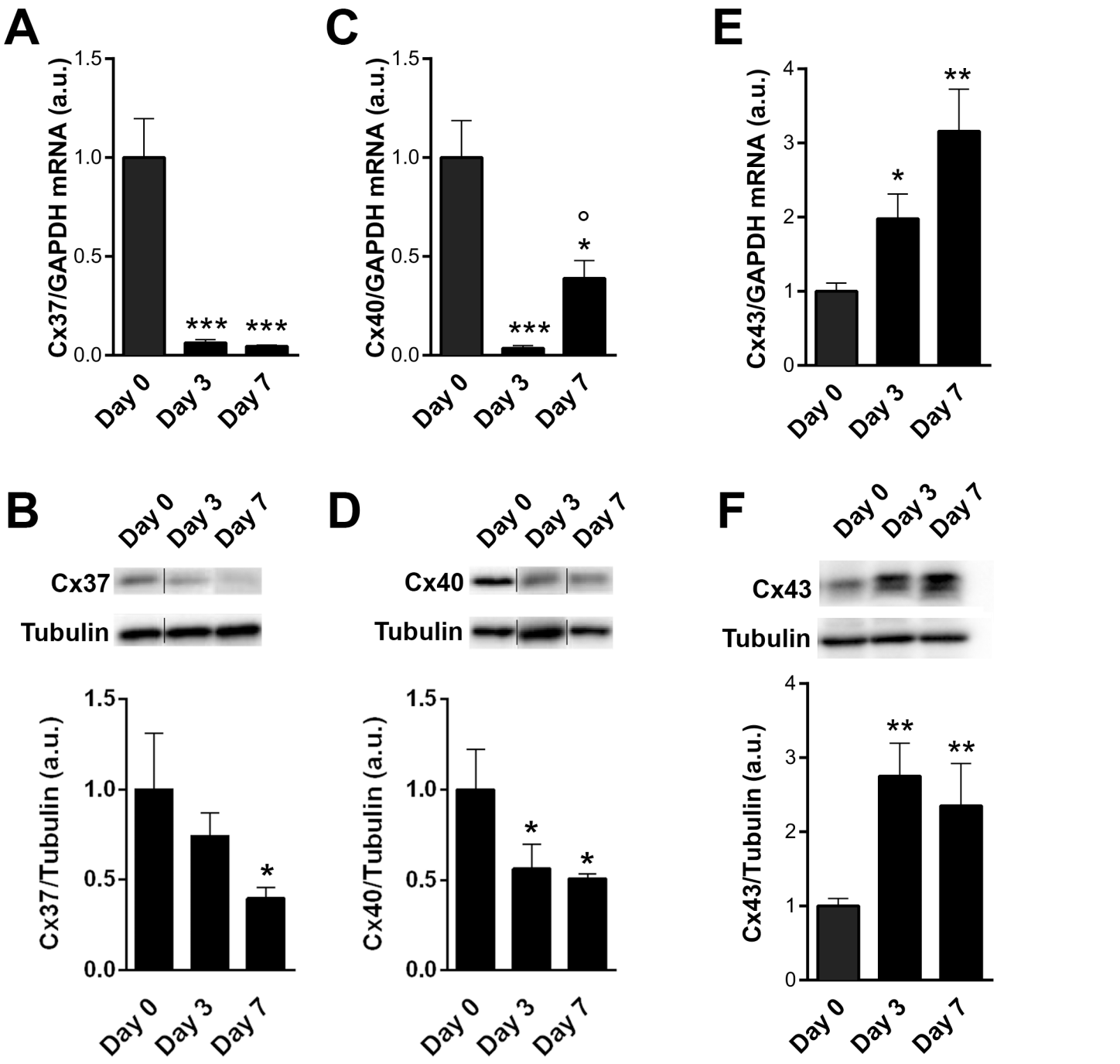

Fig 4. Expression of endothelial Cx37 and 40 are decreased, while muscular Cx43 is increased following arterial engraftment of human vein. Human veins were subjected to arterial pressure and flow for 3 and 7 days using an *ex-vivo* perfusion model. Levels of Cx37 transcript (**A**) and protein (B), Cx40 transcript (**C**) and protein (D), and Cx43 transcript (**E**) and protein (**F**). Data are mean ± SEM of 4–8 experiments. *p<0.05, **p<0.01 and ***p<0.001 versus the native segment. °p<0.05 day 3 versus day 7.

doi:10.1371/journal.pone.0138847.g004

and VSMC proliferation [12, 28], is not involved in Cx43 overexpression, in accordance with our previous findings that Cx43 expression is increased in static human vein culture [17]. The fact that Cx43 is upregulated both in vivo and ex-vivo implicate intrinsic factors in the Cx43 upregulation following vein grafting. Similarly, the contribution of bone marrow derived

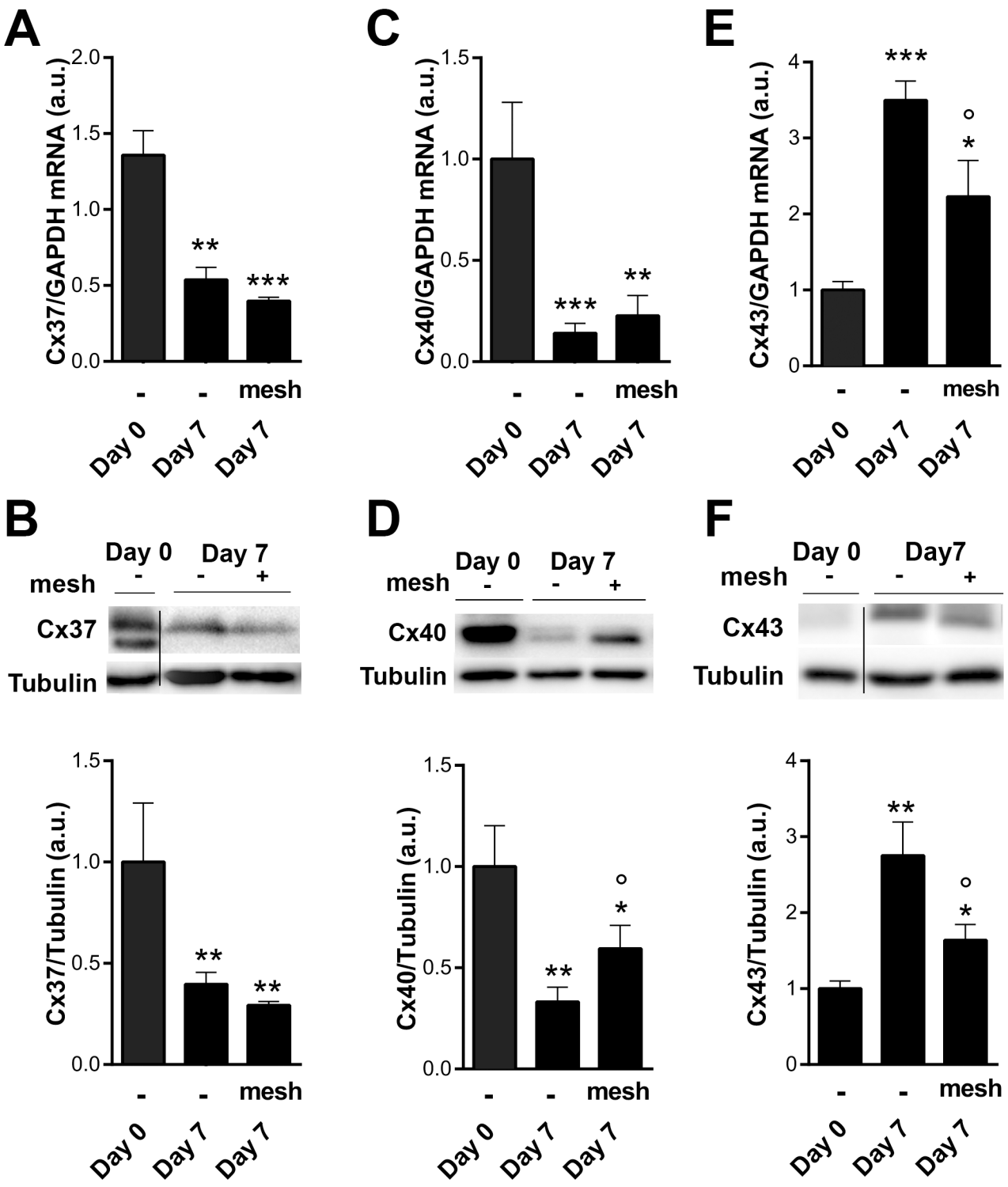

Fig 5. Cx43 overexpression following arterial engraftment is dampened by the use of an external mesh support. Human veins were subjected to arterial pressure and flow for 7 days in absence or presence of the external mesh support. Cx37 transcripts (**A**) and protein (**B**) levels remain low in presence of the mesh. Cx40 transcript (**C**) and protein (**D**) levels tend to increase in presence of the mesh. Cx43 transcript (**E**) and protein (**F**) levels are decreased by the external support. Data are mean ± SEM of 4–8 experiments. *p<0.05, **p<0.01, ***p<0.001 versus the native segment. °p<0.05 ctrl versus external mesh.

doi:10.1371/journal.pone.0138847.g005

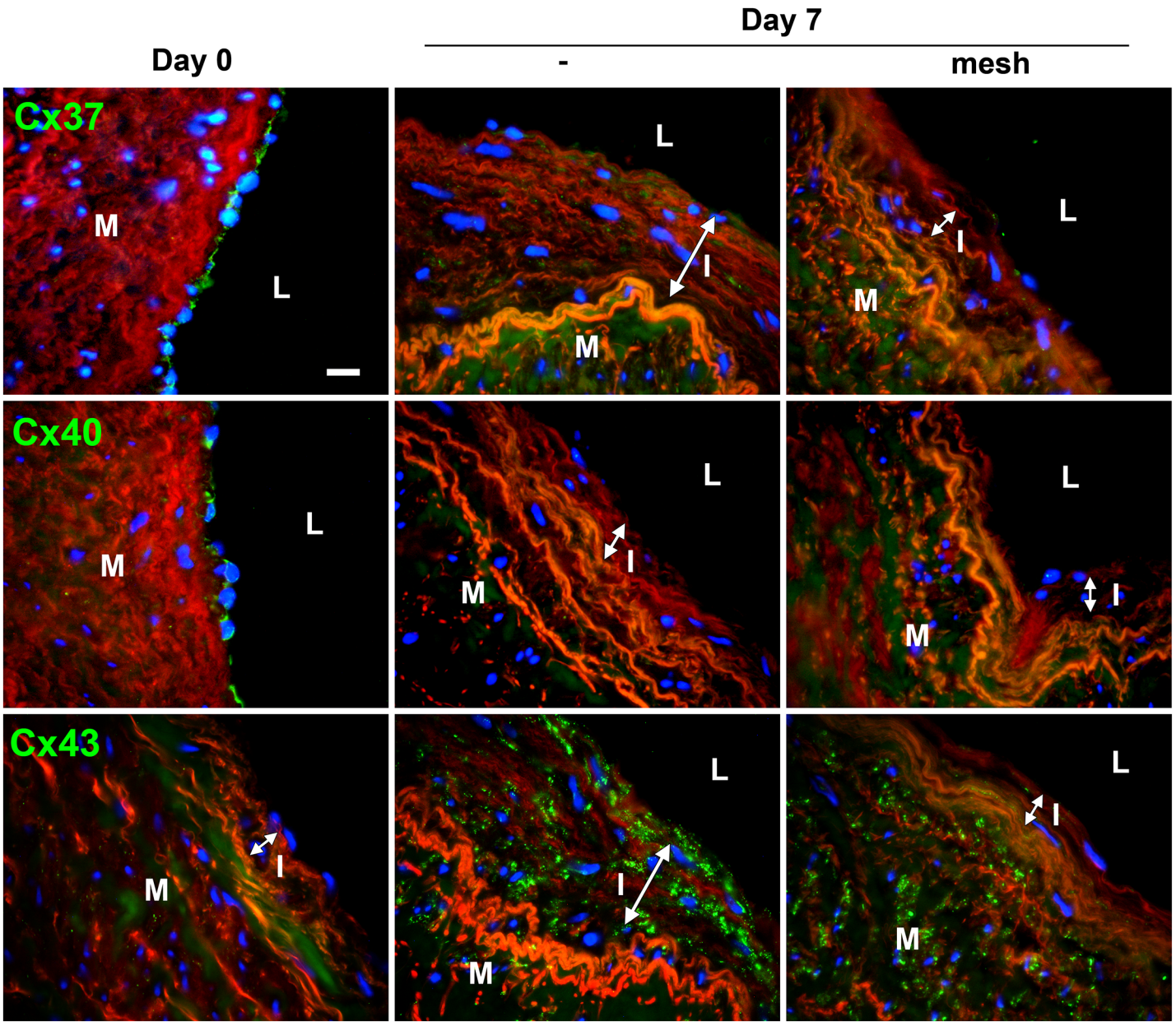

Fig 6. Expression pattern of endothelial Cx37 and 40 and muscular Cx43 following arterial engraftment of human vein. Human veins were subjected to arterial pressure and flow for 3 and 7 days using an *ex-vivo* perfusion model. Representative Cx37 (**upper panel**), Cx40 (**middle panel**) and Cx43 (**lower panel**) immunostaining after 7 days of perfusion, with or without external mesh. Connexin stainings (green) were counterstained with Evans blue staining of the elastic laminae (red). Data represent mean ± SEM of 8–9 experiments. Bar represents 50 μm. L: lumen; I: intimal hyperplasia; M: media. Data are representative of 5 experiments. Square insets represent a 3 fold magnification of images.

doi:10.1371/journal.pone.0138847.g006

progenitor cells homing to the sites of injury *in vivo* is expected to be negligible in our *ex-vivo* perfusion system.

Given the rapidity of Cx43 overexpression following rabbit grafting we propose that Cx43 is overexpressed in response to the early surgical stress, rather than flow per se. In line with this hypothesis, cFOS and cJUN, which play a key role in cell proliferation [36], cluster with the Cx43 gene GJA1 following rabbit grafting. Indeed, previous reports demonstrated that cJUN or cFOS control Cx43 promoter activity through a functional AP1 site [37, 38], hence those

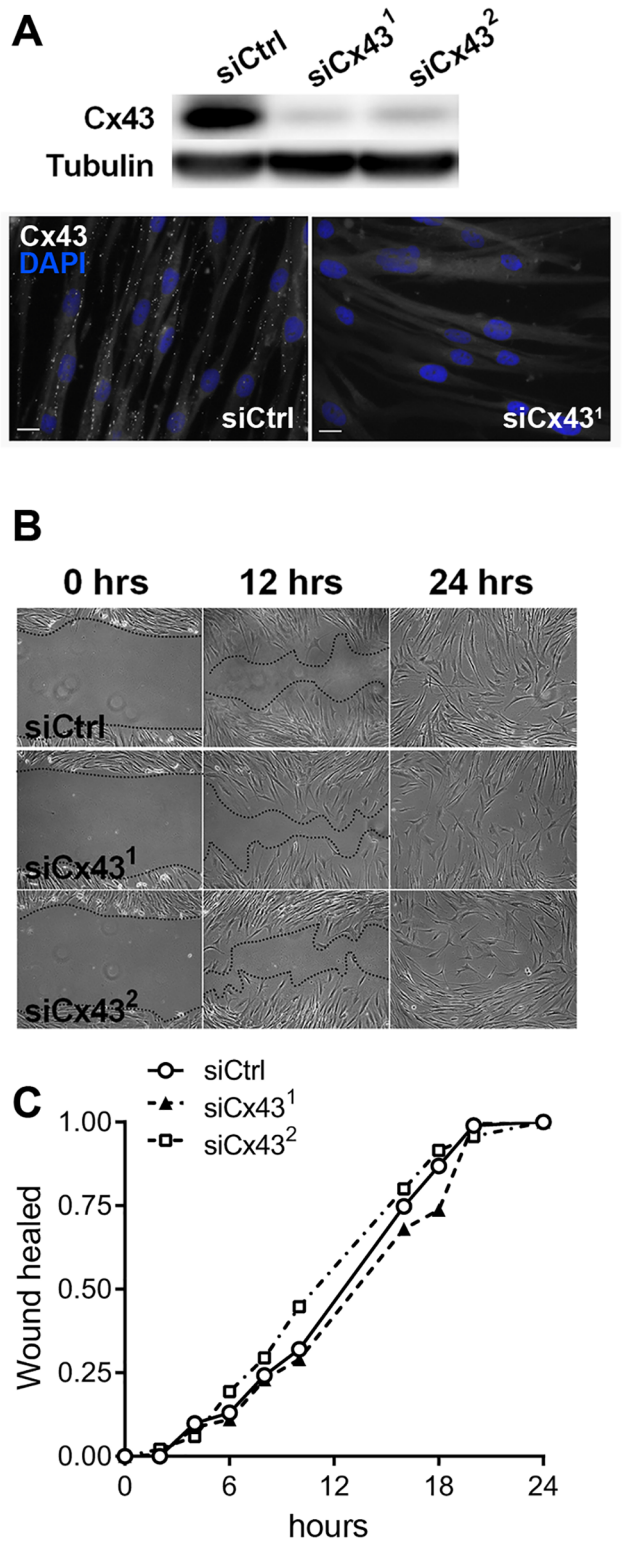

Fig 7. Cx43 knock-down reduces hVSMC proliferation. Human primary VSMC were transfected with a control siRNA (siCtrl) or Cx43 siRNAs (siCx43[1] and siCx43[2]). **A)** Representative Western blot analysis of the Cx43 over tubulin levels (**upper panel**, n = 3) and immunofluorescence staining (**lower panel**, n = 3). **B)** Human VSMC migration was assessed using scratch wound assay. Representative images of wound closure at 0, 12 and 24 hours after injury of VSMC transfected with a control siRNA (siCtrl) or two different

Cx43 siRNAs (siCx43[1] and siCx43[2]). **C)** Representative wound closure kinetic (n = 3–4) in cells transfected with the siCtrl (continuous line), siCx43[1] (dotted line) or siCx43[2] (dashed line).

doi:10.1371/journal.pone.0138847.g007

factors may control Cx43 in response to grafting. On the other hand Cx43 overexpression is partially prevented by external support, implying at least a partial regulation of Cx43 expression by hemodynamic sensitive pathways.

Although the exact mechanisms whereby arterial engraftment leads to Cx43 upregulation remain to be fully unraveled, we observed a strong correlation between the amount of IH and the levels of Cx43, suggesting a role of Cx43 in neointima formation. Conflicting data exist regarding the role of Cx43 in VSMC proliferation and IH formation [2, 5, 7]. Our study clearly supports the concept that Cx43 stimulates VSMC proliferation [2, 7]. Furthermore, both general inhibition of intercellular communication using carbenoxolone or specific blockade of Cx43-made gap junctions prevented myointimal proliferation and the development of IH in human vein grafts, suggesting that Cx43-mediated intercellular communication plays a key

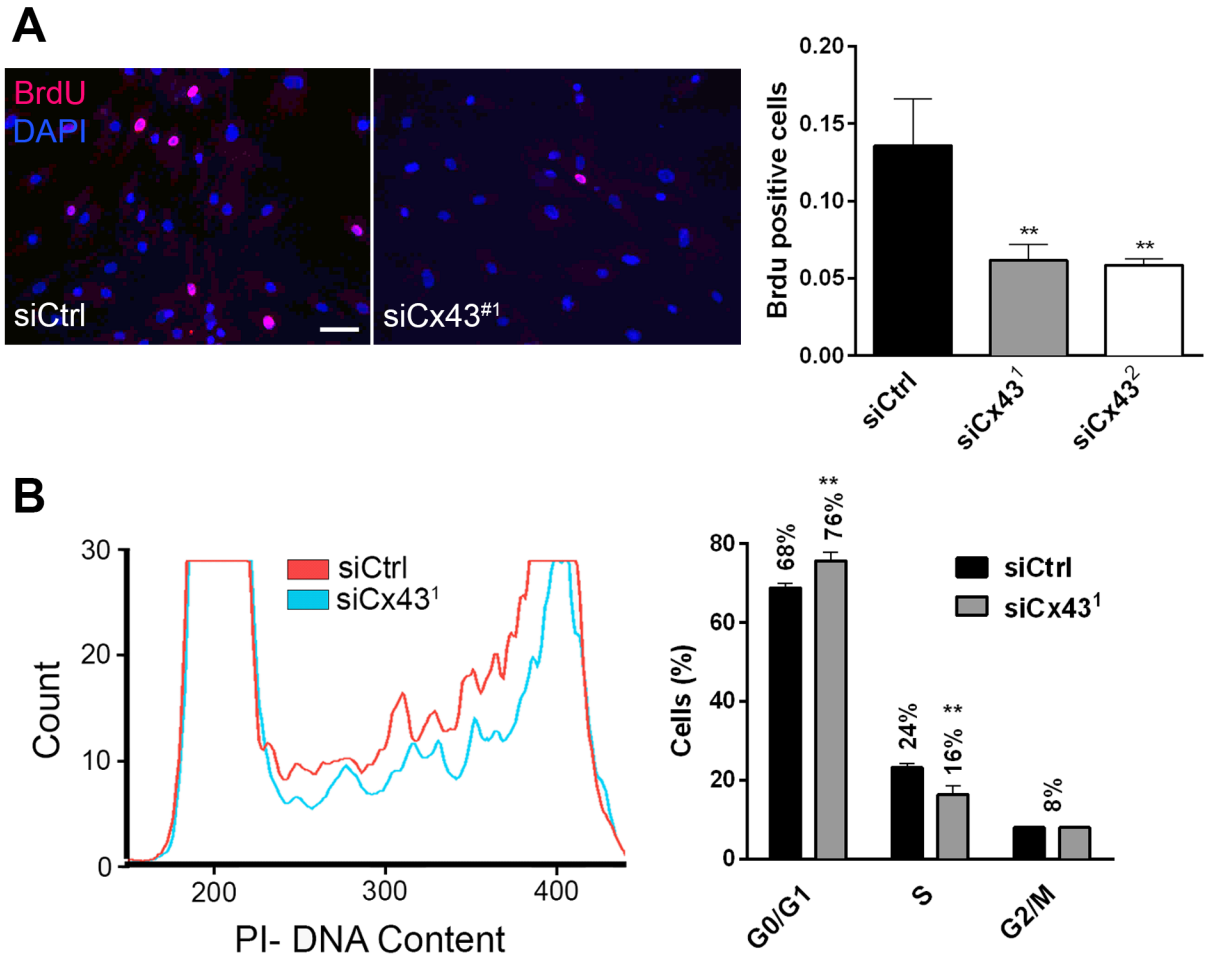

Fig 8. Cx43 knock-down does not affect human VSMC migration. Primary hVSMC were treated 24h with PDGF-BB, 48 hours after transfection with a control (siCtrl) or Cx43 (siCx43[1 or 2]) siRNAs. **A**) Representative immunofluorescence staining (left panel) and quantification of Brdu positive nuclei (right panel). Nuclei were identified with DAPI. Data represent mean ±SEM of 5 experiments. **p<0.01 versus siCtrl. Bar represents 20 μm. **B**) Representative (left panel) and quantification (right panel) of flow cytometry analysis of DNA content (propidium iodide staining). Data represent mean ±SEM of 4 experiments. **p<0.01 versus siCtrl.

doi:10.1371/journal.pone.0138847.g008

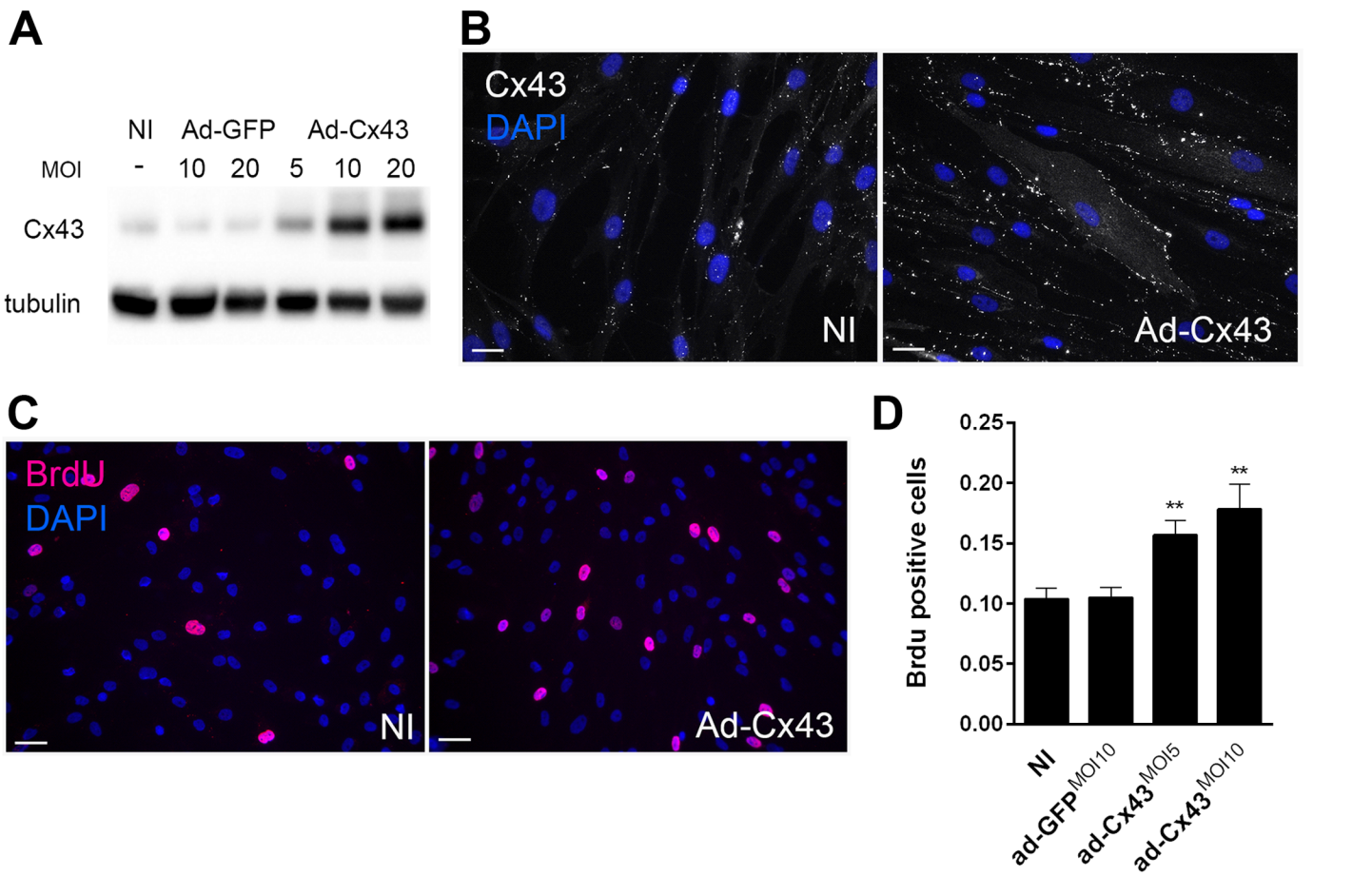

Fig 9. Cx43 overexpression promotes SMC proliferation. hVSMC were infected or not (NI) with a control adenovirus (Ad-GFP) or a human Cx43 adenovirus (Ad-Cx43) at various multiplicity of infection (MOI) as indicated. **A and B)** Representative Western blot analysis of the Cx43 over tubulin levels and Cx43 immunofluorescent staining. **C and D)** Representative immunofluorescent images and quantification of Brdu incorporation during 24h in primary hVSMC in presence of PDGF-BB. Nuclei were identified with DAPI. **B**) Bar represent 50 μm. **C**) Bar represent 25 μm. Data represent mean ±SEM of 5–6 experiments. **p<0.01 versus NI and ad-GFP.

doi:10.1371/journal.pone.0138847.g009

role in IH. The development of IH also involves VSMC migration from the media layer to the neointima region. Cx43 knock-down did not impact VSMC migration in our experimental model of wound healing, in contrast with studies showing that Cx43 participates in VSMC transmigration when stimulated with angiotensin II [7] or PDGF [2]. This discrepancy is probably due to the differences between experimental designs and wound healing assay versus transmigration assay. Studies performed in other cell types suggest an opposite role of Cx43 in cell migration [39–41], suggesting a very complex role of Cx43, which clearly depends on the model and cell type studied and warrants further pre-clinical studies before using Cx43-targeted peptides in the treatment of pathologies.

Endothelial cells (EC) are highly sensitive to hemodynamic flow and the frictional forces between blood and the endothelium [42]. Notably, the production of nitric oxide (NO) by EC is a key factor in maintaining quiescent and contractile VSMC [43]. Our data indicate that exposure to arterial hemodynamic rapidly decreases the expression of the major endothelial connexins Cx37 and Cx40, both *in-vivo* and *ex-vivo*. Cx40 [24, 25] and Cx37 [44] are required for proper eNOS expression and function. In line with these data, we previously demonstrated that the expression of the endothelial NO synthase (eNOS) is strongly reduced upon arterial

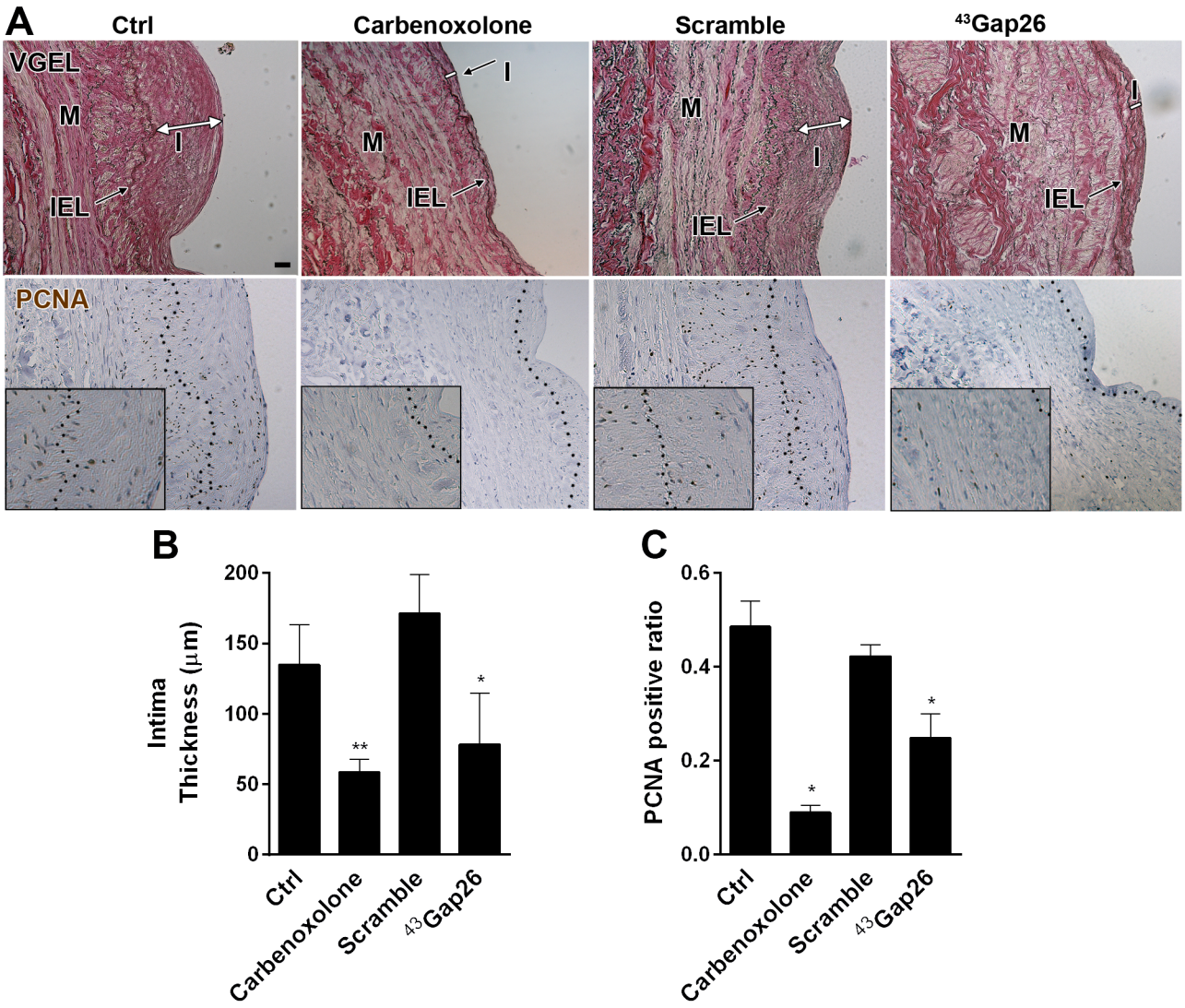

Fig 10. Inhibition of Cx43-mediated intercellular communication alleviates the development of intimal hyperplasia in human veins. 5 mm segments of opened vein were kept in static culture for 10 days in presence or not (**ctrl**), of 200 μM carbenoxolone or 200 μM ^{43}Gap26 peptide or a respective scramble peptide. **A)** Representative VGEL (**upper panel**), and PCNA (**lower panel**) stained sections showed decreased intimal thickness and cell proliferation in presence of the Cx43 inhibitors. I = intima; M = media; IEL: internal elastic lamina. Bar represents 100 μm. Square insets in PCNA staining represent a 3 fold magnification of images. **B and C)** Quantitative assessment of intima thickness (**B**) and PCNA positive area (**C**). Data represent mean ± SEM of 3–4 experiments. *p<0.05, versus ctrl.

doi:10.1371/journal.pone.0138847.g010

implantation in the EVPS [16]. Thus, despite continuous endothelial coverage as demonstrated by vWf immunostaining, it is likely that the vein graft endothelium is not fully functional when placed in an arterial environment, as suggested by a previous report [45]. In line with this hypothesis, a polymorphism in the Cx37 gene [46], as well as the loss of Cx37 (Cx37-/- mice) [47] increase the risk of atherosclerosis, which share molecular events with IH, including endothelial dysfunction and VSMC proliferation. Unfortunately external reinforcement using the mesh barely improved the expression of these endothelial markers. The combined loss of eNOS, endothelial Cx37 and Cx40, as well as other key endothelial genes likely precludes proper NO production and facilitates IH development. External meshing did not restore the expression of EC connexins Cx37 and 40. In sharp contrast, Cx43 levels, SMCs proliferation

and neointima formation were all severely blunted by the external scaffold, which we believe is a viable approach to reduce vein graft failure.

This study highlights Cx43 as an early molecular marker of IH and demonstrates that the development of pathological IH in human vein grafts requires Cx43. Further studies are required to identify the signals passing through gap junctions mediating the increased VSMC proliferation and we cannot exclude that hemi-channels also play a role in this process. Cx43 is mostly expressed by VSMC. Thus, the development of Cx43-targeted pharmacological tools provides an opportunity to manipulate VSMC proliferation while sparing EC connexins. Especially, topical delivery of mimetic peptides blocking Cx43 might provide an exciting strategy in the prevention of IH.

Supporting Information

S1 Fig. The analysis of 57 probe sets demonstrates changes in expression over time after rabbit vein graft.
(TIF)

S1 Table. List of Primer sequences.
(DOCX)

Acknowledgments

We thank Xavier Berard and for their contribution to the design and execution of this project. We thank Martine Lambelet, Danny Labes, Janine Horlbeck and Jean-Christophe Stehle for their excellent technical assistance.

Author Contributions

Conceived and designed the experiments: AL F. Allagnat F. Alonso J-AH SD C-KO J-MC SB. Performed the experiments: AL F. Allagnat F. Alonso CK CD. Analyzed the data: AL F. Allagnat F. Alonso CK J-AH SD SB CD. Contributed reagents/materials/analysis tools: C-KO CK J-AH SD SB J-MC JM. Wrote the paper: AL F. Allagnat J-AH SD C-KO J-MC JM.

References

1. Mozaffarian D, Benjamin EJ, Go AS, Arnett DK, Blaha MJ, Cushman M, et al. Heart disease and stroke statistics—2015 update: a report from the American Heart Association. Circulation. 2015; 131(4):e29–322. doi: 10.1161/CIR.0000000000000152 PMID: 25520374.
2. Chadjichristos CE, Matter CM, Roth I, Sutter E, Pelli G, Luscher TF, et al. Reduced connexin43 expression limits neointima formation after balloon distension injury in hypercholesterolemic mice. Circulation. 2006; 113(24):2835–43. doi: 10.1161/CIRCULATIONAHA.106.627703 PMID: 16769907.
3. Straub AC, Billaud M, Johnstone SR, Best AK, Yemen S, Dwyer ST, et al. Compartmentalized connexin 43 s-nitrosylation/denitrosylation regulates heterocellular communication in the vessel wall. Arteriosclerosis, thrombosis, and vascular biology. 2011; 31(2):399–407. doi: 10.1161/ATVBAHA.110.215939 PMID: 21071693; PubMed Central PMCID: PMC3056333.
4. Jia G, Mitra AK, Cheng G, Gangahar DM, Agrawal DK. Angiotensin II and IGF-1 regulate connexin43 expression via ERK and p38 signaling pathways in vascular smooth muscle cells of coronary artery bypass conduits. The Journal of surgical research. 2007; 142(1):137–42. doi: 10.1016/j.jss.2006.11.007 PMID: 17624368.
5. Liao Y, Regan CP, Manabe I, Owens GK, Day KH, Damon DN, et al. Smooth muscle-targeted knockout of connexin43 enhances neointimal formation in response to vascular injury. Arteriosclerosis, thrombosis, and vascular biology. 2007; 27(5):1037–42. doi: 10.1161/ATVBAHA.106.137182 PMID: 17332489.
6. Johnstone SR, Kroncke BM, Straub AC, Best AK, Dunn CA, Mitchell LA, et al. MAPK phosphorylation of connexin 43 promotes binding of cyclin E and smooth muscle cell proliferation. Circulation research. 2012; 111(2):201–11. doi: 10.1161/CIRCRESAHA.112.272302 PMID: 22652908; PubMed Central PMCID: PMC3405546.

7. Jia G, Cheng G, Gangahar DM, Agrawal DK. Involvement of connexin 43 in angiotensin II-induced migration and proliferation of saphenous vein smooth muscle cells via the MAPK-AP-1 signaling pathway. Journal of molecular and cellular cardiology. 2008; 44(5):882–90. doi: 10.1016/j.yjmcc.2008.03.002 PMID: 18405916; PubMed Central PMCID: PMC2765202.
8. Meens MJ, Pfenniger A, Kwak BR, Delmar M. Regulation of cardiovascular connexins by mechanical forces and junctions. Cardiovascular research. 2013; 99(2):304–14. doi: 10.1093/cvr/cvt095 PMID: 23612582; PubMed Central PMCID: PMC3695747.
9. Brisset AC, Isakson BE, Kwak BR. Connexins in vascular physiology and pathology. Antioxidants & redox signaling. 2009; 11(2):267–82. doi: 10.1089/ars.2008.2115 PMID: 18834327; PubMed Central PMCID: PMC2819334.
10. Haefliger JA, Nicod P, Meda P. Contribution of connexins to the function of the vascular wall. Cardiovascular research. 2004; 62(2):345–56. doi: 10.1016/j.cardiores.2003.11.015 PMID: 15094354.
11. Jiang Z, Wu L, Miller BL, Goldman DR, Fernandez CM, Abouhamze ZS, et al. A novel vein graft model: adaptation to differential flow environments. American journal of physiology Heart and circulatory physiology. 2004; 286(1):H240–5. doi: 10.1152/ajpheart.00760.2003 PMID: 14500133.
12. DeSart KM, Butler K, O'Malley KA, Jiang Z, Berceli SA. Time and flow-dependent changes in the p27 gene network drive maladaptive vascular remodeling. Journal of vascular surgery. 2014. doi: 10.1016/j.jvs.2014.05.015 PMID: 24953896.
13. Longchamp A, Allagnat F, Berard X, Alonso F, Haefliger JA, Deglise S, et al. Procedure for human saphenous veins ex vivo perfusion and external reinforcement. Journal of visualized experiments: JoVE. 2014;(92:). doi: 10.3791/52079 PMID: 25350681.
14. Berard X, Deglise S, Alonso F, Saucy F, Meda P, Bordenave L, et al. Role of hemodynamic forces in the ex vivo arterialization of human saphenous veins. Journal of vascular surgery. 2013; 57(5):1371–82. doi: 10.1016/j.jvs.2012.09.041 PMID: 23351647.
15. Mack CP. Signaling mechanisms that regulate smooth muscle cell differentiation. Arteriosclerosis, thrombosis, and vascular biology. 2011; 31(7):1495–505. doi: 10.1161/ATVBAHA.110.221135 PMID: 21677292; PubMed Central PMCID: PMC3141215.
16. Longchamp A, Alonso F, Dubuis C, Allagnat F, Berard X, Meda P, et al. The use of external mesh reinforcement to reduce intimal hyperplasia and preserve the structure of human saphenous veins. Biomaterials. 2014; 35(9):2588–99. doi: 10.1016/j.biomaterials.2013.12.041 PMID: 24429385.
17. Deglise S, Martin D, Probst H, Saucy F, Hayoz D, Waeber G, et al. Increased connexin43 expression in human saphenous veins in culture is associated with intimal hyperplasia. Journal of vascular surgery. 2005; 41(6):1043–52. doi: 10.1016/j.jvs.2005.02.036 PMID: 15944608.
18. Corpataux JM, Naik J, Porter KE, London NJ. The effect of six different statins on the proliferation, migration, and invasion of human smooth muscle cells. The Journal of surgical research. 2005; 129 (1):52–6. doi: 10.1016/j.jss.2005.05.016 PMID: 16087194.
19. Corpataux JM, Naik J, Porter KE, London NJ. A comparison of six statins on the development of intimal hyperplasia in a human vein culture model. European journal of vascular and endovascular surgery: the official journal of the European Society for Vascular Surgery. 2005; 29(2):177–81. doi: 10.1016/j.ejvs.2004.11.003 PMID: 15649726.
20. Dubuis C, May L, Alonso F, Luca L, Mylonaki I, Meda P, et al. Atorvastatin-loaded hydrogel affects the smooth muscle cells of human veins. The Journal of pharmacology and experimental therapeutics. 2013; 347(3):574–81. doi: 10.1124/jpet.113.208769 PMID: 24071735.
21. Martin D, Allagnat F, Gesina E, Caille D, Gjinovci A, Waeber G, et al. Specific silencing of the REST target genes in insulin-secreting cells uncovers their participation in beta cell survival. PloS one. 2012; 7 (9):e45844. doi: 10.1371/journal.pone.0045844 PMID: 23029270; PubMed Central PMCID: PMC3447792.
22. Martin D, Allagnat F, Chaffard G, Caille D, Fukuda M, Regazzi R, et al. Functional significance of repressor element 1 silencing transcription factor (REST) target genes in pancreatic beta cells. Diabetologia. 2008; 51(8):1429–39. doi: 10.1007/s00125-008-0984-1 PMID: 18385973.
23. Alonso F, Krattinger N, Mazzolai L, Simon A, Waeber G, Meda P, et al. An angiotensin II- and NF-kappaB-dependent mechanism increases connexin 43 in murine arteries targeted by renin-dependent hypertension. Cardiovascular research. 2010; 87(1):166–76. doi: 10.1093/cvr/cvq031 PMID: 20110337; PubMed Central PMCID: PMC2883896.
24. Alonso F, Boittin FX, Beny JL, Haefliger JA. Loss of connexin40 is associated with decreased endothelium-dependent relaxations and eNOS levels in the mouse aorta. American journal of physiology Heart and circulatory physiology. 2010; 299(5):H1365–73. doi: 10.1152/ajpheart.00029.2010 PMID: 20802140.

25. Le Gal L, Alonso F, Wagner C, Germain S, Nardelli Haefliger D, Meda P, et al. Restoration of connexin 40 (cx40) in Renin-producing cells reduces the hypertension of cx40 null mice. Hypertension. 2014; 63 (6):1198–204. doi: 10.1161/HYPERTENSIONAHA.113.02976 PMID: 24614215.

26. Allagnat F, Cunha D, Moore F, Vanderwinden JM, Eizirik DL, Cardozo AK. Mcl-1 downregulation by pro-inflammatory cytokines and palmitate is an early event contributing to beta-cell apoptosis. Cell death and differentiation. 2011; 18(2):328–37. doi: 10.1038/cdd.2010.105 PMID: 20798690; PubMed Central PMCID: PMC3131897.

27. Darzynkiewicz Z, Huang X. Analysis of cellular DNA content by flow cytometry. Current protocols in immunology / edited by John E Coligan [et al]. 2004;Chapter 5:Unit 5 7. doi: 10.1002/0471142735.im0507s60 PMID: 18432930.

28. Fernandez CM, Goldman DR, Jiang Z, Ozaki CK, Tran-Son-Tay R, Berceli SA. Impact of shear stress on early vein graft remodeling: a biomechanical analysis. Annals of biomedical engineering. 2004; 32 (11):1484–93. PMID: 15636109.

29. Pfenniger A, Wong C, Sutter E, Cuhlmann S, Dunoyer-Geindre S, Mach F, et al. Shear stress modulates the expression of the atheroprotective protein Cx37 in endothelial cells. Journal of molecular and cellular cardiology. 2012; 53(2):299–309. doi: 10.1016/j.yjmcc.2012.05.011 PMID: 22659288.

30. Chaytor AT, Evans WH, Griffith TM. Peptides homologous to extracellular loop motifs of connexin 43 reversibly abolish rhythmic contractile activity in rabbit arteries. The Journal of physiology. 1997; 503 (Pt 1):99–110. PMID: 9288678; PubMed Central PMCID: PMC1159890.

31. Halidi N, Alonso F, Burt JM, Beny JL, Haefliger JA, Meister JJ. Intercellular calcium waves in primary cultured rat mesenteric smooth muscle cells are mediated by connexin43. Cell communication & adhesion. 2012; 19(2):25–37. doi: 10.3109/15419061.2012.690792 PMID: 22642233; PubMed Central PMCID: PMC3804248.

32. Polacek D, Bech F, McKinsey JF, Davies PF. Connexin43 gene expression in the rabbit arterial wall: effects of hypercholesterolemia, balloon injury and their combination. Journal of vascular research. 1997; 34(1):19–30. PMID: 9075822.

33. Yeh HI, Lupu F, Dupont E, Severs NJ. Upregulation of connexin43 gap junctions between smooth muscle cells after balloon catheter injury in the rat carotid artery. Arteriosclerosis, thrombosis, and vascular biology. 1997; 17(11):3174–84. PMID: 9409308.

34. Plenz G, Ko YS, Yeh HI, Eschert H, Sindermann JR, Dorszewski A, et al. Upregulation of connexin43 gap junctions between neointimal smooth muscle cells. European journal of cell biology. 2004; 83 (10):521–30. doi: 10.1078/0171-9335-00417 PMID: 15679098.

35. Wang LH, Chen JZ, Sun YL, Zhang FR, Zhu JH, Hu SJ, et al. Statins reduce connexin40 and connexin43 expression in atherosclerotic aorta of rabbits. International journal of cardiology. 2005; 100 (3):467–75. doi: 10.1016/j.ijcard.2004.12.005 PMID: 15837092.

36. Holt J. Fos and Jun: inducible transcription factors regulating growth of normal and transformed cells. Cancer treatment and research. 1992; 63:301–11. PMID: 1363363.

37. Geimonen E, Boylston E, Royek A, Andersen J. Elevated connexin-43 expression in term human myometrium correlates with elevated c-Jun expression and is independent of myometrial estrogen receptors. The Journal of clinical endocrinology and metabolism. 1998; 83(4):1177–85. doi: 10.1210/jcem.83.4.4695 PMID: 9543137.

38. Mitchell JA, Lye SJ. Regulation of connexin43 expression by c-fos and c-jun in myometrial cells. Cell communication & adhesion. 2001; 8(4–6):299–302. PMID: 12064606.

39. Mendoza-Naranjo A, Cormie P, Serrano AE, Hu R, O'Neill S, Wang CM, et al. Targeting Cx43 and N-cadherin, which are abnormally upregulated in venous leg ulcers, influences migration, adhesion and activation of Rho GTPases. PloS one. 2012; 7(5):e37374. doi: 10.1371/journal.pone.0037374 PMID: 22615994; PubMed Central PMCID: PMC3352877.

40. Behrens J, Kameritsch P, Wallner S, Pohl U, Pogoda K. The carboxyl tail of Cx43 augments p38 mediated cell migration in a gap junction-independent manner. European journal of cell biology. 2010; 89 (11):828–38. doi: 10.1016/j.ejcb.2010.06.003 PMID: 20727616.

41. Chen CH, Mayo JN, Gourdie RG, Johnstone SR, Isakson BE, Bearden SE. The Connexin 43/ZO-1 Complex Regulates Cerebral Endothelial F-actin Architecture and Migration. American journal of physiology Cell physiology. 2015. doi: 10.1152/ajpcell.00155.2015 PMID: 26289751.

42. Davies PF. Hemodynamic shear stress and the endothelium in cardiovascular pathophysiology. Nature clinical practice Cardiovascular medicine. 2009; 6(1):16–26. doi: 10.1038/ncpcardio1397 PMID: 19029993; PubMed Central PMCID: PMC2851404.

43. Ataya B, Tzeng E, Zuckerbraun BS. Nitrite-generated nitric oxide to protect against intimal hyperplasia formation. Trends in cardiovascular medicine. 2011; 21(6):157–62. doi: 10.1016/j.tcm.2012.05.002 PMID: 22814422.

44. Pfenniger A, Derouette JP, Verma V, Lin X, Foglia B, Coombs W, et al. Gap junction protein Cx37 interacts with endothelial nitric oxide synthase in endothelial cells. Arteriosclerosis, thrombosis, and vascular biology. 2010; 30(4):827–34. doi: 10.1161/ATVBAHA.109.200816 PMID: 20081116; PubMed Central PMCID: PMC2930827.

45. Osgood MJ, Hocking KM, Voskresensky IV, Li FD, Komalavilas P, Cheung-Flynn J, et al. Surgical vein graft preparation promotes cellular dysfunction, oxidative stress, and intimal hyperplasia in human saphenous vein. Journal of vascular surgery. 2014; 60(1):202–11. doi: 10.1016/j.jvs.2013.06.004 PMID: 23911244; PubMed Central PMCID: PMC3926896.

46. Pitha J, Hubacek JA, Cifkova R, Skodova Z, Stavek P, Lanska V, et al. The association between subclinical atherosclerosis in carotid arteries and Connexin 37 gene polymorphism (1019C>T; Pro319Ser) in women. International angiology: a journal of the International Union of Angiology. 2011; 30(3):221–6. PMID: 21617605.

47. Wong CW, Christen T, Roth I, Chadjichristos CE, Derouette JP, Foglia BF, et al. Connexin37 protects against atherosclerosis by regulating monocyte adhesion. Nature medicine. 2006; 12(8):950–4. doi: 10.1038/nm1441 PMID: 16862155.

Preoperative dietary restriction reduces intimal hyperplasia and protects from ischemia-reperfusion injury

Christine R. Mauro, MD,[a] Ming Tao, MD,[a] Peng Yu, MD, PhD,[a]
J. Humberto Treviño-Villerreal, MD, PhD,[b] Alban Longchamp,[a] Bruce S. Kristal, PhD,[c]
C. Keith Ozaki, MD,[a] and James R. Mitchell, PhD,[b] *Boston, Mass*

Objective: **Whereas chronic overnutrition is a risk factor for surgical complications, long-term dietary restriction (reduced food intake without malnutrition) protects in preclinical models of surgical stress. Building on the emerging concept that acute preoperative dietary perturbations can affect the body's response to surgical stress, we hypothesized that short-term high-fat diet (HFD) feeding before surgery is detrimental, whereas short-term nutrient/energy restriction before surgery can reverse negative outcomes. We tested this hypothesis in two distinct murine models of vascular surgical injury, ischemia-reperfusion (IR) and intimal hyperplasia (IH).**

Methods: **Short-term overnutrition was achieved by feeding mice a HFD consisting of 60% calories from fat for 2 weeks. Short-term dietary restriction consisted of either 1 week of restricted access to a protein-free diet (protein/energy restriction) or 3 days of water-only fasting immediately before surgery; after surgery, all mice were given ad libitum access to a complete diet. To assess the impact of preoperative nutrition on surgical outcome, mice were challenged in one of two fundamentally distinct surgical injury models: IR injury to either kidney or liver, or a carotid focal stenosis model of IH.**

Results: **Three days of fasting or 1 week of preoperative protein/energy restriction attenuated IH development measured 28 days after focal carotid stenosis. One week of preoperative protein/energy restriction also reduced plasma urea, creatinine, and damage to the corticomedullary junction after renal IR and decreased aspartate transaminase, alanine transaminase, and hemorrhagic necrosis after hepatic IR. However, exposure to a HFD for 2 weeks before surgery had no significant impact on kidney or hepatic function after IR or IH after focal carotid stenosis.**

Conclusions: **Short-term dietary restriction immediately before surgery significantly attenuated the vascular wall hyperplastic response and improved IR outcome. The findings suggest plasticity in the body's response to these vascular surgical injuries that can be manipulated by novel yet practical preoperative dietary interventions. (J Vasc Surg 2016;63:500-9.)**

Clinical Relevance: **In view of the high clinical complication rates in the setting of cardiovascular reconstructions (and their pathophysiologic links to ischemia-reperfusion and intimal hyperplasia), short-term dietary restriction stands as a particularly attractive, pleiotropic strategy for this population to enhance patient outcomes. Whereas employment of rodent models will be useful in refining our understanding of the nutritional basis of protection and underlying molecular mechanisms, inevitably multicenter randomized clinical trials will be required to determine efficacy of such approaches in humans.**

Contemporary surgical treatments for occlusive arterial disease include endarterectomies and bypasses. These interventions carry high risk of complications during the periprocedural period, including ischemia-reperfusion (IR) injury. Furthermore, surgical treatments for occlusive arterial disease suffer from high failure rates in the longer term because of reocclusive vascular wall adaptations largely from cell proliferation-driven intimal hyperplasia (IH).[1] Although IR and IH occur on different time scales with respect to the surgical procedure and by different molecular mechanisms, they collectively lead to considerable morbidity and mortality, with mitigation strategies currently largely lacking for both.

Chronic overnutrition on calorie-dense foods and dietary restriction without malnutrition (DR, otherwise known as calorie restriction) have opposite effects on risk for cardiovascular disease and obesity-associated metabolic dysfunction.[2] Overnutrition is an accepted risk factor for cardiovascular disease as well as for surgical complications.[3] DR is best known for extending longevity and reducing age-associated morbidity in multiple species,[4,5] but it also mitigates IR to heart and brain in animal models.[6-8] The wide-ranging benefits of DR in experimental organisms have led to prospective clinical trials to evaluate potential benefits in humans, including the recently completed

From the Department of Surgery[a] and Department of Neurosurgery,[c] Brigham and Women's Hospital/Harvard Medical School; and the Department of Genetics and Complex Diseases, Harvard School of Public Health.[b]

This work was supported by grants from the National Institutes of Health (NIDDK DK090629, NIA AG036712) to J.R.M., National Institutes of Health (National Heart, Lung, and Blood Institute T32HL007734, 1F32HL117521) to C.R.M., the American Heart Association (12GRNT9510001, 12GRNT1207025) and the Lea Carpenter DuPont Vascular Surgery Fund to C.K.O., and National Institutes of Health (R01-AG25872) to B.S.K.

Author conflict of interest: J.R.M. has consulted for L-Nutra, a company that develops medical food to fight diseases, including cancer.

Additional material for this article may be found online at www.jvascsurg.org.

Correspondence: James R. Mitchell, PhD, 655 Huntington Ave 2-121, Boston, MA 02115 (e-mail: jmitchel@hsph.harvard.edu).

The editors and reviewers of this article have no relevant financial relationships to disclose per the JVS policy that requires reviewers to decline review of any manuscript for which they may have a conflict of interest.

0741-5214

http://dx.doi.org/10.1016/j.jvs.2014.07.004

Comprehensive Assessment of Long-term Effects of Reducing Intake of Energy (CALERIE) trial.[9] This phase 2 study used intensive dietary and behavioral interventions in a highly motivated nonobese population to seek 25% restriction for 2 years as measured by doubly labeled water technique. However, sustained adherence to such regimens in the general population is poor, probably because of a combination of behavioral, physiologic, psychological, and environmental (such as food availability) factors.[10]

Recently, we and others have shown that benefits of DR against surgical stress accrue rapidly—within days to weeks—in rodents and humans.[11-19] These studies demonstrate plasticity in the mammalian response to surgical stress with beneficial outcomes readily achievable by brief preoperative dietary manipulations. However, it is not currently known if such benefits extend to other models of vascular injury, such as IH. Similarly, whereas long-term overnutrition is a demonstrated risk factor for surgery, it not known how long it takes for the detrimental effects of high-fat diet (HFD) feeding on surgical outcome to occur.

Here, to provide insight into the overall plasticity of the mammalian response to acute changes in nutrition on resistance to surgical stress, we tested the effects of 2 weeks of overnutrition with or without brief periods of preoperative DR on the response to two common forms of vascular surgical trauma, IH and IR.

METHODS

Mice. Male F1 hybrids derived from C57BL/6 and DBA2 strains purchased at the age of 6 weeks (Jackson Laboratories, Bar Harbor, Me) and previously shown to respond beneficially to protein restriction[19] were used in both IR and IH models; C57BL6/J mice previously shown to respond beneficially to fasting[17] and detrimentally to long-term HFD feeding[15] were used additionally in the IH model. Animals were maintained under standard laboratory conditions with ad libitum access to chow unless otherwise noted. All experiments were approved by the appropriate Institutional Animal Care and Use Committee.

Diets. In addition to unrefined chow pellets (PicoLab Mouse Diet 20-5058; LabDiet, St. Louis, Mo) with 22% calories from fat, 55% from carbohydrate, and 23% from protein, three different diets composed of refined ingredients (lard and soybean oil for fat; sucrose, maltodextrin, and corn starch for carbohydrate; hydrolyzed casein for protein) were employed (Research Diets, New Brunswick, NJ). The HFD D12492 consisted of 60% calories from fat, 20% from protein, and 20% from carbohydrates and was delivered in a soft pellet form. The control and protein-free diets were both based on D12450BSpx and delivered in a final 1% agar form. The control diet consisted of 10% calories from fat, 70% from carbohydrate, and 20% from protein. The protein-free diet consisted of 10% calories from fat and 90% from carbohydrate and was made isocaloric to the control diet by addition of sucrose.

IR models. Renal and hepatic IR injury was induced as described previously.[19] Briefly, mice were anesthetized by isoflurane inhalation (5% induction, 2% maintenance), and body temperature was maintained on a water-circulating heat pad. Preoperative blood glucose determinations were performed on fresh blood with an Easy Check Diabetes Meter Kit (Home Aide Diagnostics, Deerfield Beach, Fla) according to the manufacturer's instructions. Ischemia was induced after a midline abdominal incision. For renal IR, the left renal pedicle was localized and the renal artery and vein were occluded for 25 or 30 minutes with an atraumatic microvascular clamp (Roboz Surgical Instrument Co, Gaithersburg, Md). The procedure was repeated immediately on the right kidney. For hepatic IR, after visualization of the liver hilum, an atraumatic clamp was placed over the portal vein, hepatic artery, and bile duct to the left and median hepatic lobes for 30 minutes. In this model, 70% of the liver tissue becomes ischemic, and blood outflow from the small intestine is preserved through the right anterior and caudate liver lobes. After inspection for signs of ischemia (purple color in kidney, pale color in liver), the wound was covered with phosphate-buffered saline-soaked gauze and the animal placed under a heating pad and an aluminum foil blanket to maintain body temperature. After release of the clamp, restoration of blood flow was confirmed by return of the ischemic organ to normal color. Animals were returned to clean cages and allowed ad libitum access to a complete diet after surgery. Blood samples were collected from a superficial nick to the tail or terminally through the renal artery for analysis of ischemic injury over a time course based on organ-specific end points determined previously.[17,19] Functional impairment was assessed in the renal IR model by measurement of serum urea or creatinine levels daily for up to 3 days after IR with QuantiChrom assay kits (BioAssay Systems, Hayward, Calif). Kidney damage was assessed by blind histologic analysis of corticomedullary tubular necrosis from serial 3-μm sections taken 100 μm apart from formalin-fixed, paraffin-embedded kidney samples stained with hematoxylin and eosin (HE). Injury was assessed in the hepatic IR model by measurement of levels of liver enzymes alanine transaminase (ALT) and aspartate transaminase (AST) in the serum for up to 24 hours after reperfusion by kinetic analysis in a 96-well format with a BioTek II microplate reader (BioTek, Winooski, Vt) and by histology from 3-μm sections from formalin-fixed, paraffin-embedded samples stained with HE. Hepatic injury was scored in HE-stained sections in a blind fashion by counting of the percentage necrotic area per field in 10 fields/section. All images were taken under the same magnification and exposure settings.

IH model. IH was induced by our validated model of low flow in the mouse carotid artery.[20] Briefly, the left common carotid artery was exposed and visualized through a midline incision with use of a surgical microscope (OPMI-MD; Carl Zeiss, Germany). A focal stenosis was created approximately 1 mm proximal to the common carotid bifurcation by tying of a 9-0 nylon suture around both the artery and a blunt 35-gauge needle (external diameter of 0.14 mm, item No. NF 35 BL; World Precision Instruments, Inc, Sarasota, Fla). After removal of the needle, the vessel diameter was reduced by about 78%. Our previous

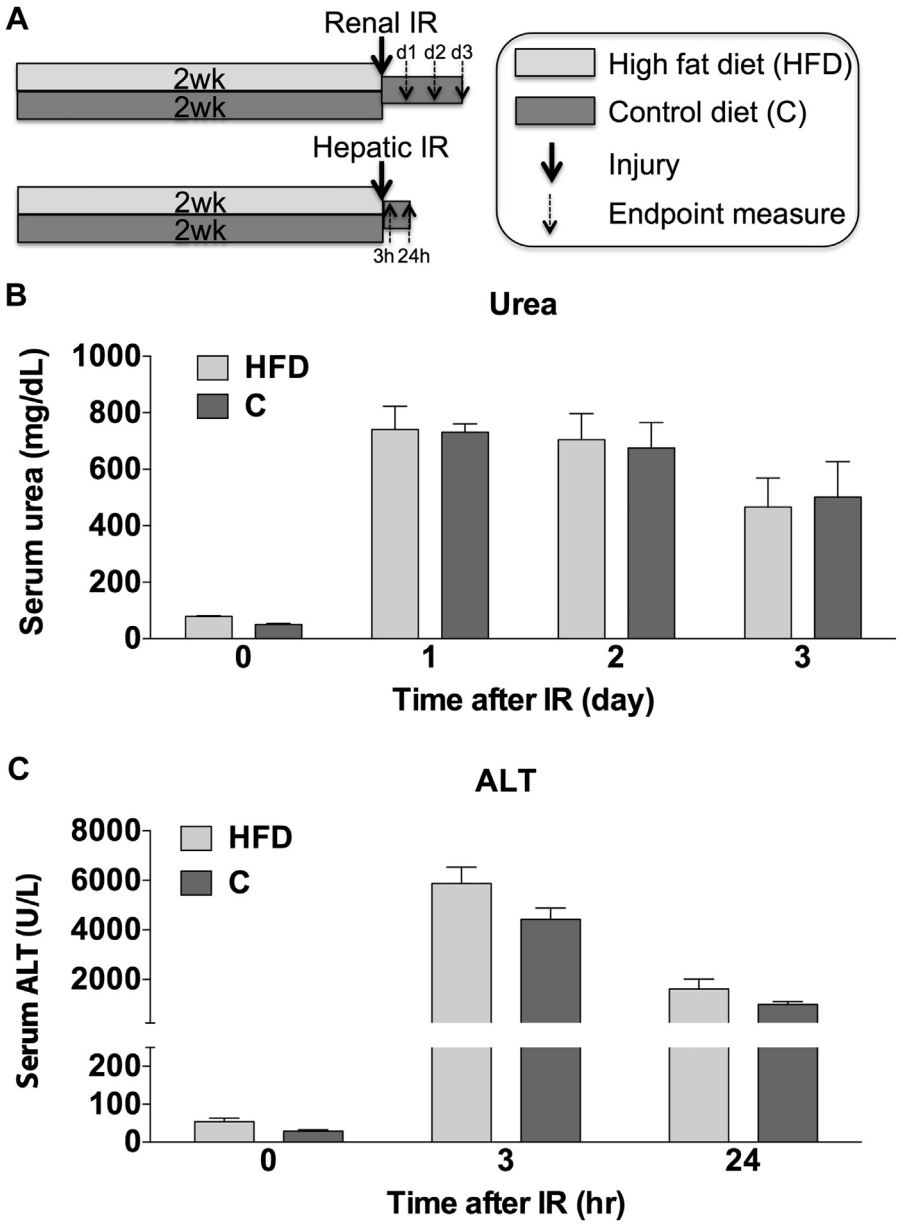

Fig 1. Influence of short-term high-fat diet (*HFD*) on outcome of ischemia-reperfusion (*IR*) injury. Two-week exposure to HFD did not worsen outcome of IR injury in male B6D2F1 mice. **A,** Experimental design. Mice were fed a low-fat control diet (*C*) or HFD for 2 weeks before onset of renal or hepatic IR injury and then returned to the low-fat control diet after surgery. Blood was drawn before injury or at the indicated times after reperfusion and analyzed for markers of renal function (urea) or liver injury (alanine transaminase, *ALT*) as indicated. **B,** Outcome of 25 minutes of bilateral renal IR injury as measured by changes in urea in serum before (time = 0) and on the indicated day after IR injury (n = 5/group). **C,** Outcome of 30 minutes of hepatic IR injury as measured by the amount of the liver enzyme ALT in serum before (time = 0) and at the indicated time after reperfusion (n = 5/group).

studies have shown that this diameter reduction will produce a reduction in luminal flow of about 85%.[20] Carotid thrombosis was not noted in this model under normal chow conditions. After creation of the focal stenosis, the surgical incision was closed, and mice were allowed to recover; all mice were returned to ad libitum feeding on a complete diet after surgery. One month later, arterial morphology was assessed on Masson trichrome-stained 6-μm sections up to 3 mm downstream of the stenosis as previously described.[20-23] Digitized images were taken and analyzed with a computerized imaging system (Zeiss Axio A1 microscope, High Resolution Camera, Vision 4.7 software for Windows; Carl Zeiss). Morphometric analysis was performed by tracing the interior surface of the lumen, the internal elastic lamina

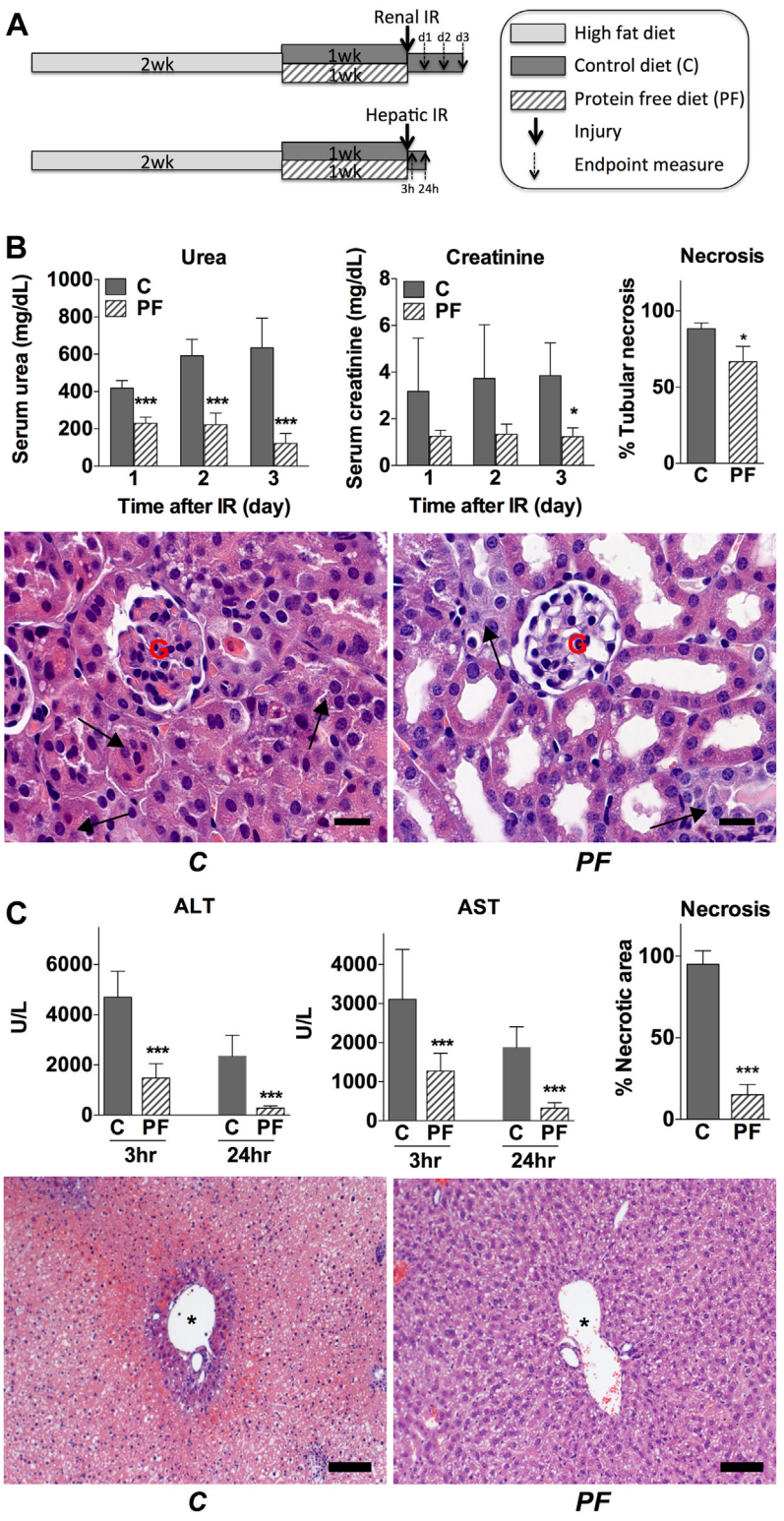

Fig 2. Influence of short-term protein-free (*PF*) dietary restriction (DR) after high-fat diet (HFD) on outcome of ischemia-reperfusion (*IR*) injury. **A,** Experimental design. Male B6D2F1 mice were fed HFD for 2 weeks followed by 1 week of low-fat control (*C*) vs low-fat PF diet before onset of renal or hepatic IR injury. All animals were returned to the low-fat control diet after surgery. **B,** Outcome of 30 minutes of bilateral renal IR injury as measured by changes in serum urea and creatinine on the indicated day after injury; n = 5/group. The percentage of tubular epithelial cell

(IEL), and the external elastic lamina (EEL). Areas were calculated from the measured circumference assuming a circular structure under in vivo conditions: luminal, intimal (= IEL − luminal), and medial (= EEL − IEL).

Statistical analyses. All data are expressed as means ± standard error of the mean. One- and two-way analysis of variance followed by Holm-Sidak correction for all pairwise multiple comparison procedures and unpaired two-tailed Student *t*-test were performed with SigmaPlot v11.0 (Systat Software Inc, San Jose, Calif) or GraphPad Prism.

RESULTS

Short-term exposure to HFD does not significantly affect outcome of renal or hepatic IR injury. Long-term exposure to HFD results in increased adiposity, systemic inflammation, and metabolic derangements. We tested the ability of short-term exposure to HFD to worsen outcome against IR injury in kidney and liver. To this end, 6-week old F1 hybrid B6D2F1 males were given ad libitum access to a refined diet composed of 60% calories from fat (HFD) or a control diet with 10% calories from fat (control chow; Fig 1, *A*). Animals consumed less of the energy-dense HFD but equal numbers of calories as animals on the control chow, gained more weight, and had a significantly higher percentage body fat than animals on control chow (Supplementary Fig 1, online only).

After 2 weeks on HFD or control chow, half of the animals in each diet group were subject to renal IR and the other half to hepatic IR. Serum drawn on days 1, 2, and 3 after reperfusion (renal) or 3 and 24 hours after reperfusion (hepatic) was used to monitor organ damage and dysfunction.

Contrary to our initial hypothesis, there were no significant differences between HFD and control chow groups in the damage suffered from 25 minutes of renal ischemia followed by reperfusion (Fig 1, *B*). Similar results were seen for hepatic IR injury with respect to release of ALT and AST, markers of liver injury, in the serum (Fig 1, *C*; Supplementary Fig 1, online only). We conclude that although long-term HFD can worsen outcome of IR injury, it does not do so in the short time of 2 weeks in this relatively healthy hybrid strain of mice.

Short-term protein-free DR improves outcome of renal and hepatic IR after HFD. We next tested the ability of short-term DR, which can lend protection against ischemic injury in as little as 6 days,[19] to protect against ischemic injury to kidneys or liver within 1 week immediately before surgery. Because protein/essential amino acid restriction and overall calorie restriction may each contribute to DR benefits,[19,24] we employed a DR regimen combining both protein and energy restriction by giving mice limited access to a protein-free diet.

Mice were exposed to HFD for 2 weeks as in the previous arm of the experiment and then fed either a control or protein-free diet for 1 week before induction of renal or hepatic IR (Fig 2, *A*). Animals on the protein-free diet consumed significantly fewer calories than animals on the control diet during the first 6 days after the switch from HFD. The protein-free group also had reduced blood glucose levels and reduced body weights relative to animals switched back to the control diet (Supplementary Fig 2, online only).

After preconditioning, animals were subject to either renal or hepatic IR. As we were predicting improvement with dietary preconditioning, we lengthened the period of renal ischemia from 25 to 30 minutes in this study arm to increase the magnitude of damage against which to measure protection. After bilateral renal IR, animals preconditioned on a protein-free diet displayed better preservation of renal function than those switched back to the control diet before surgery as measured by renal functional markers urea and creatinine in the serum (Fig 2, *B*; n = 5/group). Histologic analysis confirmed that changes in serum markers represented damage to the corticomedullary junction typical of this injury and that tubular necrosis was significantly reduced by the protein-free diet before surgery (Fig 2, *B*; n = 3/group).

Mice on the protein-free diet subjected to hepatic IR were also protected, displaying reduced ALT and AST 3 and 24 hours after injury (Fig 2, *C*; n = 15/group). This was confirmed by histologic analysis of hemorrhagic necrosis, with significant improvement in the preoperative protein-free group (Fig 2, *C*; n = 6/group).

We conclude that plasticity in the response to dietary modulation of ischemic injury in young adult male mice allows improvement in outcomes by short-term DR but not worsening of outcomes by short-term exposure to HFD.

Fasting protects against IH after HFD or normal chow. We next asked if short-term preoperative dietary interventions could modulate a fundamentally different outcome, IH, on hemodynamic changes in blood flow in a model of common carotid focal stenosis. Previously, we

necrosis in the cortex and at the cortical-medullary junction in serial sections 100 μm apart from each kidney is quantitated at right; n = 3/group. *Below*, Representative images of hematoxylin and eosin (HE)-stained kidney sections from the indicated groups harvested 3 days after injury. The *arrows* point to tubular structures in which cell death and disruption of normal structure are evident. *G*, Glomerulus; *scale bar* = 20 μm. **C,** Outcome of 30 minutes of hepatic IR injury as measured by the amount of the liver enzymes alanine transaminase (*ALT*) and aspartate transaminase (*AST*) in serum 3 and 24 hours after reperfusion; n = 15/group. The average percentage of necrosis in 10 microscopic fields per animal is quantitated at right; n = 6/group. The *asterisks* indicate the significance of the difference between groups at the indicated time point according to an unpaired, two-tailed Student *t*-test; $*P < .05$, $***P < .001$. *Below*, Representative images of HE-stained liver sections from the indicated group harvested 24 hours after injury. The *asterisk* indicates the central vein associated with portal triads; eosinophilic regions are characteristic of cell necrosis. *Scale bar* = 100 μm.

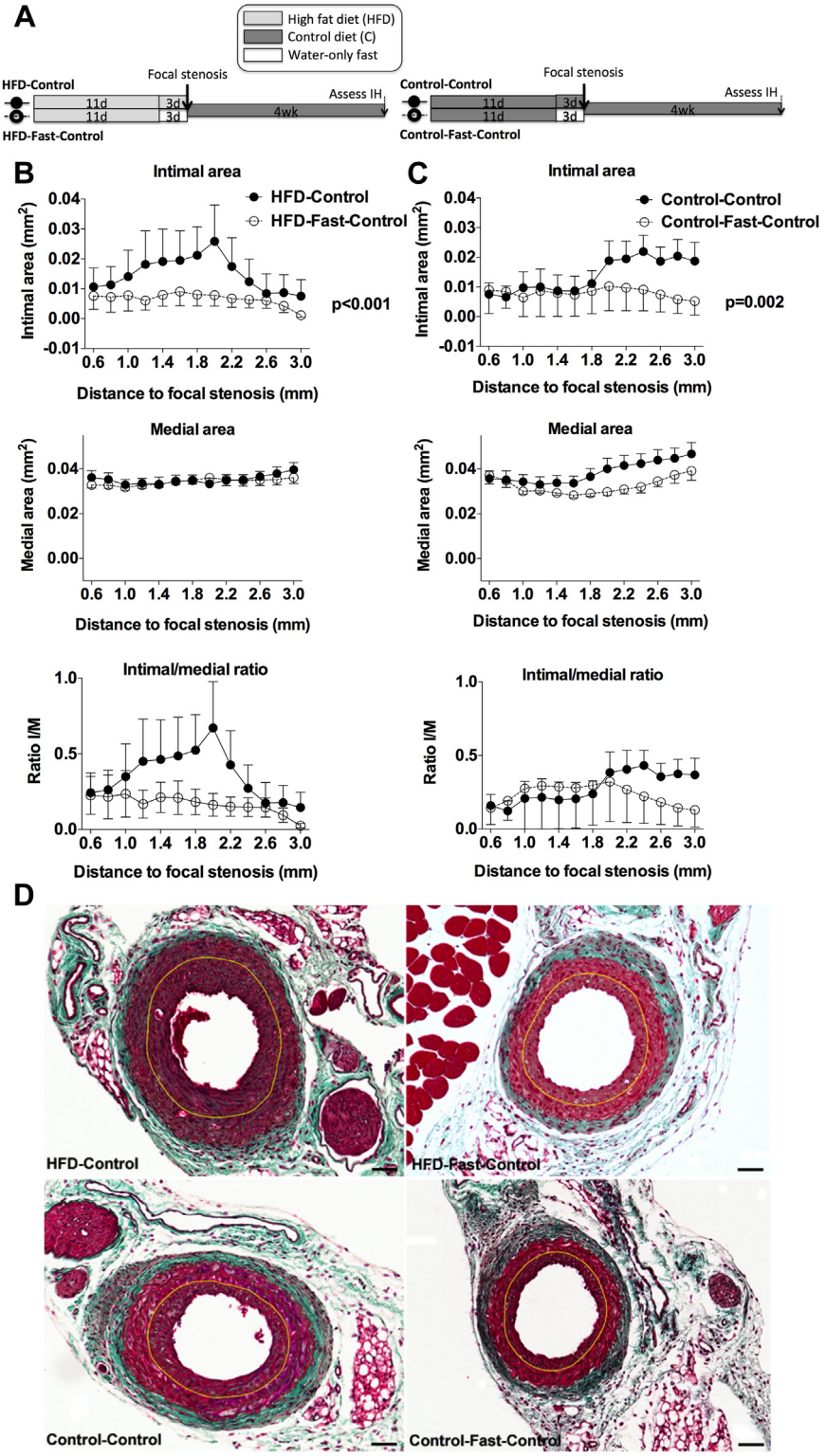

Fig 3. Influence of short-term high-fat diet (*HFD*) or fasting on intimal hyperplasia (*IH*). **A,** Experimental design. Male C57BL/6J mice were exposed for 2 weeks to HFD or low-fat control diet (*C*) for the indicated period with or without a 3-day water-only fast immediately before focal stenosis. All mice were then returned to the control diet. Four weeks later, IH was measured by histology. **B** and **C,** Intimal area, medial area, and intimal/medial area ratio at the indicated distance from the

found that long-term HFD feeding before and 4 weeks after focal stenosis exacerbates IH in C57Bl/6 mice by this model.[20]

Here, we tested whether 2 weeks of HFD exposure immediately before induction of focal stenosis had an effect on development of IH and if this could be modulated by DR. The first DR regimen that we tested was 3 days of water-only fasting, which we previously showed to protect against both renal and hepatic IR in male C57Bl/6 mice.[17] To test the effects of HFD with or without fasting on development of IH, 6-week-old male C57Bl/6 mice were exposed to HFD or control chow for 11 days and then maintained for 3 more days, on the same diet or subject to 3 days of water-only fast (Fig 3, *A*; n = 10/group). Immediately after focal stenosis, all mice were given ad libitum access to control chow for 4 weeks, and then the amount of IH was determined by histology as previously reported.[20]

Similar to IR injury, a 2-week preoperative HFD did not significantly affect the intimal hyperplastic response. However, 3 days of fasting immediately before the procedure significantly reduced IH whether the mice were previously on the HFD ($P < .001$) or a control diet ($P = .002$) (Fig 3, *B-D*). In contrast, medial areas proximal to the focal stenosis were not significantly different between diet groups; as a result, intimal/medial ratios resembled intimal areas (Fig 3, *B* and *C*).

Short-term protein-free DR attenuates IH. Because extended periods of fasting may not be feasible in clinical practice, we also tested the ability of protein-free DR to modulate IH (Fig 4, *A*). For these experiments, we used B6D2F1 hybrid males shown to respond beneficially to protein restriction to rule out any potential artifacts associated with particular inbred lines such as C57Bl/6J. We found that 1 week of protein-free DR before focal stenosis significantly reduced IH at 28 days (Fig 4, *B*; n = 10/group). In contrast, medial areas proximal to the focal stenosis were not significantly different between diet groups; as a result, intimal/medial ratios resembled intimal areas (Fig 4, *B*).

We conclude that whereas short-term HFD exposure did not worsen surgical outcome, two different short-term dietary regimens (3 days of water-only fasting and 1 week of protein-free DR) protected from IR to kidney and liver and reduced the intimal hyperplastic response to hemodynamic perturbation on focal stenosis.

DISCUSSION

Although long-term dietary habits such as DR or overnutrition can have beneficial or detrimental effects, respectively, on surgical outcome in experimental models, the potential of acute changes in food intake in the days leading up to a planned surgical procedure to alter surgical outcome has not been rigorously tested. On the basis of emerging data on the ability of mammalian metabolism and physiology to respond rapidly to changes in dietary intake, we hypothesized that short-term overnutrition would worsen surgical outcomes and that short-term DR immediately before surgery would reverse these negative effects and improve outcomes. Furthermore, we hypothesized that these effects would not be specific to IR but generally applicable to different vascular surgical outcomes, including development of IH. Whereas we found no detrimental effects of short-term (2 weeks) HFD, short-term DR markedly improved outcomes after two distinct vascular surgery injuries, IR and hemodynamically driven IH.

Long-term overnutrition resulting in obesity and type 2 diabetes is a risk factor for surgical complications. Excess adiposity makes surgical procedures technically more challenging and is also associated with reduced insulin sensitivity and increased systemic inflammation.[25,26] Here we examined a different clinical scenario, short-term overnutrition, but found no detrimental effect on IR or focal stenosis–related surgical outcomes. Although 2 weeks of HFD feeding significantly increased adiposity, it did not increase blood glucose levels. Hyperglycemia typically takes a few weeks longer to develop in HFD-fed mice and correlates with a reduction in insulin sensitivity and an increase in systemic low-grade inflammation. Thus, one can speculate that the detrimental effects of long-term overnutrition on surgery are likely to stem from perturbations in these metabolic parameters rather than directly from the absolute amount of adipose tissue. This position is supported by the observation that obesity itself often does not correlate with surgical outcome[27]; indeed, increased adiposity itself is not mutually exclusive of a healthy metabolic profile.[28]

Long-term DR is known to improve a variety of metabolic end points as well as acute stress resistance but is impractical in the clinical setting. Whereas longevity benefits in nonhuman primates on DR have been equivocal, benefits on health span (protection from age-related cancer, diabetes, and cardiovascular disease) are clear.[5,29,30] Importantly, studies suggest that humans respond to DR in beneficial ways with respect to metabolic fitness (including improved glucose homeostasis, lipid profiles, and cardiovascular performance).[31,32]

Although short-term DR has recently emerged as a powerful mediator of beneficial adaptive stress responses including protection from surgical IR,[14] the ability of short-term DR to affect IH occurring as a result of focal stenosis is remarkable, considering that the dietary intervention occurred 4 weeks before outcome assessment. Limited data on the half-life of the DR benefits suggest that such benefits are short-lived after the return to ad

focal stenosis (n = 10 mice/per group). *P* value indicates the significance of the difference between intimal areas of the indicated groups according to a two-way analysis of variance. Note the absence of differences between HFD and control diets alone on intimal area. **D,** Representative Masson trichrome-stained images under each dietary condition taken at 0.6- to 3.0-mm distance proximal to a focal stenosis. The *yellow line* depicts internal elastic lamina. *Scale bars* = 50 μm.

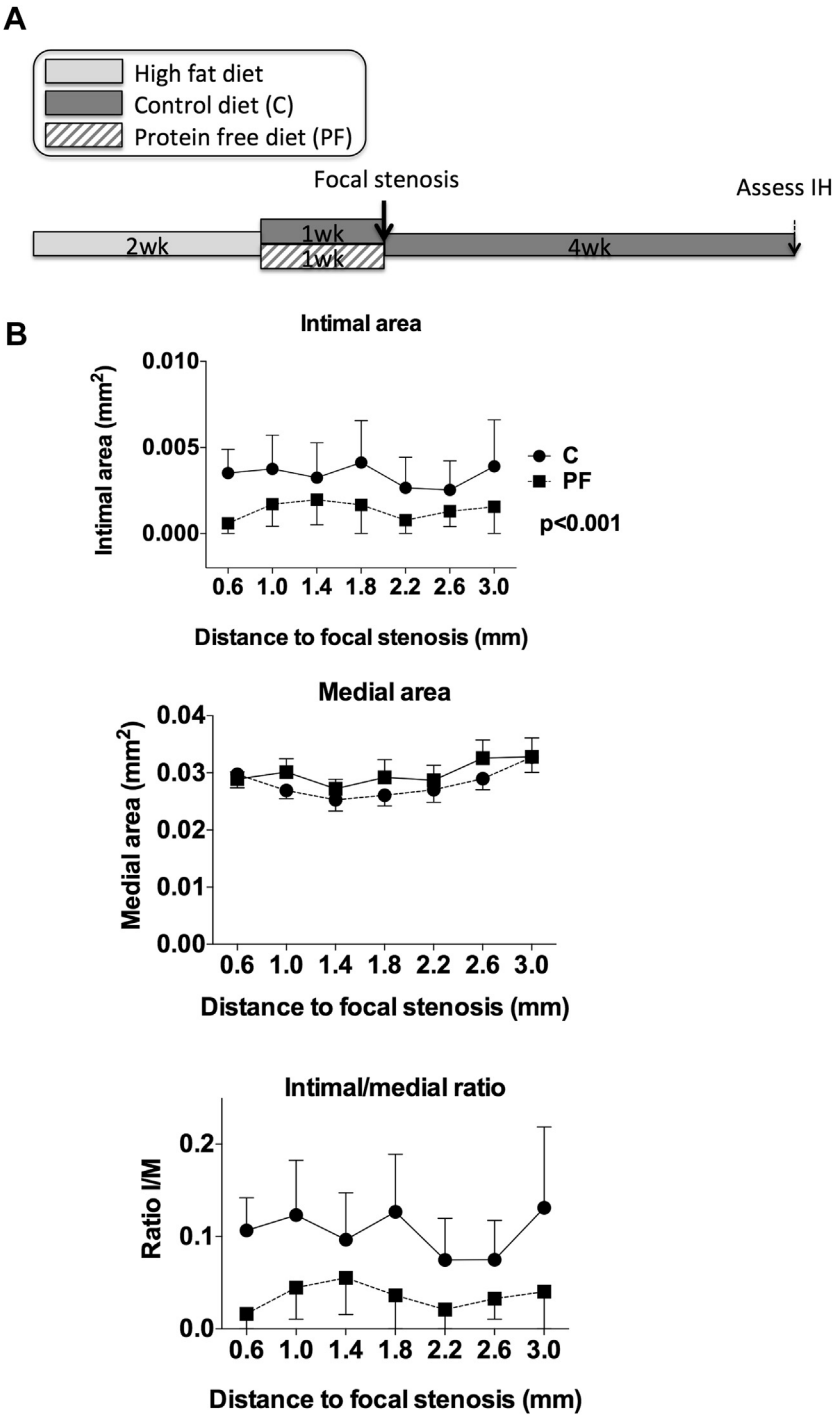

Fig 4. Influence of short-term protein-free (*PF*) dietary restriction (DR) after high-fat diet (HFD) on intimal hyperplasia (*IH*). **A,** Experimental design. After 2 weeks on HFD, male B6D2F1 animals were exposed for 1 week to a control diet with 18% calories from protein (*C*, n = 10) or an isocaloric diet lacking protein (*PF*, n = 10) before focal stenosis. All mice were then returned to control chow. Four weeks later, IH was measured by histology. **B,** Intimal area, medial area, and intimal/medial area ratio at the indicated distance from the focal stenosis. *P* value indicates the significance of the difference between intimal areas of the indicated groups according to a two-way analysis of variance.

libitum feeding on a complete diet. For example, the benefits of 3 days of fasting on survival in the renal ischemia model last approximately 3 days.[17] Similarly, the benefits of long-term DR on gene expression profiles and longevity are lost rapidly, within days to weeks.[33] Most likely, the benefits of short-term DR against IH reflect modulation of events occurring shortly after the change in hemodynamic flow that further affect later remodeling, rather than the change in flow itself, which remains perturbed because of the focal stenosis throughout the experimental period.

This study has a number of limitations. Because the nature of the injuries encumbered by IR and focal stenosis occur on very different time scales and with different causes, we did not set out a priori to define underlying mechanisms of protection. Thus, one limitation of this study is that molecular mechanisms of protection against IR and IH, and whether they are shared, are not delineated. Furthermore, in the case of IR, it is unknown if preconditioning affects reperfusion injury to other organs, such as lung, outside of the ischemic organ. A further limitation of this study is the use of two different genetic strains, the inbred C57BL/6 strain and the hybrid B6D2F1 strain, preventing direct comparison of the result of fasting and protein restriction in the IH model. Whereas such direct within-strain comparisons are important in future studies designed to elucidate underlying mechanisms, here they had the advantage of reducing the risk of identifying strain-specific, diet-specific, or interaction-specific effects with less likelihood of translating to humans.

What little is known about the mechanistic basis of protection by either long-term or short-term DR regimens points to dampening of local or systemic inflammation and upregulation of cell/organ autonomous stress resistance mechanisms, including oxidative stress resistance.[6,8,15,17] Teleologically, one can speculate that evolutionary selection under the intense pressure of nutrient/energy restriction yielded molecular pathways to maximize stress resistance under starvation conditions.[30] The amino acid starvation response activated by the amino acid sensor and eIF2α (eukaryotic translation initiation factor 2α) kinase GCN2 (general control nonderepressible 2) may be one such pathway, implicating dietary protein sensing and translational control in stress protection.[19] Interestingly, preconditioning regimens leading to equivalent functional protection against renal ischemic injury, including 3 days of water-only fasting and 4 weeks of 30% DR, have divergent effects on kidney gene expression with little overlap, consistent with the possibility of multiple underlying mechanisms of protection.[17] Further research in experimental models will be required to define such molecular effectors, leading, it is hoped, to the identification of clinically relevant targets.

Despite the risk posed by chronic overnutrition and the potential beneficial effects of short-term protein or calorie restriction before surgery, preoperative DR is rarely considered before surgery except in specific instances, for example, in bariatric surgery in which the immediate goal is to lose weight to facilitate the operation itself. The only universal dietary recommendation before surgery is overnight fasting to avoid aspiration of regurgitated solids under anesthesia. In some cases, overnight fasting has been replaced by carbohydrate energy-dense drinks up to a few hours before surgery to reduce postoperative thirst, hunger (well-being), and insulin resistance.[34] Data presented here and elsewhere[19,35] suggest that protein restriction, rather than calorie restriction, is a major determinant of short-term DR benefits. By extension, preoperative carbohydrate loading may not be mutually exclusive with short-term DR benefits, whether in the form of water-only fasting or brief protein restriction.

CONCLUSIONS

Whereas short-term overnutrition leading to increased adiposity had no effect on outcome of IR or IH examined here, protein/energy restriction imparted significant benefits in these models, suggesting clinically relevant strategies to enhance the mammalian response to injury. Clinical human trials in this arena have documented feasibility and safety of preoperative dietary interventions, including 2 weeks of very low calorie diets or 3 days of reduced food intake followed by 24 hours of water-only fasting immediately before surgery.[11,36] In view of the high clinical complication rates in the setting of cardiovascular reconstructions (and their pathophysiologic links to IR and IH), short-term DR now stands as a particularly attractive, pleiotropic strategy for this population to enhance patient outcomes.[37] Whereas employment of rodent models will be useful in refining our understanding of the nutritional basis of protection, including duration and severity of restriction, and underlying molecular mechanisms, inevitably multicenter randomized clinical trials will be required to determine safety and efficacy of such approaches in humans.

We thank Hanqiao Zheng, MD, PhD, for technical assistance.

AUTHOR CONTRIBUTIONS

Conception and design: CO, JM
Analysis and interpretation: CM, MT, PY, JT, JM
Data collection: CM, MT, PY, JT, JM
Writing the article: CM, MT, AL, CO, JM
Critical revision of the article: AL, BK, CO, JM
Final approval of the article: CM, MT, PY, JT, AL, BK, CO, JM
Statistical analysis: CM, MT, PY, JT, BK
Obtained funding: CM, BK, CO, JM
Overall responsibility: JM

REFERENCES

1. Subbotin VM. Analysis of arterial intimal hyperplasia: review and hypothesis. Theor Biol Med Model 2007;4:41.
2. Fontana L, Klein S. Aging, adiposity, and calorie restriction. JAMA 2007;297:986-94.
3. Bays HE. Adiposopathy is "sick fat" a cardiovascular disease? J Am Coll Cardiol 2011;57:2461-73.
4. Speakman JR, Mitchell SE. Caloric restriction. Mol Aspects Med 2011;32:159-221.

5. Colman RJ, Beasley TM, Kemnitz JW, Johnson SC, Weindruch R, Anderson RM. Caloric restriction reduces age-related and all-cause mortality in rhesus monkeys. Nat Commun 2014;5:3557.
6. Yu ZF, Mattson MP. Dietary restriction and 2-deoxyglucose administration reduce focal ischemic brain damage and improve behavioral outcome: evidence for a preconditioning mechanism. J Neurosci Res 1999;57:830-9.
7. Ahmet I, Wan R, Mattson MP, Lakatta EG, Talan M. Cardioprotection by intermittent fasting in rats. Circulation 2005;112:3115-21.
8. Chandrasekar B, Nelson JF, Colston JT, Freeman GL. Calorie restriction attenuates inflammatory responses to myocardial ischemia-reperfusion injury. Am J Physiol Heart Circ Physiol 2001;280:H2094-102.
9. Rochon J, Bales CW, Ravussin E, Redman LM, Holloszy JO, Racette SB, et al. Design and conduct of the CALERIE study: comprehensive assessment of the long-term effects of reducing intake of energy. J Gerontol A Biol Sci Med Sci 2011;66:97-108.
10. Anton SD, Karabetian C, Heekin K, Leeuwenburgh C. Caloric restriction to moderate senescence: mechanisms and clinical utility. Curr Transl Geriatr Exp Gerontol Rep 2013;2:239-46.
11. Van Nieuwenhove Y, Dambrauskas Z, Campillo-Soto A, van Dielen F, Wiezer R, Janssen I, et al. Preoperative very low-calorie diet and operative outcome after laparoscopic gastric bypass: a randomized multicenter study. Arch Surg 2011;146:1300-5.
12. Verweij M, van Ginhoven TM, Mitchell JR, Sluiter W, van den Engel S, Roest HP, et al. Preoperative fasting protects mice against hepatic ischemia/reperfusion injury: mechanisms and effects on liver regeneration. Liver Transpl 2011;17:695-704.
13. Bloomer RJ, Kabir MM, Trepanowski JF, Canale RE, Farney TM. A 21 day Daniel Fast improves selected biomarkers of antioxidant status and oxidative stress in men and women. Nutr Metab (Lond) 2011;8:17.
14. Robertson LT, Mitchell JR. Benefits of short-term dietary restriction in mammals. Exp Gerontol 2013;48:1043-8.
15. Nguyen B, Tao M, Yu P, Mauro C, Seidman MA, Wang YE, et al. Preoperative diet impacts the adipose tissue response to surgical trauma. Surgery 2013;153:584-93.
16. Benotti P, Blackburn GL. Protein and caloric or macronutrient metabolic management of the critically ill patient. Crit Care Med 1979;7:520-5.
17. Mitchell JR, Verweij M, Brand K, van de Ven M, Goemaere N, van den Engel S, et al. Short-term dietary restriction and fasting precondition against ischemia reperfusion injury in mice. Aging Cell 2010;9:40-53.
18. van Ginhoven TM, Dik WA, Mitchell JR, Smits-te Nijenhuis MA, van Holten-Neelen C, Hooijkaas H, et al. Dietary restriction modifies certain aspects of the postoperative acute phase response. J Surg Res 2011;171:582-9.
19. Peng W, Robertson L, Gallinetti J, Mejia P, Vose S, Charlip A, et al. Surgical stress resistance induced by single amino acid deprivation requires Gcn2 in mice. Sci Transl Med 2012;4:118ra11.
20. Tao M, Mauro CR, Yu P, Favreau JT, Nguyen B, Gaudette GR, et al. A simplified murine intimal hyperplasia model founded on a focal carotid stenosis. Am J Pathol 2013;182:277-87.
21. Longchamp A, Alonso F, Dubuis C, Allagnat F, Berard X, Meda P, et al. The use of external mesh reinforcement to reduce intimal hyperplasia and preserve the structure of human saphenous veins. Biomaterials 2014;35:2588-99.
22. Yu P, Nguyen BT, Tao M, Campagna C, Ozaki CK. Rationale and practical techniques for mouse models of early vein graft adaptations. J Vasc Surg 2010;52:444-52.
23. Yu P, Nguyen BT, Tao M, Bai Y, Ozaki CK. Mouse vein graft hemodynamic manipulations to enhance experimental utility. Am J Pathol 2011;178:2910-9.
24. Levine ME, Suarez JA, Brandhorst S, Balasubramanian P, Cheng CW, Madia F, et al. Low protein intake is associated with a major reduction in IGF-1, cancer, and overall mortality in the 65 and younger but not older population. Cell Metab 2014;19:407-17.
25. Yilmaz MB, Guray U, Guray Y, Biyikoglu SF, Tandogan I, Sasmaz H, et al. Metabolic syndrome negatively impacts early patency of saphenous vein grafts. Coron Artery Dis 2006;17:41-4.
26. Protack CD, Jain A, Vasilas P, Dardik A. The influence of metabolic syndrome on hemodialysis access patency. J Vasc Surg 2012;56:1656-62.
27. Jackson RS, Black JH 3rd, Lum YW, Schneider EB, Freischlag JA, Perler BA, et al. Class I obesity is paradoxically associated with decreased risk of postoperative stroke after carotid endarterectomy. J Vasc Surg 2012;55:1306-12.
28. Bluher M. The distinction of metabolically 'healthy' from 'unhealthy' obese individuals. Curr Opin Lipidol 2010;21:38-43.
29. Colman RJ, Anderson RM, Johnson SC, Kastman EK, Kosmatka KJ, Beasley TM, et al. Caloric restriction delays disease onset and mortality in rhesus monkeys. Science 2009;325:201-4.
30. Mattison JA, Roth GS, Beasley TM, Tilmont EM, Handy AM, Herbert RL, et al. Impact of caloric restriction on health and survival in rhesus monkeys from the NIA study. Nature 2012;489:318-21.
31. Heilbronn LK, Smith SR, Martin CK, Anton SD, Ravussin E. Alternate-day fasting in nonobese subjects: effects on body weight, body composition, and energy metabolism. Am J Clin Nutr 2005;81:69-73.
32. Trepanowski JF, Canale RE, Marshall KE, Kabir MM, Bloomer RJ. Impact of caloric and dietary restriction regimens on markers of health and longevity in humans and animals: a summary of available findings. Nutr J 2011;10:107.
33. Dhahbi JM, Kim HJ, Mote PL, Beaver RJ, Spindler SR. Temporal linkage between the phenotypic and genomic responses to caloric restriction. Proc Natl Acad Sci U S A 2004;101:5524-9.
34. Soreide E, Eriksson LI, Hirlekar G, Eriksson H, Henneberg SW, Sandin R, et al. Pre-operative fasting guidelines: an update. Acta Anaesthesiol Scand 2005;49:1041-7.
35. Verweij M, van de Ven M, Mitchell JR, van den Engel S, Hoeijmakers JH, Ijzermans JN, et al. Glucose supplementation does not interfere with fasting-induced protection against renal ischemia/reperfusion injury in mice. Transplantation 2011;92:752-8.
36. van Ginhoven TM, de Bruin RW, Timmermans M, Mitchell JR, Hoeijmakers JH, Ijzermans JN. Pre-operative dietary restriction is feasible in live-kidney donors. Clin Transplant 2011;25:486-94.
37. Mitchell JR, Beckman JA, Nguyen LL, Ozaki CK. Reducing elective vascular surgery perioperative risk with brief preoperative dietary restriction. Surgery 2013;153:594-8.

Submitted Apr 24, 2014; accepted Jul 3, 2014.

Additional material for this article may be found online at www.jvascsurg.org.

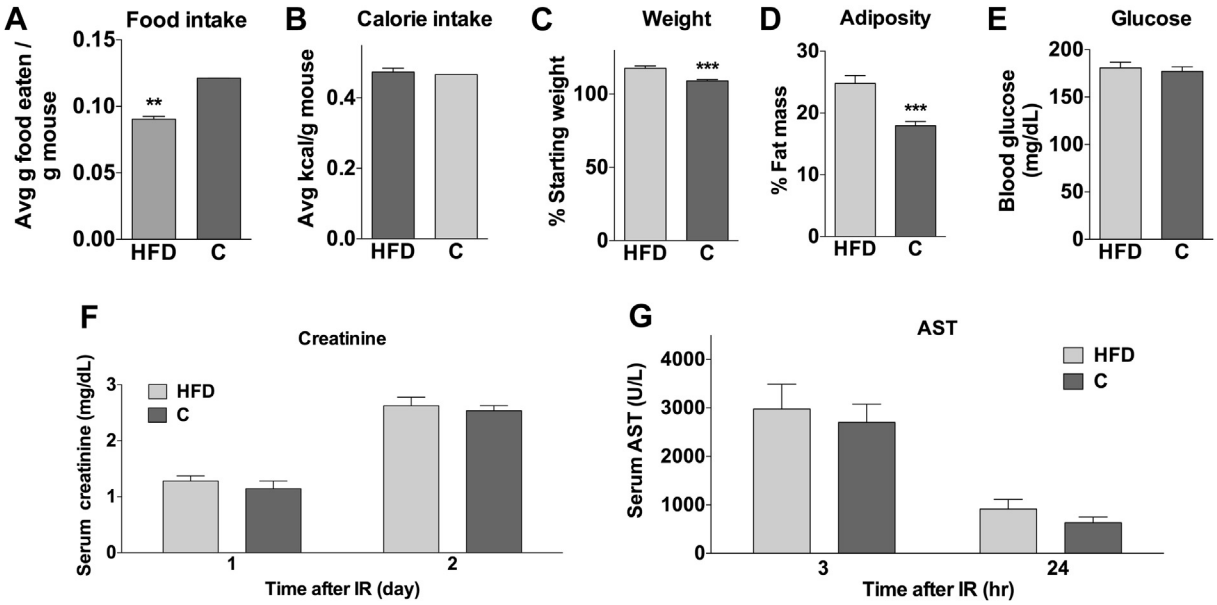

Supplementary Fig 1 (online only). Characteristics of animals on short-term exposure to high-fat diet (*HFD*) vs control low-fat diet (*C*). **A,** Food intake during a 2-week period (n = 10/group) presented as average grams of food eaten per gram of mouse. **B,** Calorie intake corrected for energy density of diet. **C,** Weight gain expressed as a percentage of starting weight. **D,** Adiposity expressed as a percentage of total body weight. **E,** Blood glucose in the fed state before harvest. **F,** Serum levels of creatinine at the indicated time after renal reperfusion (n = 5/group). **G,** Serum levels of aspartate transaminase (*AST*) at the indicated time after hepatic reperfusion (n = 5/group). The *asterisks* indicate the significance of the difference between groups according to an unpaired, two-tailed Student *t*-test; $^{**}P < .01$, $^{***}P < .001$. *IR*, Ischemia-reperfusion.

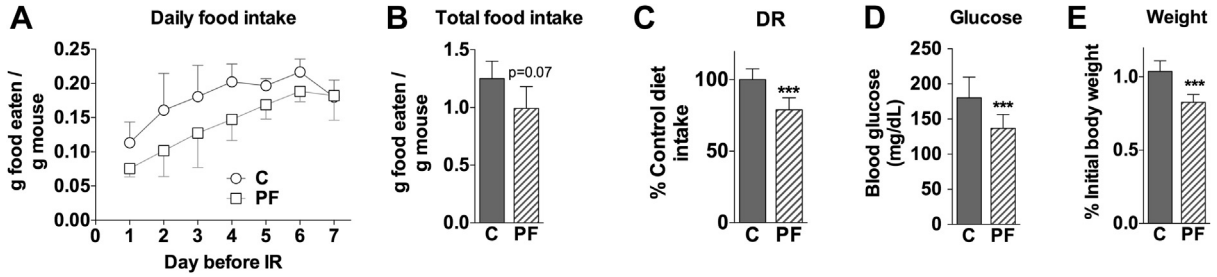

Supplementary Fig 2 (online only). Characteristics of animals on short-term protein-free (*PF*) dietary restriction (*DR*) after high-fat diet (HFD) exposure for 2 weeks. **A,** Daily food intake for 1 week before ischemia-reperfusion (*IR*) after the switch from HFD to the indicated control (*C*) or PF diet; n = 4 cages/group (20 mice/group). **B,** Total food intake 1 week before IR. **C,** DR calculated as a percentage of average food eaten by animals on the control diet. **D, E,** Blood glucose **(D)** and body weight **(E)** after 1 week on C or PF diet as indicated. The *asterisks* indicate the significance of the difference between groups according to an unpaired, two-tailed Student *t*-test; $^{***}P < .001$.